Preparation of the Polymethacrylates with Controlled Structures through the Detailed Analysis of Polymerization Products

Koichi Ute

Department of Chemistry
Faculty of Engineering Science
Osaka University
1990

Preparation of the Polymethacrylates with Controlled Structures through the Detailed Analysis of Polymerization Products

Koichi Ute

Department of Chemistry
Faculty of Engineering Science
Osaka University
1990

PREFACE

Preparation of polymers with finely controlled structure is one of the most important and interesting subjects in pure and applied polymer chemistry. For the studies of the controlled polymer synthesis, detailed analysis of polymer structures is essential, and NMR spectroscopy has played an important role in this field. Introduction of superconducting magnets together with developments of two-dimensional experiments and multinuclear measurements have brought new aspects in the characterization of polymers by NMR spectroscopy.

This dissertation deals with the anionic polymerizations of methacrylates through the detailed analysis of the resulting polymers and oligomers with the aid of high-field NMR. The structural analysis led us to the discovery of the stereoregular and living polymerization of methyl methacrylate. The dissertation also describes the on-line GPC/NMR method which has been developed as a novel technique for the characterization of polymers. These studies has been carried out under the direction of Professor Koichi Hatada in his laboratory at Osaka University from 1982 to 1990.

The author wishes to express his deep gratitude to Professor Koichi Hatada for his valuable guidance and constant encouragement throughout the present work. The author is deeply indebted to Professor Yoshio Okamoto (Nagoya University) and Associate Professor Tatsuki Kitayama for their numerous fruitful discussions.

Great acknowledgment is also made to Professor Mikiharu Kamachi, Professor Shun-ichi Murahashi and Professor Takayuki Fueno for their detailed criticisms on the thesis.

Many thanks are due to Professor Retsu Miura (Kansai Medical University), Mr. Yoshio Terawaki, Mr. Hiroshi Okuda, Mr. Toshio Shimamura (Nitto Technical Information Center Co. Ltd.), and Mr. Mamoru Imanari (JEOL Ltd.) for their helps in the NMR measure-

ments. The author also wishes to express his thanks to Associate Professor Yoshiki Matsuura, Dr. Hideo Imoto (University of Tokyo) and Mr. Ken-ichi Sakaguchi for their helpful suggestions in the X-ray studies. The author extends his appreciation to Associate Professor Tomoshige Nitta for his valuable suggestions on the flow-cell for the GPC/NMR measurements, and also to Mr. Makoto Takeuchi (JEOL Ltd.) for his experimental supports on SFC experiments.

The author feels very fortunate to have the opportunity to collaborate with Dr. Eiji Yashima, Dr. Eiji Masuda, Mr. Hideo Nakanishi, Mr. Katsuji Tanaka, Mr. Tohru Nishimura, Mr. Masanori Yamamoto, Mr. Yoshinori Tashima, and Mr. Masaharu Kashiyama. Finally, the author thanks to all the members of Hatada Laboratory for their kind helps in supporting the research activities.

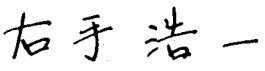

Koichi Ute

Department of Chemistry
Faculty of Engineering Science
Osaka University
November, 1990

CONTENTS

GENERAL INTRODUCTION

Properties of polymers depend not only on the chemical structure of monomeric units but also on the microstructures such as stereoregularity, comonomer composition, terminal groups, molecular weight and its distribution. It has been a challenging subject for polymer chemists to synthesize the polymers with well-defined or controlled structures. Living polymerization and stereoregular polymerization, which are the remarkable developments in modern polymer synthesis, are both promising techniques for the purpose.

The anionic polymerization of methyl methacrylate (MMA) is one of the most intensively studied polymerizations of polar vinyl monomers. MMA can be polymerized with a variety of lithium, magnesium and aluminum compounds to give polymers with a wide range of tacticities. Many papers including several review articles[1-6] have been published on MMA polymerization since the first preparation of stereoregular PMMAs by Fox *et al.*[7] and Miller *et al.*[8] in 1958. However, the complexity of the factors affecting the polymerization reaction prevented a clear understanding of the polymerization. It has been difficult to control the molecular weight and its distribution of stereoregular PMMAs.

The polymerization of MMA with butyllithium, a typical example of anionic initiator, yields the polymer which has a broad molecular weight distribution (MWD). Initiator efficiency in the polymerization is low if each polymer molecule is assumed to contain one butyl group. Most of these features are ascribed to the side reactions between the initiator and monomer[9-14]; an attack of the initiator on the monomer takes place on both olefinic and carbonyl double bonds [1,2].

Hatada and his coworkers polymerized totally deuterated MMA (MMA-*d*$_8$) with undeuterated butyllithium in toluene and in THF and analyzed the structure of the resulting polymers and oligomers by ^{1}H NMR spectroscopy[15-17]. They showed that butyl isopropenyl ketone (BIPK) formed in the polymerization mixture adds to a growing anion [3] to form an anion ended with BIPK [4]. The

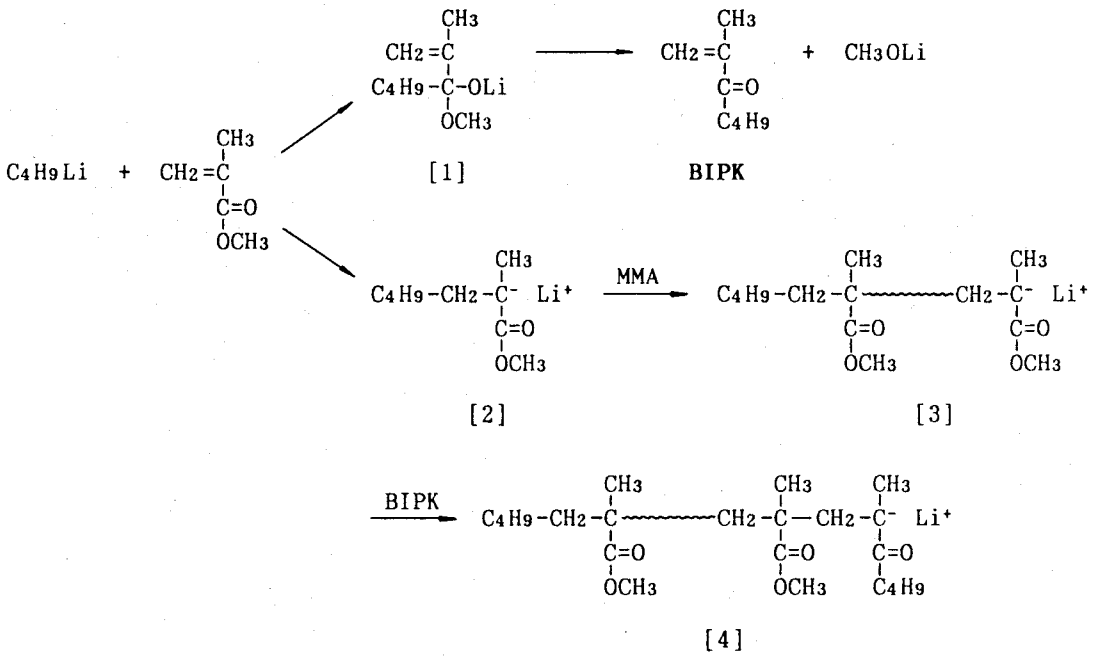

[1] BIPK [2] [3] [4]

ketone-ended anions are much less reactive than MMA-ended anions and most of them remain unreacted during the polymerization reaction. The lithium methoxide formed concomitantly with BIPK coordinates with a growing anion and generate another species of different reactivity and stereoregularity. These cause the MWD of the resultant polymer to be broad.

Self-termination of the polymer anion to form a cyclic ketone structure [6] is also responsible for the broad MWD, particularly for the polymerization conducted at above -40°C. Goode *et al.*[9] and Glusker *et al.*[10] described that a pseudo-terminated growing center [5] did not lose its activity completely and sometimes acted as the "dormant" species in the polymerization system.

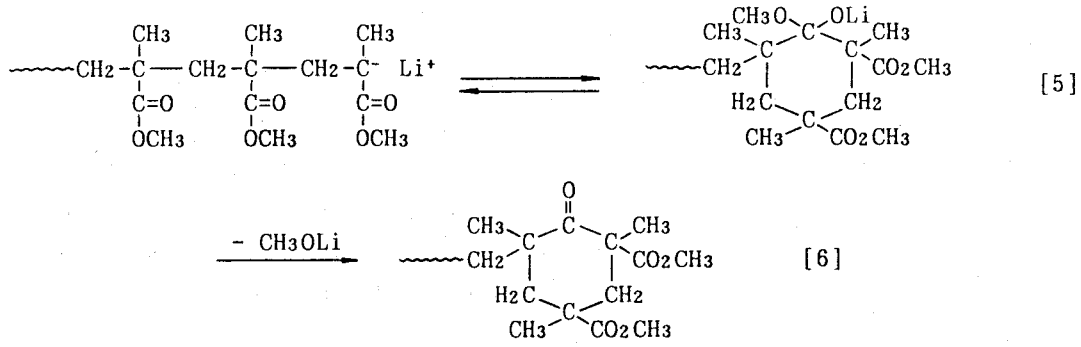

[5] [6]

The course of the cyclizing selfcondensation were investigated extensively by Lochmann and his coworkers[18,19] in terms of the character of solvent, effect of alkoxide, concentration of the reactants, and temperature, using esters of α-metallocarboxylic acids as initiator.

In the polymerization of MMA by Grignard reagents, Schlenk equilibrium [7] also makes the reaction complex.

$$2\ RMgX \rightleftharpoons R_2Mg + MgX_2 \qquad [7]$$

The exchange between "RMgBr" and "R_2Mg" is slow enough to react with monomer independently without perturbing the equilibrium[20], thus tacticity and MWD of the resulting polymer are dominated by the relative amount of these active species ('eneidic mechanism'). Ando *et al.*[21] and Matsuzaki *et al.*[22] suggested that in the polymerization of MMA by phenylmagnesium bromide active species for isotactic polymer were produced from "C_6H_5MgBr" and those for syndiotactic-rich polymer from "$(C_6H_5)_2Mg$", and that isotactic polymer was produced at relatively high temperature (> 0°C). The results are consistent with general observations that Schlenk equilibrium moves in favor of "RMgX" with increasing temperature and that "R_2Mg" does not yield isotactic PMMA.

Moreover, organomagnesium compounds are usually prepared in diethyl ether or THF, and therefore the influence of these polar molecules on the polymerization, particularly in the polymerization in a nonpolar solvent, is generally inevitable. Allen and his coworkers[23,24] carried out the polymerization of MMA in toluene initiated by homogeneous "de-etherated" alkyl and arylmagnesium bromides prepared in THF. The stoichiometric compositions of the equilibrium mixture of the initiating species (mole ratio of Br/R) were dependent on the concentration of the residual THF. It would seem likely that the initiation species under these conditions was *t*-$C_4H_9MgBr\cdot 2THF$ which forms a chiral species if one THF is displaced by a coordinated monomer [8]. However, the associated forms [9,10] should also be taken into account where the ratio of Br/R exceeds unity or the ratio of THF/R is close to unity, because $MgBr_2$, even solvated with THF, can not exist alone in toluene due to its low solubility (0.006 M).

[8]

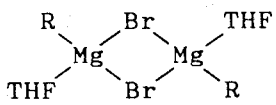

[9]

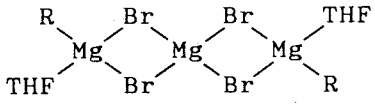

[10]

In summary, the factors affecting the anionic polymerization of MMA can be described as follows:

1. Side reaction in the initiation step (formation of isopropenyl ketone and methoxide)
2. Self-termination (or pseudotermination) of the polymer anions to form a cyclic ketone structure
3. Schlenk equilibrium
4. Influence of polar molecules
5. Association of active species.

In contrast to the above complexities, the polymerization of MMA in THF by bulky alkyllithium such as 1,1-diphenylhexyllithium (DPHLi) at low temperature proceeds in a living manner to give PMMA of a narrow MWD[25,26]. A new method of polymerization known as group transfer polymerization (GTP) was developed by Webster and his coworkers in 1983[27]; by this method methacrylates and acrylates can be polymerized using ketene silyl acetals in the presence of a nucleophilic (*e.g.* HF_2^-, CN^-) or an electrophilic (*e.g.* $ZnCl_2$, Et_2AlCl) coinitiator. GTP proceeds through a living mechanism even at room temperature which allows the preparation of polymers with a narrow MWD. However, the stereoregularities of the PMMAs prepared by DPHLi in THF and by GTP are low similarly to those of the PMMAs prepared by radical polymerization.

In 1985, the present authors found that highly isotactic PMMA (*mm* > 96 %) with a narrow MWD is produced by the polymerization of MMA in toluene at low temperature with the *t*-butylmagne-

sium bromide prepared in diethyl ether[28]. This is the first example of the living and highly stereoregular polymerization of MMA. The polymerization proceeds without a side reaction, and the number average molecular weight (*Mn*) of the polymer can be easily controlled by the initial amounts of the monomer and initiator. Later, living and highly syndiotactic (*rr* > 90 %) polymerization of methacrylates has been achieved by employing *t*-butyllithium-trialkylaluminum complex[29] and organolanthanide complex[30] as initiator. Now it has become possible to synthesize both highly isotactic and highly syndiotactic PMMAs with controlled molecular weight and MWD.

This dissertation deals with the studies on the mechanism of anionic polymerizations of methacrylates through detailed analyses of the resulting polymers and oligomers. The studies are described in the following four chapters.

Chapter 1 describes the studies on the anionic polymerization of MMA with the aid of deuterated monomer and initiator. When a totally deuterated monomer (MMA-*d*$_8$) is polymerized with an undeuterated initiator, the fragments of the initiator and the terminating reagent incorporated in the polymer chain can be easily detected by ^{1}H NMR spectroscopy without being disturbed by the strong signals due to monomeric units.

The polymer and oligomer of MMA-*d*$_8$ obtained from the polymerization with butyllithium in toluene showed a singlet peak at 2.57 ppm and a triplet at 2.40 ppm[17]. These peaks were assigned to the terminal methine proton and the methylene proton adjacent to the carbonyl group (the α-methylene protons) of BIPK units, respectively. The oligomers (*DP* = 3 - 5) of undeuterated MMA separated by HPLC were found to have a BIPK unit at the terminating end of chain from the consideration of the fragmentation pattern in their mass spectra. The structure was represented as follows:

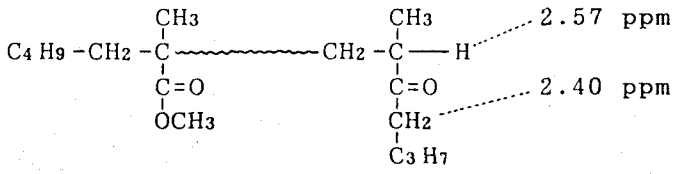

[11]

In the case of the polymer, it was difficult to obtain spectroscopic evidence specifying the location of a BIPK unit in the chain. The BIPK unit was believed to be located near the beginning of the polymer chain in view of the following observations: <i> a lower molecular weight polymer formed in the early stage of polymerization contained one BIPK unit as well as the higher molecular weight polymer formed later, <ii> BIPK monomer could be hardly detected in the reaction mixture even in the early stage of polymerization and thus was considered to be already incorporated in the polymer chain, <iii> the α-methylene protons of BIPK units showed a relatively long spin-lattice relaxation time. Thus, the following structure of the polymer was postulated in the previous paper[16]:

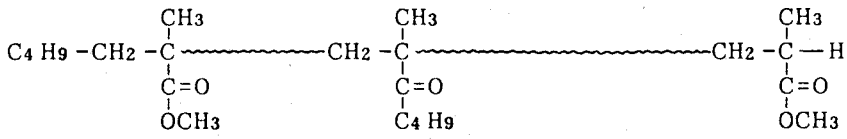

[12]

The present authors[33] extended the studies on the polymerization of MMA using deuterated monomer to the polymerization with Grignard reagent and found that the polymer and oligomer molecule of MMA-*d*8 prepared with butylmagnesium chloride in toluene at -78°C contained BIPK units in a chain as well, although the content per chain was smaller than those prepared with butyllithium. It was also found that the polymer and oligomer molecules of MMA-*d*8 had only 0.3 - 0.4 terminal methine proton which showed the signal at 2.57 ppm. We tried to find a cyclic ketone structure at the chain end [6] using ^{13}C NMR and a model compound but could detect it at most 0.05 per chain. This prompted us to look for another type of terminal methine proton signal; from the ^{1}H NMR analyses of the poly(MMA-*d*8)s prepared with several anionic initiators such as DPHLi, sodium methoxide, and *t*-butylmagnesium bromide, it was confirmed that the NMR signal of the terminal methine proton attached to an MMA unit (MMA-H, *cf.*[12]) does not resonate at 2.57 ppm but at 2.45 ppm[34]. The signal at 2.57 ppm is actually due to the methine proton attached to a BIPK unit (BIPK-H).

The location of the BIPK units in a polymer chain as well as

quantitative determination of the two types of terminal methine protons (MMA-H and BIPK-H) should provide information on the behavior of BIPK in the course of the polymerization reactions initiated with butyllithium and butylmagnesium chloride. However, the signals due to the α-methylene protons of BIPK units overlap with MMA-H signals to make the direct quantitative determination of both methine protons impossible. This problem was solved by adopting butyllithium-1,1-d_2 and butylmagnesium-1,1-d_2 bromide as initiators. The use of the partially deuterated initiators with the aid of a high-field NMR spectrometer (500 MHz) enabled us to determine not only MMA-H and BIPK-H but also the three kinds of initiator fragments *viz.* the butyl group at the α-end (initiating end, or 'left-end') of chain, the BIPK unit in the interior part of chain, and the BIPK unit at the ω-end (terminating end, or 'right-end') of chain. All the polymer molecules formed in THF with butyllithium-1,1-d_2 contained BIPK units at the ω-ends, while the polymer formed in toluene contained the BIPK or MMA terminal unit. Polymer molecules formed in the polymerization with butylmagnesium-1,1-d_2 chloride were either the pure PMMA or the PMMA having one BIPK unit at the ω-end of the chain. The results revealed that the difference of the results of polymerization is due to the difference of the behavior of BIPK in the course of the polymerization reaction.

The clear understanding of the reaction mechanism led us to a highly stereoregular and living polymerization of MMA by anionic mechanism, which is described in Chapter 2. Highly isotactic PMMAs with narrow MWD (Mw/Mn < 1.2) have been prepared by the polymerization of MMA in toluene at -78°C initiated with *t*-butylmagnesium bromide prepared in diethyl ether[28]. The polymerization proceeded in a living manner; the initiation reaction was fast and quantitative, and the propagation was slow.

The ether solution of *t*-butylmagnesium bromide contains an excess amount of $MgBr_2$ which was formed through the side reaction between *t*-C_4H_9MgBr and *t*-C_4H_9Br during the preparation [13].

$$t\text{-}C_4H_9MgBr + t\text{-}C_4H_9Br \longrightarrow (t\text{-}C_4H_9)_2 + MgBr_2 \qquad [13]$$

The excess amount of $MgBr_2$ contributes to form the initiating species of homogeneous activity and stereospecificity because the Schlenk equilibrium [7] shifts to the side of "*t*-C_4H_9MgBr" which produces highly isotactic PMMA. Polymerizations of MMA by *n*-, *iso*- and *s*-C_4H_9MgBr were also investigated in toluene at -78°C. With an increase in the bulkiness of the alkyl group, the isotacticity of the polymer increased and the MWD became narrower. Addition of $MgBr_2$ to the polymerization mixture [14] also enhanced isotacticity of the resultant polymer.

$$C_4H_9Br + BrCH_2CH_2Br + 2\ Mg \longrightarrow C_4H_9MgBr + MgBr_2 + C_2H_4 \qquad [14]$$

The propagating species in the highly isotactic and living polymerization should involve the associated form [15], considering the low solubility of $MgBr_2$. This was also suggested by the fact that the viscosity of the polymerization mixture decreased remarkably when a small amount of methanol was added to quench the living polymer anion.

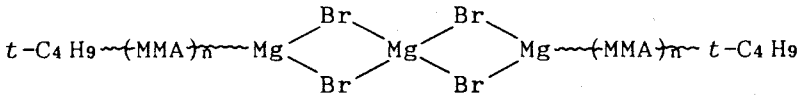

[15]

$$\xrightarrow{2\ CH_3OH} 2\ t\text{-}C_4H_9\sim(MMA)_n\sim H + 2\ CH_3OMgBr + MgBr_2$$

The living polymerization was applied to the syntheses of the highly isotactic block copolymers of methacrylates[31] and of the functional PMMAs containing a polymerizable terminal-group (macromonomers) [16][32]; an additive (*e.g.* DBU: 1,8-diazabicyclo-[5.4.0]undec-7-ene) which solves the association of polymer anions was required to proceed the end-functionalization [16].

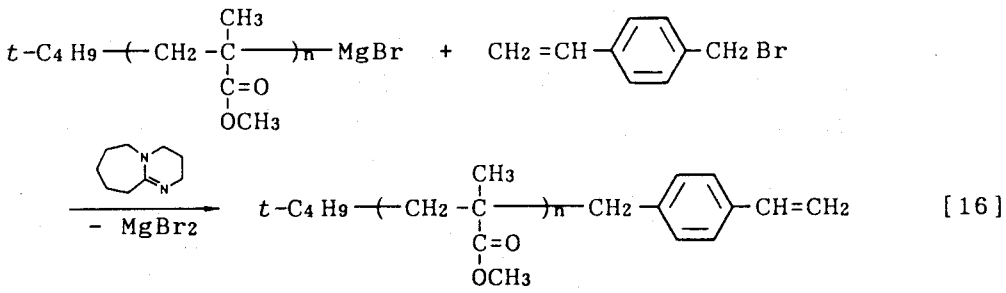

[16]

Detailed analysis of configurational sequences of oligomers or chain ends of polymers elucidates the steric course of propagation reaction. Stereostructure of the chain ends of the highly isotactic PMMA prepared with *t*-C_4H_9MgBr in toluene was investigated extensively by 2D NMR technique[35]. Configurational sequences of the oligomers isolated as reaction products from the early stage of the polymerization were also investigated by HPLC and 2D NMR spectroscopy[36]. The configuration of the α-end of the PMMA was found to be less isotactic ($m/r \approx 10$) than those of the interior monomeric sequences ($m/r > 50$). The relative amount of the four diastereomers in the trimer fraction ($mm+mr$)/($rm+rr$) was 19, also indicating that the addition of MMA to the unimer anion is less isotactic-specific than that to the higher propagating anion. These suggest that the penultimate monomeric unit of the living PMMA anion coordinates to the active sites and contributes the stereoregulation in the highly isotactic polymerization [17]. On the other hand, the m/r ratio at the ω-end showed the addition of methanol (a protonating reagent) to the PMMA anion to be almost non-stereospecific.

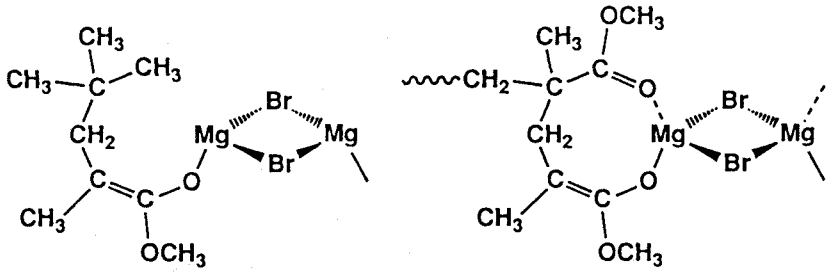

α-End In-chain [17]

The stereoregular living polymerization offers an effective means of preparing the stereoregular oligomers. The purely-isotactic (*it*-) and the purely-syndiotactic (*st*-) oligomers are considered to be good model compounds of stereoregular polymers. Chapter 3 is focused on the structural analysis of the *it*- and the *st*-oligomers of MMA.

The mixtures of MMA oligomers were prepared in toluene with *t*-C_4H_9MgBr and with *t*-C_4H_9Li-$(C_2H_5)_3Al$. The *it*- and *st*-oligomers which are composed exclusively of *meso* (*m*) sequences and

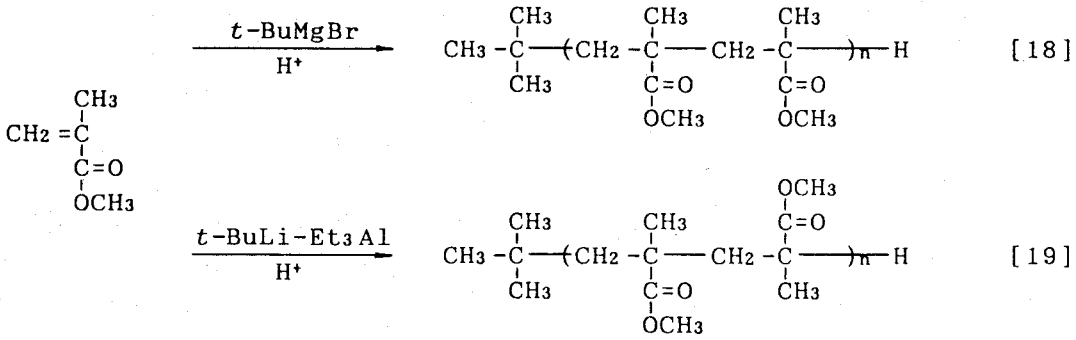

[18]

[19]

exclusively of *racemo* (*r*) sequences, respectively, were isolated from the oligomer mixtures by HPLC[37,38]. Even the octamers, for which 128 diastereomers are theoretically possible, were isolated in the stereochemically pure form (*it*- and *st*-octamers). It should be noted that these polymerization systems give the polymers and oligomers carrying the same terminal groups [18,19]. The assignments for all the ^{1}H and ^{13}C NMR signals of the oligomers were unambiguously made by 2D NMR. The chemical shifts of protons and carbons in the monomeric units of the third and farther positions from the α- and ω-ends were nearly the same as those in the corresponding stereosequences of high molecular weight PMMA.

A trimer of MMA was isolated from the oligomer mixture prepared in toluene with *t*-C_4H_9MgBr, and the molecular structure was determined by single crystal X-ray analysis[37]. The configuration of the trimer was proved to be *meso-meso*, and the conformation in the crystal was *ttg*$^{+}$*tg*$^{+}$ (as *(R,S,R)*-isomer) along the main chain skeletal sequence *t*Bu-CCCCCC-H. However, both the *it*- and *st*-oligomers were found to take the extended all-*trans* conformation in solution, from the observed patterns of the $^{4}J_{HH}$ long-range correlation peaks in the ^{1}H COSY spectra.

Supercritical fluid chromatography (SFC) has been found suitable for the rapid and detailed analysis of the *it*- and *st*-oligomers of MMA, when the temperature gradient technique and the modifier were applied[39]. Oligomer components from trimer to 20-mer separated completely and could be isolated by repeated fractionations. Separation by tacticity as well as by molecular weight was observed for a mixture of the *it*- and *st*-oligomers.

In 1978, Watanabe *et al.*[40] reported the first experiment on direct coupling of liquid chromatography to ^1H NMR using a stopped-flow technique. Recent progress in NMR spectroscopy on its sensitivity and resolution has made it possible to use the spectrometer as a real-time detector for HPLC[41,42]. Chapter 4 describes the on-line GPC/NMR method which has been developed as a novel technique for the characterization of polymers. The usefulness of the on-line GPC/NMR in the studies of polymerization reactions was demonstrated.

Determination of molecular weight by gel-permeation chromatography (GPC) requires a calibration curve, and a set of standard polystyrenes of narrow MWD are usually employed for this purpose. However, preparations of other standard polymers are generally difficult. The *Mn* of the polymer with well-defined structure can be simply determined by on-line GPC/NMR provided that the intensity ratio of the signals due to the monomeric units and the end-groups is measured with good accuracy. On-line GPC/NMR of the isotactic PMMAs prepared by the living polymerization initiated by *t*-C_4H_9MgBr has been performed on a GPC chromatograph linked to a 500 MHz NMR spectrometer[43,44]. ^1H NMR spectra of good resolution and high S/N ratio were collected over the entire chromatographic peak. The *Mn* of the solute PMMA could be directly determined from the intensities of the ^1H NMR signals due to *t*-butyl and methoxy groups because the isotactic PMMAs contains exactly one *t*-butyl group per chain. The *log*(*Mn*) *vs.* elution time plots for the three PMMA samples (*Mn* = 3160, 5260, 12600) have fallen on a single straight line. The results demonstrate the feasibility of the on-line GPC/NMR as an absolute calibration method for GPC.

The anionic polymerization of MMA often involves multiple active species with different reactivities and stereospecificities. Consequently, the resulting polymer has a broad and/or multimodal MWD, and tacticity of the polymer varies with molecular weight. It is essential for the understanding of the nature of active species in these polymerizations to examine the molecular weight dependence of tacticities of PMMA. However, fractionation of polymer is usually laborious and requires considerable amount of the polymer sample. Using the on-line GPC/NMR,

the molecular weight dependence of tacticity of the PMMAs prepared by several anionic initiators such as t-C_4H_9MgBr, n-C_4H_9-MgCl, DPHLi, t-C_4H_9Li and t-C_4H_9Li-(n-C_4H_9)$_3Al$ complex could be elucidated for a short time ($\leq$ 60 min per sample) with a small amount of the sample ($\approx$ 1 mg)[45]. The plots of intensities of the α-methyl proton resonances due to *mm*- and *rr*-triads against elution time clearly showed the variation of tacticity with molecular weight of the PMMA. On the basis of the results, the natures of active species in the polymerizations were discussed. The on-line GPC/NMR method was also useful for the structural analysis of block and random copolymers[46] and of oligomers[47].

References

1. S. Bywater, *Adv. Polym. Sci.*, **4**, 66 (1965).
2. P. Pino, U. W. Suter, *Polymer*, **17**, 977 (1976).
3. H. Yuki, K. Hatada, *Adv. Polym. Sci.*, **31**, 1 (1979).
4. B. L. Erussalimsky, E. Yu. Melenevskaya, V. N. Sgonnik, *Acta Polymerica*, **32**, 183 (1981).
5. P. E. M. Allen, D. R. G. Williams, *Ind. Eng. Chem. Prod. Res. Dev.*, **24**, 334 (1985).
6. K. Hatada, T. Kitayama, K. Ute, *Prog. Polym. Sci.*, **13**, 189 (1988).
7. T. G. Fox, B. S. Garret, W. E. Goode, S. Gratch, J. F. Kincaid, A. Spell, J. D. Stroupe, *J. Am. Chem. Soc.*, **80**, 1768 (1958).
8. R. G. Miller, B. Mills, P. A. Small, A. Turner-Jones, D. G. M. Wood, *Chem. Ind.*, **1958**, 1323.
9. W. E. Goode, F. H. Owens, W. L. Myers, *J. Polym. Sci.*, **47**, 75 (1960).
10. D. L. Glusker, E. Stiles, B. Yoncoskie, *J. Polym. Sci.*, **49**, 297 (1961).
11. B. J. Cottam, D. M. Wiles, S. Bywater, *Can. J. Chem.*, **41**, 1905 (1963).
12. D. M. Wiles, S. Bywater, *Trans. Faraday Soc.*, **61**, 150 (1965).
13. N. Kawabata, T. Tsuruta, *Makromol. Chem.*, **86**, 231 (1965).
14. S. Bywater, *Adv. Polym. Sci.*, **4**, 66 (1965).
15. K. Hatada, T. Kitayama, K. Fujikawa, K. Ohta, H. Yuki, *Polym. Bull.*, **1**, 103 (1978).
16. K. Hatada, T. Kitayama, S. Okahata, H. Yuki, *Polym. J.*, **13**, 1045 (1981).
17. K. Hatada, T. Kitayama, K. Fujikawa, K. Ohta, H. Yuki, *ACS Symp. Ser.*, **166**, 327 (1981).
18. L. Lochmann, S. Pokorny, J. Trekoval, H.-J. Adler, W. Berger, *Makromol. Chem.*, **184**, 2021 (1983).
19. A. H. E. Muller, L. Lochmann, J. Trekoval, *Makromol. Chem.*, **187**, 1473 (1986).
20. D. F. Evans, G. V. Fazakerley, *J. Chem. Soc.*, **A**, 184 (1971).

21. I. Ando, R. Chujo, A. Nishioka, *Polym. J.*, 1, 609 (1970).
22. K. Matsuzaki, H. Tanaka, T. Kanai, *Makromol. Chem.*, **182**, 2905 (1981).
23. B. O. Bateup, P. E. M. Allen, *Eur. Polym. J.*, **13**, 761 (1977).
24. P. E. M. Allen, B. O. Bateup, *Eur. Polym. J.*, **14**, 1001 (1978).
25. B. C. Anderson, G. D. Andrews, P. Arthur, Jr., H. W. Jacobson, A. J. Playtis, W. H. Sharkey, *Macromolecules*, **14**, 1599 (1981).
26. P. Lutz, P. Masson, G. Beinert, P. Rempp, *Polym. Bull.*, **12**, 79 (1984).
27. O. W. Webster, W. R. Hertler, D. Y. Sogah, W. B. Farnham, T. V. Rajanbabu, *J. Am. Chem. Soc.*, **105**, 5706 (1983).
28. K. Hatada, K. Ute, K. Tanaka, T. Kitayama, Y. Okamoto, *Polym. J.*, **17**, 977 (1985); **18**, 1037 (1986).
29. T. Kitayama, T. Shinozaki, E. Masuda, M. Yamamoto, K. Hatada, *Polym. Bull.*, **20**, 505 (1988); *Makromol. Chem. Suppl.*, **15**, 167 (1989).
30. H. Yasuda, H. Yamamoto, K. Yokota, A. Nakamura, S. Miyake, *Polym. Prepr. Jpn.*, **39**, 1602 (1990).
31. T. Kitayama, K. Ute, M. Yamamoto, N. Fujimoto, K. Hatada, *Polym. J.*, **22**, 386 (1990).
32. K. Hatada, T. Kitayama, K. Ute, E. Masuda, T. Shinozaki, M. Yamamoto, *Polym. Bull.*, **21**, 165 (1989).
33. K. Ute, T. Kitayama, K. Hatada, *Polym. J.*, **18**, 249 (1986).
34. T. Kitayama, K. Ute, K. Hatada, *Polym. J.*, **16**, 925 (1984).
35. K. Hatada, K. Ute, K. Tanaka, M. Imanari, N. Fujii, *Polym. J.*, **19**, 425 (1987).
36. K. Hatada, K. Ute, K. Tanaka, T. Kitayama, *Polym. J.*, **19**, 1325 (1987).
37. K. Ute, T. Nishimura, Y. Matsuura, K. Hatada, *Polym. J.*, **21**, 231 (1989).
38. K. Ute, T. Nishimura, and K. Hatada, *Polym. J.*, **21**, 1027 (1989).
39. K. Hatada, K. Ute, T. Nishimura, M. Kashiyama, T. Saito, M. Takeuchi, *Polym. Bull.*, **23**, 157 (1990).
40. N. Watanabe, E. Niki, *Proc. Jpn. Acad.*, **54**, 194 (1978).
41. H. C. Dorn, *Anal. Chem.*, **56**, 747A (1984).
42. D. A. Laude Jr., C. L. Wilkins, *Trends Anal. Chem.*, **5**, 230 (1986).
43. K. Hatada, K. Ute, Y. Okamoto, M. Imanari, N. Fujii, *Polym. Bull.*, **20**, 317 (1988).
44. K. Hatada, K. Ute, M. Kashiyama, M. Imanari, *Polym. J.*, **22**, 218 (1990).
45. K. Hatada, K. Ute, T. Kitayama, T. Nishimura, M. Kashiyama, N. Fujimoto, *Polym. Bull.*, **22**, 549 (1990).
46. K. Hatada, K. Ute, T. Kitayama, M. Yamamoto, T. Nishimura, M. Kashiyama, *Polym. Bull.*, **21**, 489 (1989).
47. K. Ute, M. Kashiyama, K. Oka, K. Hatada, O. Vogl, *Makromol. Chem., Rapid Commun.*, **11**, 31 (1990).

CHAPTER 1

Studies on the Anionic Polymerizations of Methyl Methacrylate Using Totally Deuterated Monomer and Undeuterated or Partially Deuterated Initiator

1.1 Introduction

Many papers have been published on the polymerization of methacrylates by organomagnesium compounds since Goode[1] and Nishioka[2] reported the polymerization of MMA by Grignard reagents in 1960. In several review articles[3-5], the polymerizations of methacrylates by organomagnesium compounds have been compiled. However, there still exist some ambiguities regarding the polymerization, particularly in the structure of the polymer, efficiency of initiator, and mechanism of polymerization. The complexity of the factors affecting the polymerization has prevented a clear understanding of this polymerization reaction, and the molecular weight and its distribution of the polymer cannot be fully controlled.

Several studies dealt with the effects of temperature and amount of THF or MgX_2 on the stereoregularity and molecular weight of the resulting polymer[6-8]. Allen and his coworkers[9] studied the mechanism of polymerization of MMA with butylmagnesium compounds in toluene-THF mixtures mainly by kinetic methods.

Chemical analysis of the reaction products is another approach to the mechanism of polymerization. Goode and his coworkers[10] studied the initiation and the termination processes in the polymerization of MMA by tritium-labeled phenylmagnesium bromide through a detailed analysis of the low molecular products of polymerization. Yasuda and his coworkers[11] investigated the elementary steps of the polymerization reaction by butylmagnesium bromide. Bateup and Allen[12] determined the amounts of the unreacted initiator and CH_3OMg^- formed during the polymerization of MMA by butylmagnesium bromide in toluene-THF mixtures.

Hatada *et al.* have developed a new method for understanding the mechanism of polymerization using totally deuterated mono-

mers[13-18]. When a deuterated monomer is polymerized by an undeuterated initiator, the fragments of the initiator and/or the terminating reagent incorporated in the polymer or oligomer chain can be detected by ^{1}H NMR spectroscopy without disturbance from the signals due to monomeric units in the chain. In this chapter, the present authors applied this method to the polymerizations of MMA by Grignard reagents to elucidate the structures of the polymerization products and the fate of the initiator during the polymerization. The studies on the polymerization of MMA with alkyllithium were extended by adopting partially deuterated initiators and high-field NMR.

1.2 Structures of the PMMAs Prepared with Butylmagnesium Chloride and with Several Other Anionic Initiators[19]

1.2.1 Structures of the MMA- and Ketone-Ended Polymer and Oligomer Molecules

Polymerizations of MMA and MMA-*d*8 with *n*-C_4H_9MgCl were carried out in toluene at -78°C for 72 h. The results are given in Table 1. The polymerizations of MMA-*d*8 were terminated by quenching the reaction mixtures with CH_3OH (denoted as D/h) or with CD_3OD (D/d), respectively. The polymerization of MMA was quenched with CH_3OH (H/h). The results of these three polymerizations were similar in yield and in molecular weight of the products. In all the polymerizations, the reaction products contained about 70 % methanol-insoluble polymer and about 30 % methanol-soluble oligomer.

Figure 1 shows ^{1}H NMR spectra of the polymer and oligomer of MMA-*d*8 (Polymer-D/h and Oligomer-D/h in Table 1). The signals at 0.8 ppm and at 1.1 ppm were assigned to the methyl and methylene protons of butyl groups, respectively, which originally came from the initiator. The triplet at 2.40 ppm is attributed to the carbonyl methylene protons of butyl pentadeuteroisopropenyl ketone (BIPK-*d*5) units incorporated into the polymer or oligomer chain[15]. BIPK-*d*5 should be formed through attack of the initiator on the carbonyl group of the monomer.

Table 1. Polymerization of MMA and MMA-*d*8 with C_4H_9MgCl in toluene at -78°C for 72 h[a]

Entry	Monomer	(mmol)	Terminating reagent	Polymer[b] Yield (%)	Polymer[b] *Mn*	Oligomer[c] Yield (%)	Oligomer[c] *Mn*
D/h	MMA-*d*8	5.39	CH_3OH	70.3	12000	29.4	989
D/d	MMA-*d*8	5.45	CD_3OD	71.0	13500	28.2	940
H/h	MMA	5.02	CH_3OH	67.1	10200[d]	30.0	940

[a] Toluene 5.0 ml, C_4H_9MgCl 0.518 mmol.
[b] Methanol-insoluble part. [c] Methanol-soluble part.
[d] Triad tacticity, *mm/mr/rr* = 31/18/51.

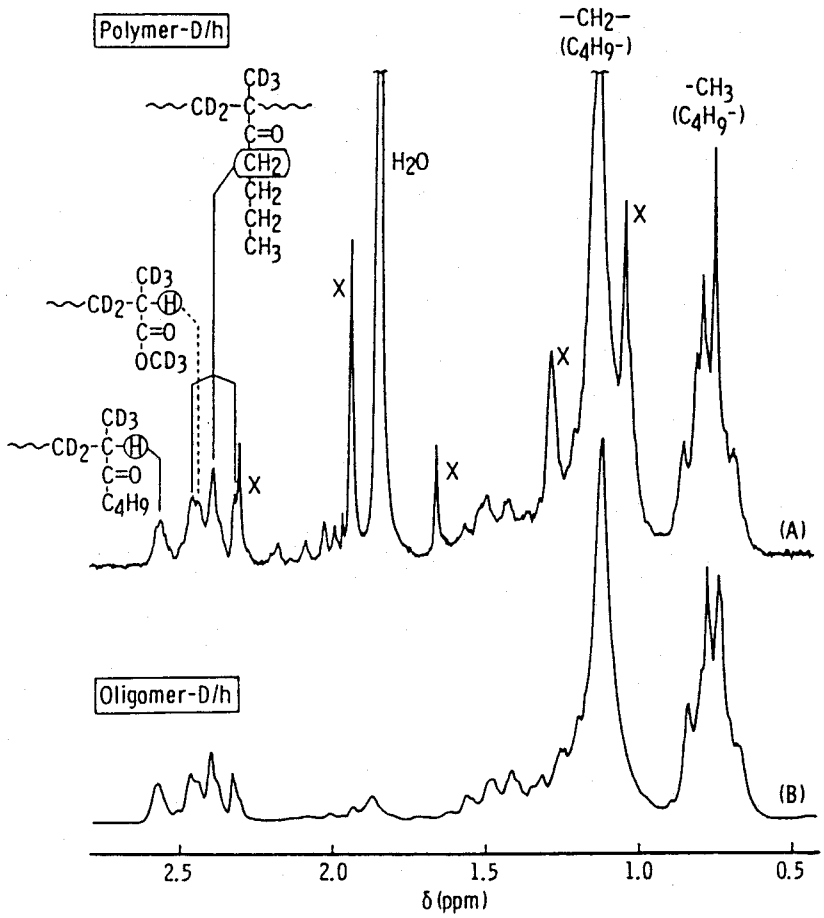

Figure 1. ^1H NMR spectra of the polymer and oligomer of MMA-*d*8 prepared with C_4H_9MgCl in toluene at -78°C. The signals labeled "X" are due to the remaining protons in the monomeric units. (Nitrobenzene-*d*5, 110°C)

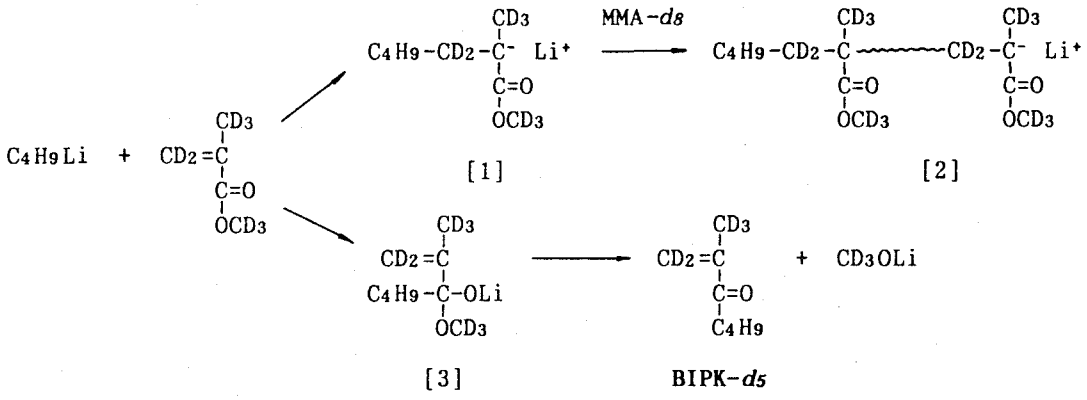

[1] [2] [3] BIPK-*d*5

The presence of the ketone unit in the chain was also evidenced by the thermal decomposition of the polymer or oligomer followed by gas chromatographic analysis.

The singlets at 2.45 and 2.57 ppm were assigned to the methine protons introduced into the ω-ends (terminating ends) from the terminating reagent (CH_3OH). The former, though it overlaps with the triplet at 2.40 ppm, is assigned to the methine proton in the terminal MMA unit. The latter is attributed to the methine proton attached to the BIPK-*d*5 unit located at the ω-end[18]. The abbreviations "MMA-H" and "BIPK-H" are used hereinafter to denote these terminal methine protons.

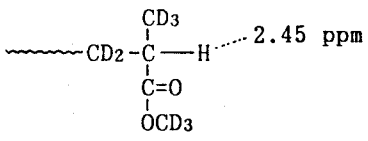

[4] MMA-H

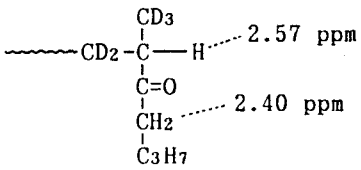

[5] BIPK-H

To confirm these assignments, ^1H NMR spectra of the poly(MMA-*d*8)s obtained by several kinds of initiators were inspected as shown in Figure 2. The polymer obtained by CH_3ONa must contain no ketone unit even if carbonyl addition occurs, and all the terminal methine proton should be MMA-H (*cf.* Figure 2D). In the polymerization by 1,1-diphenylhexyllithium (*cf.* Figure 2B) or *t*-C_4H_9MgBr (*cf.* Figure 2C), the initiator hardly attacks the carbonyl group of MMA and the reaction is living[20-23]. The poly(MMA-*d*8)s obtained by these three initiators showed a rather

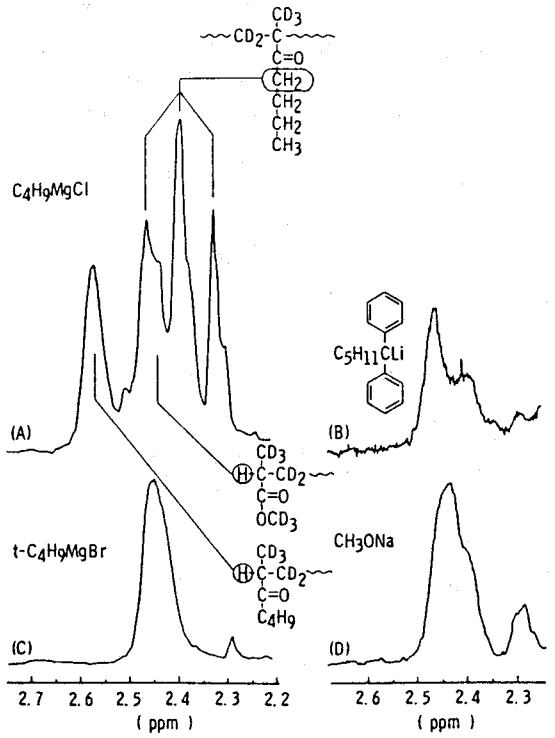

Figure 2. ^{1}H NMR spectra of polymers prepared by C_4H_9MgCl in toluene at -78°C (A), 1,1-diphenylhexyllithium in THF at -78°C (B), t-C_4H_9MgBr in toluene at -78°C (C), and CH_3ONa in diethyl ether at 50°C (D).

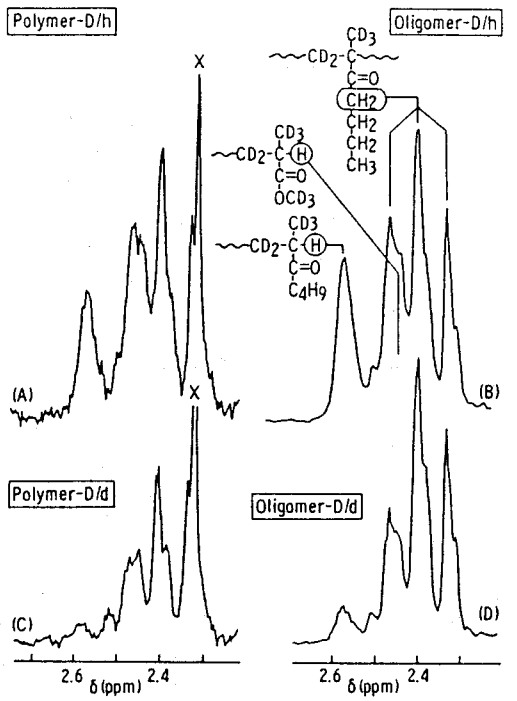

Figure 3. ^{1}H NMR spectra of the polymer and oligomer of MMA-d_8 formed in the polymerization by C_4H_9MgCl terminated with CH_3OH (A), (B), or CD_3OD (C), (D). X, signals due to the remaining protons in the monomer units.

Table 2. ^{1}H NMR signal intensities for the polymer and oligomer of MMA-d_8 prepared with C_4H_9MgCl in toluene at -78°C

Sample	Amount (10^{-3} g-hydrogen/g-sample)		
	CH_3	$-CH_2CO-$ (BIPK) + MMA-H	BIPK-H
Polymer-D/h	0.3214	0.0898	0.0214
Polymer-D/d	0.2897	0.0491	0.0034
Oligomer-D/h	4.949[a]	1.280	0.359
Oligomer-D/d	4.814[a]	0.896	0.065

[a] Ten percent of these values are due to the butyl group of dibutylisopropenylcarbinol included in the oligomer.

broad signal at about 2.45 ppm, but not at 2.57 ppm (Figures 2B, 2C, and 2D). Thus, the signal at about 2.45 ppm should be assigned to MMA-H, and the one at 2.57 ppm to BIPK-H.

The content of the two types of terminal methine protons and the initiator fragments in the polymer and oligomer obtained by *n*-C_4H_9MgCl was determined by the following procedure. Figure 3 shows the carbonyl methylene and terminal methine proton region spectra of the polymers and the oligomers of MMA-*d*$_8$ obtained in the CH_3OH- and CD_3OD-terminated polymerizations by *n*-C_4H_9MgCl (*cf.* Table 1). When the polymerization mixture was quenched by CD_3OD instead of CH_3OH, the signal at 2.57 ppm almost disappeared, and the intensities of signals around 2.4 ppm decreased to some extent (Figures 3C, and 3D), reflecting termination by deuterium.

The signal at 2.40 ppm in the spectra of Polymer-D/d and Oligomer-D/d is due only to the carbonyl methylene protons of BIPK-*d*$_5$ units. Table 2 summarizes the ^1H NMR signal intensities for methyl protons of butyl groups (0.8 ppm), carbonyl methylene protons in BIPK-*d*$_5$ units combined with MMA-H (2.4 ppm), and BIPK-H (2.57 ppm); the intensities are expressed in terms of the hydrogen content per gram of a polymer or oligomer sample. Then, the difference in the signal intensity at 2.45 ppm between Polymer-D/h and Polymer-D/d or Oligomer-D/h and Oligomer-D/d should correspond to the amount of MMA-H.

From the data in Tables 1 and 2, the numbers per chain of BIPK-H, MMA-H, and BIPK-*d*$_5$ units, and C_4H_9- groups at the α-end (initiating end) was calculated. Both the polymer and oligomer molecules contain one butyl group at the α-end. The polymer molecule has 0.3 BIPK-*d*$_5$ unit and the same amount of BIPK-H. The oligomer has 0.4 BIPK-H unit and also the same amount of BIPK-H. These values indicate that almost all the BIPK unit is located at the ω-end of the chain.

In order to obtain additional evidence for the location of the ketone unit in the chain, the heptane-soluble fraction of undeuterated MMA oligomer prepared under the same conditions were fractionated by GPC (Figure 4), and fractions from the dimer to heptamer were collected. It was found by NMR and mass spectroscopies that all these fractions contained two types of oligomers,

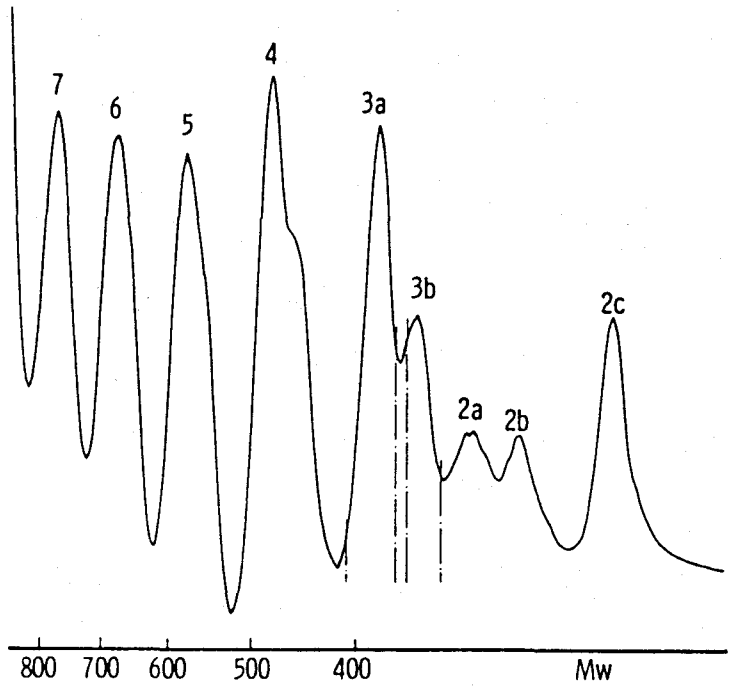

Figure 4. GPC curve of the heptane-soluble fraction of the MMA oligomer prepared with C_4H_9MgCl in toluene at -78°C.

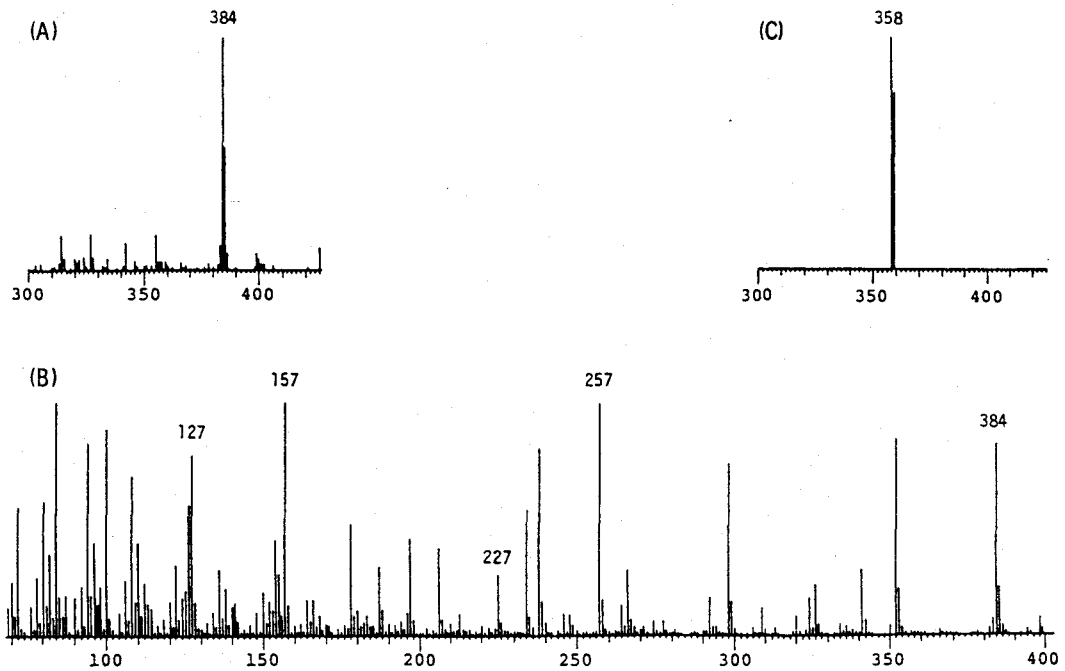

Figure 5. FD- and EI-mass spectra of the trimes ended with a BIPK unit (A), (B) and with an MMA unit (C) prepared with C_4H_9MgCl in toluene at -78°C.

which contain one ketone unit at the ω-end but none in the chain, respectively.

Figure 5 shows the FD- and the EI-mass spectra of the trimers. The FD-spectrum (Figure 5A) indicates that fraction 3a is the trimer containing one ketone unit in the chain, and the EI-spectrum (Figure 5B) indicates the presence of the ketone unit at the ω-end. Peaks at (M^+/Z) = 384, 257, 227, 157 and 127 correspond to the fragments shown below.

M^+/Z	Fragments
384	$[C_4H_9$-(MMA)-(MMA)-(BIPK)-H$]^+$
257	$[C_4H_9$-(MMA)-(MMA)$]^+$
227	[(MMA)-(BIPK)-H$]^+$
157	$[C_4H_9$-(MMA)$]^+$
127	[(BIPK)-H$]^+$

No fragments which would come from the trimer C_4H_9-(MMA)-(BIPK)-(MMA)-H or C_4H_9-(BIPK)-(MMA)-(MMA)-H were observed in the spectrum.

M^+/Z	Fragments
283	$[C_4H_9$-(MMA)-(BIPK)$]^+$
183	$[C_4H_9$-(BIPK)$]^+$

Figure 5C is the FD-mass spectrum of fraction 3b. The spectrum indicates that the fraction is the MMA trimer without a ketone unit in the chain. Similar results were obtained on the tetramer, pentamer, hexamer and heptamer. The results clearly indicate that there are two types of oligomers ending with MMA and BIPK units, respectively.

1.2.2 Cyclic Ketone and Other Structures at the Chain Ends

So long as we consider that the polymer and oligomer molecules have linear and non-branched chain structures, each molecule should have one α-end and one ω-end. However, the sum of

MMA-H and BIPK-H per polymer or oligomer molecule shown in Table 3 does not amount to unity, and this suggests the presence of other types of structure at the ω-end of the chain.

Goode *et al.*[10] reported that the principal mode of termination in the polymerization of MMA by phenylmagnesium bromide in toluene at 0°C is intramoleculer cyclization to yield a cyclic ketone at the chain end [6].

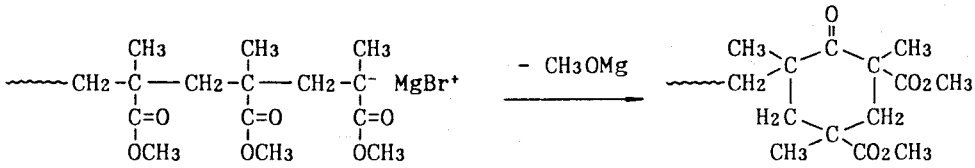

[6]

We carried out the cyclization reaction of a living PMMA anion, and studied the structure of the resulting cyclic ketone unit by ^{13}C NMR spectroscopy (*cf.* Section 1.4). The cyclic ketone unit at the ω-end of PMMA exhibited characteristic ^{13}C NMR signals at 173.3 - 173.9 ppm and 177.5 - 178.5 ppm for ester carbonyl carbons, and at 211 - 212 ppm for ketone carbonyl carbons. These signals were found to be sensitive to the stereostructure of the ketone ring. As shown in Figure 6, Oligomer-H/h shows the characteristic signals of ester carbonyl carbons of cyclic ketone terminal at 173.3 ppm and 173.6 ppm. Intensity measurements indicated that about 5 % of the oligomer contained the cyclic ketone terminal at the chain end.

In order to find out other structures at the ω-ends, ^{1}H NMR spectra of the oligomers were examined in detail. In the ^{1}H NMR spectrum of Oligomer-H/h, three weak multiplets were observed at 4.87, 4.97 and 5.08 ppm (Figure 7A). It was expected that dibutylisopropenylcarbinol was formed by the reaction of BIPK and the initiator and contained in the oligomer [7].

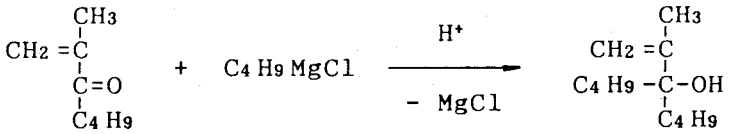

[7]

The authentic sample for this alcohol showed a pair of signals at 4.87 and 4.97 ppm due to the vinyl protons, and the signal due to the methyl protons of the isopropenyl group at 1.69 ppm. As shown in Figure 7B, the signals in the vinyl proton region of the

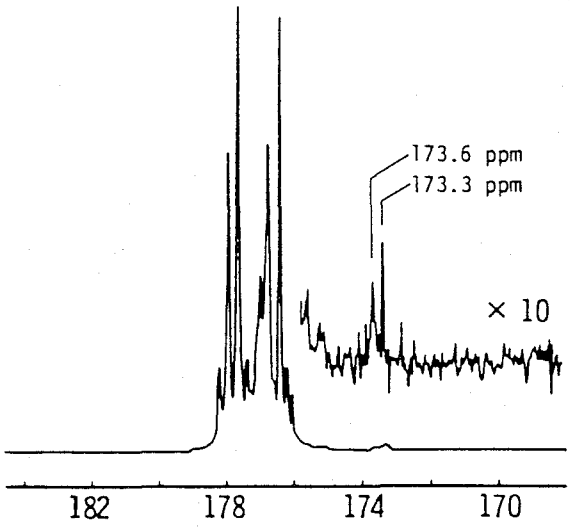

Figure 6. ^{13}C NMR spectrum of the oligo(MMA) prepared with C_4H_9MgCl in toluene at -78°C for 72 h (Oligomer-H/h).

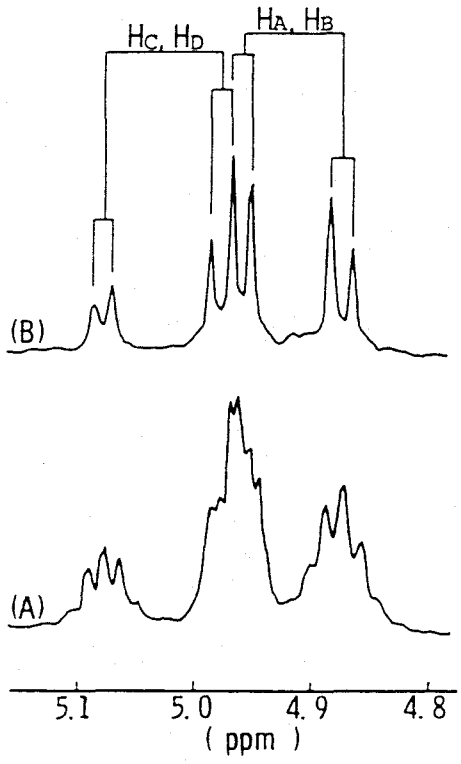

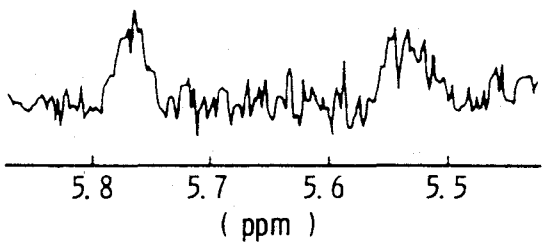

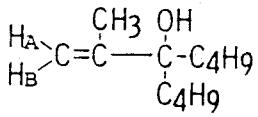

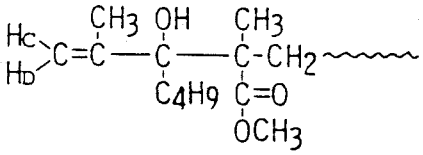

Figure 7. ^{1}H NMR spectra of vinyl protons in Oligomer-H/h. (A) Normal measurement, (B) decoupled (irradiated at 1.7 ppm).

Figure 8. ^{1}H NMR spectrum of vinyl protons in Oligomer-H/h.

oligomer changed into two pairs of typical AB quartets when irradiated around 1.7 ppm the region for the signal of the methyl protons of the isopropenyl group. The quartets at 4.87 and 4.97 ppm were assigned to the vinyl protons of dibutylisopropenylcarbinol included in the oligomer. The other quartets at 4.97 and 5.08 ppm should be due to a similar isopropenyl compound because of the similarities of the chemical shifts. The spin-lattice relaxation time, T_1, for the signal at 5.08 ppm was 2.3 s, which was significantly shorter than that for the signal at 4.87 ppm (4.4 s). The results enabled us to assign the quartets at 4.97 and 5.08 ppm to the tertiary alcoholic ω-end formed through the addition of the propagating chain end onto the carbonyl group of BIPK [8].

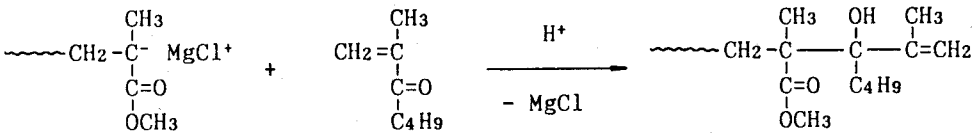

[8]

The intensity measurement indicated that about 4 % of the oligomer molecules contained this type of ω-end.

When the propagating anion attacks the carbonyl group of MMA monomer, another structure of the ω-end [9] is produced[24].

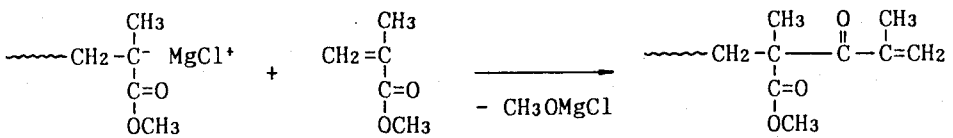

[9]

A pair of weak signals at 5.53 and 5.77 ppm whose T_1 was about 1.0 s was considered to be due to this structure (Figure 8). However, the content was estimated to be at most 0.01 per chain.

Table 3 summarizes the structures of the ω-ends of polymer and oligomer described above. The structures of chain ends of about 90 % oligomer molecules were clarified. The cyclic ketone terminal [6], tertiary alcoholic terminal [8] and linear ketone terminal [9] may also exist in polymer molecules, but they have not been detected probably owing to the lower intensities of the NMR signals.

Table 3. Structure of the ω-ends of the polymerization products of MMA prepared with C_4H_9MgCl in toluene at -78°C for 72 h

	Oligomer	Polymer
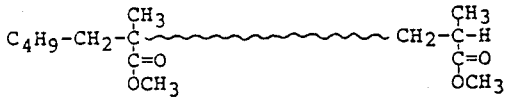	40%	40%
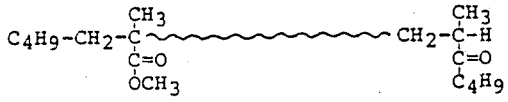	40%	30%
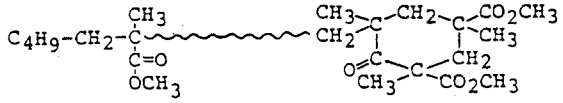	5%	—
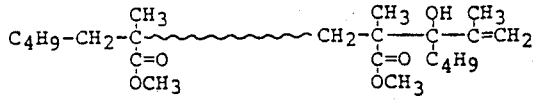	4%	—
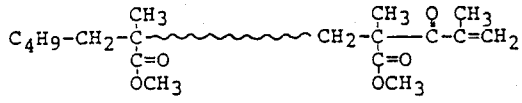	1%	—

Table 4. Fate of initiator fragments in the polymerization of MMA in toluene at -78°C for 72 h (percentage based on C_4H_9MgCl used)

C_4H_9Mg-	(Unreacted)	18
$CH_2=C(CH_3)-COC_4H_9$	(Unreacted)	8
$CH_2=C(CH_3)-C(OH)(C_4H_9)_2$		6
$C_4H_9-CH_2-C(CH_3)(CO_2CH_3)-\sim$	(Polymer)[a]	7
	(Oligomer)[a]	33
$\sim CH_2-C(CH_3)(COC_4H_9)-H$	(Polymer)[a]	2
	(Oligomer)[a]	16
$\sim C(OH)(C_4H_9)-C(CH_3)=CH_2$	(Polymer)	—
	(Oligomer)	1
	Total	91%

[a] Data refer to the polymerization of MMA-d_8.

1.2.3 Fate of the Initiator in the Polymerization

It is well known that in the polymerization of methacrylates by Grignard reagent, all the initiator used cannot be accounted for if each polymer or oligomer molecule is assumed to contain one initiator fragment. In this study, we have found that some of the polymer or oligomer molecules contained two initiator fragments, one at the α-end and the other at the ω-end as a ketone unit. The sum total of the butyl groups in the polymer and oligomer molecules was 60 % of the initiator used (Table 4). About 20 % of the initiator remained unreacted during the polymerization and was recovered as butane when the polymerization was terminated. Bateup and Allen[12] observed similar amounts of unreacted *n*-C_4H_9MgBr in the polymerization in toluene-THF mixtures. They suggest that the unreacted C_4H_9Mg- species coordinate with the active center affecting the stereoregulation. The C_4H_9- groups in unreacted BIPK and dibutylisopropenylcarbinol corresponded to 8 and 6 % of the C_4H_9MgCl used, respectively. Thus, most of the initiator fragments are now accounted for (Table 4).

1.3 Polymerizations of MMA-*d*$_8$ with Butyllithium-1,1-*d*$_2$ and Butylmagnesium-1,1-*d*$_2$ Chloride[25]

Studies on the polymers of MMA-*d*$_8$ prepared with undeuterated butyllithium[13-17] or butylmagnesium chloride[19] by 100 MHz ^1H NMR analyses permitted us to determine the amounts and structures of the initiator fragments such as the butyl group of BIPK units in a polymer chain. The location of BIPK units in a polymer chain should provide information on the behavior of BIPK in the course of polymerization reaction. As described in the previous section, NMR chemical shifts of the two types of terminal methine protons MMA-H and BIPK-H were confirmed for the poly(MMA-*d*$_8$) samples prepared with several anionic initiators. Quantitative determination of these two protons in the poly(MMA-*d*$_8$) would allow estimation of the amount of each terminal unit. However, the signals due to the α-methylene protons of BIPK units overlap

with MMA-H signals to make the direct quantitative determination of both methine protons impossible. In this section, the problem was solved by employing butyllithium-1,1-*d*2 ($C_3H_7CD_2Li$) and butylmagnesium-1,1-*d*2 ($C_3H_7CD_2MgCl$) as initiators. The use of these partially deuterated initiators with the aid of a high-field NMR spectrometer (500 MHz) enabled us to determine not only MMA-H and BIPK-H but also the three kinds of initiator fragments *viz.* the butyl group at the α-end of chain, the BIPK unit in the inner part of chain, and the BIPK unit at the ω-end of chain.

1.3.1 Polymerization of MMA-d8 with $C_3H_7CD_2Li$ in THF

Polymerization of MMA-*d*8 was carried out with $C_3H_7CD_2Li$ in THF at -78°C. The results are summarized in Table 5. The polymerization product was separated into three fractions: (A) the methanol-insoluble part; (B) the hexane-insoluble (and methanol-soluble) part; (C) the hexane-soluble part. The total yield was quantitative. *Mn* of the methanol-insoluble part was 4.76 x 10^4 by VPO, and the molecular weight distribution was broad (*Mw/Mn* = 3.20). The hexane-insoluble part had much lower *Mn*.

Figures 9a and 9b show ^1H NMR spectra of the hexane-insoluble part and the methanol-insoluble part, respectively. There appeared the signals due to the $C_3H_7CD_2$- groups incorporated in the polymer chain and the signal due to the methine proton at the ω-end of chain. The broad singlet at 2.58 ppm including small satellite signals can be assigned to BIPK-H[18,19]. In the spectral region from 2.40 ppm to 2.50 ppm, where the signals of MMA-H would appear (*cf.* Figure 11), no signal was observed for both the hexane-insoluble and the methanol-insoluble polymers. Hatada *et al.*[14] postulated that the methanol-insoluble part of the poly(MMA-*d*8) prepared with butyllithium in THF has the following chain structure:

$$C_4H_9\text{---}(\text{MMA})\text{---}[\text{-BIPK---(MMA)---}]_n\text{---MMA-H} \qquad [10]$$

The present result indicates that the poly(MMA-*d*8) molecule contains no MMA-H but BIPK-H at the ω-end of the chain.

$$C_3H_7CD_2\text{---}(\text{MMA})\text{---}[\text{-BIPK---(MMA)---}]_n\text{---BIPK-H} \qquad [11]$$

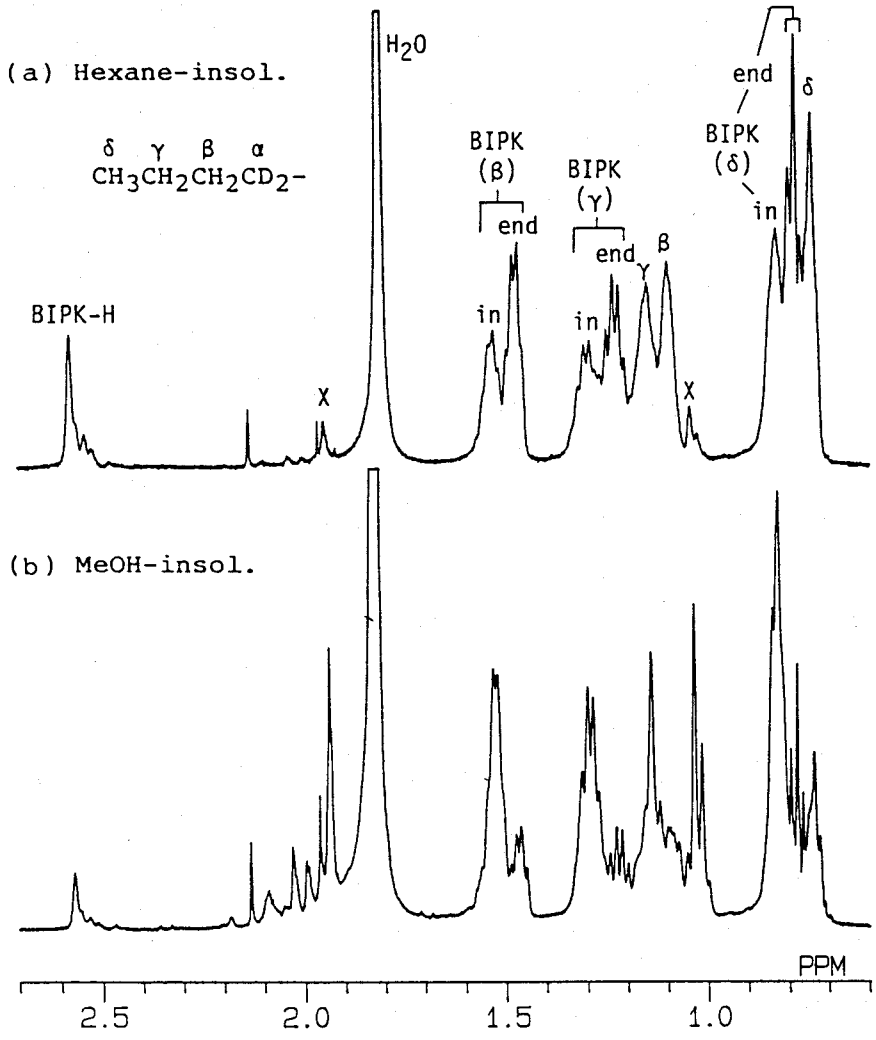

Figure 9. 500 MHz ^{1}H NMR spectra of the poly(MMA-*d*$_8$) prepared with $C_3H_7CD_2Li$ in THF at -78°C. (a) Methanol-soluble and hexane-insoluble part, (b) methanol-insoluble part. (Nitrobenzene-*d*$_5$, 110°C)
X: Signals due to the remaining protons in the monomeric unit.

Table 5. Analysis of $C_3H_7CD_2$- groups incorporated in the poly(MMA-*d*8) prepared with $C_3H_7CD_2Li$ in THF at -78°C[a] —— Contents of the initiator fragments and of the terminal methine proton (BIPK-H)[b] per chain

	Yield		*Mn*[c]	$C_3H_7CD_2$- total amount	Content per chain / mol/mol			
					$C_3H_7CD_2$-	BIPK unit		BIPK-H
	g	%	10^3	mmol	α-end[d]	interior	ω-end	
MeOH-insol	0.915	74.5	47.6[e]	0.104	1.019	3.359	1.042	0.898
hexane-insol	0.239	19.4	4.08	0.165	1.045	0.741	1.037	0.886
hexane-sol	0.073	6.6	-	0.230				
Total	1.227	100.5		0.499				

[a] MMA-*d*8 11.1 mmol, $C_3H_7CD_2Li$ 0.50 mmol, THF 10.0 ml, polymerization 24 h.

[b] There was no MMA-H detected.

[c] Determined by VPO.

[d] The amount of $C_3H_7CD_2$- group at the α-end of chain was calculated as $c(\delta_t/3 - \beta_k/2)/(\delta_t/3)$, where c, δ_t and β_k are the total amount of $C_3H_7CD_2$- group per chain, the intensity of all the δ-methyl resonances, and the intensity of combined β-methylene resonances due to BIPK units, respectively.

[e] *Mw/Mn* = 3.20 by GPC.

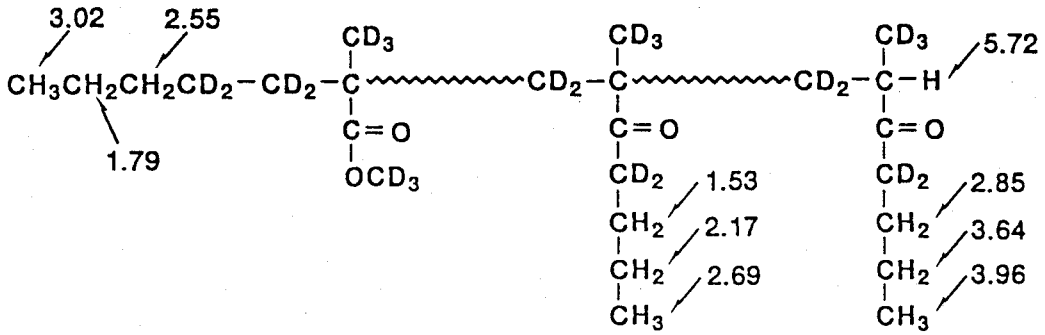

Figure 10. Spin-lattice relaxation times (T_1) for the methyl and methylene protons in the $C_3H_7CD_2$- group incorporated in the poly(MMA-*d*8) (hexane-insoluble part) prepared with $C_3H_7CD_2Li$ in THF at -78°C. (500 MHz, in nitrobenzene-*d*5 at 110°C)

The fact has been hardly revealed without introducing deuterium at the α-position of the butyl group in BIPK units.

Two broad quartets of different intensities resonating at 1.476 and 1.532 ppm are both assigned to the β-methylene protons of the $C_3H_7CD_2$- group in butyl-d_2 isopropenyl-d_5 ketone (BIPK-d_7) units. T_1 value for the former resonance was determined as 2.85 s and was about twice as large as that for the latter (1.53 s), indicating that the former is due to the BIPK unit at the chain end and the latter to those in inner part of the chain (Figure 10). The β-methylene resonance at 1.476 ppm showed correlation peaks with the γ-methylene resonance at 1.231 ppm in ^{1}H COSY, and the γ-methylene resonance with the δ-methyl resonance at 0.788 ppm (triplet). Similarly, β-methylene protons at 1.532 ppm showed connectivity to the γ-methylene protons at 1.302 ppm, and the γ-methylene protons to the δ-methyl protons at 0.832 ppm (broad singlet). The signals at 0.745, 1.102, and 1.153 ppm are attributable to the methyl and methylene protons of the $C_3H_7CD_2$- group at the α-end of chain, according to the ^{1}H COSY. Thus the 500 MHz ^{1}H NMR analysis made it possible to distinguish the three kinds of $C_3H_7CD_2$- fragments incorporated in the poly(MMA-d_8) chain. The T_1 values for the methyl and methylene protons were consistent with the segmental mobility of the three $C_3H_7CD_2$- fragments (Figure 10); the $C_3H_7CD_2$- group in the inner BIPK units should be less mobile than the $C_3H_7CD_2$- groups at the chain ends.

Table 5 provides the contents of the three kinds of $C_3H_7CD_2$- groups and of BIPK-H per chain for the methanol-insoluble and the hexane-insoluble fractions along with the *Mn*'s of the fractions. Both fractions contained one $C_3H_7CD_2$- group at the α-end of chain, and the values should be regarded as an index of accuracy of the present determinations. Both fractions also had one BIPK unit and nearly one BIPK-H at their ω-end of chain. The hexane-insoluble polymer contained totally 1.8 BIPK units per chain, whereas the methanol-insoluble one contained 4.4 BIPK units. The *Mn* of the methanol-insoluble fraction is about 12 times as large as that of the hexane-insoluble fraction while the content of BIPK in the former fraction is only about 2 times as large as that in the latter. This suggests that the methanol-insoluble

polymer has more BIPK units in the former (the α-end side) part of the chain than in the latter part (the ω-end side) as shown in the formula [12].

$C_3H_7CD_2$-(MMA)-BIPK-(MMA)-BIPK-(MMA)-BIPK-(MMA)-BIPK-H [12]

The total amount of $C_3H_7CD_2$- groups in each fraction was determined from the intensity of the ^{1}H NMR resonances due to δ-methyl protons as shown in Table 5. The results completely accounted for a material balance of the initiator used.

1.3.2 Polymerization of MMA-d8 with $C_3H_7CD_2Li$ in Toluene

Polymerizations of MMA-*d8* with $C_3H_7CD_2Li$ in toluene were carried out at -78°C for 24 h, changing the initial monomer/initiator ratio, $[M]_0/[I]_0$, from 10.7 to 41.1 mol/mol (Table 6). The polymerization products were fractionated into methanol-insoluble, hexane-insoluble and hexane-soluble parts. The yield and *Mn* of the methanol-insoluble part increased with increasing $[M]_0/[I]_0$.

Figure 11 shows ^{1}H NMR spectra of the methanol-insoluble and the hexane-insoluble parts obtained by the polymerization carried out at $[M]_0/[I]_0$ = 22.2. Besides the signals due to BIPK-H and $C_3H_7CD_2$- groups mentioned above, the signals attributable to MMA-H were detected in the spectral region from 2.4 to 2.5 ppm. The MMA-H resonance split into three peaks owing to the tacticity at the ω-end of chain. According to the ^{1}H NMR analyses of MMA oligomers[26], the three MMA-H resonances were assigned to the *-r* (*-mr* + *-rr*), *-rm* and *-mm* sequences as indicated in Figure 11. The *m/r* ratio at the ω-end of chain was determined as 64/36 from the intensities of the three signals, and the value was smaller than the *m/r* ratio for in-chain tacticity (81/19). This indicates that the termination reaction with methanol is less stereospecific than the propagation reaction.

Table 6 shows the contents of BIPK units and terminal methine protons per chain. Compared with the polymer prepared with $C_3H_7CD_2Li$ in THF, the polymer prepared in toluene contained much smaller amount of BIPK in a chain. The methanol-insoluble parts had more BIPK unit in interior part of the chain than the

Table 6. Analysis of $C_3H_7CD_2$- groups incorporated in the poly(MMA-*d*8) prepared with $C_3H_7CD_2Li$ in toluene at -78°C for 24 h[a] ——— Contents of the initiator fragments and of the terminal methine protons per chain

$C_3H_7CD_2Li$ mmol ([M]$_0$/[I]$_0$)		Yield %	*Mn*[b] 10^3	$C_3H_7CD_2$- total amount mmol	Content per chain / mol/mol				
					$C_3H_7CD_2$-	BIPK unit		BIPK-H	MMA-H
					α-end[c]	interior	ω-end		
1.04	*MeOH-insol*	53.8	16.6	0.066	1.070	0.211	0.386	0.337	0.419
(10.7)	*hexane-insol*	24.8	3.77	0.137	1.014	0.113	0.523	0.523	0.514
	hexane-sol	11.4		0.503					
	Total	90.0		0.706					
0.50	*MeOH-insol*	73.9	25.3[d]	0.067	1.136	0.325	0.393	0.380	0.338
(22.2)	*hexane-insol*	19.2	4.13	0.096	1.028	0.120	0.524	0.509	0.335
	hexane-sol	6.5		0.268					
	Total	99.6		0.431					
0.27	*MeOH-insol*	76.7	31.2	0.057	1.123	0.331	0.442	0.468	0.303
(41.1)	*hexane-insol*	13.7	4.12	0.069	0.995	0.081	0.638	0.623	0.224
	hexane-sol	3.9		0.114					
	Total	94.3		0.240					

[a] MMA-*d*8 11.1 mmol, toluene 10.0 ml, polymerization time 24 h.

[b] Determined by VPO.

[c] The amount of $C_3H_7CD_2$- group at the α-end of chain was calculated as $c(\delta_t/3 - \beta_k/2)/(\delta_t/3)$, where c, δ_t and β_k are the total amount of $C_3H_7CD_2$- group per chain, the intensity of all the δ-methyl resonances, and the intensity of total β-methylene resonances due to BIPK units, respectively.

[d] *Mw/Mn* = 3.38, triad tacticity *mm:mr:rr* = 72.4 : 17.4 : 10.2.

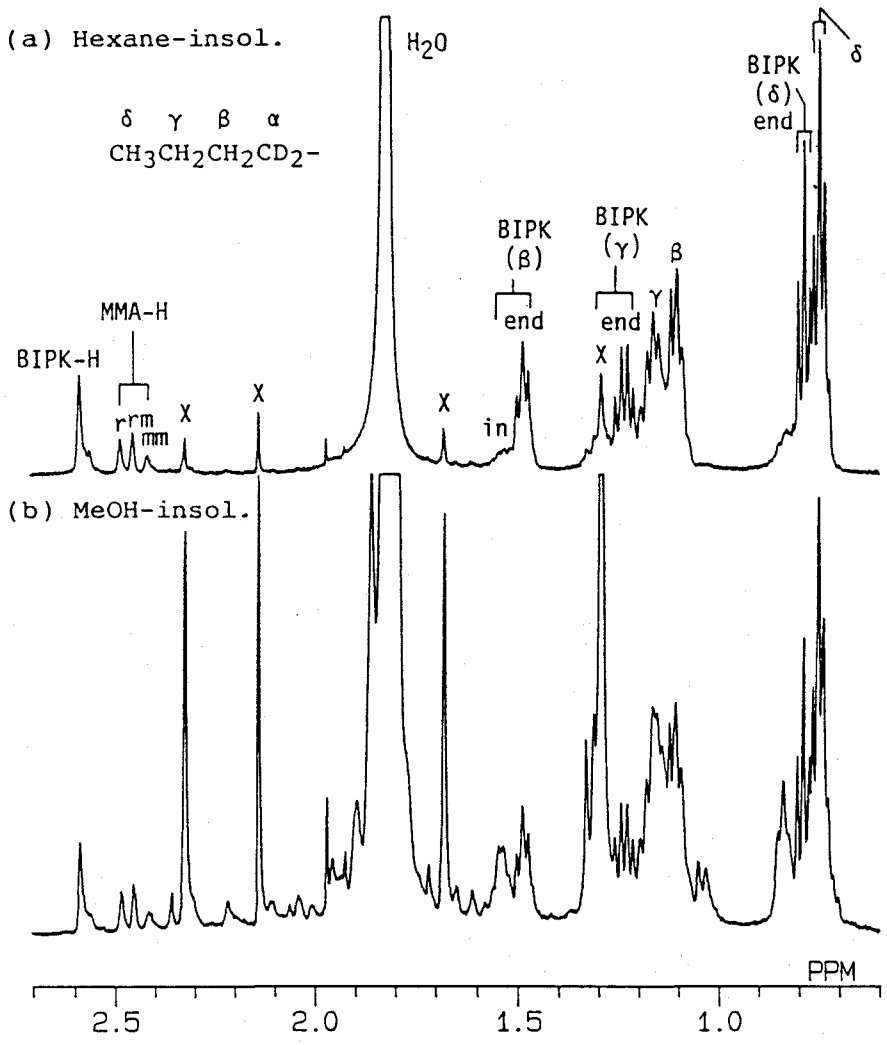

Figure 11. 500 MHz ^{1}H NMR spectra of the poly(MMA-*d*$_8$) prepared with $C_3H_7CD_2Li$ in toluene at -78°C ([MMA-*d*$_8$]$_0$/[$C_3H_7CD_2Li$]$_0$ = 22.2). (a) Hexane-insoluble part, (b) methanol-insoluble part. (Nitrobenzene-*d*$_5$, 110°C) X: Signals due to the remaining protons in the monomeric unit.

hexane-insoluble parts but less BIPK unit at the ω-end.

The content of BIPK-H agreed with the content of the BIPK unit at the ω-end of chain (Table 6). The total contents of BIPK-H and MMA-H were less than unity except for the hexane-insoluble part prepared at $[M]_0/[I]_0$ = 10.7. The fraction of the polymer chain which has BIPK-H or MMA-H was 72 - 77 % for the methanol-insoluble parts. The presence of the chains carrying some other types of structures such as a cyclic ketone terminal[10] at the ω-ends is suggested.

The results shown in Table 6 indicate that there exist the six types of poly(MMA-d_8) chains: the polymer chains which have BIPK-H and no interior BIPK unit [13], MMA-H and no interior BIPK unit [14], BIPK-H and one interior BIPK unit [15], MMA-H and one interior BIPK unit [16], BIPK-H and more than one interior BIPK units [11], and MMA-H and more than one interior BIPK units [10].

$C_3H_7CD_2$~~~~~~~~~~~~~~~~(MMA)~~~~~~~~~~~~~~~~BIPK-H [13]

$C_3H_7CD_2$~~~~~~~~~~~~~~~~(MMA)~~~~~~~~~~~~~~~~MMA-H [14]

$C_3H_7CD_2$~~~~(MMA)~~~~BIPK~~~~(MMA)~~~~BIPK-H [15]

$C_3H_7CD_2$~~~~(MMA)~~~~BIPK~~~~(MMA)~~~~MMA-H [16]

If we assume a random distribution of interior BIPK units among polymer chains, the fraction of the polymer molecules having n interior BIPK units, $P(n)$, should obey a Poisson distribution:

$$P(n) = k^n \exp(-k)/n! \qquad [17]$$

where k is the mean value of interior BIPK units per polymer molecule which is given in Table 6. For example, the fraction of the polymer molecules [13] in the methanol-insoluble part obtained at $[M]_0/[I]_0$ = 10.7 is calculated as 0.273 (= 0.810 x 0.337) using $P(0)$ = 0.810 and the content of BIPK-H (0.337). The fractions of each type were estimated as shown in Table 7.

The fractions of the polymer molecules which have more than one BIPK units in the interior part of chain ([10] and [11]) were very small (Table 7). The fractions of the polymer chain [13] in the methanol-insoluble parts were smaller by 18-24 % than that in the hexane-insoluble parts. The fraction of the polymer

Table 7. Fractions of the polymer molecules having n in-chain BIPK unit per chain, $P(n)$, and the fractions (%) of the six types of polymer chains for the poly(MMA-d_8)s prepared with $C_3H_7CD_2Li$ in toluene

Parameters and type of polymer chain		[MMA-d_8]$_0$ / [$C_3H_7CD_2Li$]$_0$					
		10.7		22.2		41.1	
		MeOH insol	*hexane insol*	*MeOH insol*	*hexane insol*	*MeOH insol*	*hexane insol*
Parameters							
	k[a]	0.211	0.113	0.325	0.120	0.331	0.081
	$P(0)$[b]	0.810	0.893	0.722	0.887	0.718	0.922
	$P(1)$[b]	0.171	0.101	0.235	0.106	0.238	0.075
	$P(\geq 2)$[c]	0.019	0.006	0.043	0.007	0.044	0.003
Fraction of polymer chain (%)							
$C_3H_7CD_2$ ~~~~~~~~~~(MMA)~~~~~~~~~~ BIPK-H		27.3	46.7	27.4	45.1	33.6	57.4
$C_3H_7CD_2$ ~~~~~~~~~~(MMA)~~~~~~~~~~ MMA-H		33.9	45.9	24.4	29.7	21.8	20.7
$C_3H_7CD_2$ ~~(MMA)~~ BIPK ~~(MMA)~~ BIPK-H		5.8	5.3	8.9	5.4	11.1	4.7
$C_3H_7CD_2$ ~~(MMA)~~ BIPK ~~(MMA)~~ MMA-H		7.2	5.2	7.9	3.6	7.2	1.7
$C_3H_7CD_2$ ~~(MMA)~~ BIPK ~~(MMA)~~$_n$ BIPK-H[d]		0.6	0.3	1.6	0.4	2.1	0.2
$C_3H_7CD_2$ ~~(MMA)~~ BIPK ~~(MMA)~~$_n$ MMA-H[d]		0.8	0.3	1.5	0.2	1.3	0.1
	Total (%)	75.6	103.7	71.7	84.4	77.1	84.8

[a] The content of in-chain BIPK units per polymer molecule (*cf.* Table 6).

[b] Obeys a Poisson distribution; $P(n) = k^n \exp(-k)/n!$.

[c] $P(\geq 2) = 1 - P(0) - P(1)$.

[d] $n \geq 2$.

chain containing no BIPK unit decreased with increasing $[M]_0/[I]_0$. This suggests that the ratio of C=C addition (formation of [1]) to C=O addition (formation of BIPK) in the reaction of $C_3H_7CD_2Li$ and MMA-d_8 slightly decreases as the initial ratio of MMA-d_8 to $C_3H_7CD_2Li$ increases.

The total amounts (in mmol) of $C_3H_7CD_2$- groups in the polymerization products corresponded to 68 - 89 % of the $C_3H_7CD_2Li$ used (Table 6). According to the previous work by Hatada *et al.*[15], the residual 11 - 32 % is attributed to the butane formed by protonation of unreacted buthyllithium rather than by metalation of the monomer[30,31], based on mass spectrometric evidence. It was suggested by Vankerckhoven and Van Beylen in the polymerization of methacrylonitrile in toluene at -78°C[32] that the unreacted butyllithium molecules are engaged in very stable and inactive associated species.

1.3.3 Polymerization of MMA-d_8 with $C_3H_7CD_2MgCl$ in Toluene

The polymerization of MMA-d_8 with butylmagnesium-1,1-d_2 chloride ($C_3H_7CD_2MgCl$) in toluene was carried out under the conditions similar to the polymerization with $C_3H_7CD_2Li$ in toluene ($[M]_0/[I]_0$ = 9.3 mol/mol). Table 8 gives the results of the polymerization, and Figure 12 shows ^1H NMR spectra of the polymers. Both the methanol-insoluble and hexane-insoluble polymers contained less BIPK units in a chain than those prepared with $C_3H_7CD_2Li$; nearly half of the polymer molecules contained no BIPK unit. The other 30 - 50 % had a BIPK unit at the ω-end of chain but very few in inner part of the chain. Thus the polymers consists of mainly [13] and [14].

The numbers of BIPK-H per chain were smaller than those of the terminal BIPK unit and the difference exceeded the experimental error. The results may indicate that there exist the polymer chains having a short and contiguous BIPK sequence at the ω-end *e.g.* as shown below [17] and that the protons of the butyl group in the penultimate BIPK unit show the chemical shifts similar to those in the terminal BIPK unit.

C_4H_9 ~~~~~~(MMA)~~~~~~ BIPK-BIPK-H [17]

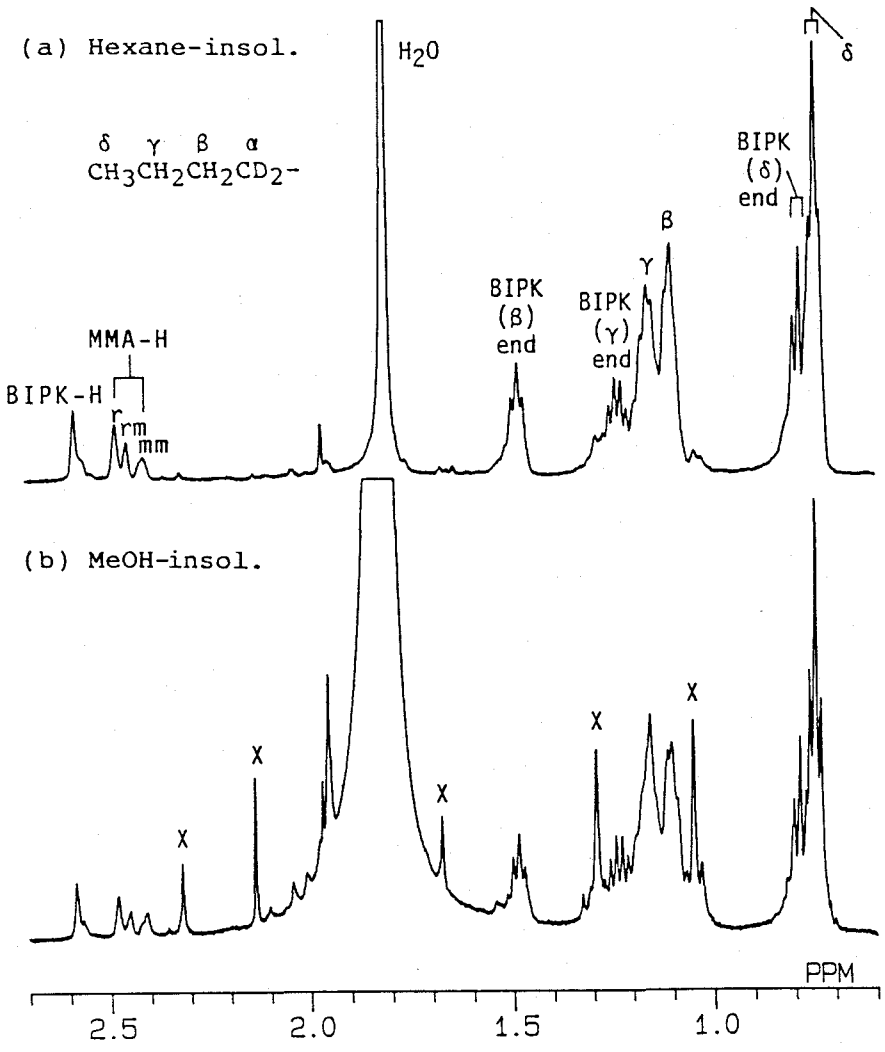

Figure 12. 500 MHz ^{1}H NMR spectra of the poly(MMA-*d*$_8$) prepared with $C_3H_7CD_2MgCl$ in toluene at -78°C. (a) Hexane-insoluble part, (b) methanol-insoluble part (Nitrobenzene-*d*$_5$, 110°C). X: Signals due to the remaining protons in the monomeric unit.

Table 8. Analysis of $C_3H_7CD_2$- groups incorporated in the poly(MMA-*d*8) prepared with $C_3H_7CD_2MgCl$ in toluene at -78°C for 72 h[a] ——— Contents of the initiator fragments and of the terminal methine protons per chain

	Yield		*Mn*[b]	$C_3H_7CD_2$- total amount	Content per chain / mol/mol				
					$C_3H_7CD_2$-	BIPK unit		BIPK-H	MMA-H
	g	%	10^3	mmol	α-end[c]	interior	ω-end		
MeOH-insol	1.555	73.4	13.1[d]	0.160	0.983	0.068	0.302	0.244	0.355
hexane-insol	0.334	15.7	2.90	0.173	1.104	0.000	0.487	0.354	0.490
hexane-sol	0.208	9.8	-	0.622					
Total	2.097	98.9		0.955					

[a] MMA-*d*8 18.5 mmol, $C_3H_7CD_2MgCl$ 2.00 mmol, toluene 20 ml.

[b] Determined by VPO (chloroform, 40°C).

[c] The amount of $C_3H_7CD_2$- group at the α-end of chain was calculated as $c(\delta_t/3 - \beta_k/2)/(\delta_t/3)$, where c, δ_t and β_k are the total amount of $C_3H_7CD_2$- group per chain, the intensity of all the δ-methyl resonances, and the intensity of combined β-methylene resonances due to BIPK units, respectively.

[d] Triad tacticity *mm:mr:rr* = 28.4 : 17.3 : 54.3.

The total amounts of terminal methine protons (MMA-H + BIPK-H) were 0.60 and 0.84 per chain for the methanol-insoluble and the hexane-insoluble parts, respectively. A part of the polymer molecules was found to have cyclic ketone or isopropenyl ketone structure at the ω-end (*cf.* Section 1.2.2).

The *m/r* ratio at the ω-end of chain was 57/43 as determined from the MMA-H resonances. The value differs from that for the in-chain sequence (*m/r* = 37/63), indicating that the stereospecificity of the termination reaction with methanol is again different from that of the chain propagation.

1.3.4 Mechanism of the Polymerizations

The structural analyses of the poly(MMA-*d*8)s mentioned above led us to the understanding of the mechanisms of the three polymerization reactions conducted under different conditions.

(A) Polymerization of MMA with butyllithium in THF

In the polymerization of MMA with butyllithium in THF, the

initiator is consumed within the first few seconds to produce the unimer anion [1] and BIPK[16]. A small part of the BIPK reacts again with butyllithium to give an alkoxide, but most of the BIPK add to growing anions rapidly because BIPK (Q = 1.02, e = 0.86)[27] is more reactive than MMA (Q = 0.74, e = 0.40)[27]. The amount of BIPK formed is larger than the amount of the anion [1][16], thus all the growing oligomer anions ended with MMA-unit [2] change to the oligomer anions ended with BIPK-unit [18] in the early stage of polymerization. The BIPK-ended anions [18] are less reactive than the MMA-ended anions [2] and remain unreacted for a while. However, once attacked by MMA, the oligomeric anion add the MMA monomer very rapidly to form the higher molecular weight chain [19].

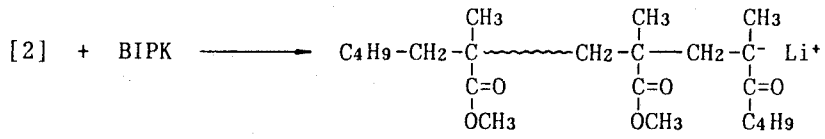

[18]

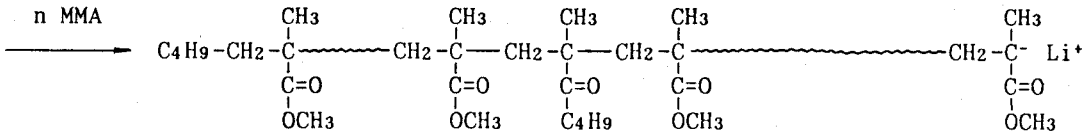

[19]

The lifetime of the growing anion [19] must be very short because the anion is soon attacked by another BIPK molecule to generate the BIPK anion again. A part of the anions alternates several times between the growing state (MMA anion) and the dormant state (BIPK anion) in the course of the polymerization. As the polymerization reaction proceeds, the MMA/BIPK ratio in the remaining monomer increases gradually making the lifetime of the MMA anion longer. This corresponds to the fact that the methanol-insoluble polymer is formed rapidly from 3 h after initiation when the amount of BIPK in the polymerization mixture becomes very small[16].

Hatada *et al.*[16] postulated that the MMA anion added no more BIPK from 3 h after initiation because there remained little BIPK in the polymerization mixture. The methanol-insoluble polymer

was consequently expected to have MMA-H at the ω-end of the chain as shown in the formula [10]. However, in this work it was found that very few MMA unit is located at the ω-end of the polymer chain. The results may indicate that the amount of the MMA anion is so small and does not exceed the amount of BIPK during the polymerization. Otherwise we must consider another mechanism which explains such a specific location of the BIPK unit in the polymer chain. Bywater suggests that the tertiary alkoxide [3] might not release lithium methoxide immediately but rather on termination of the reaction to form BIPK[28]. Thus, one possible explanation for the location of the BIPK unit at the ω-end of the polymer chain is that the tertiary alkoxide coordinates with the propagating chain end, and the ketone is formed on termination to be immediately incorporated into the ω-end of the polymer chain.

(B) Polymerization of MMA with butyllithium in toluene

The reaction between butyllithium and MMA in toluene is completed within the first few seconds. A part of butyllithium remains unreacted during the polymerization owing to the rigid aggregates in the polymerization mixture[15]. The ratio of C=O addition (formation of BIPK) to C=C addition (formation of [1]) for the polymerization in toluene (0.73)[15] is smaller than that for the polymerization in THF (1.10)[16]. Therefore, 20-46 % of the MMA-ended growing anions survives without being attacked by BIPK throughout the polymerization reaction (Table 7).

Another difference between the polymerizations in toluene and in THF is that the reactivities of growing species in toluene are not so uniform as in THF, probably due to association of the species. This is evident from the fact that methanol-insoluble fraction is formed even in the early stage of polymerization[15]. Some of the MMA-ended anion grows rapidly to give the methanol-insoluble polymer, and the others grow so slowly as to give methanol-soluble (and hexane-insoluble) polymer. In the course of chain growth, more than half of the MMA-ended anions add BIPK to form the less reactive BIPK anions; most of them remain unreacted during the polymerization and are recovered as the polymer which has the structure of the formula [13]. A small part of

the BIPK anions add MMA again to yield the higher molecular weight polymers having BIPK units in inner part of the chain. Some of the propagating species ending with MMA anion are self-terminated probably owing to the formation of a cyclic ketone terminal at the ω-end of chain. The self-termination occurs more on the species which grow so slowly.

(C) Polymerization of MMA with butylmagnesium chloride in toluene

In this polymerization, initiation reaction between butylmagnesium chloride and MMA takes place rather slowly, therefore the amount of the growing anion and BIPK in the polymerization mixture slightly increases during the polymerization reaction[29]. A considerable amount of unreacted BIPK remains after the completion of the polymerization[19]. This may be related to the stability of the alkoxide [3] in the polymerization mixture; the magnesium alkoxide may be more stable than the lithium alkoxide and release methoxide slowly to form BIPK.

The amount of BIPK formed in the polymerization with butylmagnesium chloride is smaller than that in the polymerization with butyllithium in toluene. The reactivity of the BIPK-ended anion having magnesium as a counterion should be lower than that having lithium as a counterion. Therefore an addition of BIPK to the growing anion is almost equivalent to a termination reaction. As a result, both the methanol-insoluble and the hexane-insoluble fractions contain little BIPK unit in the inner part of the chain.

1.4 Polymerization of MMA-*ds* with *t*-Butylmagnesium Bromide and Formation of a Cyclic Ketone Terminal in Living PMMA Anions

In order to get a spectroscopic evidence of the formation of a cyclic ketone terminal (CT) in PMMA, ^{13}C NMR spectrum of a cyclic trimer of MMA (dimethyl 1,3,5,5-tetramethyl-4-oxo-1,3-cyclohexanedicarboxylate) was investigated. The cyclic trimer was prepared as a model compound of CT according to Lochmann's procedure[33] and was obtained as a 55:45 mixture of the *cis*- and *trans*-isomers.

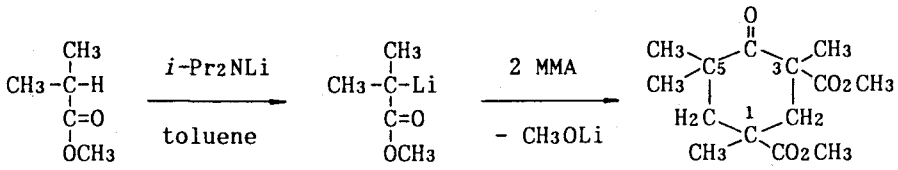

[21]

Table 9 provides the ^{1}H and ^{13}C NMR chemical shift values for the cyclic trimer. The *cis/trans* assignment was made on the basis of the nonequivalency of the two methylene protons at the 2-position of the trimer; the chemical shift difference between the methylene protons of the *cis*-isomer (1.403 ppm) is larger than that of the *trans*-isomer (0.084 ppm). The *trans*-isomer could be separated by crystallization (*mp* = 45.6 - 46.7°C) from heptane solution of the isomeric mixture.

As will be described in the next chapter, the polymerization of MMA initiated with *t*-C_4H_9MgBr in toluene at -78°C[22,23] or with 1,1-diphenylhexyllithium (DPHLi) in THF at -78°C[20,21] generates living PMMA anion. Quenching the living PMMA anions with methanol at -78°C gives the PMMAs which have MMA-H quantitatively at the ω-ends of polymer chain (Table 10, No. 1 and 3). When the living PMMA anions were allowed to stand at 0°C for 24 h before being quenched with methanol, the amount of MMA-H introduced at the ω-end of the resulting polymer decreased remarkably (Table 10, No. 2 and 4).

Figure 13 shows ^{13}C NMR spectra of the PMMAs (ketone and ester carbonyl regions). The PMMAs prepared with *t*-C_4H_9MgBr (a and b) are highly isotactic and the strong signal at 176.3 ppm is due to *mmmm* pentad. The PMMAs prepared with DPHLi (c and d) are syndiotactic, which is realized from the *rr* and *rm* centered pentad signals. The degree of polymerization is 22 for a and b, and 32 for c and d. The PMMAs which were allowed to stand at 0°C for 24 h before quenching (b and d) showed signals of weak intensity at 173.3 - 173.9 ppm and 211 - 212 ppm, whereas the PMMAs which were quenched at -78°C showed no signal around these regions. This indicates the formation of a cyclic ketone terminal at the ω-end of the poly(MMA-*d*8) chain.

The weak signals at 173.3 - 173.9 ppm are attributed to one of the two ester carbonyls of the cyclic ketone terminal, and the splitting of the signals is due to stereoisomerism of the cyclic

Table 9. ^{1}H and ^{13}C NMR chemical shifts (ppm) of a cyclic trimer of MMA (dimethyl 1,3,5,5-tetramethyl-4-oxo-cyclohexanedicarboxylate)[a]

		trans-isomer		*cis*-isomer	
		^{13}C	^{1}H	^{13}C	^{1}H
C1	(*q*-C)	39.95		40.13	
	(CH_3)	29.44	1.342	29.83	1.351
	(C=O)	178.63		177.83	
	(OCH_3)	52.26	3.697	52.18	3.717
C2	(CH_2)	39.45	2.427	42.14	1.698
			2.511		3.101
C3	(*q*-C)	53.63		53.73	
	(CH_3)	22.82	1.322	23.16	1.337
	(C=O)	173.78		173.06	
	(OCH_3)	52.36	3.724	52.23	3.640
C4	(C=O)	212.71		212.83	
C5	(*q*-C)	43.39		43.61	
	(CH_3)*a*	25.97	0.962	27.82	1.188
	(CH_3)*e*	27.89	1.141	28.15	1.148
C6	(CH_2)	44.24	1.740	43.45	1.634
			2.370		2.551

[a] Measured in $CDCl_3$ at 35.0°C.

Table 10. Formation of a cyclic ketone terminal (CT) in the living poly(MMA-*d*8) anions prepared with *t*-C_4H_9MgBr and with 1,1-diphenylhexyllithium (DPHLi) at -78°C ——— Numbers of MMA-H and CT per molecule of the poly(MMA-*d*8) obtained

No.	Initiator	*Mn*	*ω*-end		Tacticity		
			MMA-H	CT	*mm*	*mr*	*rr*
1	*t*-C_4H_9MgBr	2290	0.98	-	98	2	0
2		2290[a]	0.10	0.93	98	2	0
3	DPHLi	3300	1.0	-	1	21	78
4		3150[a]	0.0	0.75	1	21	78

[a] Allowed to stand at 0°C for 24 h before being quenched with methanol.

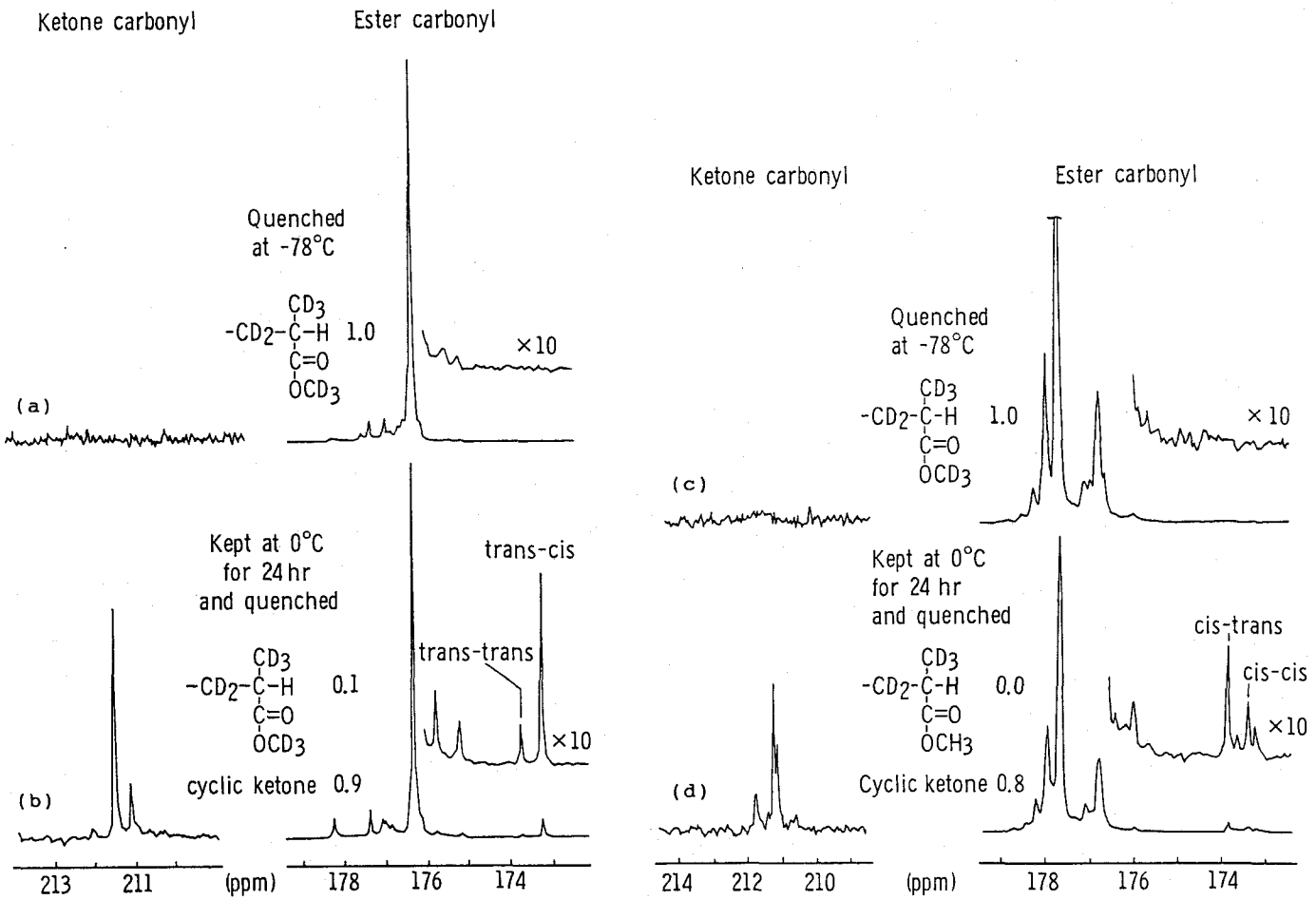

Figure 13. 25 MHz ^{13}C NMR spectra of the PMMAs prepared with *t*-C_4H_9MgBr (1/20) in toluene at -78°C for 72 h (a,b), and by 1,1-diphenylhexyllithium (DPHLi) (1/20) in THF at -78°C for 24 h (c,d). In the cases of (b) and (d), polymerization mixture was allowed to stand at 0°C for another 24 h before termination with methanol.

ketone terminal. The PMMA prepared with *t*-C_4H_9MgBr is highly isotactic and thus the cyclic terminal should be *trans-cis* and *trans-trans* structures, whereas the PMMA prepared with DPHLi is syndiotactic-rich and consequently the cyclic terminal should be predominantly *cis-cis* and *cis-trans* structures (Figure 13).

1.5 Experimental Part

1.5.1 Materials

Methyl methacrylate-*d*$_8$ was synthesized from acetone cyanohydrin-*d*$_7$ and methanol-*d*$_4$ according to the method of Crawford[34]. Isotopic purity was 99.17 % for α-CD_3, 99.12 % for $CD_2=$, and 99.85 % for OCD_3, respectively, by NMR analysis.

Butylmagnesium chloride was prepared from butyl chloride and magnesium metal in diethyl ether under nitrogen atmosphere. The concentration of the solution was found to be 0.86 mol/l by the titration with *s*-butanol using 9,10-phenanthroline as an indicator[35].

Butyllithium-1,1-*d*$_2$ was prepared from $CH_3CH_2CH_2CD_2Cl$ (32.7 mmol) and lithium powder (70 mmol) in heptane (45 ml) under dry argon atmosphere. The concentration of butyllithium-1,1-*d*$_2$ was determined as 0.839 M by acid-base titration. Butylmagnesium-1,1-*d*$_2$ chloride was prepared from $CH_3CH_2CH_2CD_2Cl$ (6.54 mmol) and magnesium (21 mmol) in diethyl ether (8 ml) under dry nitrogen atmosphere. The concentration of butylmagnesium-1,1-*d*$_2$ chloride was determined as 1.064 M by acid-base titration. $CH_3CH_2CH_2CD_2Cl$ (b.p. 77.5 - 78.0°C, purity > 99.9 % by G.C., isotopic purity = 99.41 % by NMR) was synthesized from $CH_3CH_2CH_2CD_2OD$ (118 mmol) and thionyl chloride (689 mmol) in dry pyridine (9.6 ml) in 71.3 % yield[36]. $CH_3CH_2CH_2CD_2OD$ was prepared from butyric anhydride and lithium aluminum deuteride; butyric anhydride (90.8 mmol) was reduced by lithium aluminum deuteride (Merck, 95.3 mmol) in diethyl ether and the reaction mixture was hydrolyzed with D_2O (6 ml)[37]. The yield was 69 %.

The cyclic trimer of MMA, dimethyl 1,3,5,5-tetramethyl-4-oxo-1,3-cyclohexanedicarboxylate (CT) was prepared by the procedure reported by Lochmann *et al.*[33]. Isolated yield of CT

was 50 % of the lithiated pivalate. The pure *trans*-isomer of CT was obtained by crystallization from heptane (*mp* = 45.6 - 46.7°C).

1.5.2 Polymerization

Polymerization was carried out in a sealed glass ampoule under dry nitrogen atmosphere. The reaction was terminated by adding a small amount of methanol containing hydrochloric acid and the mixture was poured into a large amount of methanol. After standing overnight, the precipitated polymer was collected by filtration, washed with methanol, and dried *in vacuo* at 60°C (methanol-insoluble part). The combined filtrates were evaporated under reduced pressure, and the residue was dissolved in 5 ml of benzene. Then the solution was poured into 200 ml of hexane. The hexane-insoluble polymer was washed with hexane and with water, and was freeze-dried with benzene (hexane-insoluble part). The hexane solution was evaporated to dryness. The hexane-soluble part was dissolved in 1 ml of chloroform-*d* and then the solution was evaporated under reduced pressure.

1.5.3 Measurements

^{1}H NMR spectra of poly(MMA-d_8)s were measured in nitrobenzene-d_5 at 110°C or in chloroform-*d* at 60°C. The NMR instruments used were JEOL JNM-FX100 and JNM-GX500 spectrometers being operated at 100 and 500 MHz, respectively. Sixty-four to 2000 scans were accumulated with the repetition time of 100 s using 90° observation pulse. The repetition time is large enough to make correct measurement of intensity. The hydrogen content in the sample was determined from the relative intensity of the signal of interest to the signals due to the remaining protons in nitrobenzene-d_5. The hydrogen content for the latter signal (0.359 gram-^{1}H/ml) was measured by the precision coaxial tubing method[38]. Spin-lattice relaxation time T_1 was determined by inversion-recovery method. ^{13}C NMR spectra were measured in chloroform-*d* solution at 55°C.

Mn was determined in chloroform solution at 40 °C or in toluene solution at 60 °C by a Hitachi 117 vapor pressure osmometer (VPO).

Field desorption (FD-) and electron impact (EI-) mass spectra were measured on a JEOL JMS-01SG-2 mass spectrometer.

Fractionation of the oligomers were performed on a JASCO TRIROTAR II high performance liquid chromatograph using a column packed with polystyrene gel (maximum porosity 3000) and a JASCO RI-162 refractive index detector. Chloroform was employed as an eluent.

References

1. W. E. Goode, F. H. Owens, R. P. Fellman, W. H. Snyder, J. E. Moore, *J. Polym. Sci.*, **46** 317 (1960).
2. A. Nishioka, H. Watanabe, K. Abe, I. Sono, *J. Polym. Sci.*, **48**, 241 (1960).
3. P. Pino, U. W. Suter, *Polymer* **17**, 977 (1976).
4. H. Yuki, K. Hatada, *Adv. Polym. Sci.*, **31**, 1 (1979).
5. B. L. Erussalimsky, E. Yu. Melenevskaya, V. N. Sgonnik, *Acta Polymerica*, **32**, 183 (1981).
6. I. Ando, R. Chujo, and A. Nishioka, *Polym. J.*, 1, 609 (1970).
7. P. E. M. Allen, C. Mair, *Eur. Polym. J.*, **20**, 697 (1984).
8. K. Matsuzaki, H. Tanaka, T. Kanai, *Makromol. Chem.*, **182**, 2905 (1981).
9. P. E. M. Allen, C. Mair, D. R. G. Williams, E. H. Williams, *Eur. Polym. J.*, **20**, 119 (1984).
10. W. E. Goode, F. H. Owens, W. L. Myers, *J. Polym. Sci.*, **47**, 75 (1960).
11. Y. Yasuda, N. Kawabata, T. Tsuruta, *J. Macromol. Sci. - Chem.*, A1, 669 (1967).
12. B. O. Bateup, P. E. M. Allen, *Eur. Polym. J.*, **13**, 761 (1977).
13. K. Hatada, T. Kitayama, H. Yuki, *Makromol. Chem., Rapid Commun.*, 1, 51 (1980).
14. K. Hatada, T. Kitayama, H. Yuki, *Polym. Bull.*, **2**, 15 (1980).
15. K. Hatada, T. Kitayama, K. Fujikawa, K. Ohta, H. Yuki, *ACS Symp. Ser.*, **166**, 327 (1981).
16. K. Hatada, T. Kitayama, S. Okahata, H. Yuki, *Polym. J.*, **13**, 1045 (1981).
17. K. Hatada, T. Kitayama, S. Okahata, H. Yuki, *Polym. J.*, **14**, 971 (1982).
18. T. Kitayama, K. Ute, K. Hatada, *Polym. J.*, **16**, 925 (1984).
19. K. Ute, T. Kitayama, K. Hatada, *Polym. J.*, **18**, 249 (1986).
20. B. C. Anderson, G. D. Andrews, P. Arthur, Jr., H. W. Jacobson, A. J. Playtis, W. H. Sharkey, *Macromolecules*, **14**, 1599 (1981).
21. P. Lutz, P. Masson, G. Beinert, P. Rempp, *Polym. Bull.*, **12**, 79 (1984).
22. K. Hatada, K. Ute, K. Tanaka, T. Kitayama, Y. Okamoto, *Polym. J.*, **17**, 977 (1985).

23. K. Hatada, K. Ute, K. Tanaka, Y. Okamoto, T. Kitayama, *Polym. J.*, **18**, 1037 (1986).
24. H. Schreiber, *Makromol. Chem.*, **36**, 86 (1960).
25. K. Ute, T. Kitayama, K. Hatada, *Polym. J.*, submitted.
26. K. Ute, T. Nishimura, K. Hatada, *Polym. J.*, **21**, 1027 (1989).
27. G. E. Ham, "Copolymerization", John Wiley & Sons Inc., New York., N.Y., 1964, p 845.
28. S. Bywater, *Adv. Polym. Sci.*, **4**, 66 (1965).
29. K. Hatada, K. Ute, T. Kitayama, M. Kamachi, *Polym. Prepr. Jpn.*, **32**, 1459 (1983).
30. N. Kawabata, T. Tsuruta, *Makromol. Chem.*, **86**, 231 (1965).
31. Ch. B. Tsvetanov, D. T. Petrova, P. H. Li, I. M. Panayotov, *Eur. Polym. J.*, **14**, 25 (1978).
32. H. Vankerckhoven, M. Van Beylen, *Eur. Polym. J.*, **14**, 189 (1978).
33. L. Lochmann, M. Rodova, J. Petranek, D. Lim, *J. Polym. Sci., Polym. Chem. Ed.*, **12**, 2295 (1974).
34. J. W. C. Crawford, *Br. Patent*, 405,699 (1934).
35. S. C. Watson, J. F. Eastham, *J. Organometal. Chem.*, **9**, 165 (1967).
36. P. J. Daughenbaugh, and J. B. Allison, *J. Am. Chem. Soc.*, **51**, 3665 (1929).
37. R. F. Nystrom, and W. G. Brown, *J. Am. Chem. Soc.*, **69**, 1197 (1947).
38. K. Hatada, Y. Terawaki, H. Okuda, *Org. Magn. Res.*, **9**, 518 (1977).

CHAPTER 2

Living and Highly Isotactic Polymerization of Methyl Methacrylate

2.1 Introduction

The polymerization of MMA in THF by bulky alkyllithium such as 1,1-diphenylhexyllithium at low temperatures proceeds in a living manner to give the PMMA of a narrow MWD[1,2]. A new method of polymerization known as group transfer polymerization (GTP) was developed by Webster and his coworkers in 1983[3]; by this method methacrylates and acrylates can be polymerized using ketene silyl acetals in the presence of a nucleophilic (*e.g.* HF_2^-, CN^-) or an electrophilic (*e.g.* $ZnCl_2$, Et_2AlCl) coinitiator. GTP proceeds through a living mechanism even at room temperature which allows the preparation of polymers with a narrow MWD. However, the stereoregularity of the PMMAs prepared by these living systems is similar to that of the PMMAs prepared by radical polymerization, and is atactic or rather syndiotactic.

Isotactic PMMA is usually prepared by an anionic initiator such as alkyllithium or Grignard reagent in a nonpolar solvent. Such a polymerization system often involves multiple active species and side reactions[4-8], making the MWD of the resulting PMMA broad (*cf.* Chapter 1). In 1985, the present authors found that highly isotactic PMMA (*mm* > 96 %) with a narrow MWD is produced by the polymerization of MMA in toluene at low temperature with the *t*-butylmagnesium bromide prepared in diethyl ether[9,10]. This was the first example of the direct preparation of highly isotactic PMMA with a narrow MWD, although it had been derived from the isotactic poly(triphenylmethyl methacrylate) prepared in THF with an organolithium compound[11,12].

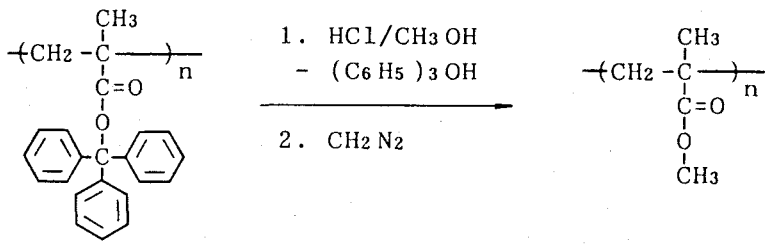

[1]

This chapter describes the polymerization of MMA by t-C_4H_9MgBr and the mechanism of formation of the highly isotactic PMMA with a narrow MWD.

2.2 Living and Highly Isotactic Polymerization of MMA with t-Butylmagnesium Bromide in Toluene[9,10]

The polymerization of MMA-d_8 with t-C_4H_9MgBr was carried out in toluene at -78°C for 72 h at the initial monomer/initiator ratio of 50/1 mol/mol. The resulting polymer showed two singlets in the ^1H NMR spectrum at 0.81 and 2.46 ppm which were assigned to the t-C_4H_9 group at the α-end of the chain and MMA-H, respectively (Figure 1). The t-C_4H_9 group was introduced into the polymer chain through the initiation reaction and the MMA-H by termination with methanol. Measurements of absolute intensity of these signals and Mn of the polymer indicated the polymer molecule to contain one t-C_4H_9 group at the α-end and one MMA-H at the ω-end. This indicates that there occurs no side reaction in the polymerization, and that the polymer molecule has the structure as shown below.

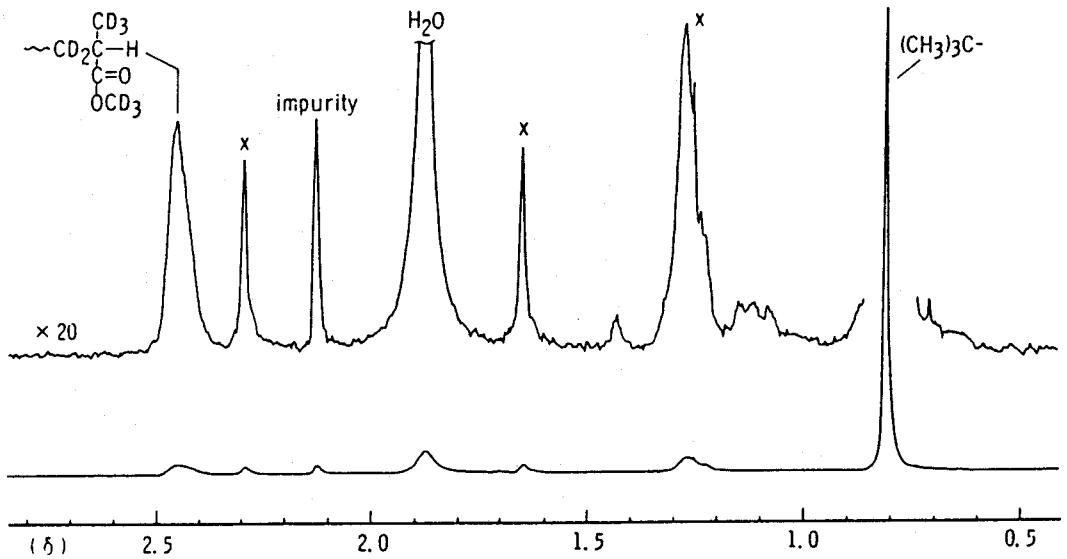

Figure 1. 100 MHz ^1H NMR spectrum of the poly(MMA-d_8) prepared with t-C_4H_9MgBr in toluene at -78°C (Mn = 5100, nitrobenzene-d_5, 110°C). X: Signals due to the remaining protons in the monomeric units.

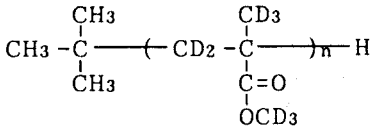

[2]

The poly(MMA-*ds*) molecule prepared in toluene at -40°C with *t*-C_4H_9MgBr contained one *t*-C_4H_9 group at the α-end of the chain but the content of MMA-H was less than unity (0.87). This indicates that there occurred side reactions such as spontaneous termination reaction through the formation of a cyclic ketone terminal at the ω-end. The cyclization reaction is much enhanced at 0°C and about 90% of the propagating species formed the cyclic ketone terminal when the species prepared in toluene at -78°C was kept at 0°C for 24 h (*cf.* Chapter 1.4).

Polymerization of MMA was carried out with *t*-C_4H_9MgBr in toluene at -78°C at various ratios of monomer to initiator. The results are shown in Table 1. The *Mn*'s of the polymer measured by GPC, VPO and by end-group assay using ^1H NMR spectroscopy agreed well with each other, and also with the value calculated from the amount of the monomer consumed and the initiator used. Thus the *Mn* of the polymer can be easily controlled by changing the ratio of initial amounts of MMA and initiator. In all the cases, the polymer was highly isotactic and of low polydispersity. The *Mw/Mn* ratios were about 1.1. The rate of polymerization was small at -78°C, and was enhanced at -40°C. However, the MWD of the PMMA formed by the polymerization at -40°C was broader than those of the PMMA prepared at -78°C (Table 1, No.6).

The polymerization were conducted in toluene at -78°C for different polymerization times. The results are shown in Figure 2. The *Mn* increased proportionally to the polymer yield. The amounts in mmol of polymer molecules was independent of the yield, and were equal to the amount of *t*-C_4H_9MgBr used. These results indicate that the polymerization has a "living" character.

The polymerization reaction was followed in toluene-*ds* at -78°C by measuring the intensities of vinylidene methylene proton signals of MMA. The signal of *t*-C_4H_9MgBr at 1.58 ppm disappeared on the addition of MMA, indicating a fast initiation reaction. The propagation was very slow compared to the initia-

Table 1. Polymerization of MMA with t-C_4H_9MgBr in toluene at -78°C[a]

No.	t-C_4H_9MgBr	Time	Yield	Tacticity / %			*Mn*				*Mw*
	mmol	h	%	*mm*	*mr*	*rr*	VPO	GPC	^{1}H NMR	Calcd	*Mn*
1	0.20	24	73	96.3	3.6	0.1	3660	3510	3560	3700	1.14
2	0.40[c]	72	100	96.5	3.2	0.3	4930	5650	4940	5060	1.10
3	0.11	120	100	96.8	2.9	0.3	10100	10400	9520	9160	1.10
4	0.10	145	99	96.7	3.0	0.3	21200	21200	20800	19900	1.08
5	0.20[d]	24	100	96.0	3.1	0.9	6100	5600	-	5060	1.43
6	0.40[e]	24	100	1.4	19.2	79.4	16500	14500	-	2560	3.10

[a] MMA 10.0 mmol, toluene 5 ml.

[b] Determined by GPC.

[c] MMA 20.0 mmol, toluene 10 ml.

[d] Polymerization at -40°C.

[e] (t-C_4H_9)$_2$Mg was used as an initiator.

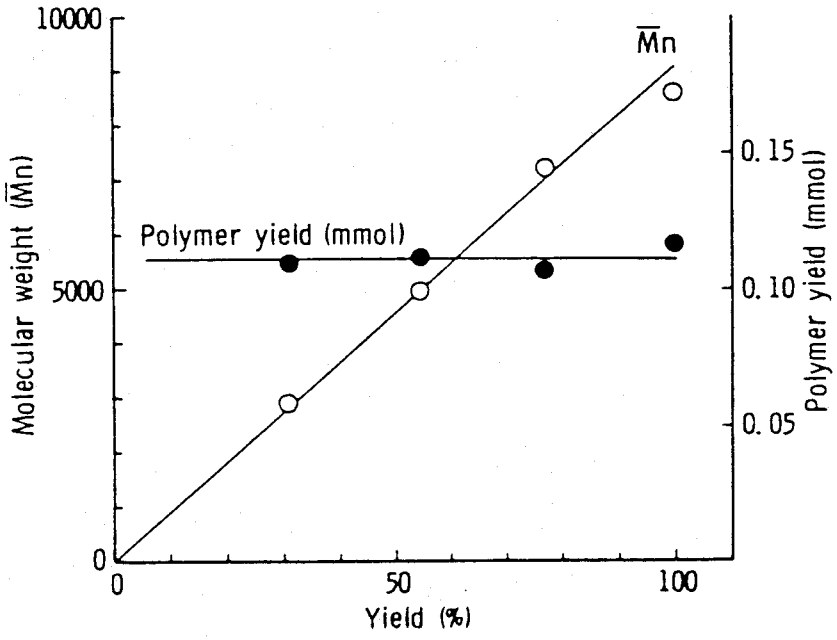

Figure 2. Relationship between *Mn* and polymer yield in the polymerization of MMA by t-C_4H_9MgBr in toluene at -78°C; the polymerizations were conducted for different polymerization times. MMA, 10 mmol; t-C_4H_9MgBr, 0.11 mmol; toluene, 5 ml.

tion reaction, and the rate of the polymerization fitted to first order plots.

$$R_p = -\frac{[MMA]}{dt} = 4.3 \times 10^{-4} [t\text{-}C_4H_9MgBr]_0 [MMA] \qquad [3]$$

Thus, fast and quantitative initiation and slow propagation as well as the living character of the resultant polymer anion are responsible for the formation of the PMMA with a narrow MWD.

Grignard reagent is considered to exist in the well-known Schlenk equilibrium:

$$2\ t\text{-}C_4H_9MgBr \rightleftharpoons (t\text{-}C_4H_9)_2Mg + MgBr_2 \qquad [4]$$

The t-C_4H_9MgBr used in this study was prepared in diethyl ether and was found to contain Mg^{2+} 2.2 times as much as carbanion (t-C_4H_9Mg- group). The $MgBr_2$ should be formed through an Wurtz type reaction between t-C_4H_9MgBr and t-C_4H_9Br during preparation of the Grignard reagent.

$$t\text{-}C_4H_9MgBr + t\text{-}C_4H_9Br \longrightarrow (t\text{-}C_4H_9)_2 + MgBr_2 \qquad [5]$$

This suggests that the Schlenk equilibrium is in favor of the side of "t-C_4H_9MgBr". In order to study the relation between Schlenk equilibrium and the results of polymerization, initiators with various ratios of $[Mg^{2+}]/[t\text{-}C_4H_9Mg]$ were prepared by mixing certain amounts of t-C_4H_9MgBr obtained in diethyl ether and $(t\text{-}C_4H_9)_2Mg$, and used for the polymerization of MMA in toluene at -78°C. The results are given in Table 2. When the ratios of $[Mg^{2+}]/[t\text{-}C_4H_9Mg]$ were larger than 1.5, highly isotactic PMMAs with narrow MWD were formed and the *Mn*'s agreed well with the calculated values. The polymers obtained by the initiator with $[Mg^{2+}]/[t\text{-}C_4H_9Mg]$ of 0.87 - 0.95 had trimodal MWD, suggesting the coexistence of at least three propagating species with different stereoregularities (Figure 3). The molecular weight dependence of tacticity of the PMMA was further investigated by the on-line GPC/NMR method in Chapter 4.4.

^1H NMR studies on the mixtures of t-C_4H_9MgBr and $(t\text{-}C_4H_9)_2Mg$ of various $[Mg^{2+}]/[t\text{-}C_4H_9Mg]$ ratios were attempted at -78°C but unsuccessful owing to poor resolution of the spectra at this

Table 2. Polymerization of MMA with t-C_4H_9MgBr/$(t\text{-}C_4H_9)_2Mg$ in toluene at -78°C for 24h[a]

$[Mg^{2+}]$	Yield	Tacticity/ %			*Mn*		*Mw*
$[t\text{-}C_4H_9Mg]$	%	*mm*	*mr*	*rr*	Obsd[b]	Calcd	*Mn*
0.53	100	2	16	82	14400	3060	2.85
0.87	96	32	22	46	4910	2940	54.0
0.95	97	88	6	6	3760	2970	16.6
1.06	100	96	4	0	3190	3060	1.83
1.50	98	96	4	0	3260	3000	1.15
2.24	69	96	4	0	2230	2130	1.10

[a] MMA 10 mmol, $[MMA]_0/[t\text{-}C_4H_9Mg]$=30 mol/mol, toluene 5 ml.

[b] Determined by GPC.

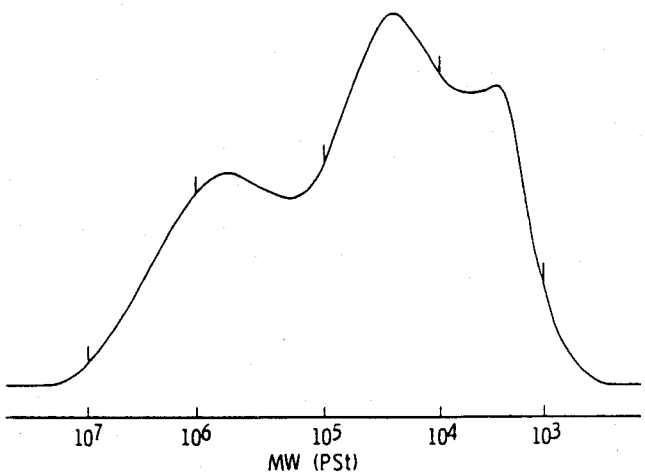

Figure 3. GPC curves of PMMA prepared by t-$C_4H_9MgBr/(t\text{-}C_4H_9)_2Mg$ ($[Mg^{2+}]/[t\text{-}C_4H_9Mg]=0.87$) in toluene at $-78°C$ for 24 h. MMA, 10 mmol; $[MMA]/[t\text{-}C_4H_9Mg]=30$ mol/mol; toluene, 5 ml. PMMA: $\bar{M}_n=4910$, $\bar{M}_w/\bar{M}_n=54.0$, tacticity $(I, H, S)=(32, 22, 46)$.

temperature. The measurements at -40°C in toluene were successful and the spectra are presented in Figure 4. The t-C_4H_9MgBr prepared in diethyl ether ($[Mg^{2+}]/[t\text{-}C_4H_9Mg]$ = 2.24) showed a singlet at 1.35 ppm, and $(t\text{-}C_4H_9)_2Mg$ ($[Mg^{2+}]/[t\text{-}C_4H_9Mg]$ = 0.53) at 1.31 ppm. The mixtures, the $[Mg^{2+}]/[t\text{-}C_4H_9Mg]$ ratio of which were between 0.57 and 0.87, exhibited two singlets at 1.33 and 1.35 ppm. With a decrease of the ratio of $[Mg^{2+}]/[t\text{-}C_4H_9Mg]$ from 0.87 to 0.57 the intensity of the peak at 1.35 ppm decreased and the intensity of the peak at 1.33 ppm increased. The mixture with $[Mg^{2+}]/[t\text{-}C_4H_9Mg]$ = 0.55 showed the resonance similar to that of $(t\text{-}C_4H_9)_2Mg$.

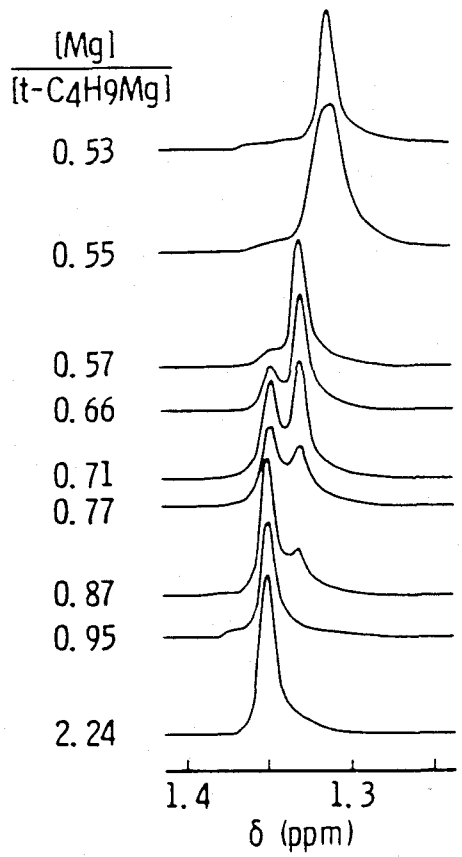

Figure 4. ^1H NMR spectra of t-$C_4H_9MgBr/(t\text{-}C_4H_9)_2Mg$ with various ratios of $[Mg^{2+}]/[t\text{-}C_4H_9Mg]$ in toluene-d_8 at -40°C. $[t\text{-}C_4H_9Mg]$ = 0.055 M; ether/toluene-d_8 = 1/5 v/v.

From the results described in Table 2 and Figure 4, it is believed that "*t*-C_4H_9MgBr" and "$(t\text{-}C_4H_9)_2Mg$" give a highly isotactic and a syndiotactic PMMA, respectively, and that the species which shows the ^1H NMR signal at 1.33 ppm gives a syndiotactic-rich polymer. Matsuzaki *et al.* suggested that in the polymerization of MMA by phenylmagnesium bromide, active species for isotactic polymer were "C_6H_5MgBr" and those for syndiotactic-rich polymer were "$(C_6H_5)_2Mg$"[7]. Isotactic polymerization has never been observed with dialkylmagnesium initiators with the single exception of dibenzylmagnesium prepared from dibenzylmercury[13].

Figure 5 shows ^{13}C NMR signals of carbonyl carbons in the PMMA prepared by *t*-C_4H_9MgBr in toluene at -78°C (No.4 in Table 1). Two weak signals of equal intensities due to *mmrm* and *mmmr* pentads are observed besides a strong signal due to an *mmmm* pentad, but no other pentad signals. Therefore, the steric defect in the polymer chain can be depicted as follows:

···——DDDDDLLLLL——···

This means that one *racemo* enchainment causes inversion of isotactic propagating species, and that stereoregulation in this polymerization is chain-end controlled. This polymer had *DP* of about 200 and 3.0 % heterotactic triads. So there exist about three switching points of monomer placements in a polymer chain. 2D NMR analysis[14] revealed that the configurational dyad sequence at the ω-end was not regular, showing the reaction between the propagating anion and the terminating reagent (methanol) was not stereospecific (*cf.* Sections 2.4 and 2.5).

Table 3 shows the results of polymerizations in toluene at -78°C with *n*-, *iso*-, *s*- and *t*-butylmagnesium bromides. *n*-C_4H_9-MgBr gave syndiotactic PMMAs in low yields, and the tacticities depended on the initiator concentration probably due to the coexistence of isotactic and syndiotactic active species. The *Mn*'s of the polymers were much larger than the expected values and the MWDs were very broad. As the alkyl group became bulkier, the isotacticity of the polymer increased greatly and the MWD became narrower. In the polymerization by *s*-C_4H_9MgBr and *t*-C_4H_9MgBr the initiator efficiencies were almost 100%, and the

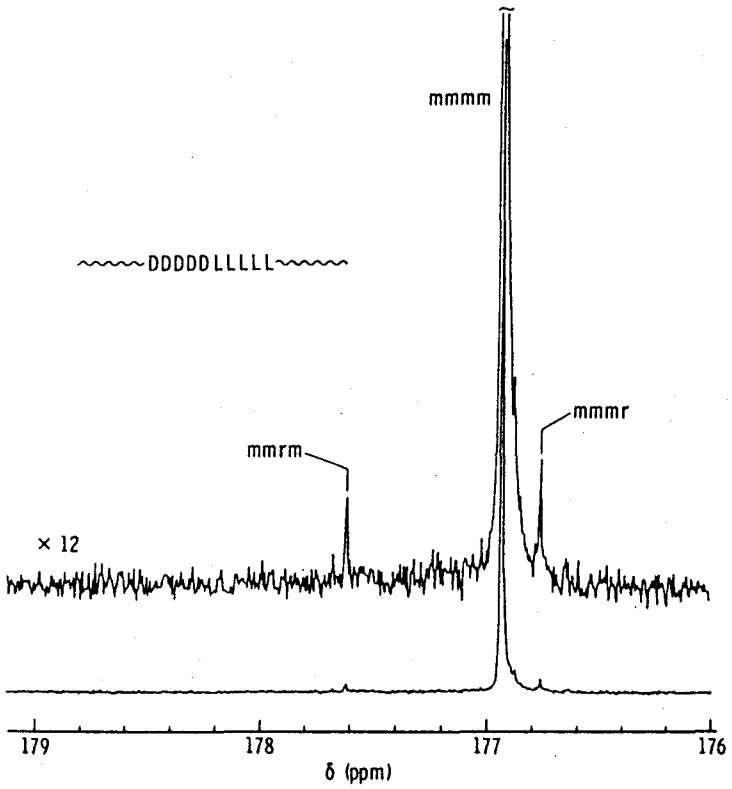

Figure 5. ^{13}C NMR signal of the carbonyl carbon in the PMMA prepared with *t*-C_4H_9MgBr in toluene at -78°C. Nitrobenzene-*d*$_5$, 110°C, 100 MHz.

Table 3. Polymerization of MMA with butylmagnesium bromides in toluene at -78°C for 72 h[a]

C_4H_9	$[Mg^{2+}]$ / $[C_4H_9Mg]$	Yield / %	Tacticity / %			*Mn*		*Mw* / *Mn*
			mm	*mr*	*rr*	GPC	Calcd	
n-C_4H_9[c]	1.0	8.1	11.0	15.3	73.7	12000	1680	13.4
	1.0	14.1	20.5	15.2	64.3	7420	760	11.2
iso-C_4H_9	1.1	33.1	92.5	5.4	2.1	5540	2270	2.29
	2.5[d]	21.7	95.5	4.5	0.0	4410	1140	2.12
s-C_4H_9	1.2	100	95.5	4.5	0.0	4930	5060	1.29
	2.4[d]	94.5	96.8	3.2	0.0	4680	4790	1.21
t-C_4H_9	2.2	100	97.4	2.6	0.0	5010	5060	1.18

[a] MMA 20 mmol, C_4H_9MgBr 0.40 mmol, toluene 10 ml.

[b] The Grignard reagent was prepared in the presence of 1,2-dibromoethane ($CH_2BrCH_2Br + Mg \longrightarrow C_2H_4 + MgBr_2$).

MWDs were narrow. t-C_4H_9MgBr gave the PMMA with the highest isotacticity and the narrowest MWD. It is expected from the results in Table 3 that the bulky alkyl group prevents the Grignard reagent from being involved in the side reaction and makes the polymerization living to produce the PMMA with a narrow MWD. Salonen and his coworker[15] studied the reactions of ethyl α-(2-furyl) acrylate with various alkylmagnesium halides. CH_3MgI reacted with the acrylate completely in 1,2-manner. The extent of 1,2-addition decreased with an increase in the bulkiness of alkyl group and t-C_4H_9MgCl reacted only in 1,4-manner. The results are consistent with those of our polymerizations.

$[Mg^{2+}]/[C_4H_9Mg]$ values for butylmagnesium bromides other than n-C_4H_9MgBr exceeded unity, and the values became larger as the butyl group became bulkier. The effect of $MgBr_2$ was confirmed by the fact that the isotacticities of the polymers prepared with iso-C_4H_9MgBr and s-C_4H_9MgBr increased and the MWDs were narrowed on the addition of excess amount of $MgBr_2$ (Table 3). It should be noted that the rate of polymerization was reduced on the addition of $MgBr_2$.

The structure of the initiating species in our isotactic-specific polymerization with t-C_4H_9MgBr is not clear at present, but the following structures, [6], [7], [8] and [9], may be proposed. In this polymerization, the efficiency of the initiator is almost 100%, isotacticity of the polymer is extremely high and MWD is narrow. These suggest that the initiating site should be homogeneous in reactivity and stereospecificity.

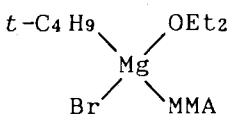

[6]

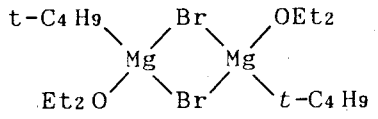

[7]

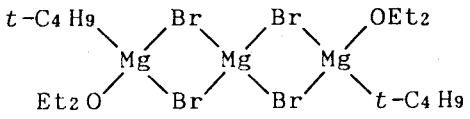

[8]

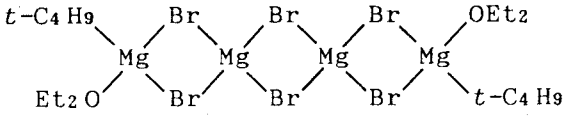

[9]

Allen and Williams[6] proposed the structure similar to [6] as the initiating species in the polymerization of MMA in toluene with "de-etherated" t-C_4H_9MgBr prepared in THF, on the basis that the isotactic initiating sites should be chiral. However, in our polymerization the stereoregulation is chain-end controlled (*cf.* Figure 5) and the initiating sites are not necessarily chiral. The solubility of ether-solvated $MgBr_2$ in toluene may be low as indicated by Allen and Mair[5]. Moreover, the viscosity of the polymerization mixture decreased remarkably when a small amount of methanol was added to quench the living anion [10].

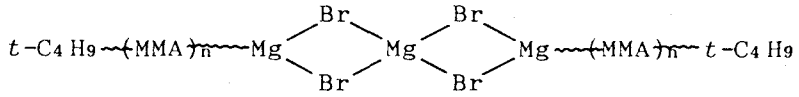

$$\xrightarrow{2\ CH_3OH} \quad 2\ t\text{-}C_4H_9\text{-}(MMA)_n\text{-}H \ + \ 2\ CH_3OMgBr \ + \ MgBr_2 \qquad [10]$$

Then, the structures [8] and [9] may possibly be considered as the initiating species, particularly [9], in which two t-C_4H_9Mg- groups are located apart from each other enough to act independently as the initiating sites of the same reactivity and stereoregularity. The association of the propagating anions may serve to prevent the side reactions such as the terminating reaction through the formation of a cyclic ketone unit at the ω-end.

In conclusion, t-C_4H_9MgBr prepared in diethyl ether exists as "t-C_4H_9MgBr" itself, and causes no side reaction in the polymerization of MMA in toluene at -78°C to produce highly isotactic PMMA with a narrow MWD. The reaction is completely living, and the amounts of the propagating species are the same as that of the initiator used and constant during the polymerization at -78°C.

2.3 Preparation of Block and Random Copolymers of Methacrylates with High Stereoregularity[16]

Stereoregularity in the anionic polymerization of methacrylates usually depends on the structure of the ester groups, and thus highly stereoregular copolymer of methacrylate is often

difficult to prepare. Hence, the preparation of the copolymers with high stereoregularity is a challenging subject, and the control of stereoregularity of the copolymer will provide a new aspect of control of properties of the copolymer. The living and highly isotactic polymerization system with t-C_4H_9MgBr was applied to copolymerizations of MMA with other methacrylates. Highly isotactic block and random copolymers could be prepared.

Polymerization of ethyl methacrylate (EMA) with the living isotactic PMMA anion prepared at -60°C was examined under several conditions. The results are given in Table 4. Figure 6 shows a GPC curve of the block copolymer of MMA and EMA with a degree of polymerization *DP* of each block of 59 and that of PMMA formed at the same $[MMA]_0/[t\text{-}C_4H_9MgBr]_0$ ratio as the block copolymerization. The chromatogram of the block copolymer showed a narrow MWD of the copolymer and did not show any peak in the range of the elution volume where the control PMMA showed its peak, indicating that all the living PMMA anions add EMA to form the block copolymer. All the block copolymers were highly isotactic and the *Mn* agreed well with the calculated values, although the MWD's became broader as the poly(EMA) block length became longer. Triblock isotactic copolymers with a fairly narrow MWD and high isotacticity were also obtained as shown in Table 4.

The homopolymerization of EMA by t-C_4H_9MgBr in toluene at -60°C also yielded highly isotactic polymer but the polymer showed a bimodal MWD. Numbers of polymer molecules in both the higher and lower molecular weight fractions were found to be almost constant during the polymerization, and *Mn*'s for both the fractions increased linearly with conversion. The results suggest that the species giving these fractions were both living and highly isotactic-specific. Since the *Mn* of the higher molecular weight fraction was about 10 times as large as that of the lower molecular weight fraction, one can assume that the rate constant for propagation at the active species giving the former fraction is about 10 times as large as that at the species giving the latter fraction.

The polymerization of MMA by the poly(EMA) anions formed with t-C_4H_9MgBr was carried out in toluene at -60°C to obtain

Table 4. Preparation of isotactic PMMA-*block*-poly(EMA) with *t*-C_4H_9MgBr in toluene at -60°C[a]

MMA	EMA	$[M]_0$	Yield	*Mn*		*Mw*	MMA/EMA[d]	Tacticity/%		
mol	mol	$[I]_0$	%	Obsd[b]	Calcd	*Mn*	in polymer	*mm*	*mr*	*rr*
0.70	0.70	100[e]	97	12500	10800	1.29	59/59	97	2	1
0.50	0.90	280	88	26900	26900	2.11	97/151	95	3	2
0.30	0.91	300	99	27200	30900	1.76	64/182	95	3	2
1.18	0.25	285	100	29700	29200	1.42	35/50/200[f]	97	2	1
0.80	0.40	90[e]	100	8200	9400	1.17	25/28/25[f]	95	3	2

[a] $[MMA+EMA]_0$/toluene = 2.0 (mol/l), $[Mg^{2+}]/[t\text{-}C_4H_9\text{-}]$ = 1.70.
[b] Determined by VPO. [c] Determined by GPC.
[d] Number of monomeric units per chain determined by chemical composition and *Mn* data for the copolymer.
[e] $[Mg^{2+}]/[t\text{-}C_4H_9\text{-}]$ = 2.21.
[f] Triblock copolymer, PMMA-*block*-poly(EMA)-*block*-PMMA.

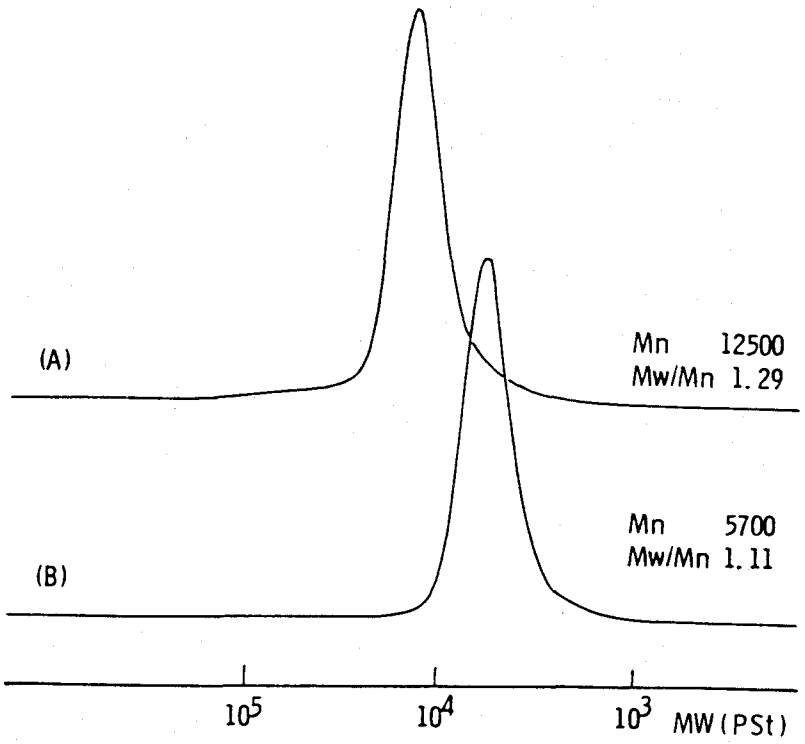

Figure 6. GPC curves of PMMA-*block*-poly(EMA) (A) and PMMA (B) prepared with *t*-C_4H_9MgBr in toluene at -60°C. (A) MMA 700 mmol, EMA 700 mmol, *t*-C_4H_9MgBr 14 mmol, toluene 700 ml, (B) MMA 10 mmol, *t*-C_4H_9MgBr 0.2 mmol, toluene 5 ml.

further information on the living nature of the poly(EMA) anion. Figure 7 shows a GPC curve of the block isotactic copolymer obtained and that of poly(EMA) formed at the same $[EMA]_0/[t\text{-}C_4H_9MgBr]_0$ ratio. Both the higher and the lower molecular weight peaks in the chromatogram of the control poly(EMA) shifted to the higher molecular weight side upon the block copolymerization. The number of polymer molecule in each fraction was found to be almost constant. The results indicate the living character of both the higher and the lower molecular weight poly(EMA) anions at -60°C. Molecular weight dependence of the copolymer composition in the block copolymer was analyzed by using the on-line GPC/NMR method and is described in Chapter 4.5.

Conventional copolymerization of MMA and EMA with $t\text{-}C_4H_9MgBr$ in toluene at -60°C also gave highly isotactic copolymer with a bimodal MWD. The copolymer was found to have a random comonomer sequence distribution as described below. The amount of the higher molecular weight fraction increased as EMA content in the initial monomer mixture increased. The result suggests that the active species giving the higher molecular weight copolymer is formed mainly in the initiation reaction of EMA with $t\text{-}C_4H_9MgBr$.

^{13}C NMR chemical shifts of carbonyl carbons in the copolymer of MMA and EMA are sensitive to triad comonomer sequence as well as pentad tacticity. Figure 8 shows carbonyl carbon spectra of the isotactic PMMA-*block*-poly(EMA), isotactic poly(MMA-*ran*-EMA), and radically prepared poly(MMA-*co*-EMA), all of which have 1:1 composition. High stereoregularity of the block and random copolymers made the spectra much simpler as compared with that of the radically prepared poly(MMA-*co*-EMA). The signals of MMA- and EMA-centered sequences in *mmmm* configurational pentad showed splittings due to the triad monomer sequences. The peak assignments were made by comparing the spectra of the isotactic copolymers with different compositions and are shown in the figure. Both of the relative peak intensities *MMM*:(*MME*+*EMM*):*EME* and *EEE*:(*EEM*+*MME*):*MEM* (*M*; MMA unit, *E*; EMA unit) were 1:2:1, indicating that the monomer sequence distributions of both MMA- and EMA-centered triads are completely random.

The block copolymer shows two strong signals at 176.51 and 176.37 ppm due to MMA and EMA sequences in *mmmm* configuration,

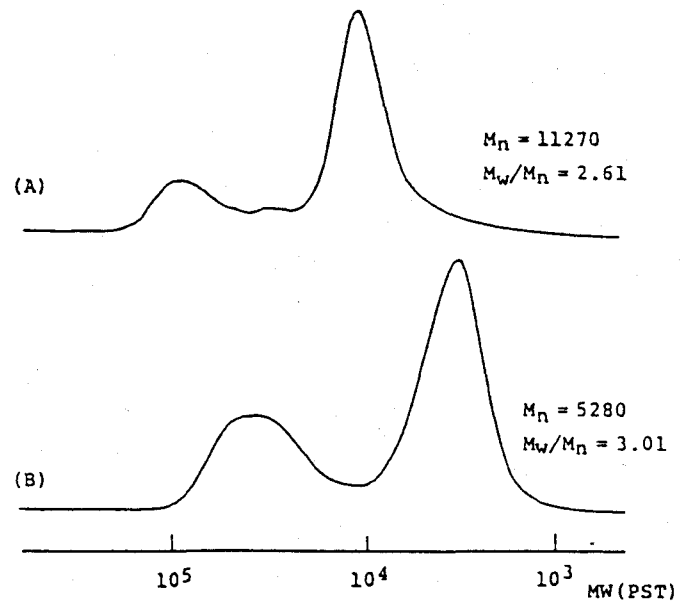

Figure 7. GPC curves of poly(EMA)-*block*-PMMA (A) and poly(EMA) (B) prepared with *t*-C_4H_9MgBr in toluene at -60°C. (A) MMA 50 mmol, EMA 50 mmol, *t*-C_4H_9MgBr 1.0 mmol, (B) EMA 10 mmol, *t*-C_4H_9MgBr 0.2 mmol.

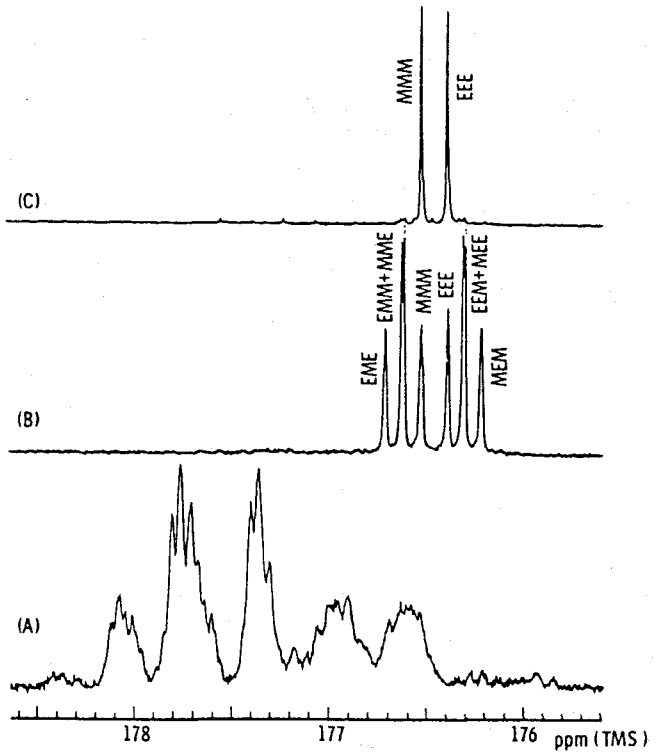

Figure 8. 125 MHz ^{13}C NMR spectra of PMMA-*block*-poly(EMA) (A), poly(MMA-*ran*-EMA) (B) prepared with *t*-C_4H_9MgBr in toluene at -60°C, and poly (MMA-*co*-EMA) prepared with AIBN in toluene at 60°C (C), measured in $CDCl_3$ at 55°C. (M and E denote MMA and EMA monomeric units, respectively.)

respectively. Weak signals of equal intensity observed at 176.60 and 176.28 ppm were assigned to MME and MEE triad in *mmmm* configuration, which should exist at the switching point of the PMMA block and the poly(EMA) block. Thus the block copolymer could be distinguished from the mixture of PMMA and poly(EMA) by ^{13}C NMR spectroscopy. Some other small peaks due to chain end units were also observed in the spectrum of the block copolymer.

2.4 Stereochemistry of the Oligomerization of MMA by *t*-Butylmagnesium Bromide in Toluene at -78°C[17,18]

Investigations on the oligomerizations of vinyl monomers provide useful information on the corresponding polymerization. Yoshino *et al.* studied the structures of the oligomers of isopropyl acrylate formed with phenylmagnesium bromide to elucidate the stereoregulation in the polymerization[19,20]. Hogen-Esch and his coworkers have extensively studied the stereochemistry of anionic oligomerizations of vinylpyridines[21,22] and vinyl sulfoxide[23,24] using chromatographic and NMR spectroscopic techniques. However, little has been reported on the stereoregular oligomerization of acrylate[25] or methacrylate[26-28] monomer. Wulff *et al.*[26] and Okamoto *et al.*[27] studied asymmetric oligomerizations of triphenylmethyl methacrylate with 1,1-diphenylhexyllithium- and fluorenyllithium-(-)-sparteine complexes, respectively, in toluene at -78°C. Hogen-Esch and his coworkers carried out the anionic oligomerization of MMA in THF by lithio or sodio methyl isobutyrate followed by termination with CH_3I or $^{13}CH_3I$ and determined the structure of the symmetrical oligomers by gas chromatography and ^{13}C NMR spectroscopy[28].

In this section, isotactic oligo(MMA)s were prepared by the polymerization of MMA with *t*-C_4H_9MgBr in toluene at -78°C and their configurational sequences were investigated to gain a more detailed understanding of stereoregulation in the polymerization.

The oligomers were isolated as reaction products from the early stage of the polymerization. The crude oligomers were fractionated into dimer to octamer by GPC. Each fraction was

further separated into stereoisomers by HPLC on a silica gel column using the mixtures of butyl chloride and acetonitrile as eluent. The structural elucidation of these oligomers are described in Chapter 3.

Figure 9 shows GPC curves of the MMA oligomers obtained in the polymerization for 5 - 120 min. The *Mn*'s of the oligomers were close to the calculated values and the MWDs were narrow, indicating the living character of the polymerization. The oligomers obtained from the polymerization for 15 min mostly contained dimer to octamer but no unimer. The nonexistence of unimer suggests that the unimer anion is much more reactive than the dimer anion. A similar trend was observed in the oligomerization of MMA initiated by methyl α-lithioisobutyrate[29,30] and also in the anionic asymmetric polymerization of triphenylmethyl methacrylate[27].

Each oligomer was separated into the individual diastereomers by HPLC (Figure 10) and the stereosequence of each isomer was determined by ^{1}H COSY and X-ray analysis (*cf.* Chapter 3) as indicated in the figure. The relative amount of the *m*- and *r*-dimers reflects that the addition of methanol (a proton source) to the dimer anion is non-stereospecific. The addition of methanol is almost non-stereospecific for the oligomer anions up to octamer as realized from the *m*/*r* ratios at their ω-ends (for trimer, $(mm+rm)/(mr+rr) = 0.8$), and the addition to the polymer anion was also found to be non-stereospecific[14] (Figure 11). It is not so surprising but should be noted that the addition of methanol to the propagating chain end is not stereospecific while the addition of monomer is highly isotactic-specific ($m/r > 50$). The addition of a proton to the oligomer anion of isopropyl acrylate formed with phenylmagnesium bromide was reported to be highly stereospecific as well as the addition of monomer to the anion[19,20]; the reason for the difference from our result is not clear at present.

The *m*/*r* ratio at the α-end of the trimer was 18.6 ($= (mm+mr)/(rm+rr)$) and values between 10 and 20 were obtained for higher oligomers (Figure 11), indicating that the addition of MMA to the unimer anion is less isotactic-specific than that to the higher propagating anion. This suggests that the penultimate

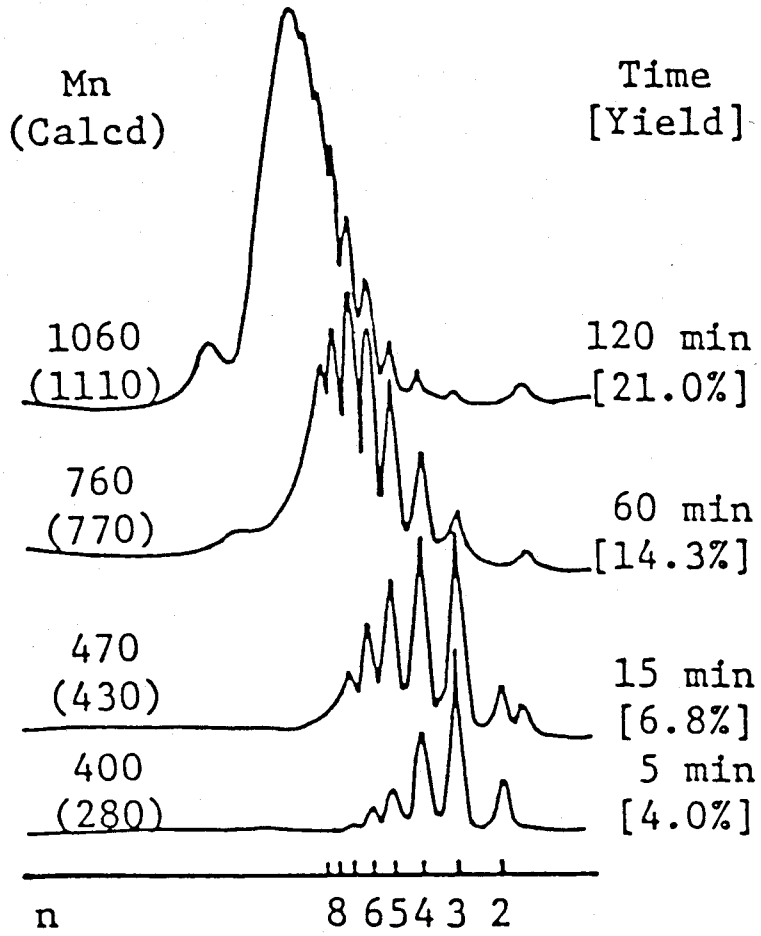

Figure 9. GPC curves of MMA-oligomers prepared with *t*-C_4H_9MgBr in toluene at -78°C for various polymerization times.

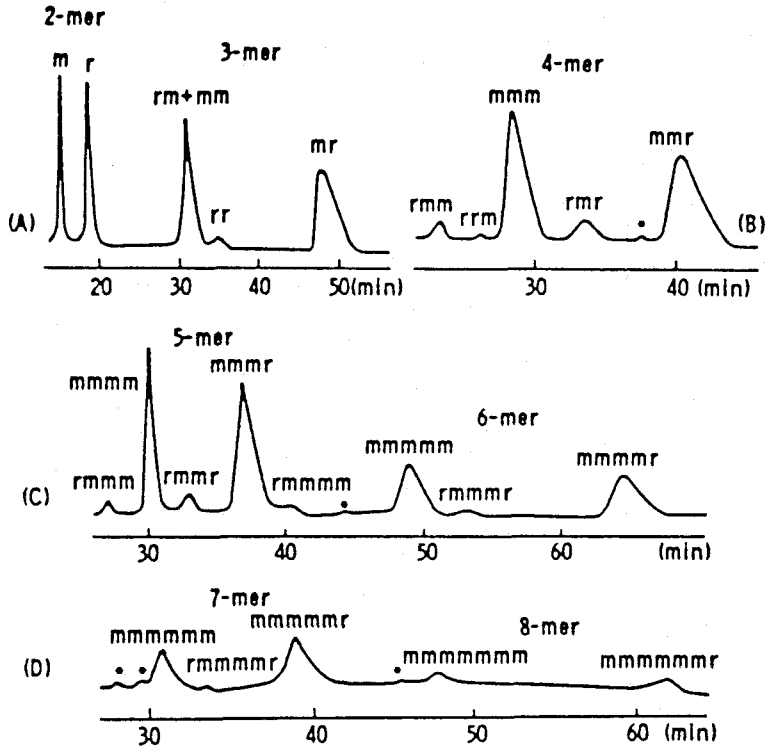

Figure 10. HPLC traces of the MMA-oligomers prepared with *t*-C_4H_9MgBr in toluene at -78°C for 15 min. Eluent, C_4H_9Cl/CH_3CN = 97.5/2.5 (A), 96/4 (B), 95/5 (C), 88/12 (D); column, silica gel, 4.6 mm(*i.d*) x 250 mm; detector, RI.

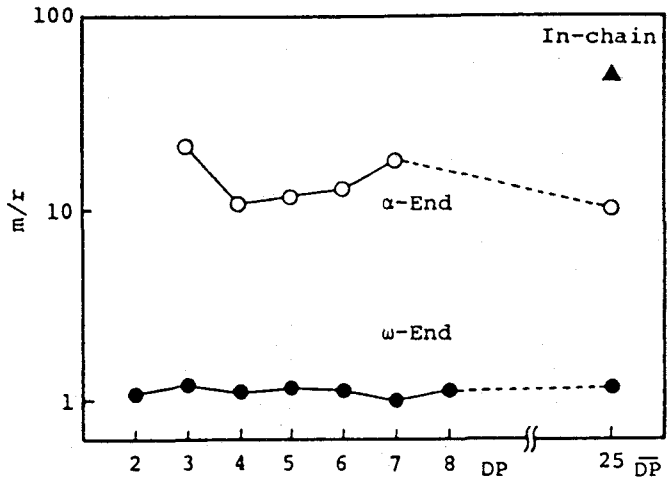

Figure 11. *meso/racemo* ratios at the α- and ω-ends of the MMA-oligomers obtained from the polymerization with *t*-C_4H_9MgBr in toluene at -78°C for 15 min. The *meso/racemo* ratio for the PMMA of *DP* = 25 are also shown.

monomeric unit of the propagating anion coordinates to the active cites and contributes the stereoregulation in the highly isotactic polymerization [11].

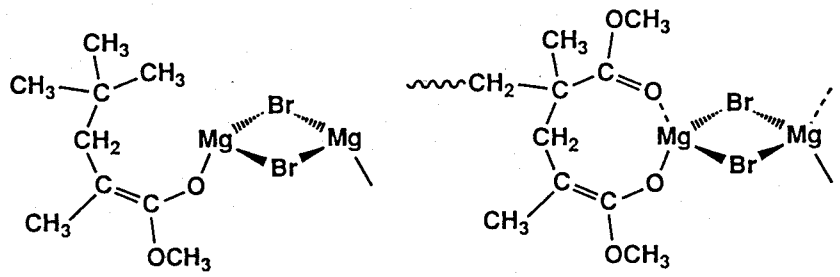

[11]

α-End In-chain

Further, the penultimate monomeric unit is considered to stabilize the propagating anion forming the active species for the living polymerization. On the other hand, the the unimer anion should be so labile that the unimer is hardly detected in the polymerization product.

2.5 Two-dimensional NMR Spectra of the Isotactic PMMA Prepared with *t*-Butylmagnesium Bromide and Detailed Examination of Tacticity[14]

Detailed investigation of the configurational sequence of an oligomer or low molecular weight polymer often provides significant information on the steric course of addition of monomer in anionic polymerization. However, this is not so easy since the resonances due to end groups and/or monomeric units located at α- and ω-ends sometimes overlap closely with the signals sensitive to the configurational sequences in chain.

Recently, two-dimensional (2D) NMR has been used in the field of polymer chemistry to make absolute tacticity assignments[31-39], investigation of monomer sequence distribution[40-42] and structural analysis of polymer and oligomer[35,43-46].

In this work we studied the structures of the isotactic PMMA prepared with *t*-C_4H_9MgBr extensively using 2D NMR, and made the peak assignments for the end groups and the monomeric units at and near the polymer ends, leading to the exact determination of

tacticity of PMMA. NMR signals due to the monomeric units at α-end may depend on the kind of initiator used, but those at ω-end should not be so different even if the polymers are prepared with different initiators. Accordingly, the peak assignments for the ω-end in this study will be applicable to most of the PMMA or oligo(MMA) prepared by anionic initiators.

Figure 12 shows a 400 MHz ^{1}H NMR spectrum of the PMMA prepared with t-C_4H_9MgBr in toluene at -78°C. The *Mn* of the PMMA was determined as 2530 by VPO and the *Mw/Mn* value determined by GPC was 1.20. It is evident from the α-CH_3 and CH_2 signals that the PMMA is highly isotactic, though signals due to the monomeric units at and near the α- and ω-ends also appear in this region. The peak assignments were made with the aid of 2D NMR spectra as described below. The numbering system for the monomeric units in the PMMA is also displayed in Figure 12. The polymer gave ^{1}H COSY and 2D *J*-resolved spectra that are shown in Figures 13 and 14.

Window functions such as sine-bell and sine-square function are commonly employed in the Fourier transform of 2D NMR data matrices in order to suppress peak broadening. In this work, the window functions also served to emphasize the correlation peaks originate from polymer-end groups, since relaxation times of the protons are much different between in-chain monomeric units and polymer-end groups.

The multiplet in the methine region (*cf.* Figure 12) between 2.39 and 2.54 ppm was assigned to the methine proton at the ω-end (ω_1-CH) and disappeared when the polymerization was terminated using CD_3OD[47]. The *J*-resolved spectrum clearly shows that the multiplet consists of two multiplets centered at 2.49 and 2.45 ppm (Figure 14), the intensity ratio of which was approximately 6:4 from a broadband decoupled ^{1}H spectrum displayed in the top of Figure 14. The occurrence of the two methine peaks is due to the tacticity of dyad at the ω-end. The lower field peak of higher intensity can be assigned to the methine proton of *racemo* dyad (ω_1-CH(*r*)) and the higher field peak of lower intensity to *meso* dyad (ω_1-CH(*m*)), according to the detailed ^{1}H NMR studies of the MMA oligomers (Chapter 3).

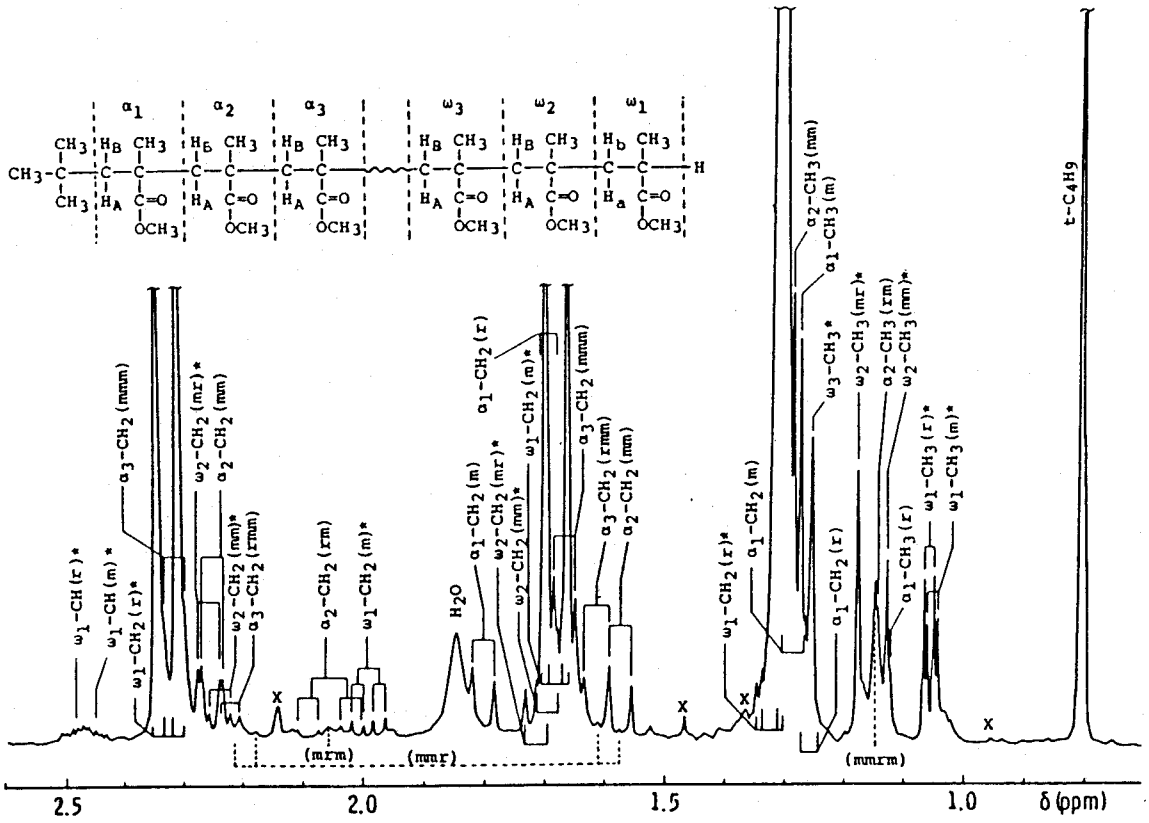

Figure 12. 400 MHz ^{1}H NMR spectrum of the isotactic PMMA prepared with *t*-C_4H_9MgBr in toluene at -78°C (*Mn* = 2530). Signals due to the end groups and monomeric units at and near the α- and ω-ends are indicated according to the numbering system shown in the figure. The methyl signal of *mmrm* pentad and the methylene signals of *mmr* and *mrm* tetrads are also indicated with dashed lines. "x" denotes signals due to impurities. (Nitrobenzene-*ds*, 110°C)

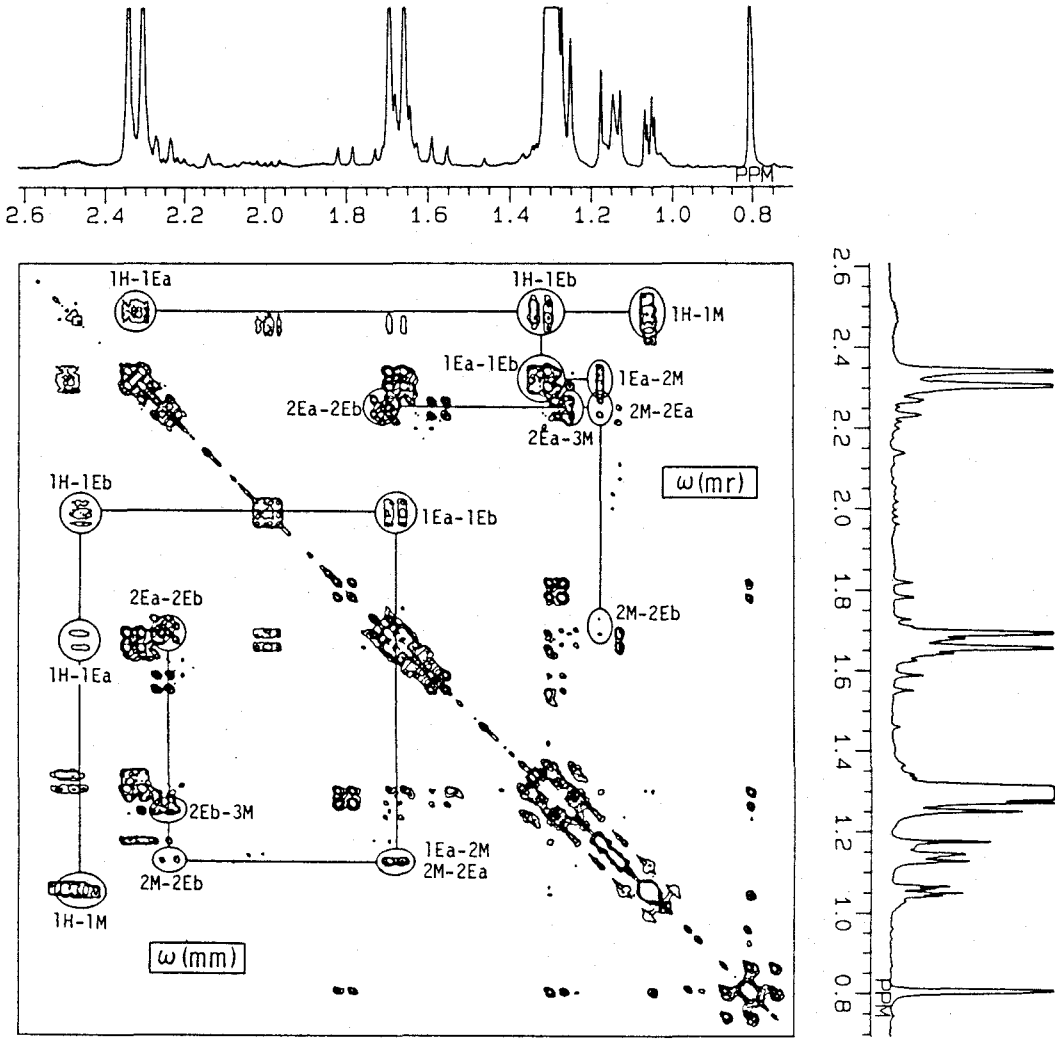

Figure 13. 400 MHz ^{1}H COSY spectrum of the isotactic PMMA prepared with *t*-C_4H_9MgBr in toluene at -78°C. Series of off-diagonal signals due to the $\omega(mm)$ and $\omega(mr)$ structures are indicated in this figure (*cf.* Figure 17). Peak numbers show protons correlated with each other; e.g. "1H-1E" denotes the correlation signal between ω_1-CH and ω_1-CH_2. M, E and H represent methyl, methylene and methine protons, respectively.

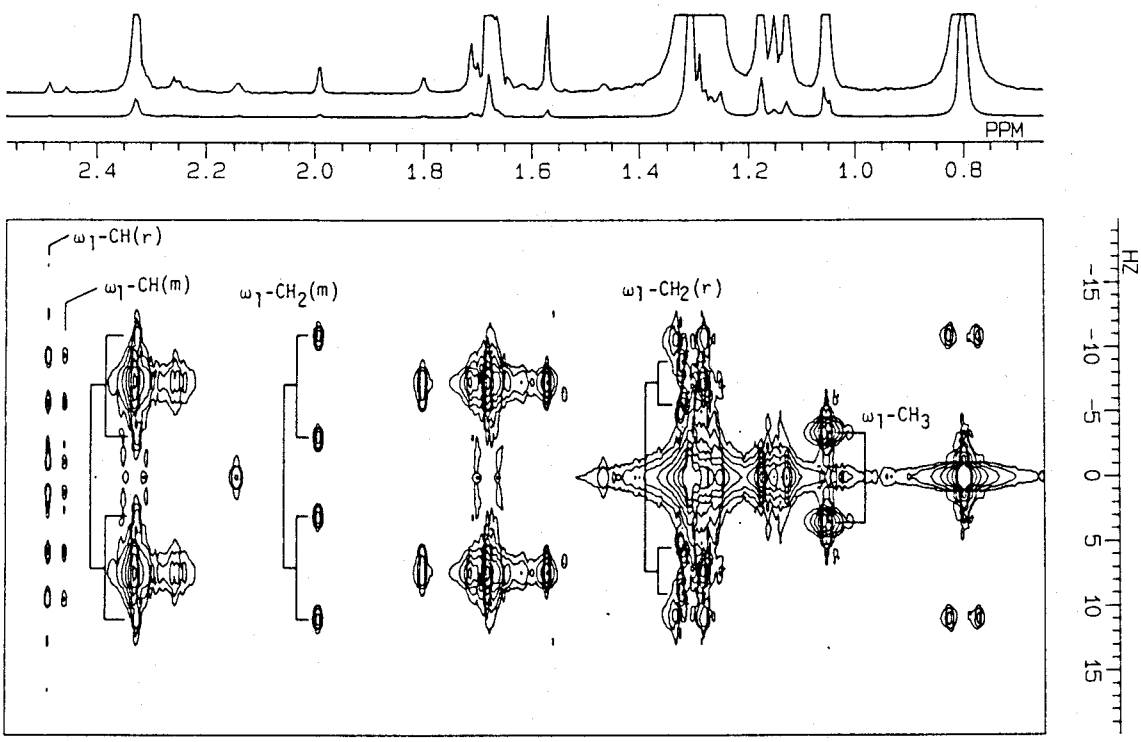

Figure 14. Two-dimensional *J*-resolved spectrum of the isotactic PMMA prepared with *t*-C_4H_9MgBr in toluene at -78°C. The spectrum shown above is the projection to the F_1-axis (broad-band decoupled spectrum).

Four peaks in the syndiotactic α-methyl region around 1.05 ppm were found to be actually two overlapped doublets at 1.04$_5$ and 1.06$_3$ ppm from the *J*-resolved spectrum. In the ^{1}H COSY spectrum these two doublets show connectivity with the peaks of ω_1-CH(*r*) and ω_1-CH(*m*), respectively ([ω(*mr*)1H-1M] and [ω(*mm*)1H-1M] in Figure 13), and the intensity ratio is about 6:4. Thus, the doublet at 1.06$_3$ ppm is assigned to ω_1-CH$_3$(*r*) and that at 1.045 ppm to ω_1-CH$_3$(*m*).

The quartet at 1.98 ppm is best seen as a doublet of doublets with the coupling constants J_{gem} and J_{vic} of -14.0 and 7.9 Hz, and is assigned to one of the ω_1-CH$_2$(*m*) methylene protons since the correlation signals with ω_1-CH(*m*) were observed in the COSY spectrum [ω(*mm*)1H-1Eb]. The COSY spectrum shows that the partner proton resonates at 1.68 ppm and overlapps with the strong doublet at 1.67 ppm [ω(*mm*)1Ea-1Eb]. This partner proton signal also correlates with ω_1-CH(*m*) [ω(*mm*)1H-1Ea]. The partnership of these two protons is also evident by ^{13}C-^{1}H COSY spectra and the carbon of ω_1-CH$_2$(*m*) was found to resonate at 42.44 ppm (Figure 15). Analogous to the way that the ω_1-CH$_2$(*m*) methylene signals were identified, the signals of ω_1-CH$_2$(*r*) protons were detected at 1.32 and 2.32 ppm, both of them overlapped by strong signals due to in-chain monomeric units. The *J*-resolved spectrum indicated each signal to be the doublet of doublets with J_{vic} = 3.5 and 7.7 Hz, respectively, and J_{gem} = -14.3 Hz. The chemical shift between these two ω_1-CH$_2$(*r*) protons is much larger than that between the signals of two ω_1-CH$_2$(*m*) protons, which supports our *meso/racemo* assignments (Chapter 4). The *vicinal* coupling constants between ω_1-CH$_2$ and ω_1-CH protons reflect the conformation of the dyad at the ω-end.

Two singlets at 1.175 and 1.128 ppm were assigned to ω_2-CH$_3$ protons in *mr* and *mm* triads (ω_2-CH$_3$(*mr*) and ω_2-CH$_3$(*mm*)), respectively. The former correlates with ω_1-CH$_2$(*r*) proton at 2.32 ppm [ω(*mr*)1Ea-2M] and the latter with ω_1-CH$_2$(*m*) proton at 1.68 ppm [ω(*mm*)1Ea-2M]. The intensity ratio is again 6:4. These two singlets also correlate with the carbon resonances at 21.11 and 21.66 ppm, respectively (Figure 16), which are recognized as methyl carbon signals by DEPT spectrum. The presence of *rm* and *rr* triads at the ω-ends can be neglected because the configura-

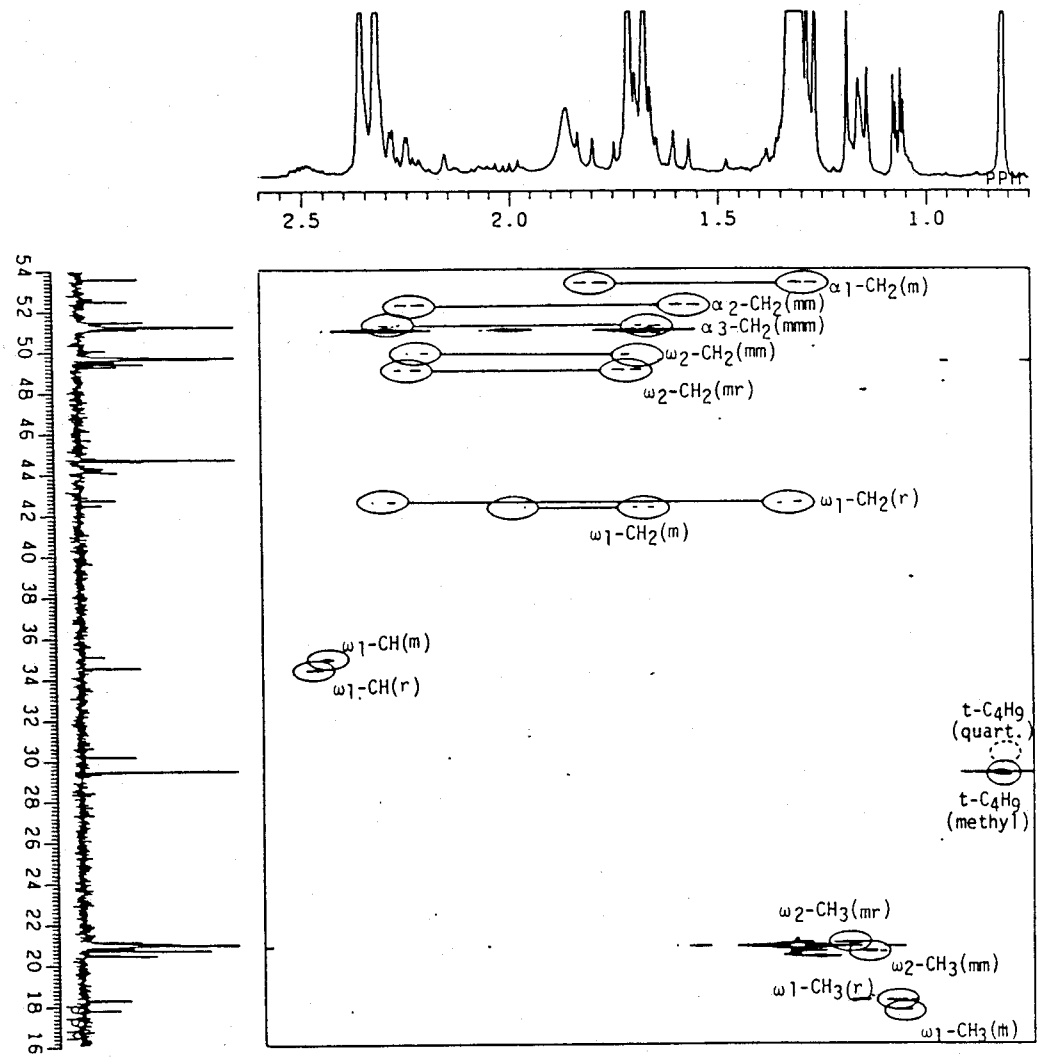

Figure 15. ^{13}C-^{1}H COSY spectrum of the PMMA prepared with *t*-C_4H_9MgBr in toluene at -78°C.

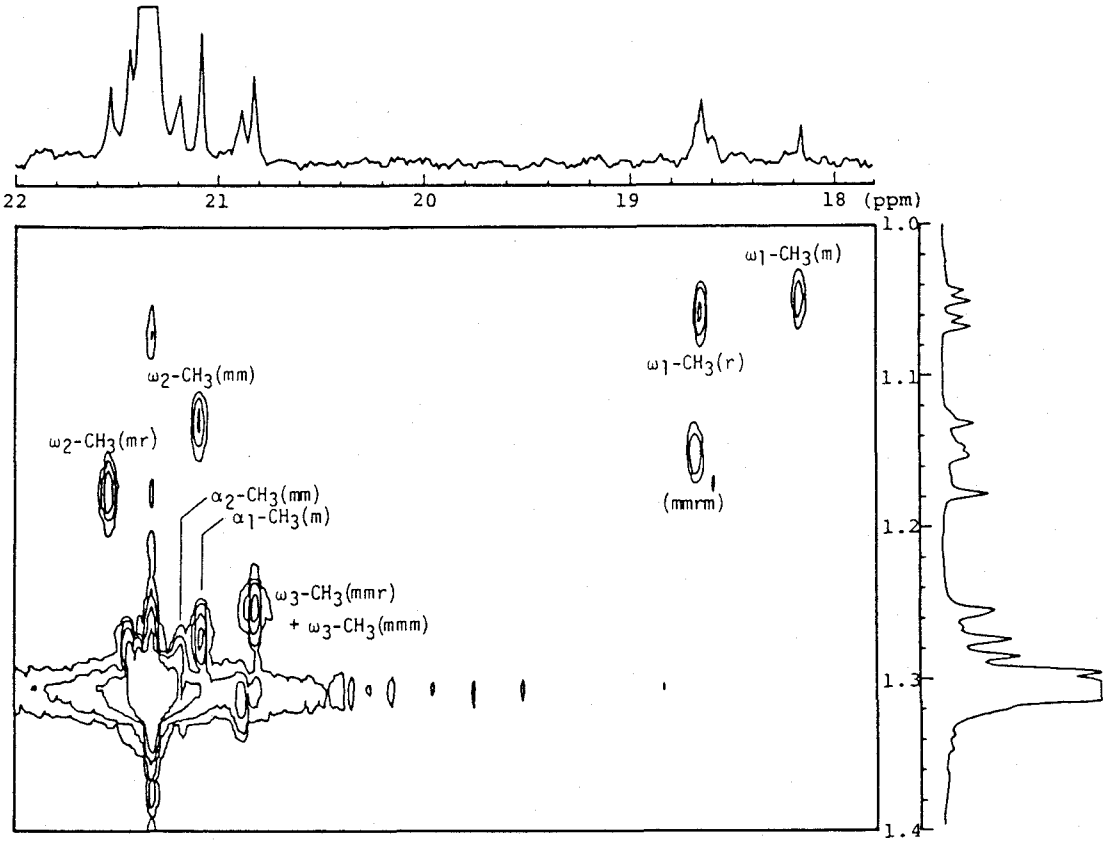

Figure 16. Expansion of the methyl region of the ^{13}C-^{1}H COSYspectrum of the PMMA prepared with *t*-C_4H_9MgBr in toluene at -78°C.

tional sequence of in-chain monomeric units is highly isotactic.

The signal of ω_2-CH_3(*mr*) is also related with the doublets at 2.25 [ω(*mr*)2M-2Ea] and 1.71 ppm [ω(*mm*)2M-2Eb] which are strongly correlated with each other [ω(*mr*)2Ea-2Eb]. This pair of doublets should be due to ω_2-CH_2(*mr*) protons. A small doublet at 2.24 ppm was assigned to one of the ω_2-CH_2(*mm*) protons since it shows cross peak to ω_2-CH_3(*mm*) signal [ω(*mm*)2M-2Eb]. The partner proton signal is proved to be located at 1.69 ppm from the COSY spectrum [ω(*mm*)2Ea-2Eb].

Singlet at 1.25 ppm shows connectivity with the ω_2-CH_2(*mr*) signal at 2.25 ppm [ω(*mr*)2Ea-3M] and with the ω_2-CH_2(*mm*) signal at 2.24 ppm [ω(*mm*)2Eb-3M], and thus, the singlet is the overlap of two resonances due to ω_3-CH_3(*mmr*) and ω_3-CH_3(*mmm*). The peak intensity is nearly equal to the sum of intensities of the signals due to ω_2-CH_3(*mr*) and ω_2-CH_3(*mm*) protons. This indicates that the dyad tacticity between ω_2- and ω_3-monomeric units is exclusively isotactic. Block copolymer of *t*-C_4H_9-(MMA-*d*$_8$)$_{10}$-*block*-(MMA)$_{10}$-H did not show the peak at 1.25 ppm, providing additional evidence for the assignment.

The signals of methylene protons beyond ω_2-unit and methyl protons beyond ω_3-unit are considered to belong to strong signals due to the in-chain methyl and methylene protons.

The methyl and methylene signals of the monomeric units at and near the α-end are also observed apart from the signals of in-chain protons. A set of methylene proton signals located at 1.28 and 1.80 ppm shows connectivity with *t*-C_4H_9 signal in the ^{1}H COSY spectrum and is assigned to α_1-CH_2(*m*) protons (*cf.* [α(*mm*)tB-1Ea] and [α(*mm*)tB-1Eb] in Figure 17). Non-equivalence of these two protons is due to the fact that they are adjacent to a chiral center at the α_1-quaternary carbon.

The singlet at 1.27_3 ppm shows connectivity with α_1-CH_2(*m*) proton at 1.80 ppm [α(*mm*)1Eb-1M], and thus, is assigned to the α_1-CH_3(*m*) signal. The α_1-CH_3(*m*) singlet also correlates with the doublet at 1.57 ppm [α(*mm*)1M-2Ea] which strongly correlates with the doublet at 2.25 ppm [α(*mm*)2Ea-2Eb]. This pair of doublets is assigned to α_2-CH_2(*mm*) protons. The singlet at 1.28_2 ppm shows a cross peak to one of the α_2-CH_2(*mm*) signals [α(*mm*)2Eb-2M], and is attributed to α_2-CH_3(*mm*) protons. The

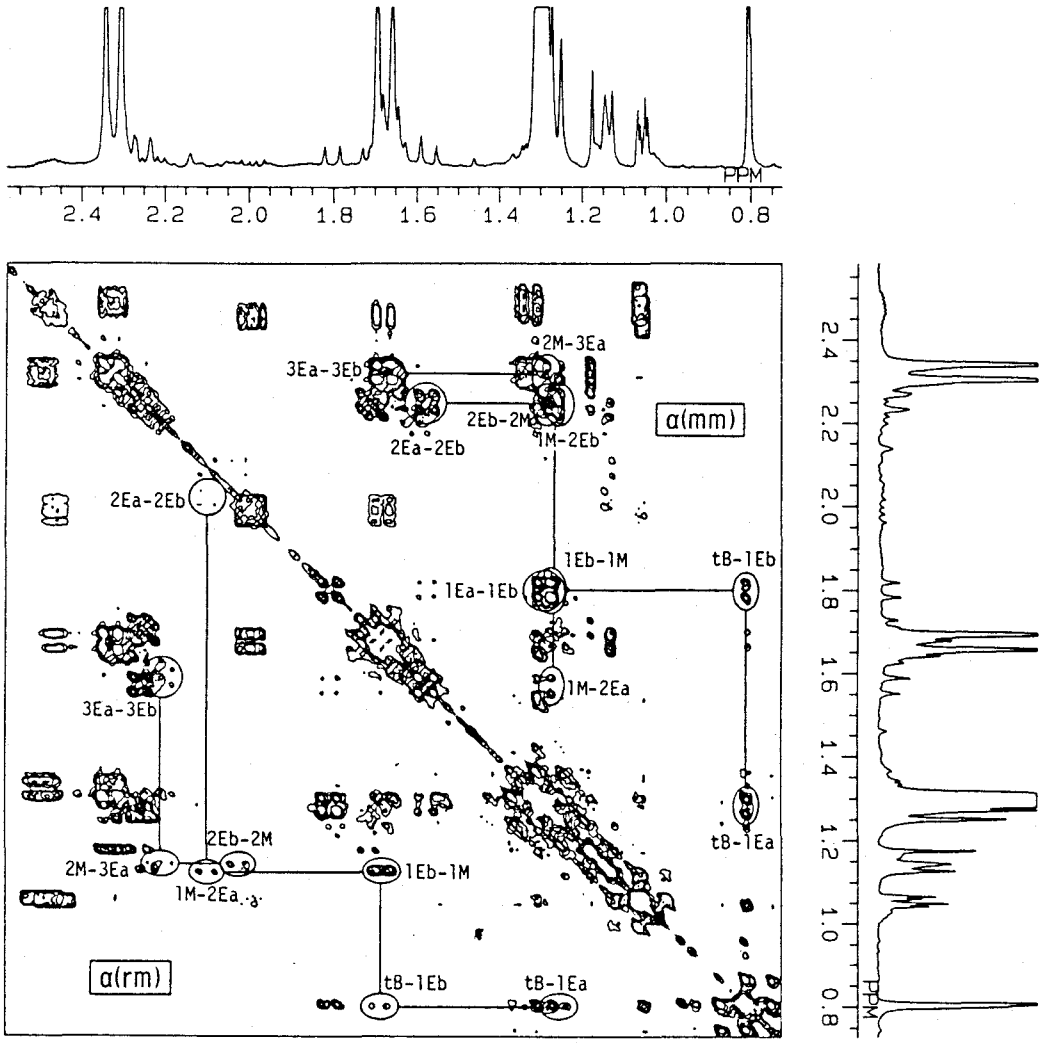

Figure 17. 400 MHz ^{1}H COSY spectrum of the isotactic PMMA prepared with t-C_4H_9MgBr in toluene at -78°C. Series of off-diagonal signals due to the $\alpha(mm)$ and $\alpha(rm)$ structures are indicated in this figure. "tB" denotes the t-C_4H_9 group at the α-end. Other designations follow the system adopted in Figure 13.

signal of α_2-CH_3(*mm*) shows connectivity with the signals at 1.66 and 2.32 ppm due to another set of methylene protons [α(*mm*)2M-3Ea], *cf.* [α(*mm*)3Ea-3Eb], indicating these signals to be assigned to α_3-CH_2(*mmm*).

All the pairs of methylene proton signals mentioned above can be seen clearly in the ^{13}C-^{1}H COSY spectrum (Figure 15). ^{13}C NMR signals of the ω-end methine carbons (ω_1-CH(*r*) and ω_1-CH(*m*)) and the α-end *t*-butyl group can be easily assigned from the ^{13}C-^{1}H COSY spectrum. The signal assignments for ^{13}C NMR spectrum thus obtained are shown in Figures 15 and 16.

To understand the mechanism of polymerization, it is important to elucidate the detailed tacticity at the ends of the polymer chain. The structural investigation of the trimers and tetramers obtained in the polymerization of MMA by *t*-C_4H_9MgBr in toluene at -78°C indicated that the tacticity at the α-end was mostly isotactic though the isotacticity was not so high as that of in-chain sequence[17]. The sequence of correlation peaks indicated by α(*rm*) in Figure 17 shows that there occurs some *racemo* enchainment at the α_1-end of the polymer chain. The signals of methyl and methylene protons at and near the α(*rm*)-end are very weak in intensity and is hardly detectable in the normal one-dimensional NMR spectrum, but they can easily be observed in the COSY spectrum as described below.

In Figure 17, one can find a couple of doublets at 1.26 and 1.69 ppm; this correlates with the signal of the α-end *t*-butyl protons [α(*rm*)tB-1Ea, α(*rm*)tB-1Eb]. These doublets correlate with each other [α(*rm*)1Ea-1Eb], and are assigned to α_1-CH_2(*r*). One of the α_1-CH_2(*r*) protons show connectivity with α_1-CH_3(*r*) protons at 1.13 ppm [α(*rm*)1Eb-1M]. The peak assignments for α_2-CH_2(*rm*), α_2-CH_3(*rm*) and α_3-CH_2(*rmm*) were made similarly from Figure 17 (*cf.* Figure 12). The intensity ratio of α_1-*mm* and α_1-*rm* is estimated to be about 10:1 from the intensities of α_1-CH_2(*m*) and α_2-CH_2(*rm*) signals.

In summary, correlation diagrams of the methyl and methylene protons for triad sequences at α- and ω-ends are shown in Figure 18. Proton pairs which showed correlation peaks in the COSY spectrum are connected by arrows.

Chemical shifts of the protons in the α-*mm*, α-*mr*, ω-*mm* and

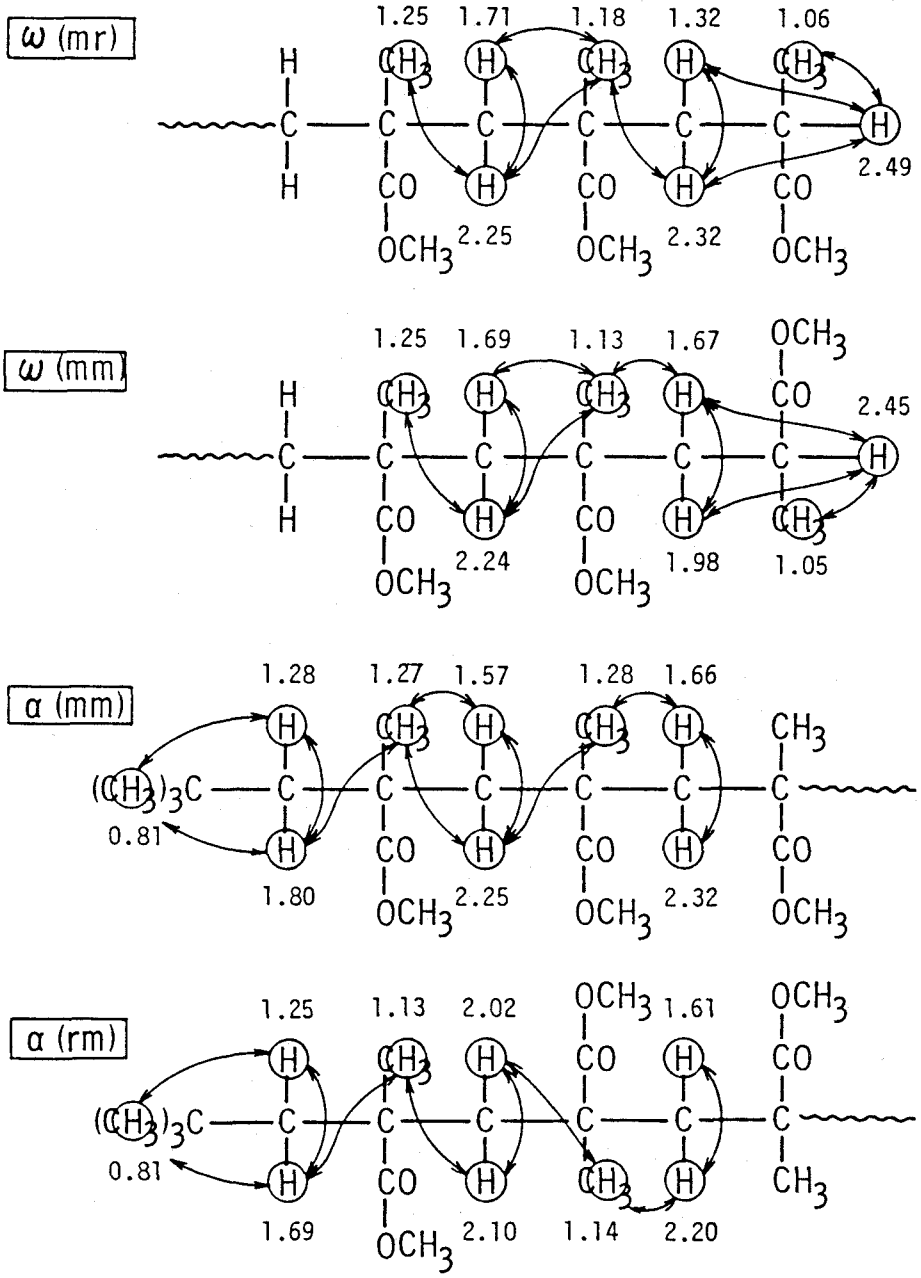

Figure 18. The correlation diagram of the protons at and near the $\omega(mm)$, $\omega(mr)$, $\alpha(mm)$ and $\alpha(rm)$-ends in the isotactic PMMA. Protons which show correlation peaks in the COSY spectrum are connected with arrows. Values shown are chemical shifts from HMDS in ppm.

ω-*rm* dyads are summarized in Figure 19 together with those in the *m*- and *r*-dimers, *mm*-, *mr*-, *rm*- and *rr*-trimers[17] and *mmmm* and *mmrm* pentads of PMMA. It is noteworthy that chemical shifts of the methyl and methylene protons at and near the α- and ω-ends of the PMMA agree with those of the oligomers in the corresponding stereochemical sequences.

The signals of the α-CH_3 and CH_2 groups in the first two and the last two monomeric units at the α- and ω-ends overlapped with the resonances of in-chain α-CH_3 groups as summarized below.

α-CH_3 region	Assignment	δ (ppm)
Syndiotactic; *rr*	ω_1-CH_3 (*m*)	1.04$_5$
(1.01 - 1.08 ppm)	ω_1-CH_3 (*r*)	1.06$_3$
	α_1-CH_3 (*r*)	1.12$_5$
Heterotactic; *mr*	ω_2-CH_3 (*mm*)	1.12$_8$
(1.12 - 1.19 ppm)	α_2-CH_3 (*rm*)	1.14$_0$
	ω_2-CH_3 (*mr*)	1.17$_5$
	α_1-CH_2 (*r*)	1.25
Isotactic; *mm*	α_1-CH_3 (*m*)	1.27$_3$
(1.23 - 1.39 ppm)	α_1-CH_2 (*m*)	1.28
	α_2-CH_3 (*mm*)	1.28$_2$
	ω_1-CH_2 (*r*)	1.32

In order to determine exact triad tacticity from the α-CH_3 signals, the following peak assignments must be taken into consideration: (i) the methylene signals are eliminated; (ii) α_1-CH_3 and ω_1-CH_3 signals are counted out by definition of triad tacticity; (iii) the signals of α_2-CH_3 and ω_2-CH_3 should be excluded from the point of view of polymerization mechanism. Therefore, the most exact triad tacticity of the interior monomeric sequences, *I*, *H* and *S*, at the level of our knowledge can be calculated using the following equations.

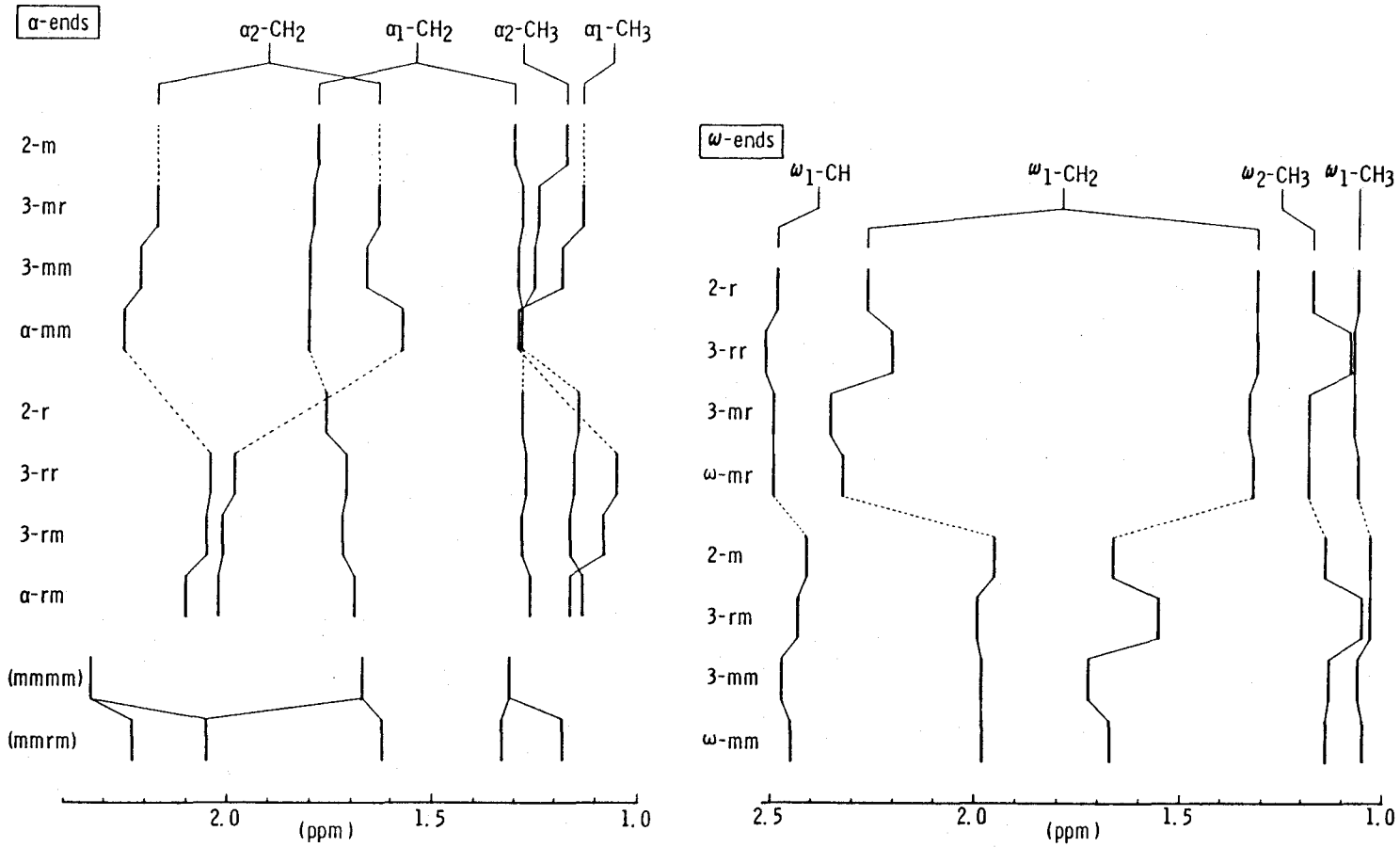

Figure 19. ^{1}H NMR chemical shifts of α_1-, α_2-, ω_1- and ω_2-CH_3, α_1-, α_2- and ω_1-CH_2, and ω_1-CH protons in the dimers, trimers and the isotactic polymer of MMA prepared with t-C_4H_9MgBr in toluene at -78°C.

$$s_c = s - [\omega_1\text{-}CH_3(m+r)]$$
$$= s - 3P$$

$$h_c = h - [\alpha_1\text{-}CH_3(r)] - [\alpha_2\text{-}CH_3(rm)] - [\omega_2\text{-}CH_3(mm+mr)]$$
$$= h - 3R(\alpha)P - 3R(\alpha)P - 3P$$
$$= h - 3.6P$$

$$i_c = i - [\alpha_1\text{-}CH_2(m+r)]/2 - [\alpha_1\text{-}CH_3(m)] - [\alpha_2\text{-}CH_3(mm)]$$
$$- [\omega_1\text{-}CH_2(r)]/2$$
$$= i - P - 3(1 - R(\alpha))P - 3(1 - R(\alpha))P - (1 - R(\omega))P$$
$$= i - 6.8P$$

$$P = [t\text{-}C_4H_9]/9$$

$$R(\alpha) = \alpha_1(m)/\alpha_1(m+r)$$
$$= \alpha_2(mrm)/\alpha_2(mm+rm) \qquad (\because\ \alpha_2(rr),\ \alpha_2(mr) = 0)$$
$$= [\alpha_2\text{-}CH_2(rm)]/([\alpha_1\text{-}CH_2(m)] + [\alpha_2\text{-}CH_2(rm)])$$
$$= 0.1$$

$$R(\omega) = \omega_1(r)/\omega_1(m+r)$$
$$= \omega_2(mr)/\omega_2(mm+mr) \qquad (\because\ \omega_2(rr),\ \omega_2(rm) = 0)$$
$$= [\omega_2\text{-}CH_3(mr)]/[\omega_2\text{-}CH_3(mm+mr)]$$
$$= 0.6$$

$$S = s_c/(i_c + h_c + s_c)$$

$$H = h_c/(i_c + h_c + s_c)$$

$$I = i_c/(i_c + h_c + s_c)$$

Here, s, h and i denote intensities of the signals in the regions of 1.01 - 1.08 ppm, 1.12 - 1.19 ppm, and 1.23 - 1.39 ppm, respectively. $[t\text{-}C_4H_9]$ represents the intensity of the signal due to the t-C_4H_9 group; the intensities of other signals are represented in a similar manner. P designates the intensity of one proton in a polymer chain. The subscript c indicates the calibrated value. $R(\alpha)$ and $R(\omega)$ are fractions of *racemo* enchainment at the α- and ω-ends. The triad tacticity, I, H and S, of the PMMA thus calculated were 95.8, 3.5 and 0.7 %, respectively.

Table 1 shows the calibrated tacticities of several PMMAs obtained by t-C_4H_9MgBr at -78°C in toluene at various ratios of

the monomer to the initiator. The calibrated tacticities revealed that the isotacticity of interior monomeric sequences was independent of molecular weight. In other words, the stereoregulating power of the propagating species in the isotactic polymerization of MMA by *t*-C_4H_9MgBr in toluene does not change in the course of polymerization, though it is slightly lower at the initiation process.

2.6 Experimental Part

2.6.1 Materials

MMA, MMA-*ds* and EMA were purified by distillation, and then distilled twice over calcium dihydride under high vacuum just before use. Toluene was purified in the usual manner and then distilled under high vacuum after treatment with butyllithium.

t-C_4H_9MgBr was prepared in diethyl ether from *t*-butyl bromide and magnesium. The amounts of *t*-C_4H_9Mg- group, Mg^{2+} and Br^- were determined by acid-base titration, chelatometric titration and precipitation titration (Fajans's method), respectively. *n*-C_4H_9MgBr, *iso*-C_4H_9MgBr and *s*-C_4H_9MgBr were prepared and analyzed similarly. *iso*-C_4H_9MgBr and *s*-C_4H_9MgBr were also prepared in the presence of 1,2-dibromoethane to obtain a solution of the reagent containing an excess amount of $MgBr_2$.

$$C_4H_9Br + 2\,Mg + BrCH_2CH_2Br \longrightarrow C_4H_9MgBr + MgBr_2 + CH_2{=}CH_2$$

$(t\text{-}C_4H_9)_2Mg$ was synthesized by adding a large amount of dioxane to the diethyl ether solution of *t*-C_4H_9MgBr. The initiators with various ratios of $[Mg^{2+}]/[t\text{-}C_4H_9Mg]$ were prepared by mixing certain amounts of *t*-C_4H_9MgBr obtained in diethyl ether and $(t\text{-}C_4H_9)_2Mg$. A small amount of precipitate was formed during the mixing and the supernatant liquid was used as the initiator solution.

2.6.2 Procedures

Polymerization was initiated by adding monomer with a hypo-

dermic syringe slowly to an initiator solution in toluene cooled to the polymerization temperature. The reaction vessel was then sealed off. Polymerization was terminated by adding methanol containing HCl (2 N) equivalent to the Mg^{2+} at the reaction temperature. The reaction mixture was poured into a large amount of hexane to precipitate the polymeric product. The precipitate was collected by filtration, washed with hexane and then water several times, and dried under vacuum at 60°C. The polymer thus obtained was dissolved in benzene and the insoluble material was filtered off. The polymer was recovered from the solution by freeze-drying.

2.6.3 Measurements

The molecular weights of the polymers were measured on a Hitachi 117 vapor pressure osmometer (VPO) in toluene at 60°C or on a JASCO FLC-A10 GPC chromatograph equipped with a Shodex GPC column A-80M (50 cm x 2) and KF-802.5 (30 cm x 1) with maximum porosity of 5 x 10^7 and 4 x 10^4, respectively, using THF as an eluent. The GPC chromatogram was calibrated against standard polystyrene samples. The molecular weights were also determined from the relative intensities of the ^1H NMR signals due to the t-C_4H_9 and OCH_3 groups.

NMR spectra were recorded on a JEOL GX-400 spectrometer using 15 %(*w/v*) solution in nitrobenzene-d_5 at 110°C. The instrument were operated with a frequency of 400 MHz for ^1H and 100 MHz for ^{13}C. ^1H chemical shifts were referred to the residual protons in the *ortho*-position of nitrobenzene-d_5 and converted to hexamethyl disiloxane (HMDS) scale as nitrobenzene - HMDS = 7.352 ppm. ^{13}C chemical shifts were measured similarly (nitrobenzene - HMDS = 121.31 ppm).

The ^1H COSY experiment employed a recycle time of 1.2 s, with 100 transients being collected for each t_1 value. A delay time of 200 ms was adopted for long-range enhancement and also for enhancement of the signals from the polymer ends. A total of 512 spectra, each consisting of 1024 data points, were accumulated, with a frequency range of 1350 Hz in both dimensions. In the ^{13}C-^1H COSY experiment, ^1H-^1H was broad-band decoupled as well as ^{13}C-^1H decoupling[48].

References

1. B. C. Anderson, G. D. Andrews, P. Arthur, Jr., H. W. Jacobson, A. J. Playtis, W. H. Sharkey, *Macromolecules*, **14**, 1599 (1981).
2. P. Lutz, P. Masson, G. Beinert, P. Rempp, *Polym. Bull.*, **12**, 79 (1984).
3. O. W. Webster, W. R. Hertler, D. Y. Sogah, W. B. Farnham, T. V. Rajanbabu, *J. Am. Chem. Soc.*, **105**, 5706 (1983).
4. P. E. M. Allen, B. O. Bateup, *Eur. Polym. J.*, **14**, 1001 (1978).
5. P. E. M. Allen, C. Mair, *Eur. Polym. J.*, **20**, 697 (1984).
6. P. E. M. Allen, D. R. G. Williams, *Ind. Eng. Chrm. Prod. Res. Dev.*, **24**, 334 (1985).
7. K. Matsuzaki, H. Tanaka, T. Kanai, *Makromol. Chem.*, **182**, 2905 (1981).
8. K. Hatada, T. Kitayama, K. Fujikawa, K. Ohta, H. Yuki, *ACS Symp. Ser.*, **166**, 327 (1981).
9. K. Hatada, K. Ute, K. Tanaka, T. Kitayama, Y. Okamoto, *Polym. J.*, **17**, 977 (1985).
10. K. Hatada, K. Ute, K. Tanaka, Y. Okamoto, T. Kitayama, *Polym. J.*, **18**, 1037 (1986).
11. Y. Okamoto, K. Ohta, K. Hatada, H. Yuki, *ACS Symp. Ser.* **166**, 353 (1981).
12. M. A. Doherty, T. E. Hogen-Esch, *ACS Polym. Prep.*, **25(2)**, 5 (1984).
13. A. Soum, N. D'Accorso, M. Fontanille, *Makromol. Chem. Rapid Commun.*, **4**, 471 (1983).
14. K. Hatada, K. Ute, K. Tanaka, M. Imanari, N. Fujii, *Polym. J.*, **19**, 425 (1987).
15. J. Salonen, G.-A. Holmberg, *Acta Chem. Scand.*, **B31**, 719 (1977).
16. T. Kitayama, K. Ute, M. Yamamoto, N. Fujimoto, K. Hatada, *Polym. J.*, **22**, 386 (1990).
17. K. Hatada, K. Ute, K. Tanaka, T. Kitayama, *Polym. J.*, **19**, 1325 (1987).
18. K. Hatada, K. Ute, T. Kitayama, K. Tanaka, M. Imanari, N. Fujii, *Polym. J.*, **21**, 447 (1989).
19. T. Yoshino, H. Iwanaga, K. Kuno, *J. Am. Chem. Soc.*, **89**, 677 (1967).
20. T. Yoshino, H. Iwanaga, *J. Am. Chem. Soc.*, **90**, 2434 (1968).
21. T. E. Hogen-Esch, C. F. Tien, *Macromolecules*, **13**, 207 (1980).
22. A. H. Soum, T. E. Hogen-Esch, *Macromolecules*, **18**, 690 (1985).
23. M. A. Buese, T. E. Hogen-Esch, *Macromolecules*, **17**, 118 (1984).
24. M. A. Buese, T. E. Hogen-Esch, *J. Am. Chem. Soc.*, **107**, 4509 (1985).
25. C. F. Tien, T. E. Hogen-Esch, *J. Polym. Sci., Polym. Chem. Ed.*, **17**, 281 (1979).
26. G. Wulff, R. Sczepan, A. Steigel, *Tetrahedron Lett.*, **27**, 1991 (1986).
27. Y. Okamoto, E. Yashima, T. Nakano, K. Hatada, *Chem. Lett.*, 759 (1987).
28. R. A. Volpe, T. E. Hogen-Esch, A. H. E. Muller, F. Gores, *Polym. Prep., Am. Chem. Soc., Div. Polym. Chem.*, **28**(2), 423 (1987).
29. L. Lochmann, S. Pokorny, J. Trekoval, H.-J. Adler, W. Berger, *Makromol. Chem.*, **184**, 2021 (1983).
30. A. H. E. Muller, L. Lochmann, J. Trekoval, *Makromol. Chem.*, **187**, 1473

(1986).
31. S. Macura, L. R. Brown, *J. Magn. Reson.*, **53**, 529 (1983).
32. P. A. Mirau, F. A. Bovey, *Macromolecules*, **19**, 210 (1986).
33. M. W. Crowther, N. M. Szeverenyi, G. C. Levy, *Macromolecules*, **19**, 1333 (1986).
34. G. P. Gippert, L. R. Brown, *Polym. Bull.*, **11**, 585 (1984).
35. M. D. Bruch, F. A. Bovey, R. E. Cais, *Macromolecules*, **17**, 2547 (1984).
36. H. N. Cheng, G. H. Lee, *Polym. Bull.*, **13**, 549 (1985).
37. M. D. Bruch, F. A. Bovey, R. E. Cais, J. H. Noggle, *Macromolecules*, **18**, 1253 (1985).
38. F. C. Schilling, F. A. Bovey, M. D. Bruch, S. A. Kozlowski, *Macromolecules*, **18**, 1418 (1985).
39. C. Chang, D. D. Muccio, T. St. Pierre, *Macromolecules*, **18**, 2337 (1985).
40. H. N. Cheng, G. H. Lee, *Polym. Bull.*, **12**, 463 (1984).
41. M. D. Bruch, F. A. Bovey, *Macromolecules*, **17**, 978 (1984).
42. S. A. Heffner, F. A. Bovey, L. A. Verge, P. A. Mirau, A. E. Tonelli, *Macromolecules*, **19**, 1628 (1986).
43. G. J. Ray, R. E. Pauls, *Makromol. Chem.*, **186**, 1135 (1985).
44. W. F. Reynolds, M. A. Winnik, R. G. Enriquez, *Macromolecules*, **19**, 1105 (1986).
45. M. D. Bruch, J. K. Bonesteel, *Macromolecules*, **19**, 1622 (1986).
46. R. E. Cais, J. M. Kometani, *Macromolecules*, **18**, 1354 (1986).
47. T. Kitayama, K. Ute, K. Hatada, *Polym. J.*, **16**, 925 (1984).
48. J. A. Wilde, P. H. Bolton, *J. Magn. Resn.*, **59**, 343 (1984).

CHAPTER 3

Stereoregular Oligomers of Methyl Methacrylate

3.1 Introduction

As mentioned in Chapter 2.4, detailed investigation of the configurational sequence of oligomers or low molecular weight polymers provides information on the stereochemistry associated with the early stage of the polymerization reaction. Moreover, model oligomers are valuable in themselves for the study of the stereochemical configuration of polymer chains[1-3]. Since Fujishige[4,5] reported ^{1}H NMR spectra of the MMA-dimers and trimers prepared with CH_3ONa as an initiator in 1978, several laboratories reported the stereochemical analysis using NMR spectroscopy of the MMA-oligomer series (from unimer to pentamer) prepared by the radical polymerization with tetraphenylethane initiators[6], by the radical telomerizations with thiophenol[7], and by group transfer polymerization[8]. The above polymerization systems are not stereospecific (rather syndiotactic) and thus the resultant MMA oligomers consist of comparable amount of some stereoisomers. Cacioli and his coworkers[9] prepared the MMA oligomer [1] by the radical telomerization with cobalt (II) porphyrin, and investigated the preferred conformations of the MMA oligomers by ^{1}H COSY experiments; they isolated three of four possible stereoisomers of the pentamer (n = 3). Volpe *et al.*[10] prepared the "symmetric" oligomer of MMA [2] by the initiation with lithio- and sodio methyl isobutyrate enolate in THF followed by termination with methyl iodide, and demonstrated the ^{13}C NMR spectrum of the mixture of three isomers of of six possible stereoisomers of hexamer (n = 4).

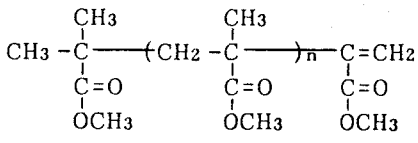

[1]

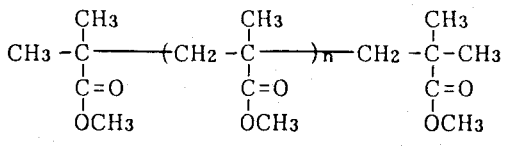

[2]

The polymerization of MMA initiated with *t*-C_4H_9MgBr in toluene at -78°C gives highly isotactic (*it*-) PMMA (*mm* ≥ 97%) with a narrow MWD[11,12]. On the other hand, the polymerization with *t*-C_4H_9Li-trialkylaluminum complex in toluene at -78°C affords highly syndiotactic (*st*-) PMMA (*rr* ≥ 90%) with a narrow MWD[13,14]. The pure-isotactic and pure-syndiotactic MMA oligomers which are composed exclusively of *meso* (*m*) dyads and exclusively of *racemo* (*r*) dyads, respectively, can be prepared and isolated effectively through these polymerization systems by the aid of HPLC technique[15,16] Even the octamers for which 128 diastereomers are theoretically possible, are isolated stereochemically pure. It should be noted that these polymerization systems provide the polymers and oligomers carrying the same terminal groups.

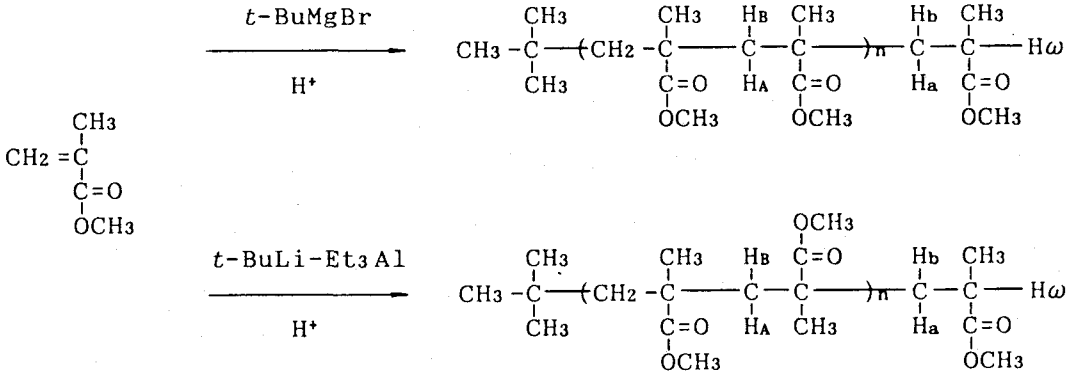

The MMA oligomers are denoted by the sequential arrangement of *m* and *r* dyads preceded with the degree of polymerization (n) (*e.g.* *3mm*, *4rrr*). Although the propagation step is highly stereospecific, the termination reaction with methanol exhibits low stereospecificity in both polymerization systems. Therefore, two series of *it*-oligomers *2m*, *3mm*, *4mmm*, *5mmmm*, ... (**Mm**) and *2r*, *3mr*, *4mmr*, *5mmmr*, ... (**Mr**), and two series of *st*-oligomers *2m*, *3rm*, *4rrm*, *5rrrm*, ... (**Rm**) and *2r*, *3rr*, *4rrr*, *5rrrr*, ... (**Rr**) are produced in the polymerization systems.

3.2 ^{1}H and ^{13}C NMR Spectra of the Pure Isotactic and Pure Syndiotactic Oligomers from Dimer to Octamer[17,18]

In this section, ^{1}H and ^{13}C NMR spectra of the pure diastereomers isolated from these oligomer mixtures have been investigated in detail. These stereoregular oligomers are considered to be good model compounds of stereoregular polymers.

3.2.1 ^{1}H NMR Spectra and the Stereostructures of the Dimers to Octamers

Figure 1 shows HPLC traces (trimer and tetramer fraction) of the *it*-oligomer prepared with *t*-C_4H_9MgBr (A), and of the *st*-oligomer prepared with *t*-$C_4H_9Li/(C_2H_5)_3Al$ complex (B). Both oligomers consisted of two series of diastereomers **Mm** + **Mr**, and **Rm** + **Rr**. Each isomer was collected separately, and the stereostructure was determined by ^{1}H NMR spectroscopy. Figure 2 demonstrates the ^{1}H DQF-COSY of the *it*-hexamer *6mmmmm* measured in $CDCl_3$. The assignment of the methyl and methylene proton signals can be made by the use of the network of correlation peaks beginning with the strong singlet at 0.85 ppm due to the *t*-C_4H_9 group and ending with the multiplet at 2.45 ppm due to the ω-end methine proton ($H\omega$).

The *meso/racemo* assignment was based on the fact that the chemical shift between the nonequivalent methylene protons in an *in-chain* monomeric unit is larger for *meso* sequences than for *racemo* sequences while that in the ω-end unit is larger for *racemo* sequences than for *meso* sequences; this was confirmed by the X-ray crystallographic analysis of the *it*-trimer *3mm* as described in the next section. The assignment of the ^{1}H NMR signals and the determination of stereostructures for other oligomers were carried out in similar manners.

The chemical shifts of methylene protons of the *it*-oligomers **Mm** from dimer to octamer are displayed in simplified bar graphs in Figure 3, together with those of highly isotactic PMMA. The monomeric units in the MMA oligomers (*6mmmmm* for example) are numbered as follows.

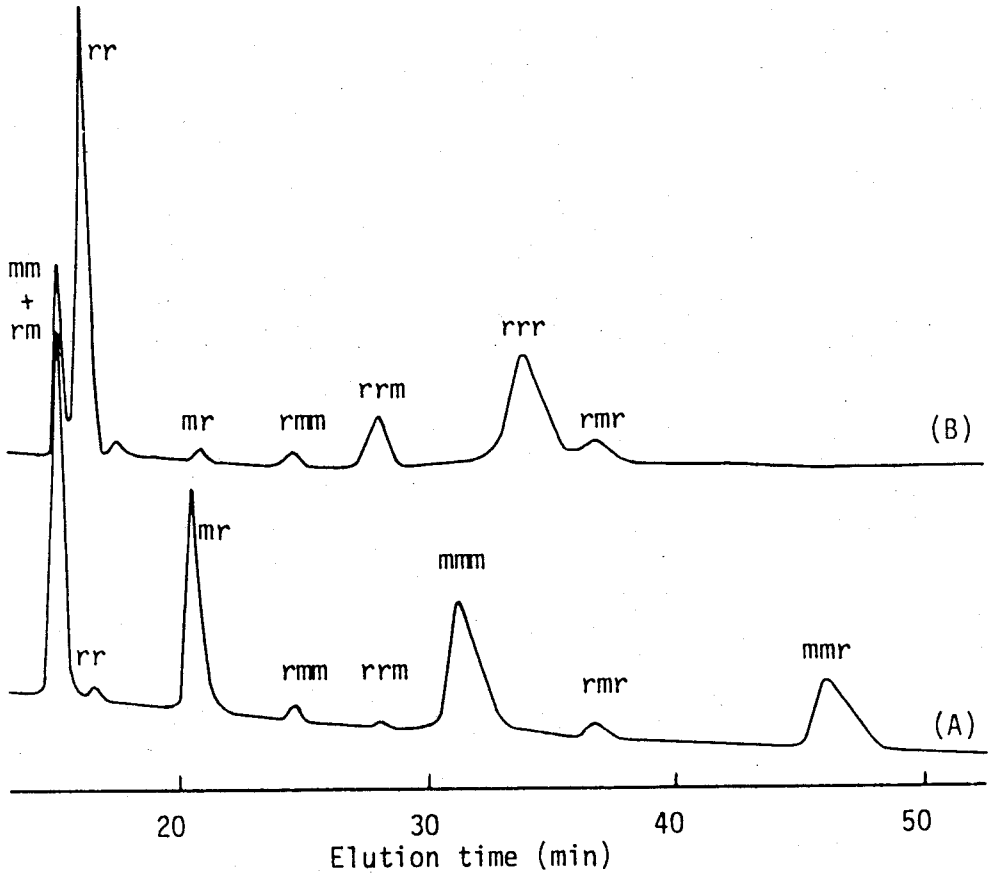

Figure 1. HPLC traces of the MMA trimers and tetramers obtained from the polymerization by *t*-C_4H_9MgBr in toluene at -78°C (A) and by *t*-$C_4H_9Li/(C_2H_5)_3Al$ in toluene at -78°C (B). Eluent, *n*-C_4H_9Cl/CH_3CN = 96/4; column, Develosil 100-5, 0.46(*i.d.*) x 25cm; detector, RI.

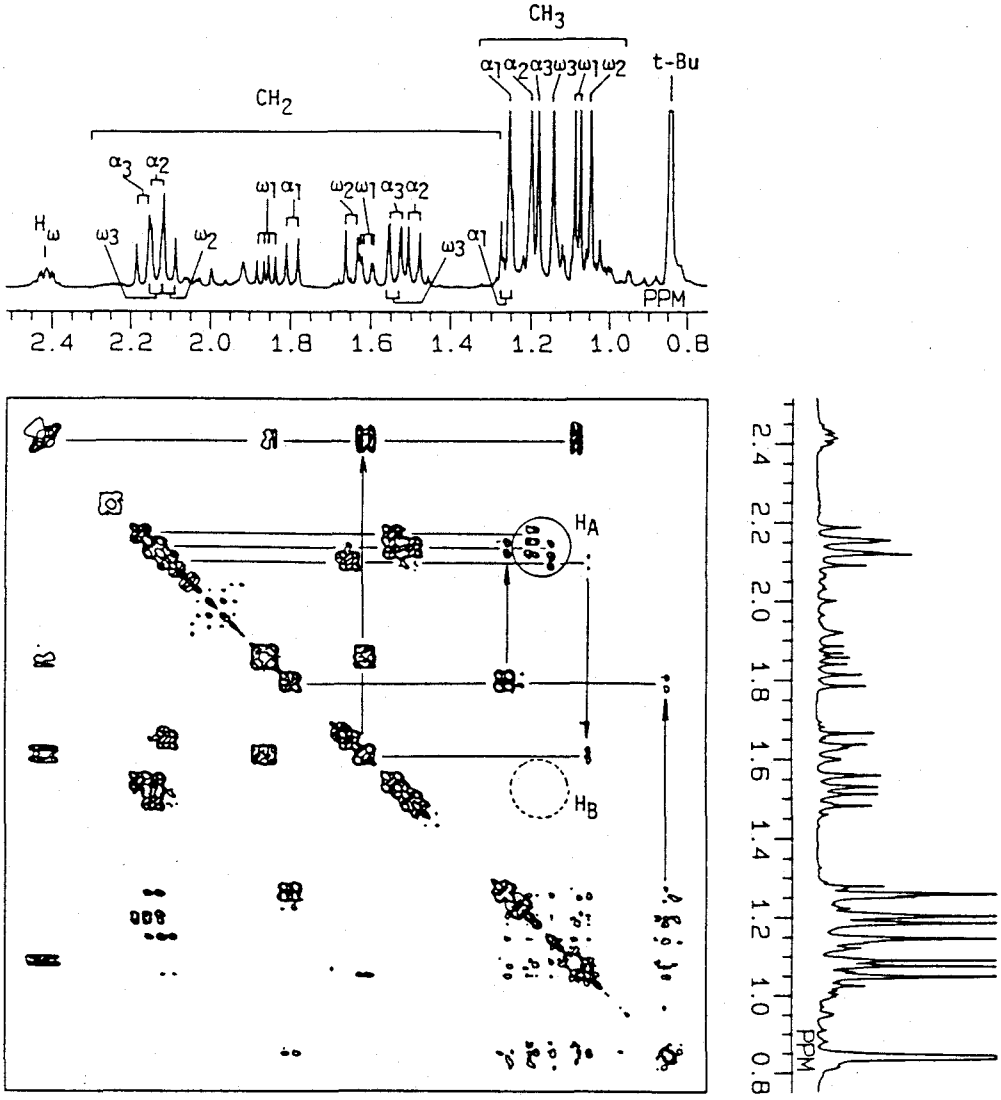

Figure 2. 500 MHz ^{1}H DQF-COSY spectrum of the pure-isotactic hexamer of MMA (*6mmmmm*) prepared with *t*-BuMgBr in toluene at −78°C ($CDCl_3$, 35°C).

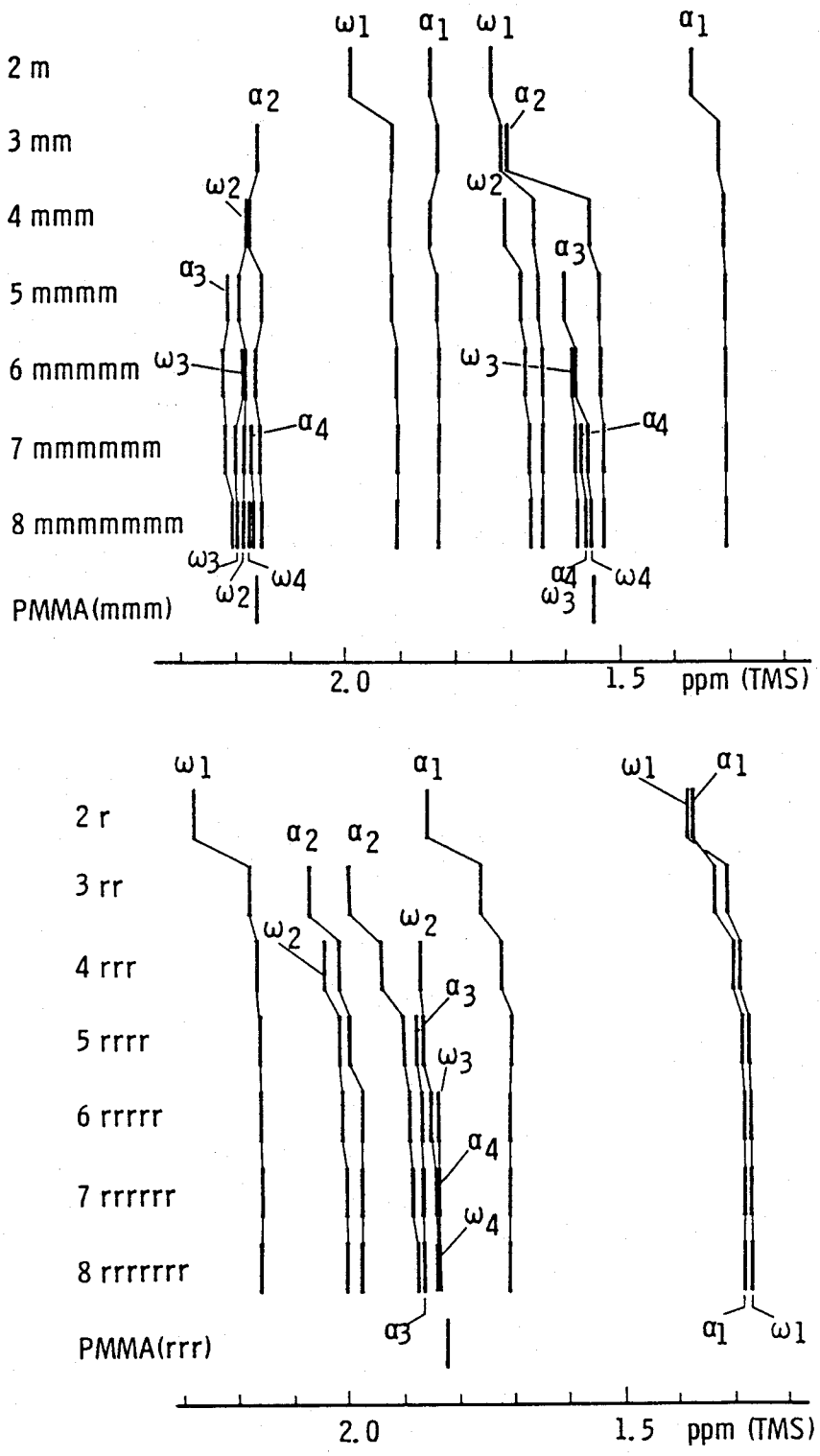

Figure 3. ^{1}H NMR chemical shifts of the methylene protons in *it*- and *st*-oligomers of MMA and in *it*- and *st*-PMMA ($CDCl_3$, 55°C).

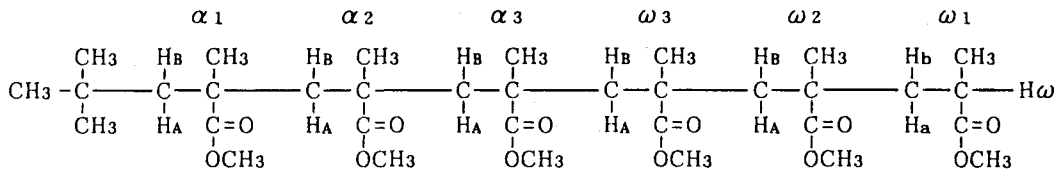

The proton signals due to α_1- and ω_1-units are observed apart from the other signals. On the other hand, the methyl and methylene protons in the monomeric units of the third and farther positions from the α- and ω-ends resonate at nearly the same position with those of *it*-PMMA. A similar tendency was found in the *st*-oligomers **Rr** (Figure 3). Methylene protons of **Rr** are nonequivalent in the α_1-, α_2-, ω_1- and ω_2-units, while the nonequivalency almost disappeared in the third and farther monomeric units from the α- and ω-ends. The chemical shift of the α_4-CH_2 protons agreed with those of the methylene protons in highly syndiotactic PMMA (*rrr*-tetrad). These results indicate that the magnetic environments in the third and farther monomeric units from the terminal groups are very similar to those in the polymer chain. Therefore, the pentamers and the higher oligomers should provide fairly good models in the NMR studies of stereoregular PMMA.

The chemical shift of Hω in the four diastereomer series **Mm**, **Mr**, **Rm** and **Rr** does not depend on the degree of polymerization over the pentamers (Figure 4), and the chemical shift values for the **Mm**-, **Mr**-, **Rm**- and **Rr**-hexamers are 2.445, 2.477, 2.359 and 2.481 ppm, respectively. It is thus possible to determine the stereostructure of the ω-end triads by the chemical shift value of Hω. The ω-end stereosequence can also be determined from the chemical shift between the nonequivalent ω_1-CH_2 protons (Table 1). The extent of nonequivalency is largest in the **Rm** series, and decreases discontinuously in the order of **Rr**, **Mr** and **Mm**. These rules should be applicable to any other oligomers and polymers of MMA which have a methine hydrogen at the ω-end of chain; such oligomers and polymers should be formed for example by disproportionation or chain transfer reaction in radical polymerization, or by living anionic polymerization terminated with protonating reagent.

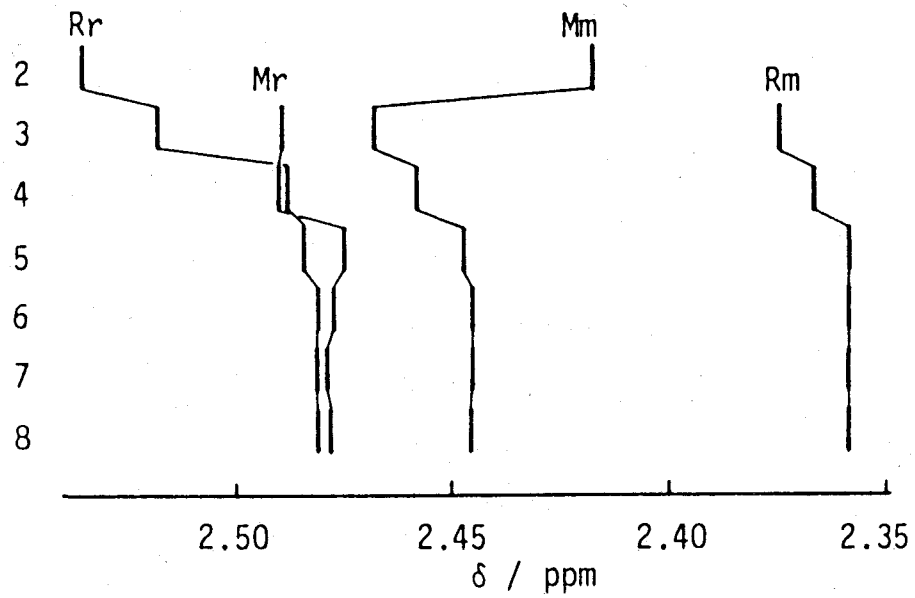

Figure 4. ^{1}H NMR chemical shift of the ω_1-CH protons in the MMA oligomers ($CDCl_3$, 55°C).

Table 1. The range of chemical shifts between the nonequivalent methylene protons (H_A and H_B) and the range of $^{3}J_{HH}$ coupling constants between the ω-end methine ($H\omega$) and methylene (H_a and H_b) protons in the MMA oligomers from trimer to octamer[a]

Stereo-structure	α_2- $\omega_2$units	ω-end unit		
	$\delta(H_A)-\delta(H_B)$	$\delta(H_a)-\delta(H_b)$	$^{3}J(H_a-H\omega)$	$^{3}J(H_b-H\omega)$
	ppm	ppm	Hz	Hz
***mm*···*mm* (Mm)**	0.48 - 0.64	0.20 - 0.27	8.5 - 8.6	2.8 - 3.0
***mm*···*mr* (Mr)**		0.42 - 0.48	8.2 - 8.4	3.4
***rr*···*rr* (Rr)**	0.00 - 0.17	0.86 - 0.88	8.4 - 8.6	3.4
***rr*···*rm* (Rm)**		1.00 - 1.03	8.0 - 8.2	3.7 - 3.9

[a] In $CDCl_3$ at 35.0°C.

3.2.2 Conformation of the MMA Oligomers in Solution

^{1}H NMR spectroscopy provides significant information regarding not only the configuration but also the conformation of the MMA oligomers. Schilling and his coworkers[19] observed in the ^{1}H COSY spectrum of the *it*-PMMA a cross peak between the *mmmm* methyl resonance and the *mmm erythro* methylene resonance but not the *threo* resonance and interpreted the peak to arise from weak $^4J_{HH}$-couplings (1 - 2 Hz) through a "W"-shaped four-bond path. Similar $^4J_{HH}$ connectivities were reported by Cacioli *et al.*[9] and by Johns *et al.*[20] for the telomers of MMA [1] (n = 2 - 4) prepared by radical polymerization with cobalt(II) tetraphenylporphyrin as chain transfer reagent.

In a similar manner, inspection of long-range $^4J_{HH}$ connectivities observed in ^{1}H DQF-COSY (see Figure 2 for example) indicated the all-extended conformation of the *it*-oligomers (*tt...tt* form along the skeletal sequence *t*-C_4H_9-(C-C)$_n$-CH_3). Among the two nonequivalent methylene protons in each monomeric unit, only one of them showed correlation peaks with the protons of the two neighboring methyl groups due to $^4J_{HH}$ coupling. For instance, the $^4J_{HH}$ correlation was observed between CH_3 and H_A (one of the nonequivalent methylene protons resonating at the higher frequency) but not between CH_3 and H_B (the other one) in the an ^{1}H DQF-COSY spectrum of *6mmmmm* (Figure 2). This indicates the four-bond planar "W" arrangement between the respective protons in a highly preferred conformation of the MMA units.

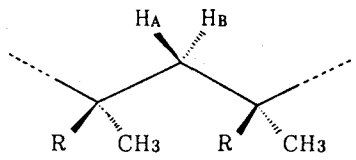

R = CO_2CH_3 [3]

The "W" arrangement in all the CH_2-C-CH_3 groups in a chain requires that one of the methylene protons and the methyl carbon should be in the *trans* state, that is, that the main chain backbone be in the repeated *tt* conformation. In the repeated *tt* conformation, H_A is flanked by carbonyl groups and H_B by methyl groups, which results in the larger chemical shift value of H_A than H_B.

The ^{1}H DQF-COSY of the *st*-oligomers also showed $^4J_{HH}$ connectivities between the methyl and methylene protons; the methylene protons in the monomeric units at the α_1- to α_3- and ω_1- to ω_3-positions are nonequivalent even in the *st*-oligomers. In contrast to the *it*-oligomer, both the nonequivalent methylene protons in a monomeric unit of the *st*-oligomer showed $^4J_{HH}$ connectivity to only one of the two neighboring methyl groups. For example, H_A (one of the nonequivalent methylene protons resonating at the higher frequency) in the α_2-unit of the pure-syndiotactic pentamer *5rrrr* showed a correlation peak only with α_1-CH_3, while H_B (the other one) in the same unit showed a correlation peak only with α_2-CH_3 (Figure 5). In the same way, H_A in the ω_2-unit showed connectivity only to ω_2-CH_3 whereas H_B to α_3-CH_3. These observations are explained if we assume the all-extended conformation [4].

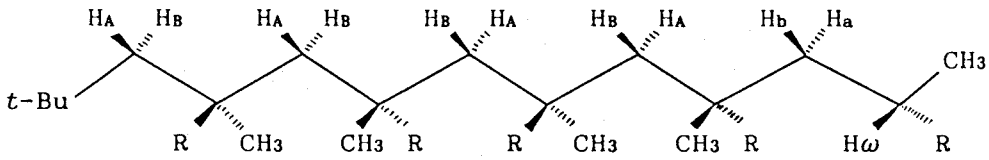

[4]

Preference of near *trans* conformation was also suggested by the conformational statistics on *it*- and *st*-PMMAs[21,22].

The preferred conformation of the ω-end C-CH_2-C-Hω arrays can be determined from the $^3J_{HH}$ *vicinal* coupling constants between Hω and the ω_1-CH_2 protons (Table 1). The coupling constant between Hω and Ha (the methylene proton resonates at the higher frequency) is about 8.4 Hz regardless of the stereostructure of the oligomers, which indicates that these two *vicinal* protons are nearly in the *trans* state. $^3J_{HH}$ between Hω and Hb (the other methylene proton) of about 3.4 Hz indicates the *gauche* arrangement of the protons. Therefore the preferred conformation of the ω-end is *trans* form along C-CH_2-C-CH_3 [5] irrespective of the stereostructure of the ω-end dyad. The *trans* form along the skeletal sequence C-CH_2-C-CO_2CH_3 [6] also accounts for the *vicinal* couplings mentioned above but is rejected for the following reasons: (i) both Ha and Hb should be in the *gauche* state with respect to ω_1-CH_3 since $^4J_{HH}$-connectivity was not detected

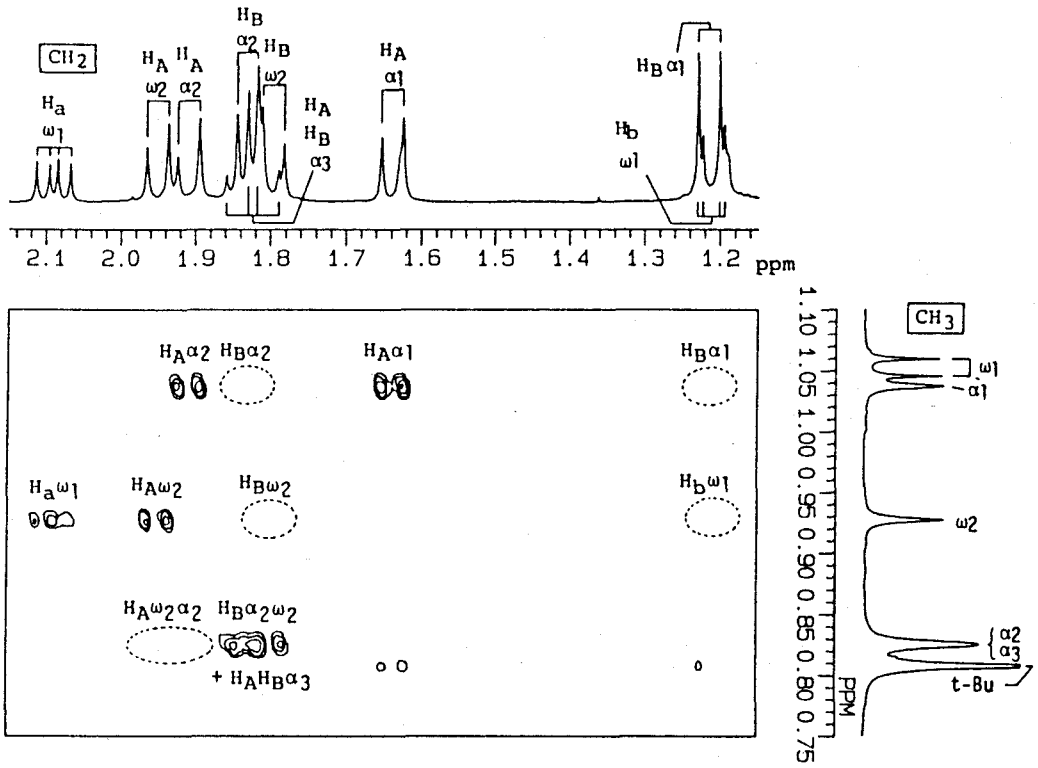

Figure 5. ^{1}H DQF-COSY spectrum (methyl and methylene proton region) of the pure syndiotactic pentamer (*5rrrr*) prepared with *t*-$C_4H_9Li/(C_2H_5)_3Al$ in toluene at -78°C ($CDCl_3$, 35°C, 500 MHz). The missing $^{4}J_{HH}$ connectivities are enclosed with dashed line.

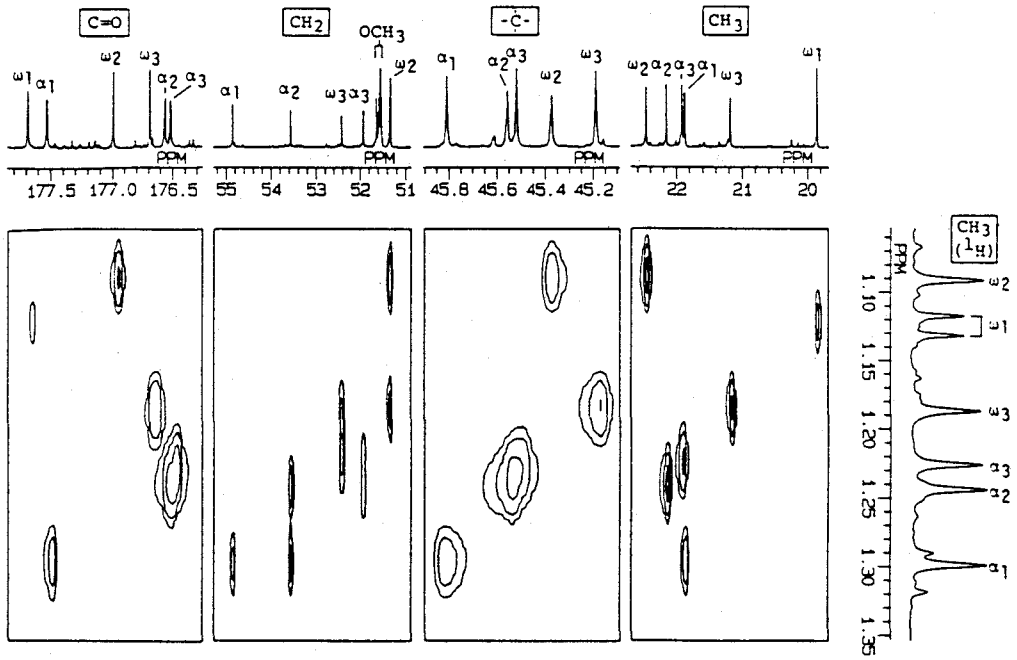

Figure 6. 125 MHz long-range $^{13}C-^{1}H$ COSY (COLOC) spectrum of the pure isotactic hexamer (*6mmmm*) ($CDCl_3$, 55°C).

between the methylene and methyl resonances, (ii) conformational energy calculations on the *meso* and *racemo* dimers[2,3] and X-ray crystallographic determination on *3mm* supported the conformation of [5], (iii) the chemical shifts of H_a and H_b can be reasonably explained if the ω-end conformation of [5] is assumed. Fujishige[4] reported similar values of the *vicinal* coupling constants for the MMA-dimers and trimers prepared with CH_3OLi; however, the proposed ω-end conformation is different from ours because their assignment is now proved to be incorrect.

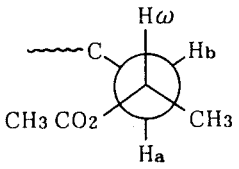

[5]

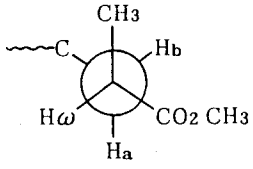

[6]

3.2.3 ^{13}C NMR Chemical Shifts of the MMA Oligomers

The complete assignment of the ^1H NMR signals permitted unambiguous assignment of the ^{13}C NMR signals of the stereoregular oligomers by measuring the long-range ^{13}C-^1H COSY (COLOC). In Figure 6 are shown the COLOC spectrum of *6mmmmm* as a typical example. Carbonyl carbons and quaternary carbons showed correlation peaks with methyl protons through $^3J_{CH}$, and $^2J_{CH}$ couplings, respectively. Methylene carbons showed $^3J_{CH}$ connectivity to the two neighboring methyl groups. Correlation peaks due to $^1J_{CH}$ coupling were also observed between the methyl carbons and protons. Thus, the signal assignment of all but methoxy carbons was achieved.

Figure 7 shows the ^{13}C NMR signals of all the MMA oligomers studied. The signals attributable to the carbons in the α_1- and ω_1-units are apart from those in the other monomeric units, and their chemical shifts reached nearly constant values over trimer. The chemical shifts of the carbons in the monomeric units up to the third monomeric units from the terminal groups seemed to be influenced by the structures of the end groups. The signals due to the α_4- and ω_4-units roughly agreed with those of PMMAs.

According to the above considerations, we calculated the ^{13}C

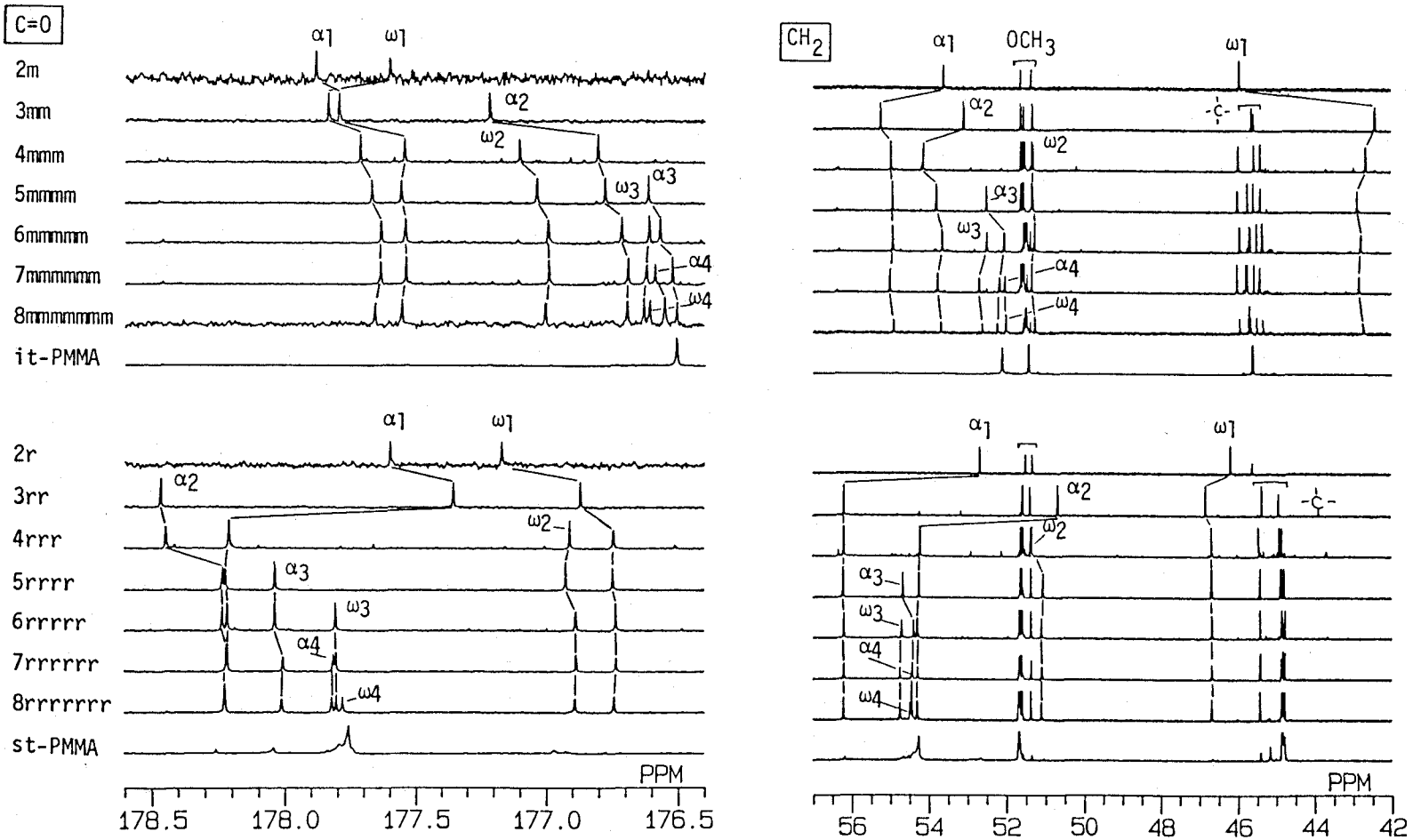

Figure 7-1. 125 MHz ^{13}C NMR spectra of the MMA oligomers (C=O and CH_2) from dimer to octamer and of the *it*- and *st*-PMMAs ($CDCl_3$, 55°C).

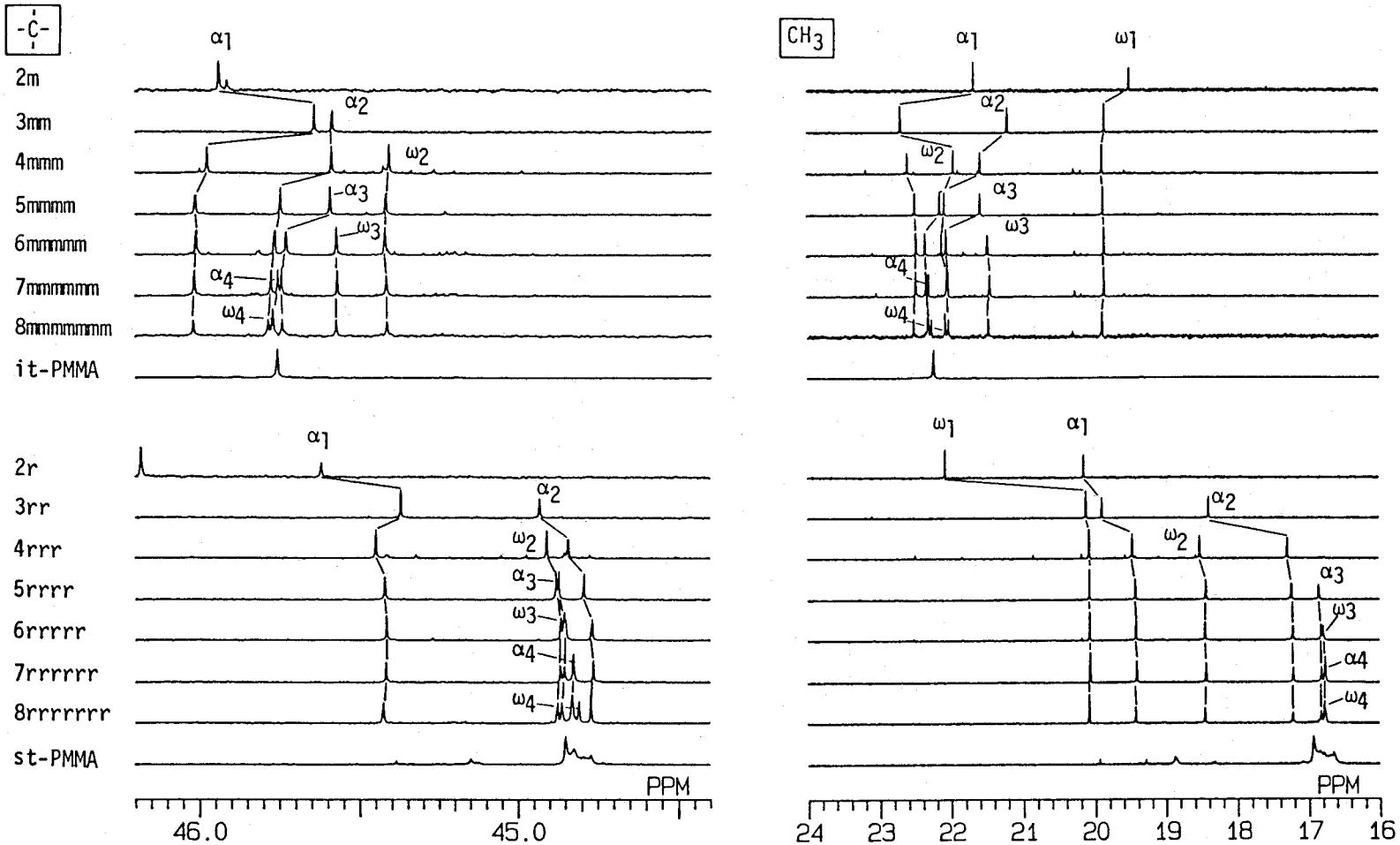

Figure 7-2. 125 MHz ^{13}C NMR spectra of the MMA oligomers (quaternary and CH_3) from dimer to octamer and of the *it*- and *st*-PMMAs ($CDCl_3$, 55°C).

chemical shifts of the oligomers by the following equations:

$$\delta_{calc} = R + P\alpha(i) + P\omega(j)$$

where R is the standard value (ppm) for the carbon of interest, and $P\alpha(i)$ and $P\omega(j)$ are the shift parameters for the monomeric unit to which the carbon belongs (Table 2). The chemical shifts for the *it*- and *st*-PMMA (tetrads and pentads) were employed as the R values for the corresponding oligomer series (**Mm** and **Rr**). $P\alpha(\geq 4)$ and $P\omega(\geq 4)$ were set at zero since the chemical shifts of the carbons in the fourth and farther monomeric unit were considered to be unaffected by the end-groups. $P\alpha(i)$ for the monomeric unit at the i-th position from the α-end and $P\omega(j)$ for the monomeric unit at the j-th position from the ω-end were evaluated from the chemical shifts of the octamers. For instance, $P\alpha(2)$ for the carbonyl carbon of **Mm** series (0.13 ppm) was defined as the difference in the chemical shift values of the carbonyl carbon in the *mmmm* pentad of *it*-PMMA (176.51 ppm) and that in the α_2-unit of *8mmmmmmm* (176.64 ppm). $P\omega(3)$ for the carbonyl carbon of **Mm** series (0.22 ppm) was defined likewise based on the shift value of the ω_3-unit of *8mmmmmmm* (176.73 ppm). Then the chemical shift value for the α_2-carbonyl carbon of the *it*-tetramer *4mmm*, for example, is thus given by the sum of these three parameters:

$$R + P\alpha(2) + P\omega(3) = 176.51 + 0.13 + 0.22 = 176.86 \text{ (ppm)}.$$

The observed value (δ_{obs}) was 176.80 ppm. This scheme was applied to all carbons of the oligomers and the results are shown in Table 3. The agreement between the observed and calculated values should be considered fairly well since the standard deviation of ^{13}C chemical shift measurements for oligomers was evaluated to be 0.02 - 0.04 ppm[25]. Particularly, the agreement over the hexamer was excellent for all the carbons.

The shift parameters may be widely used for the assignment of the ^{13}C NMR signals due to the "terminal units" in PMMA, although the terminal group at the α-end depends on the initiating species employed in the polymerization.

Table 2. Parameters for the calculation of the ^{13}C NMR chemical shifts (δ_{calc}) of the isotactic and syndiotactic MMA-oligomers[a]

Carbon	Shift parameters R, P$\alpha(i)$, P$\omega(j)$ / ppm					
	R	Pα(1)	Pα(2)	Pα(3)	Pω(3)	Pω(2)	Pω(1)
Isotactic (***mm...m***)							
C=O	176.51	1.08	0.13	0.03	0.22	0.53	1.18
CH_2	52.26	2.77	1.54	-0.14	0.47	-0.76	-9.43
Quat.	45.77	0.28	0.00	0.03	-0.16	-0.32	-9.17[b]
CH_3	22.18	-0.16	0.12	-0.11	-0.72	0.33	-2.29
Syndiotactic (***rr...r***)							
C=O	177.71	0.51	0.51	0.30	0.09	-0.82	-0.97
CH_2	54.29	1.94	0.01	0.21	0.47	-2.92	-7.61
Quat.	44.89	0.53	-0.12	0.01	0.01	0.01	-9.52[b]
CH_3	17.10	2.97	0.12	-0.28	-0.33	1.35	2.33

[a] The chemical shift (δ_{calc}, in $CDCl_3$ at 55°C) of the carbon in the monomeric unit at the i-th position from the α-end and the j-th position from the ω-end is calculated by $\delta_{calc} = R + P\alpha(i) + P\omega(j)$, where $P\alpha(\geq 4) = 0$ and $P\omega(\geq 4) = 0$.
[b] Parameter for the ω-end methine carbon.

Table III-1. ^{13}C chemical shifts (δ_{obs}) and the difference between calculated (δ_{calc}) and observed values for the MMA oligomers (carbonyl carbons)

Oligomer	δ_{obs} ($\delta_{calc}-\delta_{obs}$)/ppm							
	α_1	α_2	α_3	α_4	ω_4	ω_3	ω_2	ω_1
2*m*	177.88							177.60
	(+0.24)							(+0.22)
3*mm*	177.79	177.21						177.83
	(+0.02)	(−0.04)						(−0.11)
4*mmm*	177.54	176.80					177.10	177.71
	(+0.05)	(+0.06)					(−0.03)	(−0.02)
5*mmmm*	177.56	176.78	176.61				177.04	177.67
	(+0.03)	(−0.14)	(+0.15)				(0.00)	(+0.02)
6*mmmmm*	177.54	176.60	176.57			176.71	176.99	177.63
	(+0.05)	(+0.04)	(−0.03)			(+0.02)	(+0.05)	(+0.06)
7*mmmmmm*	177.54	176.64	176.52	176.59		176.69	176.99	177.64
	(+0.05)	(0.00)	(+0.02)	(−0.08)		(+0.04)	(+0.05)	(+0.05)
8*mmmmmmm*	177.59	176.64	176.54	176.59	176.66	176.73	177.04	177.69
	(0.00)	(0.00)	(0.00)	(−0.08)	(−0.15)	(0.00)	(0.00)	(0.00)
2*r*	177.60							177.17
	(−0.20)							(+0.08)
3*rr*	177.35	178.47						176.87
	(+0.96)	(−1.07)						(+0.17)
4*rrr*	178.21	178.45					176.91	176.74
	(+0.01)	(−0.14)					(+0.28)	(0.00)
5*rrrr*	178.22	178.23	178.03				176.92	176.74
	(0.00)	(−0.01)	(+0.07)				(−0.03)	(0.00)
6*rrrrr*	178.21	178.23	178.03			177.80	176.88	176.73
	(+0.01)	(−0.01)	(−0.02)			(0.00)	(+0.01)	(+0.01)
7*rrrrrr*	178.21	178.21	178.01	177.81		177.80	176.88	176.73
	(+0.01)	(+0.01)	(0.00)	(−0.10)		(0.00)	(+0.01)	(+0.01)
8*rrrrrrr*	178.22	178.22	178.01	177.82	177.78	177.80	176.89	176.74
	(0.00)	(0.00)	(0.00)	(−0.11)	(−0.07)	(0.00)	(0.00)	(0.00)

Table III-2. ^{13}C chemical shifts (δ_{obs}) and the difference between calculated (δ_{calc}) and observed values for the MMA oligomers (methylene carbons)

Oligomer	δ_{obs} ($\delta_{calc}-\delta_{obs}$)/ppm							
	α_1	α_2	α_3	α_4	ω_4	ω_3	ω_2	ω_1
2*m*	53.62							45.90
	(+0.65)							(−1.53)
3*mm*	55.25	53.09						42.42
	(+0.25)	(−0.05)						(+0.27)
4*mmm*	54.99	53.68					51.30	42.66
	(+0.04)	(+0.59)					(+0.06)	(+0.17)
5*mmmm*	54.96	53.81	52.51				51.30	42.87
	(+0.07)	(−0.01)	(+0.08)				(+0.20)	(−0.04)
6*mmmmm*	55.01	53.72	52.12			52.57	51.40	42.85
	(+0.02)	(+0.08)	(0.00)			(+0.16)	(+0.10)	(−0.02)
7*mmmmmm*	55.02	53.77	52.17	52.03		52.70	51.40	42.82
	(+0.01)	(+0.03)	(−0.05)	(+0.23)		(+0.03)	(+0.10)	(+0.01)
8*mmmmmmm*	55.03	53.80	52.12	52.10	52.10	52.73	51.50	42.83
	(0.00)	(0.00)	(0.00)	(+0.16)	(+0.16)	(0.00)	(0.00)	(0.00)
2*r*	52.67							46.18
	(+0.64)							(+0.51)
3*rr*	56.21	50.67						46.83
	(+0.49)	(+0.71)						(+0.06)
4*rrr*	56.21	54.21					51.33	46.68
	(+0.02)	(+0.56)					(+0.25)	(0.00)
5*rrrr*	56.23	54.25	54.68				51.36	46.68
	(0.00)	(+0.05)	(+0.29)				(+0.01)	(0.00)
6*rrrrr*	56.21	54.30	54.40			54.71	51.36	46.67
	(+0.02)	(0.00)	(+0.10)			(+0.05)	(+0.01)	(+0.01)
7*rrrrrr*	56.22	54.29	54.44	54.44		54.76	51.37	46.68
	(+0.01)	(+0.01)	(+0.06)	(−0.15)		(0.00)	(0.00)	(0.00)
8*rrrrrrr*	56.23	54.30	54.50	54.50	54.50	54.76	51.37	46.68
	(0.00)	(0.00)	(0.00)	(−0.21)	(−0.21)	(0.00)	(0.00)	(0.00)

Table III-3. ^{13}C chemical shifts (δ_{obs}) and the difference between calculated (δ_{calc}) and observed values for the MMA oligomers (quaternary carbons)

Oligomer	δ_{obs} ($\delta_{calc}-\delta_{obs}$)/ppm							
	α_1	α_2	α_3	α_4	ω_4	ω_3	ω_2	ω_1[a]
2*m*	45.90							36.26
	(−0.17)							(+0.34)
3*mm*	45.63	45.58						36.69
	(+0.26)	(−0.13)						(−0.06)
4*mmm*	45.97	45.63					45.41	36.62
	(+0.08)	(−0.02)					(+0.07)	(−0.02)
5*mmmm*	46.01	45.75	45.59				45.42	36.57
	(+0.04)	(+0.02)	(+0.05)				(+0.03)	(+0.03)
6*mmmmm*	46.01	45.76	45.73			45.57	45.42	36.56
	(+0.04)	(+0.01)	(+0.07)			(+0.04)	(+0.03)	(+0.04)
7*mmmmmm*	46.02	45.76	45.76	45.70		45.57	45.42	36.56
	(+0.03)	(+0.01)	(+0.04)	(+0.07)		(+0.04)	(+0.03)	(+0.04)
8*mmmmmmm*	46.05	45.77	45.80	45.80	45.80	45.61	45.45	36.60
	(0.00)	(0.00)	(0.00)	(−0.03)	(−0.03)	(0.00)	(0.00)	(0.00)
2*r*	45.62							35.66
	(−0.19)							(−0.41)
3*rr*	45.37	44.93						35.42
	(+0.06)	(−0.15)						(−0.04)
4*rrr*	45.45	44.84					44.91	35.37
	(−0.03)	(−0.06)					(0.00)	(0.00)
5*rrrr*	45.42	44.79	44.88				44.87	35.37
	(0.00)	(−0.02)	(+0.03)				(+0.03)	(0.00)
6*rrrrr*	45.42	44.77	44.90			44.90	44.90	35.36
	(0.00)	(0.00)	(0.00)			(0.00)	(0.00)	(+0.01)
7*rrrrrr*	45.42	44.77	44.90	44.90		44.90	44.90	35.36
	(0.00)	(0.00)	(0.00)	(−0.01)		(0.00)	(0.00)	(+0.01)
8*rrrrrrr*	45.42	44.77	44.90	44.90	44.90	44.90	44.90	35.37
	(0.00)	(0.00)	(0.00)	(−0.01)	(−0.01)	(0.00)	(0.00)	(0.00)

Table III-4. ^{13}C chemical shifts (δ_{obs}) and the difference between calculated (δ_{calc}) and observed values for the MMA oligomers (α-methyl carbons)

Oligomer	δ_{obs} ($\delta_{calc}-\delta_{obs}$)/ppm							
	α_1	α_2	α_3	α_4	ω_4	ω_3	ω_2	ω_1
2*m*	21.67							19.51
	(+0.68)							(+0.50)
3*mm*	22.69	21.19						19.85
	(−1.39)	(+1.44)						(−0.07)
4*mmm*	21.95	21.57					22.59	19.89
	(+0.07)	(+0.01)					(−0.19)	(0.00)
5*mmmm*	22.07	22.14	21.57				22.49	19.87
	(−0.05)	(+0.16)	(−0.22)				(+0.02)	(+0.02)
6*mmmmm*	22.04	22.35	22.11			21.47	22.47	19.86
	(−0.02)	(−0.05)	(−0.04)			(−0.01)	(+0.04)	(+0.03)
7*mmmmmm*	22.03	22.34	22.04	22.31		21.44	22.48	19.86
	(−0.01)	(−0.04)	(+0.03)	(−0.13)		(+0.02)	(+0.03)	(+0.03)
8*mmmmmmm*	22.02	22.30	22.07	22.30	22.30	21.46	22.51	19.89
	(0.00)	(0.00)	(0.00)	(−0.12)	(−0.12)	(0.00)	(0.00)	(0.00)
2*r*	22.07							20.14
	(−0.65)							(−0.59)
3*rr*	20.11	18.39						19.89
	(−0.37)	(+0.18)						(−0.74)
4*rrr*	20.06	17.29					18.52	19.46
	(+0.01)	(−0.40)					(−0.35)	(−0.03)
5*rrrr*	20.07	17.23	16.85				18.44	19.42
	(0.00)	(−0.01)	(−0.36)				(+0.01)	(+0.01)
6*rrrrr*	20.07	17.22	16.82			16.79	18.45	19.42
	(0.00)	(0.00)	(0.00)			(−0.02)	(0.00)	(+0.01)
7*rrrrrr*	20.07	17.22	16.83	16.80		16.77	18.45	19.42
	(0.00)	(0.00)	(−0.01)	(+0.30)		(0.00)	(0.00)	(+0.01)
8*rrrrrrr*	20.07	17.22	16.82	16.80	16.80	16.77	18.45	19.43
	(0.00)	(0.00)	(0.00)	(+0.30)	(+0.30)	(0.00)	(0.00)	(0.00)

3.2.4 Segmental Mobility of the Pure Isotactic and Pure Syndiotactic Oligomers of MMA

The ^{13}C-T_1 values for the *it*-hexamer (*6mmmmm*) and *st*-hexamer (*6rrrrr*) were measured in toluene-d_8 at 35°C (125 MHz). The results are shown in Figure 8. The T_1's of the carbonyl, methylene, quaternary and methyl carbons decreased gradually as the monomeric unit came apart from the terminal groups. However, the T_1 values were much longer than those for PMMA, even in the α_3- or ω_3-unit in the hexamers. The T_1 values for the *st*-hexamer were smaller than those for the *it*-hexamer as to the corresponding carbon of the corresponding monomeric unit. This suggests lower segmental mobility of the *st*-oligomers than the *it*-oligomers.

The ^{13}C-T_1 measurements were also carried out on a 1:1 mixture of *6mmmmm* and *6rrrrr* in toluene-d_8 or in *N,N*-dimethylformamide-d_7 at 35°C. However, the T_1 values for the respective carbons (including methoxy carbons; T_1 = 2.1 - 2.8 s for *6mmmmm* and 1.5 - 2.8 s for *6rrrrr*) showed little difference from those measured in the solutions of individual *it*- or *st*-hexamer, indicating no appreciable interaction between the *it*- and *st*-hexamers (stereocomplex formation) under these conditions. Further studies are now under way on this problem.

3.3 Structure of the Isotactic Trimer in Crystal[24]

In the literatures[4-10] cited in Section 3.1, the configurational assignment (*meso/racemo* assignment) of the monomeric sequences in the oligomeric products were made on the basis of the nonequivalency of the methylene protons; the chemical shift difference between the signals of the two methylene protons (H_A and H_B) in a given monomeric unit should be larger for *meso* sequences than for *racemo* sequences.

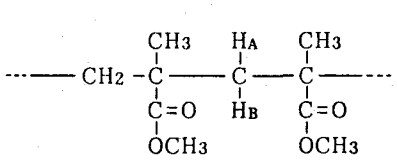

meso sequence

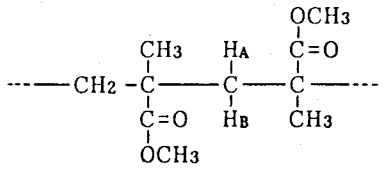

racemo sequence

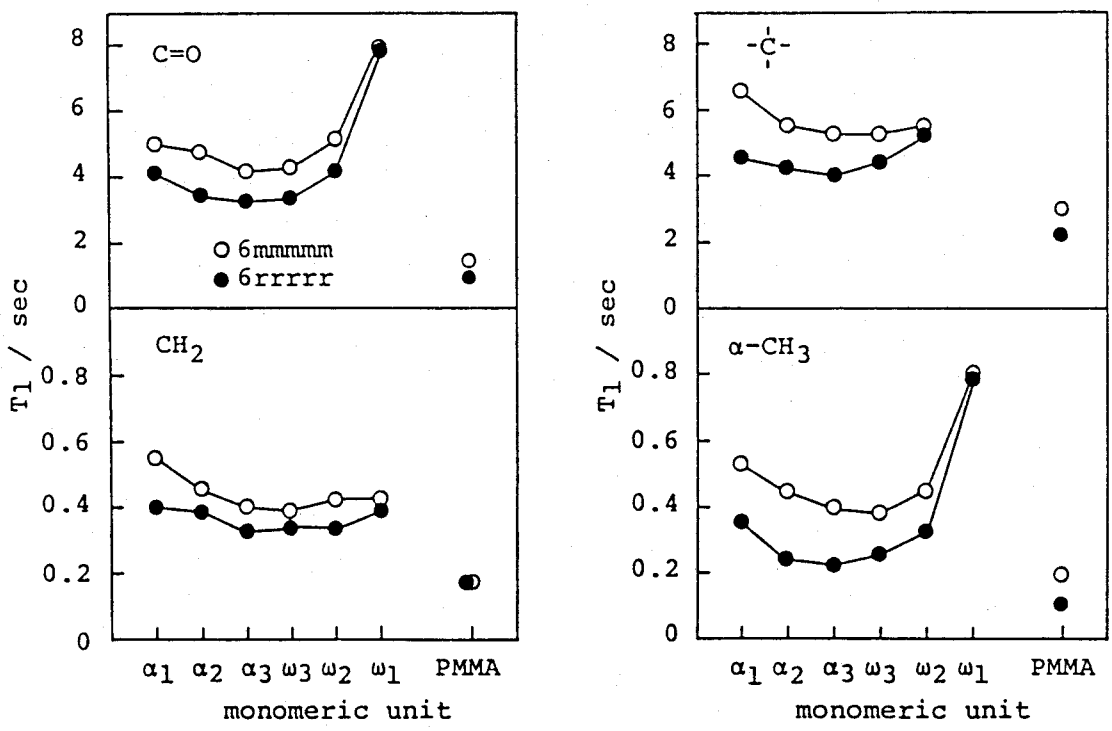

Figure 8. ^{13}C-T_1 values for the pure isotactic and the pure syndiotactic hexamers of MMA (*6mmmmm* and *6rrrrr*) and for the *it*- and *st*-PMMAs measured in toluene-*d*8 at 35°C (125 MHz).

This nonequivalency was successfully adopted for the interpretation of the ^{1}H NMR spectra of highly isotactic and highly syndiotactic PMMAs[26,27], leading to the first establishment of tacticity determination by NMR spectroscopy. However, there has been doubt as to whether the larger extent of nonequivalency for *meso* methylene protons is held even at the chain-end units. In the present work, this was found not true for the ω-end unit, and the definite *meso/racemo* assignment has been made for the signals of methylene protons at the ω-end of chain based on the X-ray analysis of a crystallized trimer.

3.3.1 X-ray Crystallographic Determination of the Trimer

The mixture of isotactic oligomers of MMA was prepared with *t*-C_4H_9MgBr in toluene at -78°C. Figure 1A shows the HPLC trace of the oligomer mixture (the trimer and tetramer region). Crystals of *3mm* were grown from the heptane solution of the fraction *3mm+3rm* (*3mm/3rm* = 48/3), and one of them was subjected to the X-ray single crystal analysis.

Table 4 gives crystallographic details and Figure 9 shows the ORTEP drawing of *3mm*. Crystal symmetry demands the crystal consisting of a racemic mixture of the (*R*, *S*, *R*) and (*S*, *R*, *S*) isomers. Only the (*R*, *S*, *R*) configuration of the quaternary carbons (C6, C11, C16) is shown in the figure. All the atomic parameters and torsional angles in the present work are given in the (*R*, *S*, *R*) form. Repetition of the three monomeric units (α_1, α_2, ω_1) in the (*R*, *S*, *R*) form between C5 and C16 produces an isotactic PMMA chain, and therefore the trimer is assigned to the *meso-meso* (*mm*) diastereomer.

The conformation of the main chain is *ttg*$^+$*tg*$^+$ along the skeletal sequence C4-C5-C6-C10-C11-C15-C16-H28 (Table 5). All the ester groups take planar *S-cis* conformation. The plane of the ester group of α_1-unit (O1=C8-O2-C9) occurs approximately perpendicular to the plane defined by the adjoining skeletal bonds (C5-C6-C10), with the carbonyl group oriented to the opposite side (*anti*) of the α-methyl carbon (C7). The plane of the ester group of α_2-unit (O3=C13-O4-C14) appreciably deviated from perpendicular to the plane defined by the adjoining skeletal bonds (C10-C11-C15) which is in a *tg*$^+$ state. The *interdyad* bond

Table 4. Crystal data and relevant diffraction data for **3mm**

mol formula	$C_{19}H_{34}O_6$	diffractmeter	Rigaku AFC5R
mol wt.	358.48	λ(CuKα) (Å)	1.5418
recryst. solvent	heptane	ω-2θ scan	1.0 + 0.15tanθ
crystal system	*monoclinic*	scan speed (deg/min)	4
space group	$P2_1/n$	$2\theta_{max}$ (deg)	125
a (Å)	10.146	octants measured	*hkl; -hkl*
b (Å)	24.742	total unique data	3390
c (Å)	9.025	obsd data ($\|F\|>3\sigma(\|F\|)$)	2718
β (deg)	109.02	no. of parameters	362
V (Å^3)	2121.1	max Δ/σ in final cycle	0.159
Z	4	R	0.050
D_{calcd} (g/cm^3)	1.123	R_w[a]	0.052
μ(CuKα) (cm^{-1})	6.4	goodness of fit[b]	1.47
cryst. size (mm)	0.3 x 0.2 x 0.2		

[a] $R_w = [\Sigma w(|F_o|-|F_c|)^2/\Sigma w|F_o|^2]^{1/2}$; $w = 1/\sigma^2(|F_o|)$.
[b] $g.o.f = [\Sigma w(|F_o|-|F_c|)^2/(N_{obsd} - N_{parms})]^{1/2}$.

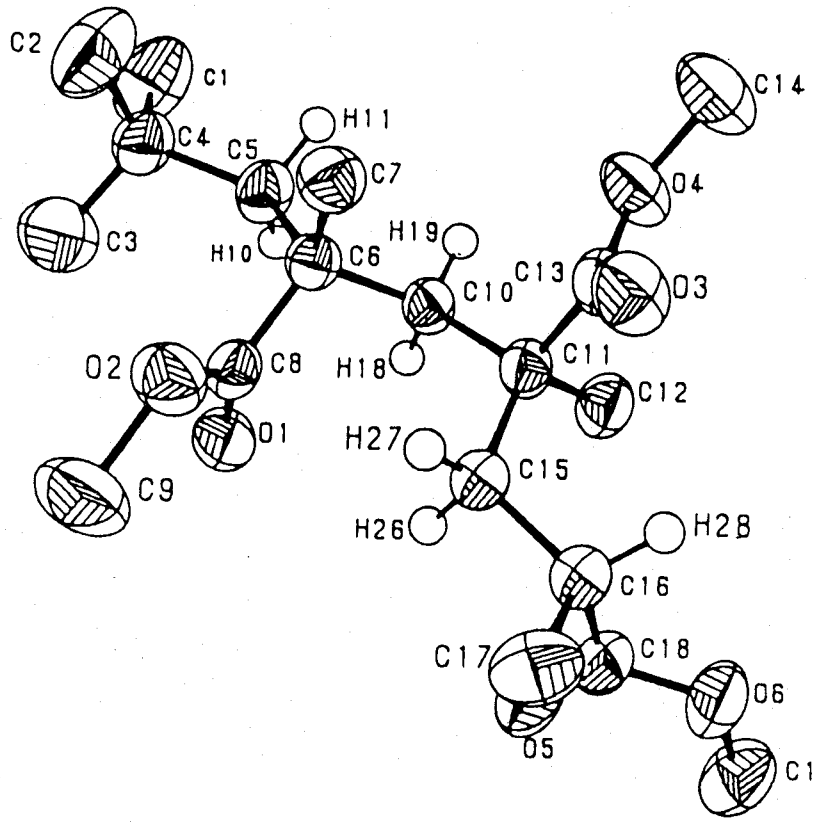

Figure 9. The ORTEP drawing of **3mm** [(*R*,*S*,*R*)-form]. Methyl hydrogen atoms are omitted in this figure.

Table 5. Selected bond lengths, angles and torsional angles for **3mm**[a]

Monomeric Units					
α_1		α_2		ω_1	
Bond Lengths (Å)					
C4 - C5	1.554				
C5 - C6	1.562	C10- C11	1.554	C15- C16	1.538
C6 - C7	1.532	C11- C12	1.546	C16- C17	1.538
C6 - C8	1.517	C11- C13	1.523	C16- C18	1.498
C6 - C10	1.565	C11- C15	1.537	C16- H28	1.003
C8 - O1	1.204	C13- O3	1.201	C18- O5	1.195
C8 - O2	1.339	C13- O4	1.332	C18- O6	1.333
C9 - O2	1.453	C14- O4	1.447	C19- O6	1.452
Bond Angles (deg)					
C4 -C5 -C6	124.6	C6 -C10-C11	121.0	C11-C15-C16	116.8
C5 -C6 -C10	103.5	C10-C11-C15	112.3	C15-C16-H28	109.6
C7 -C6 -C8	113.2	C12-C11-C13	106.8	C17-C16-C18	107.2
C6 -C8 -O2	113.4	C11-C13-O4	112.2	C16-C18-O6	112.2
O1 -C8 -O2	122.4	O3 -C13-O4	122.2	O5 -C18-O6	122.3
C8 -O2 -C9	115.1	C13-O4 -C14	116.8	C18-O6 -C19	116.2
Torsional Angles (deg)					
C4 -C5 -C6 -C10	170.4	C6 -C10-C11-C15	51.4	C11-C15-C16-H28	27.6
C5 -C6 -C10-C11	169.9	C10-C11-C15-C16	168.1		
C7 -C6 -C8 -O1	-171.9	C12-C11-C13-O3	-117.7	C17-C16-C18-O5	86.3
O1 -C8 -O2 -C9	1.6	O3 -C13-O4 -C14	1.6	O5 -C18-O6 -C19	-1.2
				H26-C15-C16-H28	147.5
				H27-C15-C16-H28	-93.8

[a] The estimated standard deviations for bond lengths, bond angles and torsional angles involving only non-hydrogen atoms are 0.003 - 0.005 Å, 0.2 - 0.3 deg and 0.2 - 0.4 deg, respectively.

angles CH_2-C-CH_2 are 103.5° for C5-C6-C10 in a *tt* state, and 112.3° for C10-C11-C15 in a *tg*$^+$ state, which agrees well with the values calculated by conformational statistics for four-bond segments embedded in PMMA chains[21]. The unusually large values for the *intradyad* bond angles C-CH_2-C, which were described in the literatures[21,22,28,29], are also observed (Table 5). Bond lengths and bond angles for side chains show little difference among the three monomeric units.

The molecular structure of PMMA was investigated by crystallographic studies on isotactic PMMA[28], wide-range X-ray scattering of syndiotactic PMMA[29], and conformational energy calculations on the several monomeric sequences embedded in PMMA chains[21,22]. Single crystal structure analysis of the MMA oligomers will provide another approach to the molecular structure of PMMA.

3.3.2 Nonequivalency of the Methylene Protons

Figure 10 shows ^{1}H NMR spectra of the MMA trimers *3mm*, *3mr*, *3rm* and *3rr*. The configuration of the interior sequence of *3mm* and *3mr* should be *meso*, since *3mm* and *3mr* are the predominant trimers isolated from the mixture of highly isotactic oligomers prepared with *t*-C_4H_9MgBr. The comparable yields of the *ω-meso* (*3mm*) and the *ω-racemo* (*3mr*) isomers resulted from the non-stereospecific reaction of the isotactic-specific anion with the protonating reagent (methanol). The ^{1}H NMR spectrum of *3mm* (Figure 10a), whose structure is now confirmed by the X-ray single crystal analysis, and the spectrum of the other isomer *3mr* (Figure 10b) clearly indicate that the chemical shift between the methylene protons in the ω-end (ω_1) unit (H_a and H_b) is smaller for m-sequence than for *r*-sequence. On the other hand, the chemical shift between the methylene protons in the interior (α_2) unit (H_A and H_B) is larger for *m*-sequences of *3mm* and *3mr* than for *r*-sequences of *3rm* and *3rr*, the predominant trimers isolated from the highly syndiotactic oligomers prepared with *t*-C_4H_9Li-$(C_2H_5)_3Al$ complex (Figures 10c and 10d). The chemical shifts between the nonequivalent methylene protons of the trimers (H_A and H_B, H_a and H_b) are summarized in Table 6.

The *ttg*$^+$*tg*$^+$ form, the conformation which *3mm* adopts in its

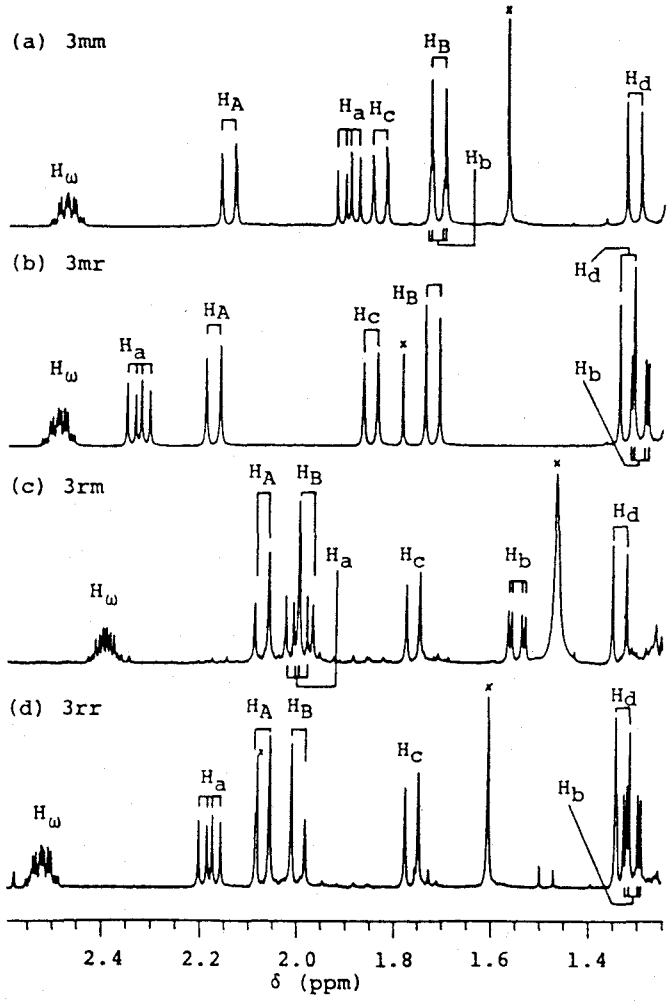

Figure 10. ^{1}H NMR spectra (methine and methylene protons region) of **3mm** (a), **3mr** (b), **3rm** (c) and **3rr** (d) measured in $CDCl_3$ at 35°C (500 MHz).

Table 6. The chemical shifts between the methylene protons in α_2 units (H_A, H_B) and ω_1 units (H_a, H_b) and the $^{3}J_{HH}$ coupling constants between the ω-end methine proton ($H\omega$) and H_a, H_b for **3mm**, **3mr**, **3rm** and **3rr**[a]

	3mm	**3mr**	**3rm**	**3rr**
$\delta(H_A)-\delta(H_B)$ /ppm	0.43	0.45	0.07	0.09
$\delta(H_a)-\delta(H_b)$ /ppm	0.19	1.03	0.45	0.87
$^{3}J(H_a-H\omega)$ /Hz	8.7	8.6	8.1	8.5
$^{3}J(H_b-H\omega)$ /Hz	2.4	3.2	3.9	3.2

[a] In $CDCl_3$ at 35°C.

crystal, accounts for the small extent of nonequivalency between H_a and H_b, but does not for the large extent of nonequivalency between H_A and H_B; it would be realized from Figure 9 that magnetic environment is quite similar for H_A (H18) and H_B (H19). The nonequivalencies of the methylene protons in interior and ω-end units of the trimers can be explained if we assume the more extended, *ttttg'* form in solution for the main chains of all the four trimers.

3.4 Supercritical Fluid Chromatography of the Stereoregular Oligomers of MMA[30]

Supercritical fluid chromatography (SFC) has been applied to the separation of the homologous species of styrene oligomers[31-33] and other oligomers[34] such as oligosiloxanes[35] and oligoethyleneglycols[36,37]. As far as we are aware of, no paper has been published on the separation of stereoisomers of oligomer components by SFC. The usefulness of HPLC in the separation of stereoisomers of MMA oligomers was realized recently[4-10,15-18]; the stereoisomers of MMA oligomers from dimer to octamer were separated by using silica gel as stationary phase and a mixture of butyl chloride and acetonitrile as mobile phase. In the present work, packed column SFC has been used to the analysis of the isotactic and syndiotactic oligomers of MMA prepared by the stereoregular living polymerizations with t-C_4H_9MgBr and t-C_4H_9Li-$(C_2H_5)_3Al$ complex.

Isotactic-specific polymerization of MMA was initiated with t-C_4H_9MgBr ([MMA]/[t-C_4H_9MgBr] = 50 mol/mol) in toluene at -78°C, and the reaction was terminated 120 min after the initiation by adding a small amount of methanol to the polymerization mixture. The yield of the oligomeric products was 20 % (Sample A). Syndiotactic-specific polymerization of MMA was carried out with t-C_4H_9Li/$(C_2H_5)_3Al$ complex ([Al]/[Li] = 2/1 mol/mol, [MMA]/[t-C_4H_9Li] = 5 mol/mol) in toluene at -78°C. The polymerization reaction was terminated with methanol 180 min after the initiation to give the oligomer mixture. The mixture was poured into hexane and the insoluble part (57.7%) was subjected to the SFC

analysis (Sample B). The standard sample of the purely isotactic heptamer (*mmmmmm* + *mmmmmr*) was isolated by GPC from Sample A. The standard sample of the purely syndiotactic pentamer of MMA (*rrrr*) was isolated by HPLC from the oligomer mixture prepared with *t*-C_4H_9Li-$(C_2H_5)_3Al$ complex and was purified by recrystallization.

Figure 11 shows GPC curves of the isotactic oligomer of MMA prepared with *t*-C_4H_9MgBr (Sample A) and of the syndiotactic oligomer of MMA prepared with *t*-C_4H_9Li-$(C_2H_5)_3Al$ (Sample B).

The SFC traces of Samples A and B are shown in Figures 12a and 13a, respectively. The pressure at the bottom of column (p_b) was set 198 kg/cm^2 for the measurements. The oligomer components from trimer to 20-mer separated completely. All the analysis finished within 15 min. The standard sample of the syndiotactic pentamer of MMA (*rrrr*) exhibited the elution peak at the same retention time as the peak numbered 5 in the SFC of Sample B (Figure 13b). Mass spectrum of the fraction #8 isolated from Sample A showed the parent peak at *M/Z* = 859 (Figure 14), indicating that peak #8 in Figure 12a is attributable to the octamer ($C_{44}H_{74}O_{16}$ = 859.1).

The fractions #7 and #9 of Sample A were collected three times, and then analyzed by SFC again; the fractions showed elution peaks at their original positions accompanied by small satellite peaks (Figures 12b and 12c). ^1H NMR analysis of the fraction #7 from Sample A yielded the spectrum of good signal-to-noise ratio by an overnight (15 h) measurement as shown in Figures 15a and 15b (in chloroform-*d* at 35°C and 500 MHz, 90° observation pulse, pulse repetition = 15 s, 3600 scans). In the ^1H NMR measurement, the signal at 1.52 ppm due to H_2O was suppressed by the gated homonuclear irradiation. The spectrum agreed well with the spectrum of the isotactic heptamer of MMA (*mmmmmm* + *mmmmmr*)(Figures 15c and 15d). These demonstrate the feasibility of the ^1H NMR analysis of the fraction collected by SFC.

The complete separation of oligomer components and the rigid assignments for them enabled the determination of *Mn* and *Mw/Mn* for Samples A and B (Table 7). The values determined by SFC and by GPC roughly agreed with each other, however, the values deter-

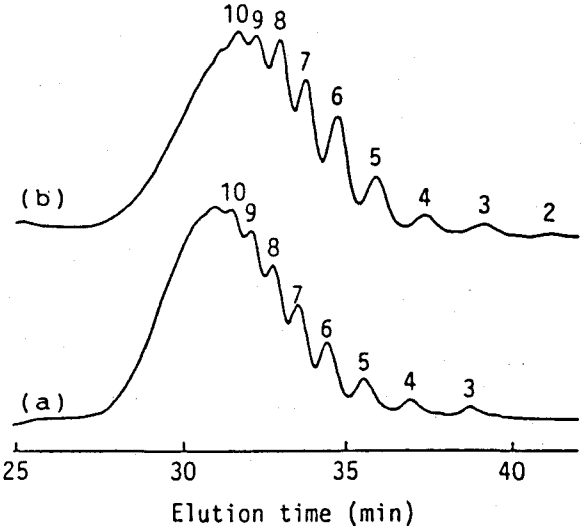

Figure 11. GPC traces of the MMA oligomers prepared with *t*-C_4H_9MgBr (Sample A)(a) and with *t*-$C_4H_9Li/(C_2H_5)_3Al$ (Sample B)(b).

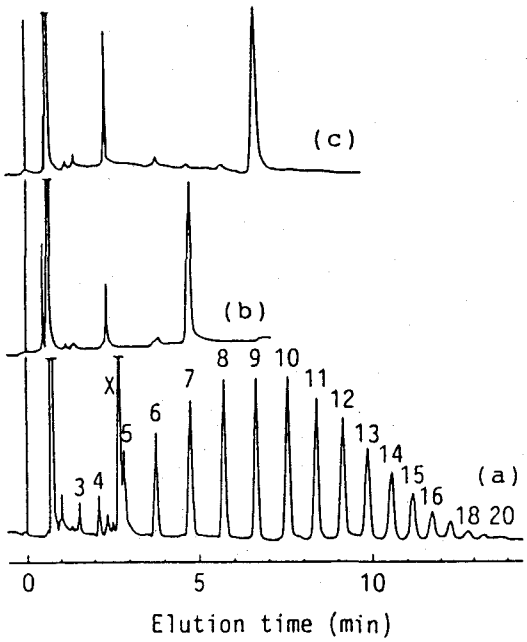

Figure 12. SFC traces of the isotactic oligomer of MMA prepared with *t*-C_4H_9MgBr in toluene at -78°C (Sample A)(a) and of the fractions #7 (b) and #9 (c) collected three times from Sample A. Mobile phase: CO_2 0.3 ml/min, C_2H_5OH 0.025 ml/min; column temp: 110°C (initial), 50°C (final); pressure at the bottom of column (p_b): 198 kg/cm^2.

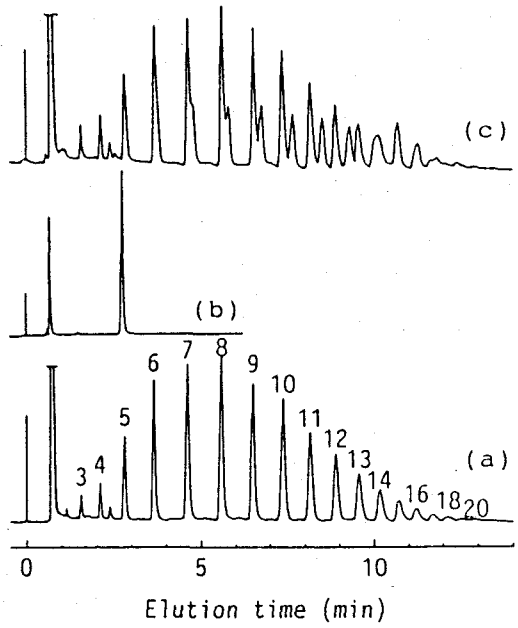

Figure 13. SFC traces of the syndiotactic oligomer of MMA prepared with *t*-$C_4H_9Li/(C_2H_5)_3Al$ in toluene at -78°C (Sample B)(a), the standard sample of the syndiotactic (*rrrr*) pentamer (b) and of the mixture of Samples A and B (A:B = 1:2)(c). The experimental conditions are the same as in Figure 13.

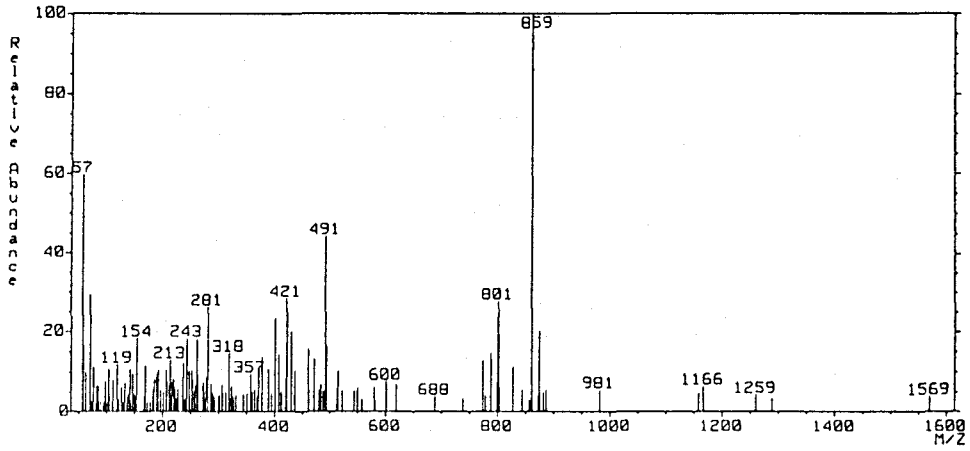

Figure 14. Mass spectrum of the fraction #8 of Sample A collected by SFC.

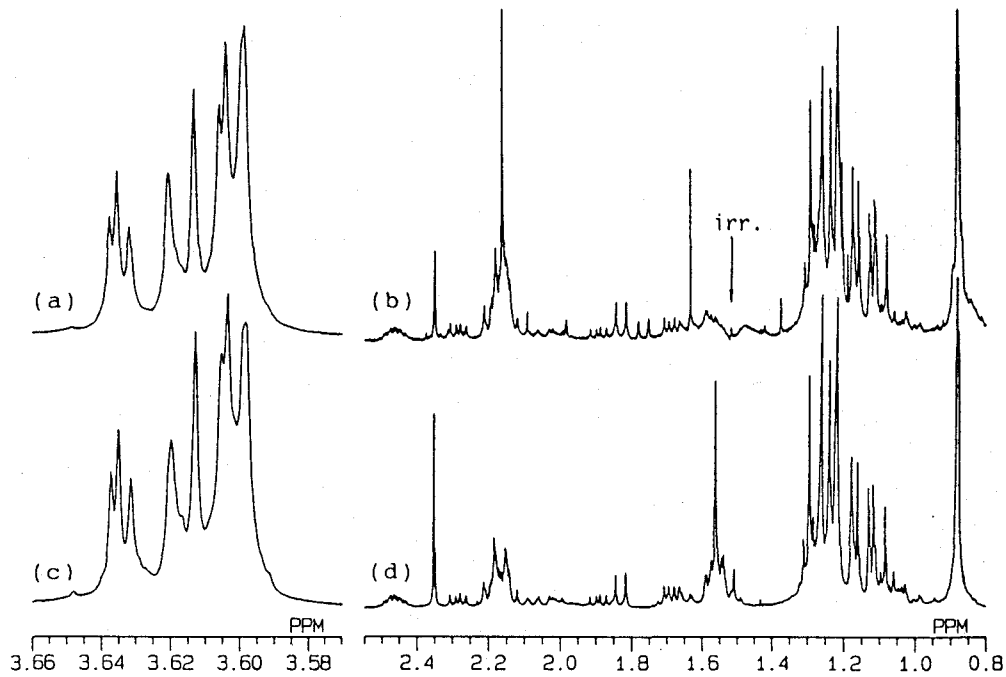

Figure 15. ^{1}H NMR spectra of the fraction #7 isolated from Sample A using SFC (a and b) and of the isotactic heptamer of MMA (*mmmmmm* + *mmmmmr*) (c and d). ($CDCl_3$, 35°C, 500 MHz)

Table 7. The *Mn* and *Mw/Mn* values for the MMA oligomers (Samples A and B) determined by GPC and by SFC

Method	Sample A		Sample B	
	Mn	*Mw/Mn*	*Mn*	*Mw/Mn*
GPC	987	1.09	920	1.10
SFC	924	1.05	893	1.11

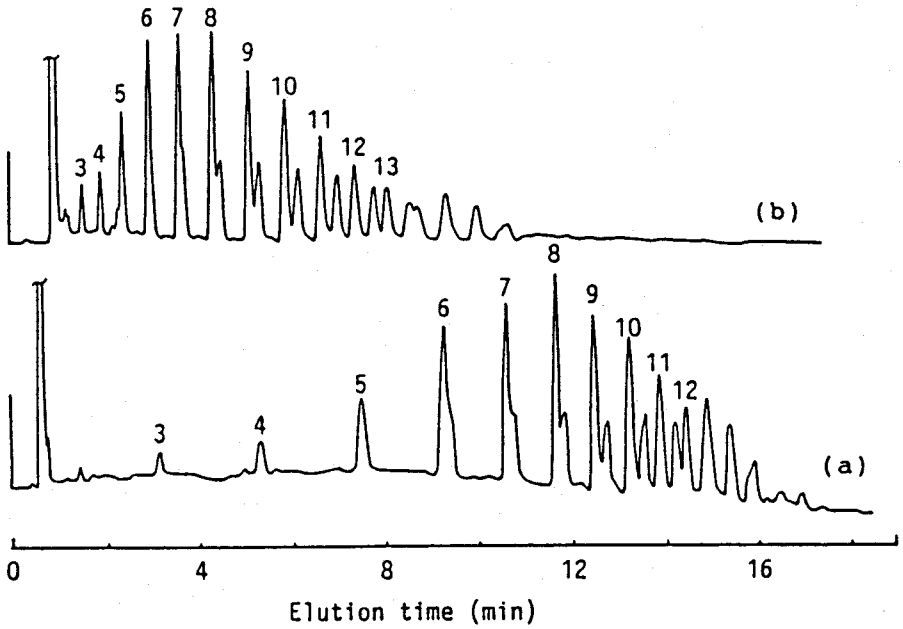

Figure 16. SFC traces for the mixture of the isotactic and syndiotactic oligomers of MMA (Sample A : Sample B = 1 : 2). Pressure at the bottom of column (p_b): (a) 156 kg/cm^2, (b) 219 kg/cm^2.

mined by SFC should be considered as more reliable because of the complete separation of the components.

The *mm*$\cdots$*m* isomer eluted faster than the *rr*$\cdots$*r* isomer in the normal phase HPLC analysis[16]. In contrast, the isotactic oligomers had slightly longer retention time in the SFC analysis than the syndiotactic oligomers of the corresponding degree of polymerization. This can be realized more easily in the SFC curve for a 1:2 mixture of Samples A and B (Figure 13c). The difference between the isotactic and syndiotactic oligomers in retention time became obvious over heptamer. The oligomer components from octamer to 12-mer each showed two distinct peaks of nearly 1:2 ratio due to the stereoisomers. The peaks arising from the isotactic 13-mer and the syndiotactic 14-mer joined to give a single broad peak again.

The SFC pattern showed dependency on p_b (Figure 16). In the SFC curve recorded at p_b of 156 kg/cm^2 (Figure 16a), the peaks due to the isotactic 12-mer and the syndiotactic 13-mer overlapped whereas the peaks due to the isotactic 14-mer and the syndiotactic 15-mer overlapped in the SFC recorded at 219 kg/cm^2 (Figure 16b). As p_b increased, separation of the higher molecular weight components was improved and the retention time was shortened.

The elution peak "X" due to an unknown compound was observed between the peaks due to the tetramer and pentamer in the chromatogram recorded at p_b of 198 kg/cm^2 (Figure 12a), whereas it was observed between the peaks due to the pentamer and hexamer in the chromatogram recorded at 219 kg/cm^2 (not shown). This indicates that the unknown compound has the dissolution property much different from that of the MMA-oligomers. The structural analysis of the unknown compound was not possible because of the unexpectedly small amount of the fraction for its strong UV-absorbtion.

The results described above show that SFC is suitable for the rapid and detailed analysis of the MMA oligomers and also for the fractionation of the oligomer components. The stereoregular oligomers of MMA provide good standard materials for SFC analysis because they are free from the peak-broadening due to stereoisomers of the oligomer components.

3.5 Experimental Part

3.5.1 Preparation of the MMA-oligomers

The *it*-oligomers were prepared by the living polymerization of MMA with *t*-C_4H_9MgBr in toluene at -78°C ([MMA]/[*t*-C_4H_9Mg-] = 50 mol/mol). The reaction was terminated 15 min after initiation by adding a small amount of methanol to the polymerization mixture. The solvent and unreacted monomer were removed by distillation, and the inorganic salts were removed by centrifugation. The yield of the oligomeric products was 7.5 %, and the *Mn* was 470. The oligomer mixture was fractionated by HPLC on a column (0.72 x 50 cm) packed with silica gel using the butyl chloride and acetonitrile mixtures as an eluent (*n*-BuCl/CH_3CN = 96/4 - 80/20)[15]. A Shodex SE-11 RI-detector was used. The diastereomer ratio for the trimers were *mm/mr/rm/rr* = 48/45/3/1 by ^1H NMR spectroscopy. Crystals of *3mm* were grown from the heptane solution of the fraction *3mm+3rm* (*3mm/3rm* = 48/3). The crystals were purified by recrystallization, and one of them was subjected to the X-ray structure analysis.

The *st*-oligomers were prepared by the oligomerization of MMA with *t*-C_4H_9Li-$(C_2H_5)_3Al$ in toluene at -78°C for 3 h ([Li]/[Al] = 1/2 mol/mol, [MMA]/[*t*-C_4H_9] = 1/5 mol/mol) The yield of the oligomer mixture was 93% and the *Mn* was 570. The diastereomer ratio for the trimer fraction were *mm/mr/rm/rr* = 0/1/29/70.

3.5.2 NMR Spectroscopy

^1H and ^{13}C NMR spectra were measured in $CDCl_3$ at 55°C using a JEOL JNM-GX500 spectrometer. Spin-lattice relaxation time (T_1) was determined by the inversion recovery method in toluene-*d*$_8$ or in *N,N*-dimethylformamide-*d*$_7$ at 35°C using a sealed NMR sample tube under nitrogen atmosphere. Double-quantum filtered (DQF) ^1H COSY[38] and long-range ^{13}C-^1H COSY with ^1H broad-band decoupling (COLOC; correlation spectroscopy via long range coupling)[39] were performed by using the pulse sequences included in a JEOL PLEXUS (ver. 1.5) software package. The typical conditions for two-dimensional measurements are as follows. The DQF-COSY experiments employed a recycle time of 2.5 s, with 16 transients being collected for each t_1 value. A total of 512

spectra, each consisting of 1024 data points, were accumulated within a frequency range of 1600 Hz in both dimensions. The COLOC experiments employed a recycle time of 1.5 s, with 256 transients being collected for each t_1 value. A total of 128 spectra, each consisting of 8192 data points, were accumulated, covering 1600 Hz in F_1 dimension and 21000 Hz in F_2 dimension. The data matrix was zero-filled to 256 x 8192 points before the double Fourier transformation.

3.5.3 SFC and GPC measurements

SFC was performed on a JEOL JSF-880 chromatograph equipped with a column (1.7 x 250 mm) packed with octadecylsilane-treated silica gel (particle size 5 μm). The system consists of two computer-controlled pumps[40,41], one is for the delivery of liquefied CO_2 as mobile phase (flow rate = 300 μl/min), and the other for the delivery of ethanol as modifier (flow rate = 25 μl/min). Concentration of the modifier in the mobile phase was kept constant throughout the experiments. The pressure at the bottom of column was regulated by a release valve within ± 1 kg/cm^2 of the desired pressure. An UV detector JEOL CAP-UV01 (operated at the wave length of 210 nm) fitted with a cell of 1 μl in volume and 5 mm in light path was employed. The amount of sample used for the analysis was 0.3 mg of the oligomer dissolved in 1.0 μl of dichloromethane. The column temperature was initially set 110°C and was cooled down to 50°C at the rate of 4°C/min after injection of the sample.

GPC was performed on a JASCO TRIROTAR-II chromatograph equipped with a GPC column (30 x 500 mm, maximum porosity = 3 x 10^3) and with a Shodex SE-61 RI detector, using chloroform as eluent. Mass spectra were recorded on a JEOL JMS-DX303HF operated at field-desorption (FD) mode.

3.5.4 X-ray Crystallographic Determination of 3mm

X-ray data were collected with a Rigaku AFC-5R automated four circle diffractometer using CuKα radiation (λ = 1.5418 Å) in the ω-2θ scan mode. The space group was determined uniquely based on the systematic extinctions: $h + l = 2n + 1$ for *h0l*, $h = 2n + 1$ for *h00*, $k = 2n + 1$ for *0k0* and $l = 2n + 1$ for *00l*. Unit

cell parameters were derived from a least-squares calculation based on 20 intense reflections whose 2θ angles fell in the range of 44-46°. Three standard reflections monitored every 100 reflections during data collection indicated no appreciable decay. No absorption correction was made.

The structure was solved by the direct method using MULTAN 78[42]. The E map corresponding to the largest combined figure of merit revealed all non-hydrogen atoms. Positions for the non-hydrogen atoms were refined with anisotropic thermal parameters[43]. Difference electron density maps indicated clearly the locations of hydrogen atoms.

References

1. Y. Tanaka, H. Sato, K. Saito, K. Miyashita, *Makromol. Chem., Rapid Commun.*, **1**, 551 (1980).
2. H. Sato, Y. Tanaka, K. Hatada, *Makromol. Chem., Rapid Commun.*, **3**, 175 (1982).
3. H. Sato, Y. Tanaka, K. Hatada, *J. Polym. Sci., Polym. Phys. Ed.*, **21**, 1667 (1983).
4. S. Fujishige, *Makromol. Chem.*, **177**, 375 (1976).
5. S. Fujishige, *Makromol. Chem.*, **179**, 2251 (1978).
6. A. Bledzki, H. Balard, D. Braun, *Makromol. Chem.*, **189**, 2807 (1988).
7. J. -M. Bessiere, B. Boutevin, L. Sarraf, *J. Polym. Sci.*, **A26**, 3275 (1988).
8. T. Konishi, Y. Tamai, M. Fujii, Y. Einaga, H. Yamakawa, *Polym. J.*, **21**, 329 (1989).
9. P. Cacioli, D. G. Hawthorne, S. R. Johns, D. H. Solomon,E. Rizzardo, R. I. Willing, *J. Chem. Soc., Chem. Commun.*, 1355 (1985).
10. R. A. Volpe, T. E. Hogen-Esch, A. H. E. Muller, F. Gores, *Polym. Prep., Am. Chem. Soc., Div. Polym. Chem.*, **28**(2), 423 (1987).
11. K. Hatada, K. Ute, K. Tanaka, T. Kitayama, Y. Okamoto, *Polym. J.*, **17**, 977 (1985).
12. K. Hatada, K. Ute, K. Tanaka, Y. Okamoto, T. Kitayama, *Polym. J.*, **18**, 1037 (1986).
13. T. Kitayama, T. Shinozaki, E. Masuda, M. Yamamoto, K. Hatada, *Polym. Bull.*, **20**, 505 (1988).
14. T. Kitayama, T. Shinozaki, E. Masuda, M. Yamamoto, K. Hatada *Makromol. Chem. Suppl.*, **15**, 167 (1989).
15. Y. Okamoto, E. Yashima, T. Nakano, K. Hatada, *Chem. Lett.*, 759 (1987).
16. K. Hatada, K. Ute, K. Tanaka, T. Kitayama, *Polym. J.*, **19**, 1325 (1987).
17. K. Hatada, K. Ute, K. Tanaka, M. Imanari, N. Fujii, *Polym. J.*, **19**, 425 (1987).

18. K. Ute, T. Nishimura, K. Hatada, *Polym. J.*, **21**, 1027 (1989).
19. F. C. Schilling, F. A. Bovey, M. D. Bruch, S. A. Kozlowski, *Macromolecules*, **18**, 1418 (1985).
20. S. R. Johns, R. I. Willing, D. A. Winkler, *Makromol. Chem., Rapid Commun.*, **8**, 17 (1987).
21. M. Vacatello, P. J. Flory, *Macromolecules*, **19**, 405 (1986).
22. P. R. Sundararajan, *Macromolecules*, **19**, 415 (1986).
23. K. Ute, T. Nishimura, K. Hatada, Y. Matsuura, K. Sakaguchi, *Polym. Prepr. Jpn.*, **37**, 2480; E432 (1988).
24. K. Ute, T. Nishimura, Y. Matsuura, K. Hatada, *Polym. J.*, **21**, 231 (1989).
25. R. Chujo, K. Hatada, R. Kitamaru, T. Kitayama, H. Sato, Y. Tanaka, *Polym. J.*, **19**, 413 (1987).
26. F. A. Bovey, G. V. D. Tiers, *J. Polym. Sci.*, **44**, 173 (1960).
27. A. Nishioka, H. Watanabe, K. Abe, Y. Sono, *J. Polym. Sci.*, **48**, 241 (1960).
28. H. Kusanagi, H. Tadokoro, Y. Chatani, *Macromolecules*, **9**, 531 (1976).
29. R. Lovell, A. H. Windle, *Polymer*, **22**, 175 (1981).
30. K. Hatada, K. Ute, T. Nishimura, M. Kashiyama, T. Saito, M. Takeuchi, *Polym. Bull.*, **23**, 157 (1990).
31. R. E. Jentoft, T. H. Gouw, *J. Polym. Sci.*, B7 811 (1969).
32. E. Klesper, W. Hartman, *J. Polym. Sci, Polym. Lett. Ed.*, 15 9 (1977); *ibid*, 15, 713 (1977).
33. J. C. Fjeldsted, W. P. Jackson, P. A. Peaden, M. L. Lee, *J. Chromatogr. Sci.*, 21, 222 (1983).
34. F. P. Schmitz, B. Gemmel, "*Oligomer separation by supercritical fluid chromatography using gradient elution*" S. Parvez, T. Miyazaki, H. Parvez Eds., Supercritical Fluid Chromatography and Micro-HPLC. VSP, Utrecht, 1989, Progress in HPLC, vol 4, pp 73-85.
35. Y. Hirata, F. Nakata, *J. Chromatogr.*, **295** 315 (1984); *ibid*, 315, 31 (1984); *ibid*, **315**, 39 (1984).
36. B. E. Richtar, *J. HRC & CC*, **8**, 297 (1985).
37. K. Matsumoto, S. Tsuge, Y. Hirata, *Anal. Sci.*, **2**, 3 (1986).
38. U. Piantini, O. W. Sorensen, R. R. Ernst, *J. Am. Chem. Soc.*, **104**, 6800 (1982).
39. H. Kessler, C. Crisinger, J. Zarbock, H. R. Loosli, *J. Magn. Resn.*, **50**, 331 (1984).
40. T. Saito, M. Takeuchi, *JEOL News*, **23A**, 47 (1987).
41. T. Saito, M. Takeuchi, "*Development of an intelligent cascade pump which can perform microdelivery independent of compressibility of fluid*", S. Parvez, T. Miyazaki, H. Parvez, Eds., Supercritical Fluid Chromatography and Micro-HPLC. VSP, Utrecht, 1989, Progress in HPLC, vol 4, pp 25-51.
42. P. Main, S. E. Hull, L. Lessinger, G. Germain, J-P. Declercq, M. M. Woolfson, "*A System of Computer Programs for the Automatic Solution of Crystal Structures from X-ray Diffraction Data*", University of York.
43. T. Ashida, "HBLS V", The Universal Crystallographic Computing System Osaka, Osaka University, 1979, p. 53.

CHAPTER 4

Analysis of Polymers by On-line GPC/NMR

4.1 Introduction

Since its introduction in 1964[1], gel permeation chromatography (GPC) has gained wide acceptance as a standard tool for the determination of the molecular weight and its distribution in polymers. Determination of molecular weight distribution (MWD) provides significant information not only for the studies of polymer properties but also for the studies of polymerization reactions because MWD reflects the mechanism of polymer-formation.

As described in the previous chapters, the polymerization of MMA by an anionic initiator such as Grignard reagent and alkyllithium often involves multiple active species with different reactivities and stereospecificities. The resulting polymer has consequently a broad and/or multimodal MWD, and microstructures of the polymers such as tacticity varies with molecular weight. It is essential for the understanding of the nature of active species in these polymerizations to examine the molecular weight dependence of the microstructures. However, fractionation of polymer by GPC is usually laborious and requires considerable amount of the polymer sample.

Recent progress in NMR spectrometer on the sensitivity and resolution has made it possible to use the spectrometer as a real-time detector for GPC[2-6]. In comparison with other conventional GPC detectors, ^{1}H NMR is an information-rich detector. For example, the ^{1}H NMR provides a wealth of structural information regarding the degree of polymerization, the stereoregularity and the copolymer composition, whereas some other detectors provide only a net property of the polymer molecules.

The continuous-flow LC-^{1}H NMR experiment was first reported in 1979[7]. Recent review articles[8,9] demonstrated the feasibility of an NMR spectrometer as a detector for HPLC, although they are limited mostly to theoretical and technical considerations. This chapter describes the on-line GPC/NMR method which has been

developed as a novel technique for the characterization of polymers. The usefulness of the on-line GPC/NMR method using a 500 MHz ^{1}H NMR spectrometer in the studies of polymerization reactions was examined.

4.2 Instrumentation for the On-line GPC/NMR Method

Figure 1 illustrates the on-line GPC/NMR system on which the present works were performed. The on-line GPC/NMR system consisted of a JASCO TRI ROTAR-V chromatograph and a JEOL JNM-GX500 spectrometer (a 16-bit A/D converter was installed).

A 2 mm or a 3 mm (*i.d.*) glass tubing with tapered structure at both ends was employed as an NMR observation flow-cell (Figure 2b); the detection volume was 0.060 and 0.140 ml, respectively. Similar type of a flow-cell was used in the on-line HPLC/NMR experiments[10,11]. In our preliminary work[2], we used the NMR flow-cell without tapered structure at both ends (Figure 2a) and detected slight broadening of the elution band probably due to the turbulent flow in the inlet path of the flow-cell. Later[3], the tapered structures at both ends was found to remove the axial dispersion almost completely as described in the next section.

The flow-cell was mounted in the proton probe designed specially for the GPC/NMR system. The chromatograph equipped with a GPC column was placed about 2 m from the superconducting magnet, and the connections between the chromatograph and the flow-cell were made with a 3 m Teflon tubing (0.3 mm *i.d.*).

Chloroform-*d* or chloroform containing 10 % of chloroform-*d* was used as an eluent. The ^{2}D NMR signal of the eluent was satisfactorily intense for internal lock and shimming of the magnetic field. Background signals due to the small amount of impurities in the eluent, except for the signal of H_2O, could be eliminated by subtracting the base line absorbance. Flow rate of the eluent, size and maximum porosity of a column, the amount of sample used, and the conditions for NMR data acquisition are dependent on the purpose of the analysis; the conditions will be specified in each section.

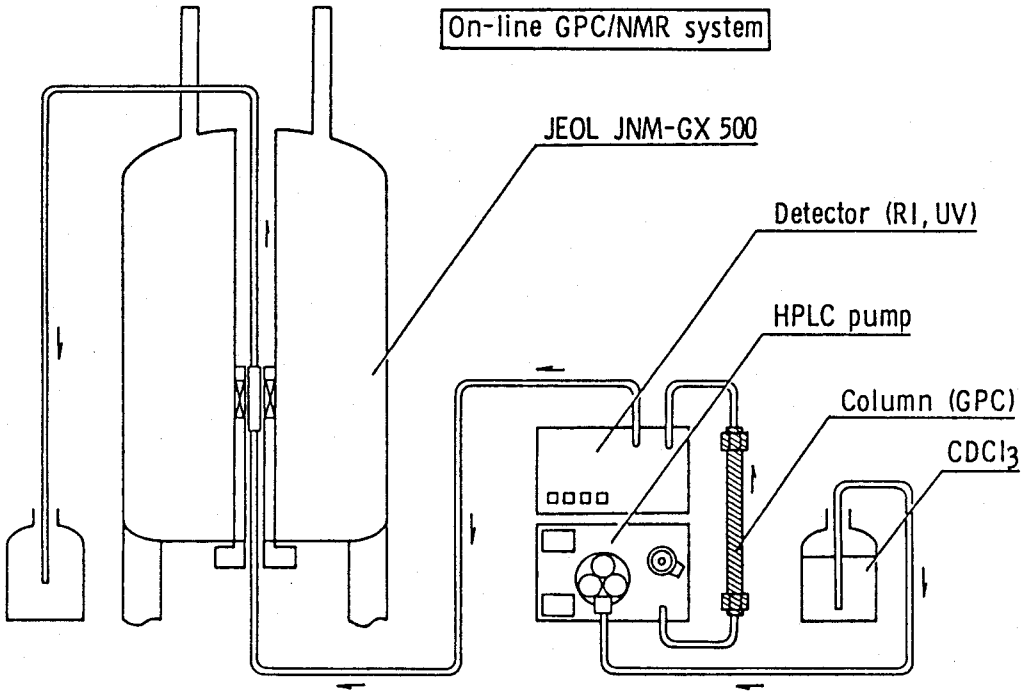

Figure 1. The schematic diagram of the on-line GPC/NMR system.

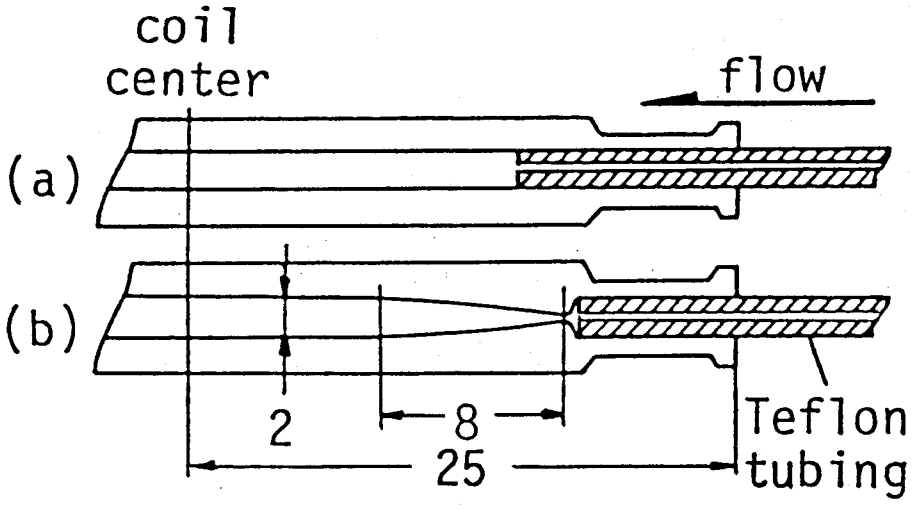

Figure 2. The 2 mm (*i.d.*) NMR observation flow-cell with (b) and without tapered structure (a) at both ends. The figures indicate the lengh in mm.

4.3 Determination of Molecular Weight and Its Distribution by the Absolute Calibration Method Using the PMMAs with Well-Defined Structure[2,3]

Determination of molecular weight by GPC requires making a calibration curve, for which a set of standard polystyrenes with narrow MWD are usually used. Preparation of other standard polymers with different molecular weights and narrow MWD are generally difficult or laborious, and much attention has been given to empirical means of deriving calibrations for other polymers from that for polystyrene[12]. The only exception at present is dual detection of a GPC chromatogram by a combination of UV or refractive index (RI) method with low angle light-scattering, in which the weight-average molecular weight (*Mw*) of a given polymer can be determined without a calibration curve[13].

The usefulness of a polymer having a known amount of chromophore groups per chain for absolute molecular weight calibration in GPC has been noted recently[14]. This technique was applied to the determination of instrumental broadening in GPC using the polystyrene polymerized with bis(3-phenylazo)benzoyl peroxide and the chromatograph equipped with a variable wavelength UV detector which is sensitive to both the chromophore and polymer[15].

NMR spectrometer is sensitive to mass concentration and also to the *Mn* of the solute polymer if the polymer molecule contains a known amount of end groups per chain. In this chapter the potential feasibility of the on-line GPC/NMR technique was realized in the preparation of an accurate calibration curve for highly isotactic PMMA with one t-C_4H_9- group at the α-end of the polymer chain.

The isotactic PMMAs used in this work were prepared by the living polymerization with t-C_4H_9MgBr in toluene at -78°C[16]. The PMMA-molecule contains one t-C_4H_9- group at the α-end of the chain and the *Mn* can be determined by relative intensities of the ^1H NMR signals due to t-C_4H_9- and CH_3O- groups as follows:

$$Mn = MW(\text{monomer-unit}) \times [3I(OCH_3)/I(t\text{-}C_4H_9)] + MW(\text{end-groups})$$

where MW(monomer-unit) = $C_5H_8O_2$ = 100 and MW(end-groups) = C_4H_9 +

H = 58. Table 1 gives the molecular weight and tacticity of the three PMMA samples used in this work.

A Shodex GPC column KF-802.5 (30 cm x 0.8 cm, maximum porosity = 2 x 10^4) was used for the present analysis. A 5 mm glass tubing (inner diameter = 2 mm) having a tapered structure at both ends was used for the NMR observation flow cell. Chloroform-*d* containing 0.5 % ethanol-d_6 was used as an eluent and the flow rate was 0.2 ml/min. The spin-lattice relaxation time (T_1's) for the CH_3O- and *t*-C_4H_9- resonances were found to be 1.02 s and 0.51 s, respectively. Thus, 45° observation pulse (2.9 μs) and the repetition time of 3.0 s were employed for correct measurement of intensity (magnetization recovers theoretically 98.5 % and 99.9 % of equilibrium state for CH_3O- and *t*-C_4H_9- resonances, respectively). The amounts of samples loaded were 0.4 mg, 0.5 mg and 0.9 mg for the PMMAs of *Mn* = 12600, 5260 and 3160, respectively. The ^1H NMR data, each consisting of 8192 data points covering 4500 Hz, were collected over the entire chromatographic peak and stored as 8 coadded scans every 24 s. A line broadening factor of 0.55 Hz was applied.

Figure 3 shows the GPC/NMR data of the isotactic PMMA with *Mn* of 12600. The cross section at 3.60 ppm, where the methoxy protons resonate, gives the ^1H NMR-detected GPC chromatogram. The ^1H NMR-detected GPC chromatograms of the three PMMA samples are shown in Figure 4, together with those recorded with an RI detector. The peak shapes of both the ^1H NMR-detected and RI-detected chromatograms are very similar to each other, and the difference in elution times due to difference in the void volume of the connecting path.

The ^1H NMR spectrum of the PMMA (*Mn* = 12600) stored as a single file for the elution time from 33.6 to 34.0 min (*cf.* Figure 4) is shown in Figure 5. The signal to noise ratio (S/N) for the *t*-C_4H_9- end group is 7.2. The *Mn* of the PMMA detected in this file was calculated to be 11800 from the intensities of the signals due to the CH_3O- and *t*-C_4H_9- groups. Similarly, spectra with good resolution and high S/N were obtained for most of the files. The files which exhibit the *t*-C_4H_9- signal with

Table 1. Characterization of PMMA samples

Mn[a]	*Mw/Mn*		Tacticity / %		
	GPC/RI	GPC/NMR	*mm*	*mr*	*rr*
3160	1.19	1.15	95.3	4.3	0.4
5260	1.13	1.13	96.9	3.0	0.1
12600	1.18	1.13	97.7	2.1	0.2

[a] Determined by ^{1}H NMR.

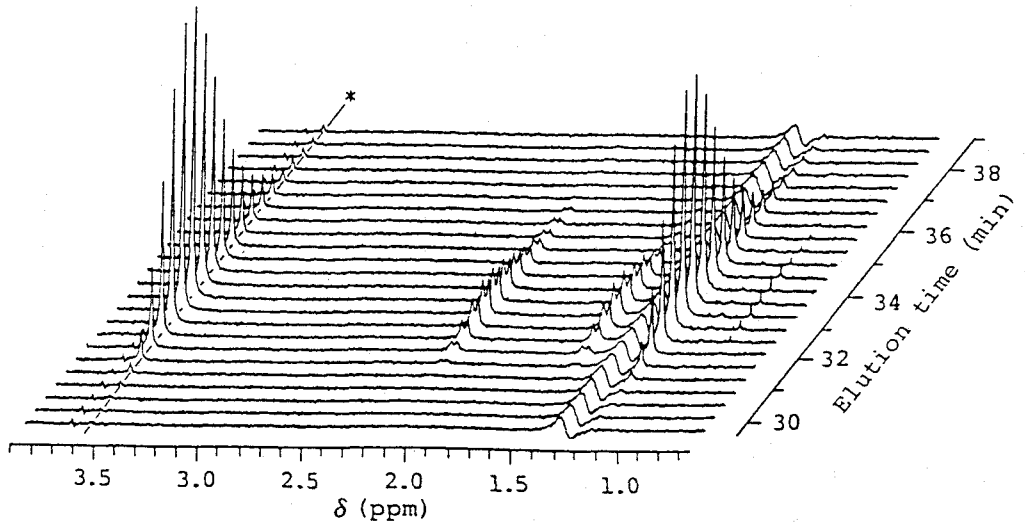

Figure 3. On-line GPC/NMR data of isotactic PMMA (*Mn* = 12600). Cross sections at 3.60 ppm (*) where the methoxy proton resonates give the ^{1}H NMR-detected GPC curve (see Figure 4).

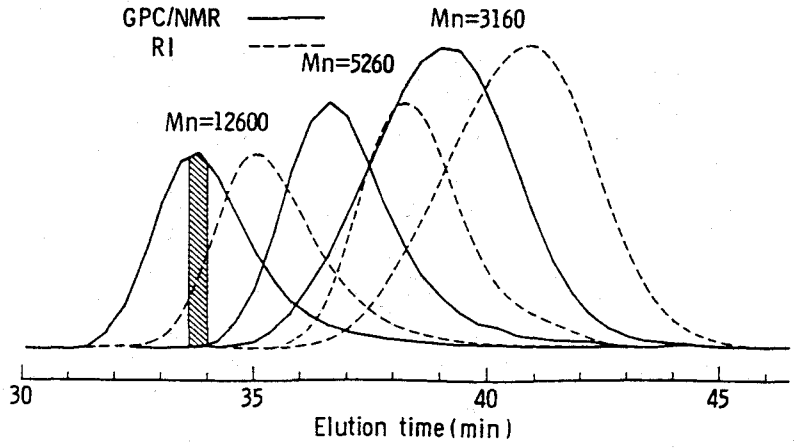

Figure 4. The ^{1}H NMR-detected GPC curves of the isotactic PMMAs with *Mn*'s of 12600, 5260 and 3160. These curves were obtained by plotting the intensity of the methoxy proton signal (3.60 ppm). The RI-detected GPC curves are also shown.

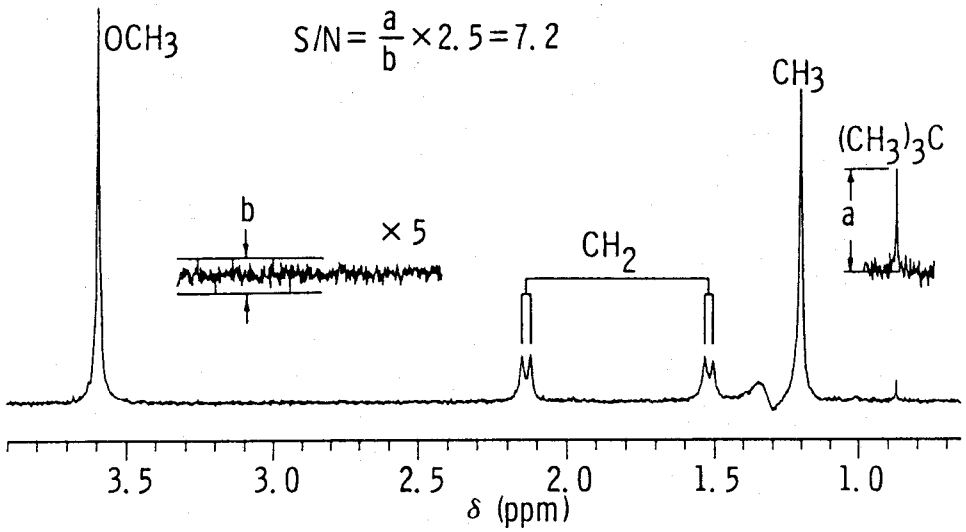

Figure 5. The ^{1}H NMR spectrum of the isotactic PMMA (*Mn* = 12600) stored as a single file at the elution time from 33.6 to 34.0 min. (45° pulse, 8 scans, 8192 data points covering 4500 Hz, line-broadening factor of 0.55 Hz.) *Mn* of the PMMA detected in this file was calculated to be 11800 from the equation:

$$Mn = \text{MW(monomer-unit)} \times DP + \text{MW(end-groups)},$$

where $DP = [3I(\text{OCH}_3)/I(t\text{-C}_4\text{H}_9)] = 117$, MW(monomer-unit) = $C_5H_8O_2$ = 100, MW(end-groups) = C_4H_9 + H = 58.

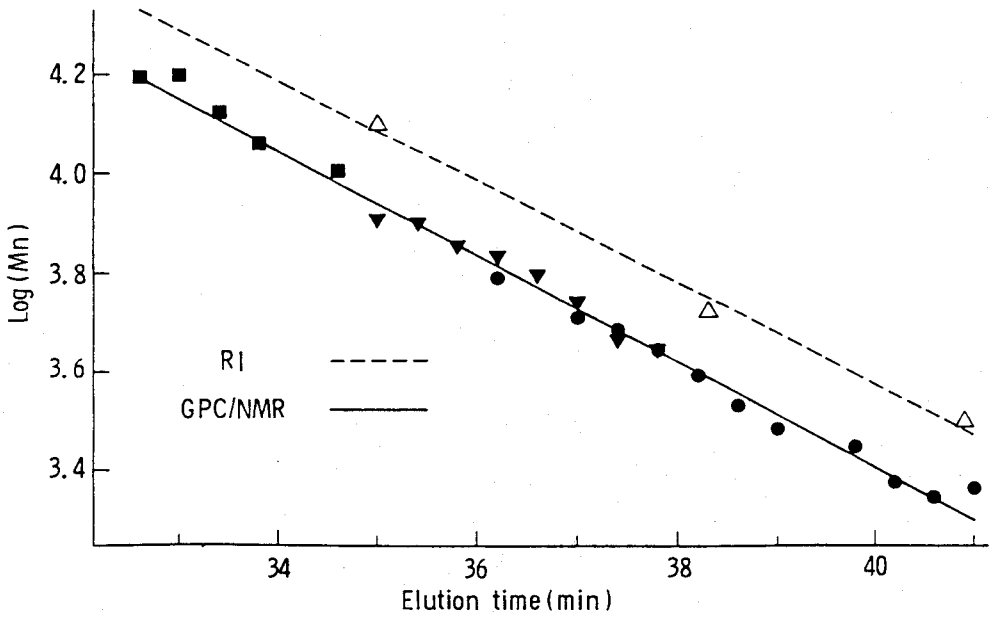

Figure 6. Plots of *log(Mn)* of isotactic PMMAs determined from the intensity ratio for the ^{1}H NMR signal of CH_3O- to *t*-C_4H_9- against elution time; *Mn* = 12600 (■), 5260 (▼), 3160 (●). The calibration curve made by plotting *log(Mn)* of the isotactic PMMAs against the peak-maximum elution time using RI-detection is also shown (△ and broken line). The flow-cell with tapered structure (Figure 2b) was employed.

the S/N less than 5 were added with 2 or 3 contiguous files so that the ratio exceeded 5. Thus the *Mn* of each fraction can be determined directly from the ^{1}H NMR spectrum. This is one of the great advantages of the on-line GPC/NMR system over dual detection systems such as UV-RI detectors or a variable wavelength UV-detector which requires calibration of the detected intensity of absorption due to end-groups and polymers for the real molecular weight.

The logarithm of the *Mn* determined from the ^{1}H NMR spectrum in each file is plotted against the elution time. The plots for all the three PMMA samples fall on a single straight line as shown in Figure 6 (solid line). The slope of the straight line is close to that of the calibration curve made by plotting *log(Mn)* for the three PMMA samples (*Mn* = 12600, 5260 and 3160) against the peak-maximum elution time using an RI-detector (broken line in Figure 6). The calibration curve made by the GPC/RI method in this way is not completely correct because the *Mw/Mn* values of 1.13 - 1.19 for the PMMA samples (Table 1) are not small enough to regard their *Mn*'s as the *Mn* at the peak-maximum elution time. Thus, the linear relation of *log(Mn) versus* elution time obtained by this on-line GPC/NMR experiment should be the most accurate calibration curve for highly isotactic PMMA. The *Mw/Mn* values calculated from the GPC/NMR method agreed well with those obtained from the normal GPC/RI method using standard polystyrenes as shown in Table 1.

In our preliminary work[2] we conducted similar experiments using the NMR flow-cell without a tapered structure at both ends (*cf.* Figure 2a) and found that the slopes of *log(Mn) versus* elution time curve for the PMMA samples of different *Mn*'s differed slightly from each other (Figure 7). The phenomenon was considered due to broadening of the elution band by the turbulent flow in the inlet path of the flow-cell. The present results clearly show that the tapered structure at both ends of the cell almost completely remove broadening.

The results mentioned here indicate the usefulness of on-line GPC/NMR for absolute calibration of molecular weight when polymer samples of well defined structure are available. It is noteworthy that a single sample with a broad MWD is enough to

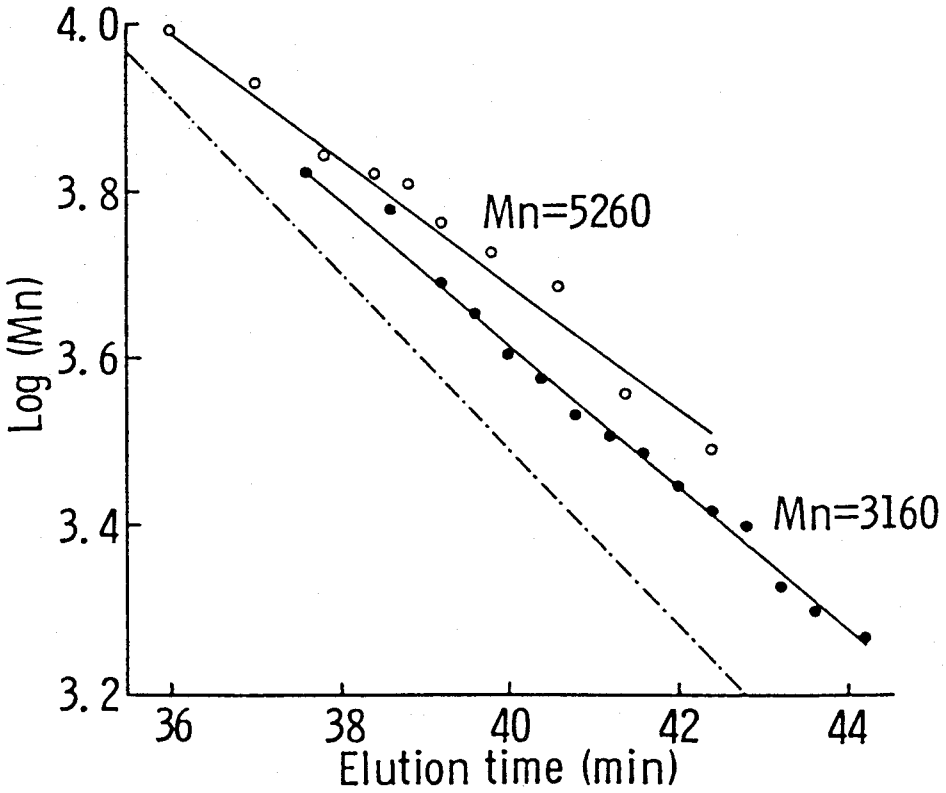

Figure 7. Plots of *log(Mn)* of isotactic PMMAs against elution time obtained from the on-line GPC/NMR measurement using the flow-cell without tapered structure; *Mn* = 5260 (○), 3160 (●).

make the calibration curve if the number of end groups per chain is well defined. On-line detection by ^1H NMR offers not only the absolute calibration curve but also information on the molecular weight dependency of some polymer-properties such as tacticity or copolymer composition at the same time. Thus, efforts for preparing the polymers of controlled structure should be encouraged for providing on-line GPC/NMR with suitable polymer samples.

4.4 Molecular Weight Dependence of Tacticity of the PMMAs Prepared by Anionic Initiators[4]

As mentioned in Chapter 2, polymerization of MMA in toluene with the *t*-C_4H_9MgBr prepared in diethyl ether yields highly isotactic PMMA with a narrow MWD. The *t*-C_4H_9MgBr solution contained excess amount of $MgBr_2$ which was formed through the side reaction between *t*-C_4H_9MgBr and *t*-C_4H_9Br during the preparation.

$$t\text{-}C_4H_9MgBr + t\text{-}C_4H_9Br \longrightarrow (t\text{-}C_4H_9)_2 + MgBr_2$$

Owing to the excess amount of $MgBr_2$, the Schlenk equilibrium shifts to the side of "*t*-C_4H_9MgBr" which produces highly isotactic PMMA.

$$(t\text{-}C_4H_9)_2Mg + MgBr_2 \rightleftharpoons 2\ t\text{-}C_4H_9MgBr$$

Accordingly, the isotacticity of the PMMA prepared by *t*-C_4H_9MgBr depends strongly on the amount of $MgBr_2$ in the initiator solution; the *t*-C_4H_9MgBr solution whose $[Mg^{2+}]/[t\text{-}C_4H_9Mg]$ ratio was larger than 1.5 gave highly isotactic polymer and that with the ratio less than unity gave less isotactic or syndiotactic polymer.

Figure 8a shows the ^1H NMR-detected GPC trace of the PMMA prepared with *t*-C_4H_9MgBr ($[Mg^{2+}]/[t\text{-}C_4H_9Mg] = 0.87$) in toluene at -78°C. The chromatogram was obtained by monitoring the methoxy proton resonance at 3.59 ppm. The polymer has a trimodal MWD,

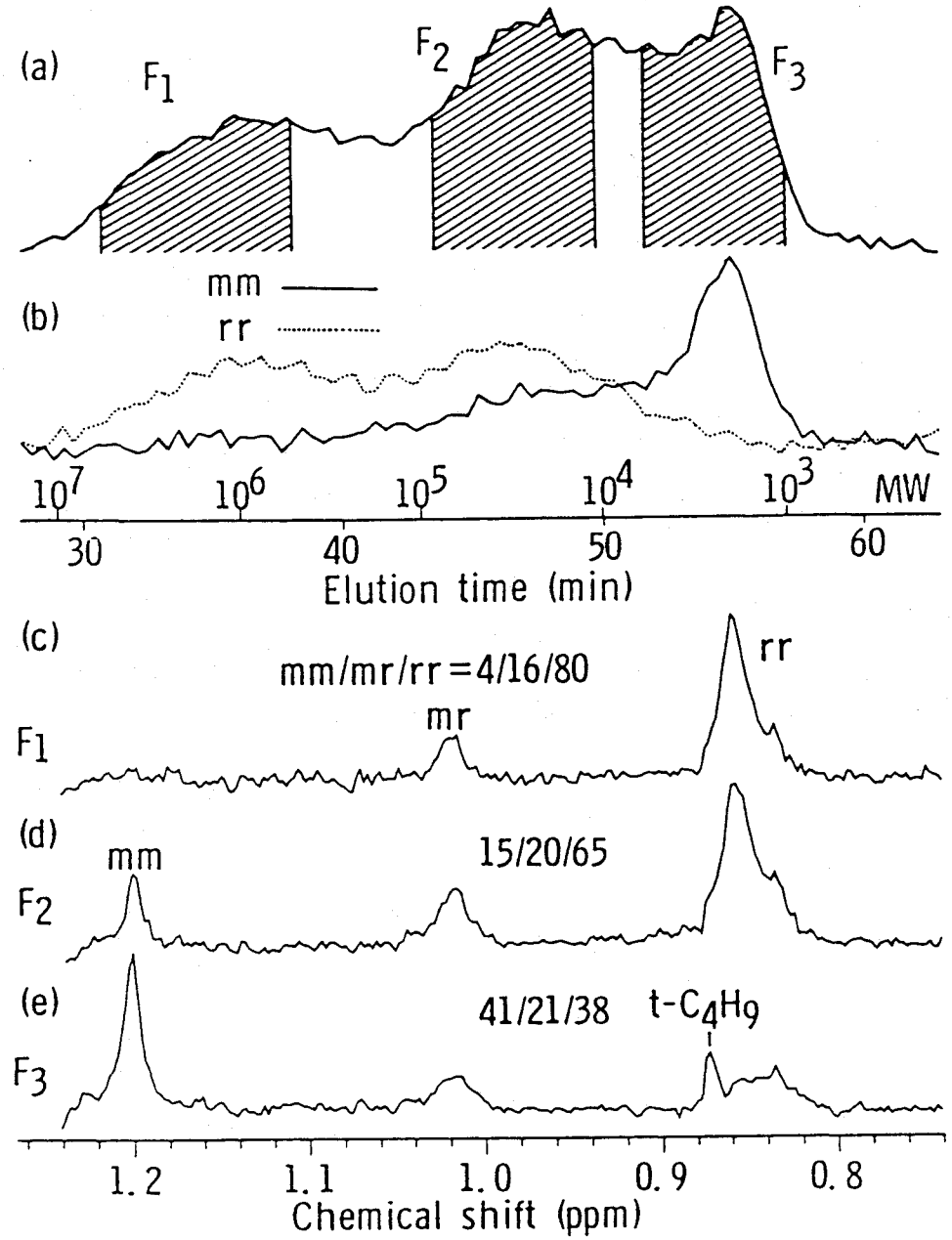

Figure 8. The ^{1}H NMR-detected GPC traces obtained by monitoring the methoxy proton resonance at 3.59 ppm (a) and the α-methyl proton resonances at 0.86 ppm (·····) and 1.20 ppm (——) due to *rr*- and *mm*-triads, respectively (b). The NMR signals due to α-methyl protons of the PMMA eluted in the elution periods F_1 (c), F_2 (d) and F_3 (e) are also shown.

and the ^{1}H NMR spectra acquired in the elution periods F_1, F_2 and F_3 (*cf.* Figure 8a) show that the tacticity of the higher molecular weight part is syndiotactic (Figure 8c) while those of the lower molecular weight parts are less syndiotactic (Figure 8d) or stereoblock-like (Figure 8e). The molecular weight dependence of tacticity can also be illustrated in a continuous form by plotting the signal intensities of the α-methyl proton resonances at 0.86 and 1.20 ppm due to the *rr*- and *mm*-triads, respectively, against elution time (Figure 8b). It is very clear that the fraction of syndiotactic triad increases with an increase in molecular weight of the polymer. The results suggest that the high molecular weight part with high syndiotacticity (*cf.* Figure 8c) was produced from the species generated by "(t-C_4H_9)$_2$Mg" and that the isotactic part which has lower molecular weight and a relatively narrow MWD (*cf.* Figure 8e) was produced from the species generated mainly by "t-C_4H_9MgBr".

Figure 9 shows the results of GPC/NMR analysis for the PMMA obtained by n-C_4H_9MgCl in toluene at -78°C[17]. The Grignard reagent was also prepared in diethyl ether but contained a stoichiometric amount of Mg^{2+} ([Mg^{2+}]/[n-C_4H_9Mg] = 1.0). As shown in Figure 9, the PMMA has a broad MWD and the higher molecular weight part is more syndiotactic than the lower molecular weight one. Probably the situation is similar to that of the polymerization by t-C_4H_9MgBr mentioned above, although the MWD is unimodal. It was reported that PMMA formed with n-C_4H_9MgCl was a mixture of isotactic and syndiotactic PMMAs as evidenced by thin layer chromatography[18] and competitive adsorption to silica gel[19]. The GPC/NMR analysis clearly shows that the syndiotactic part had higher molecular weight than the isotactic one.

The PMMA prepared with 1,1-diphenylhexyllithium (DPHLi) in toluene at -78°C is highly isotactic. However, the MWD of the polymer is very broad. GPC/NMR analysis revealed that the isotacticity of the polymer increased with increasing molecular weight and that the high molecular weight part was almost 100 % isotactic in triad (Figure 10). The results indicate that the reactivity of the propagating species has a wide distribution and the species with the higher reactivity are more isotactic-specific. The difference in the structure of the propagating species

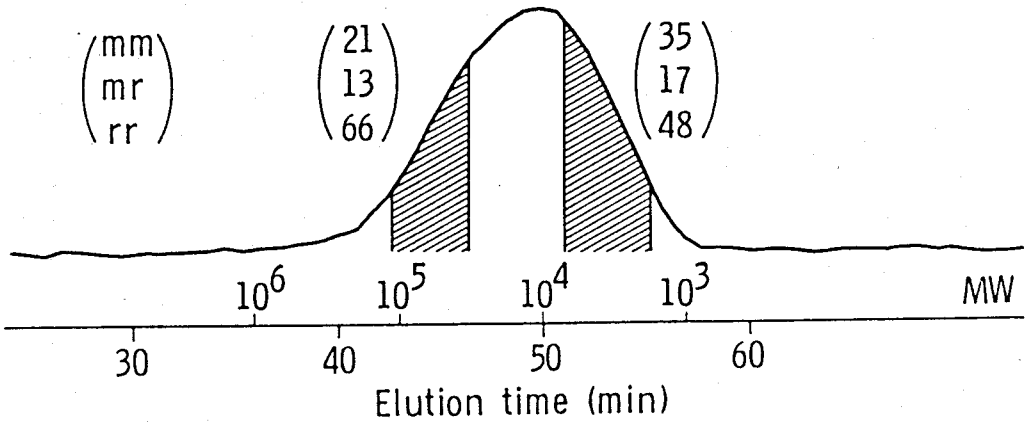

Figure 9. ^{1}H NMR-detected GPC trace of the PMMA prepared with *n*-C_4H_9MgCl in toluene at -78°C (monitoring the methoxy proton resonance at 3.59 ppm) and the triad tacticities of the eluting fractions.

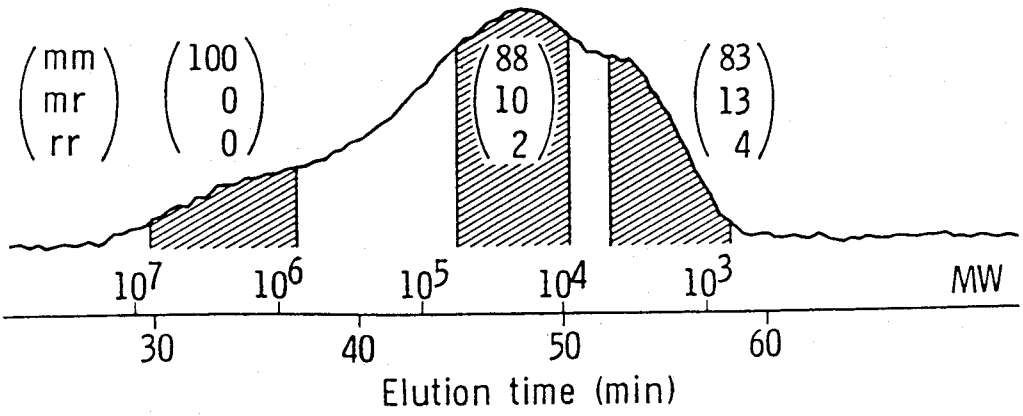

Figure 10. ^{1}H NMR-detected GPC trace of the PMMA prepared with 1,1-diphenylhexyllithium in toluene at -78°C (monitoring the methoxy proton resonance at 3.59 ppm) and the triad tacticities of the eluting fractions.

may be caused partly by the association among the DPHLi molecules in toluene at low temperature. The number average molecular weight of the polymer was much larger than the theoretical value calculated from the polymer yield and the initial monomer/initiator ratio, which indicates the association of DPHLi. Wiles and Bywater[20] reported a similar variation of isotacticity with molecular weight for the PMMA formed with DPHLi in toluene at -30°C; the isotactic triad contents in fractionated PMMAs varied from 75 % (Mv = 10^4) to 95 % (Mv = 10^6).

Polymerization of MMA with t-C_4H_9Li in toluene at -78°C gave isotactic-rich PMMA with a broad but unimodal MWD[21,22]. Figure 11 shows an NMR-detected GPC trace and a variation of isotactic triad content with molecular weight. Similarly to the DPHLi-initiated polymerization, the isotacticity increased with increasing molecular weight. However, the distribution of the propagating species in regard to reactivity in the polymerization by t-C_4H_9Li seems much narrower than that in the polymerization by DPHLi. The difference may result from different degree of association of these initiators.

It was recently found that a mixture of t-C_4H_9Li and trialkylaluminum (R_3Al) such as triethyl-, tri-n-butyl- or tri-n-octylaluminum gave highly syndiotactic polymers of MMA and other methacrylates with narrow MWD in toluene at low temperatures[21,22]. As described above, t-C_4H_9Li itself gave an isotactic PMMA with a broad MWD. Addition of R_3Al increased the syndiotacticity of the PMMA and at the ratio of R_3Al/t-$C_4H_9Li \geq 3$ highly syndiotactic PMMAs with a narrow MWD were produced. At the ratio of 1.0 the PMMA with stereoblock-like tacticity and with a bimodal MWD formed in a low yield.

The PMMA prepared with t-C_4H_9Li-(n-C_4H_9)$_3$Al (Al/Li = 1.0) in toluene at -78°C was analyzed by on-line GPC/NMR as shown in Figure 12. Figure 12a is a contour plot of the GPC/NMR data and the spectra of the cross section at 49.2 and 57.2 min are shown in Figures 12b and 12c, respectively. These clearly indicate that the lower molecular weight part is syndiotactic and the higher molecular weight one is highly isotactic. Addition of R_3Al to t-C_4H_9Li generates syndiotactic propagating species for MMA by the formation of a weak complex between t-C_4H_9Li and (n-

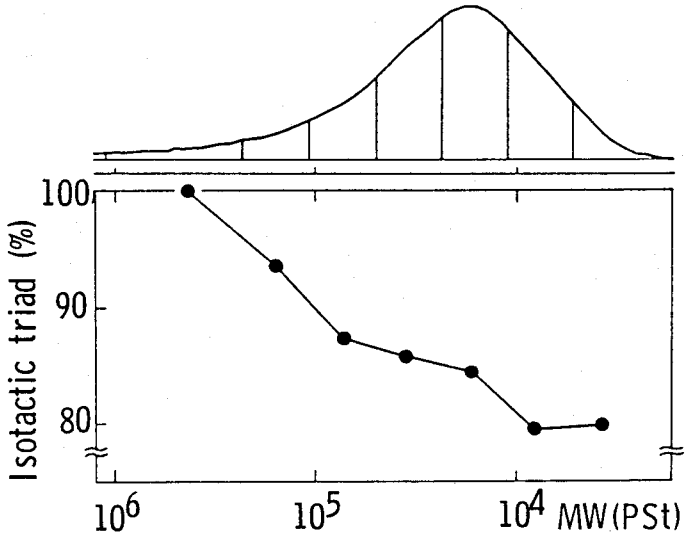

Figure 11. ^{1}H NMR-detected GPC trace of the PMMA prepared with *t*-C_4H_9Li in toluene at -78°C and the plot of the *mm*-triad content for the seven regions.

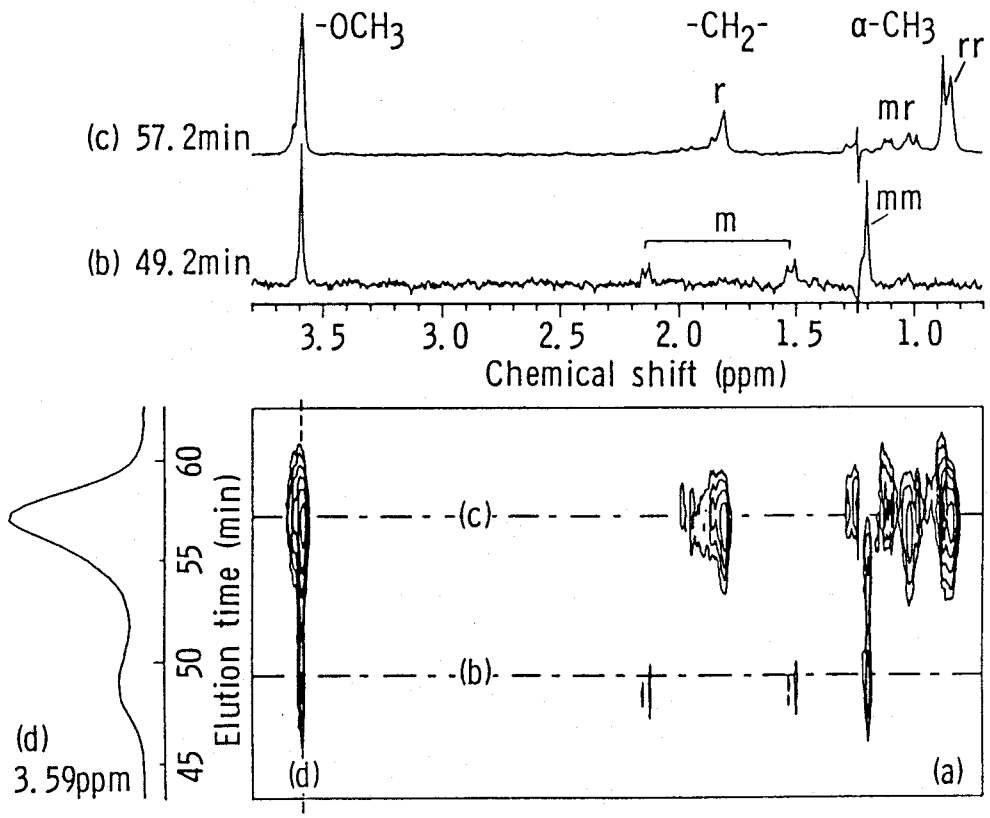

Figure 12. A contour plot (a) and cross sections (b-d) of the on-line GPC/NMR data for the PMMA prepared with *t*-C_4H_9Li-(*n*-C_4H_9)$_3$Al (Al/Li = 1.0) in toluene at -78°C.

$C_4H_9)_3Al$ and at the ratios of Al/Li ≥ 3 all the *t*-C_4H_9Li molecules are involved in the syndiotactic species. At the ratio of 1.0 there exist isotactic and syndiotactic propagating species concomitantly to give a mixture of isotactic and syndiotactic PMMAs. The mixture forms stereocomplex in toluene at low temperature so that the polymerization mixtures gels, which causes the low yield of the polymer.

4.5 Molecular Weight Dependence of Chemical Composition of the Copolymers of Methacrylates[5]

The properties of copolymers depend primarily on their chemical compositions, and the chemical compositions of copolymers often depend on their molecular weights. Molecular weight dependence of the compositions of copolymers has been determined by fractionation and subsequent compositional analysis of the fractions. However, this method requires much time and rather large amount of sample. A recent review by Mori[23] describes that dual-detector systems, such as UV-RI, or multiple wavelengths detections with an IR or UV detector, can be used for the determination of copolymer composition in GPC. In these methods, the monomer units to be distinctively detected are often limited by either their molecular structure or their combination.

In this section, the potential feasibility of the GPC/NMR method is described on the analysis of the chemical compositions of block and random copolymers of MMA and butyl methacrylate (*n*-BuMA) obtained by anionic polymerization. The molecular weight dependencies of the chemical compositions of these copolymers determined by the GPC/NMR experiment gave us important information on the copolymerization mechanism.

A Shodex GPC column K-80M (30 cm x 0.8 cm, maximum porosity = 3 x 10^7) was used. Chloroform-*d* was used as an eluent and the flow rate was 0.2 ml/min. Sixty degree pulse and the repetition time of 1.0 s were employed in the ^1H NMR measurement. The injected sample was 1.0 mg each. The ^1H NMR data, each consisted of 8192 data points covering 4500 Hz, were collected over the

entire chromatographic peak and stored as 24 coadded scans every 24 s. A line broadening factor of 0.55 Hz was applied. A Shodex SE-61 RI detector was also used for the detection.

Polymerization of MMA by *t*-C_4H_9MgBr in toluene at low temperature gives highly isotactic PMMA with narrow MWD. The polymerization system is living and permits us to prepare the block copolymer of MMA with other methacrylates[24]. In this work, the PMMA-*block*-poly(*n*-BuMA) was prepared by the polymerization of *n*-BuMA with the living isotactic PMMA formed with *t*-C_4H_9MgBr in toluene at -60°C. The poly(MMA-*ran*-*n*-BuMA) was prepared by adding *t*-C_4H_9MgBr to the mixture of MMA and *n*-BuMA ($[MMA]_o/[n\text{-BuMA}]_o=2/1$) in toluene at -78°C. The results of these copolymerizations are shown in Table 2. The *Mn* of the copolymers agreed well with the expected value, indicating the initiator efficiency to be close to unity, although multimodal MWD's were observed. Figure 13 shows 500 MHz ^1H NMR spectra of the copolymers measured in $CDCl_3$ at 35°C. It is evident from the α-CH_3 and CH_2 signals that the copolymers are highly isotactic.

Figure 14 shows the GPC/NMR data of the PMMA-*block*-poly(*n*-BuMA). The GPC chromatograms corresponding to MMA and *n*-BuMA units can be obtained form the cross sections at 3.59 ppm (OCH_3) and 3.95 ppm (OCH_2), respectively. Relative intensities of the chromatograms were normalized to represent the mole ratios of MMA and *n*-BuMA units: the cross sections at every 0.02 ppm covering the respective peak areas were accumulated and normalized. The results are shown in Figure 15-1. Thus, the copolymer composition can be directly determined from the elution curves A and B at any specified region in the chromatogram. This is one of the great advantages of this on-line GPC/NMR system over dual detection systems such as UV-RI detectors, which require calibration of the detected intensity for the real chemical composition. The ratio of the areas under the elution curves A and B (33.6 : 66.4) agreed well with the mole ratio of MMA and *n*-BuMA units in the block copolymer (34.3 : 65.7) as determined from the ^1H NMR spectrum measured under the static conditions (Figure 13-A). The chromatogram C (Figure 15-1C) obtained by summation of the two chromatograms A and B coincided well with that obtained with

Table 2. Preparation of Poly(MMA)-*block*-poly(*n*-BuMA) and Poly(MMA-*ran*-*n*-BuMA) with *t*-C_4H_9MgBr in Toluene[a]

	MMA/*n*-BuMA in feed	$[M]_0$ / $[I]_0$	Time (hr)	Yield (%)	*Mn* (VPO)	*Mw*/*Mn*	MMA/*n*-BuMA in polymer[b]	Tacticity(%) *mm*	*mr*	*rr*
Block[c]	34.4/65.6	87.5	4.5+24	100	10500	2.44	34.3/65.7	97	3	0
Random[d]	66.3/33.7	101.0	72	99	11200	3.88	67.2/32.8	97	3	0

[a] $[MMA+n\text{-BuMA}]_0$/toluene = 2.0 mol/L.

[b] Determined from ^1H NMR spectra measured in $CDCl_3$ at 35°C.

[c] MMA 40mmol, *n*-BuMA 76.4mmol, temperature -60°C; Mn(calcd)=11100.

[d] MMA 6.7mmol, *n*-BuMA 3.4mmol, temperature -78°C; Mn(calcd)=11500.

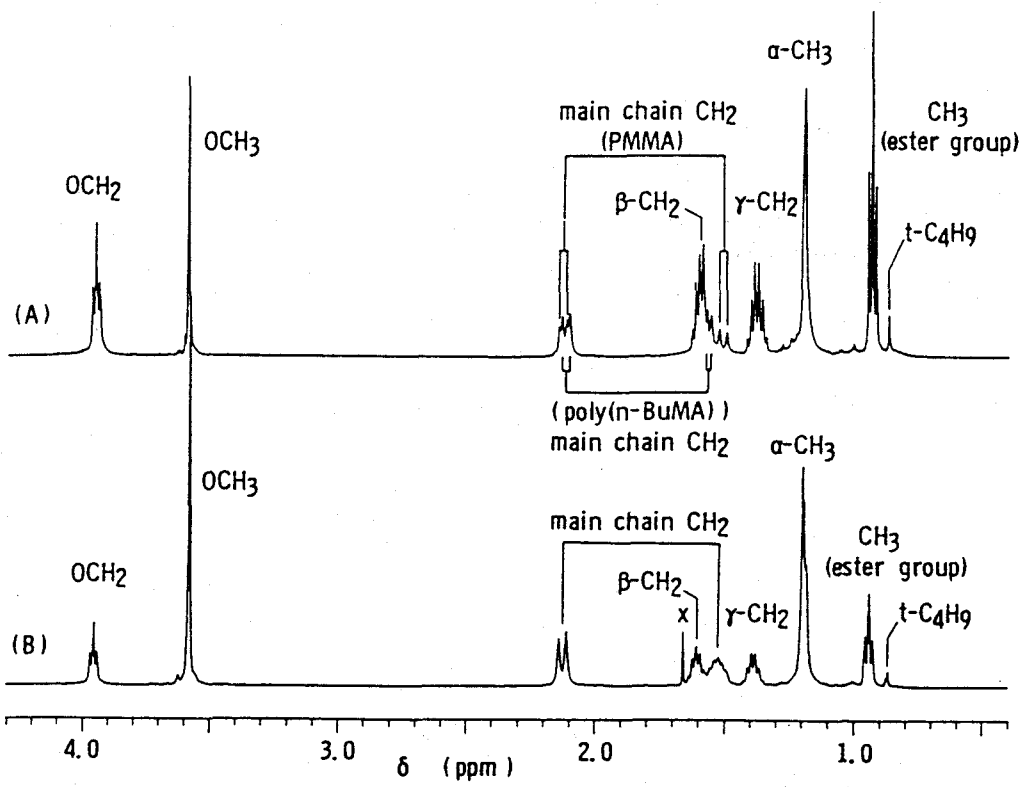

Figure 13. 500 MHz ^1H NMR spectra of PMMA-*block*-poly(*n*-BuMA) (A) and poly(MMA-*ran*-*n*-BuMA) (B) prepared with *t*-C_4H_9MgBr in toluene at -60°C and -78°C, respectively ($CDCl_3$, 35°C).

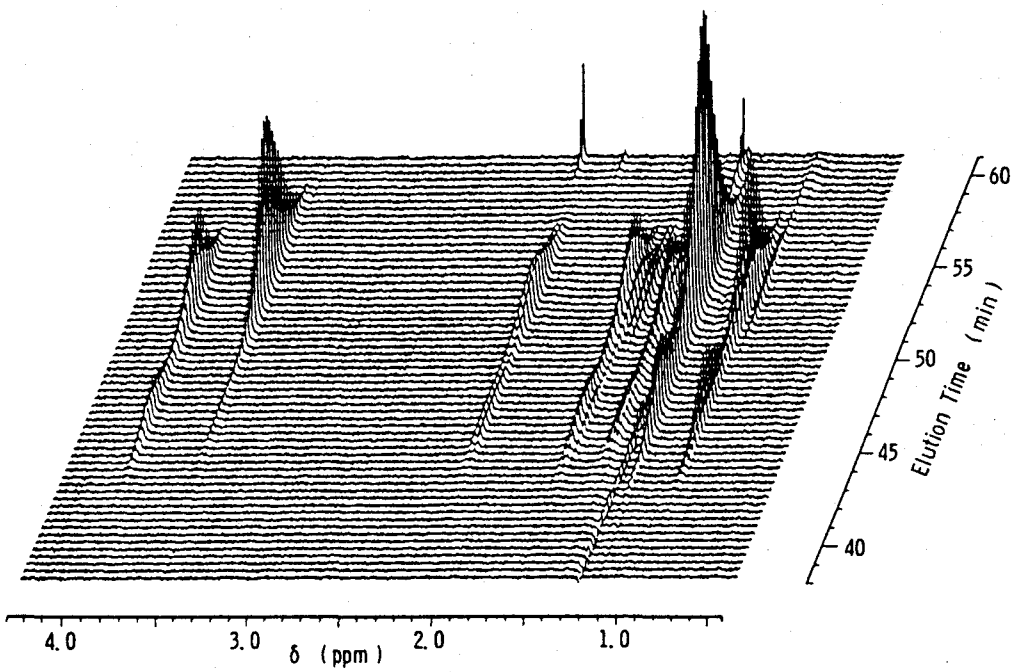

Figure 14. On-line GPC/NMR data of PMMA-*block*-poly(*n*-BuMA).

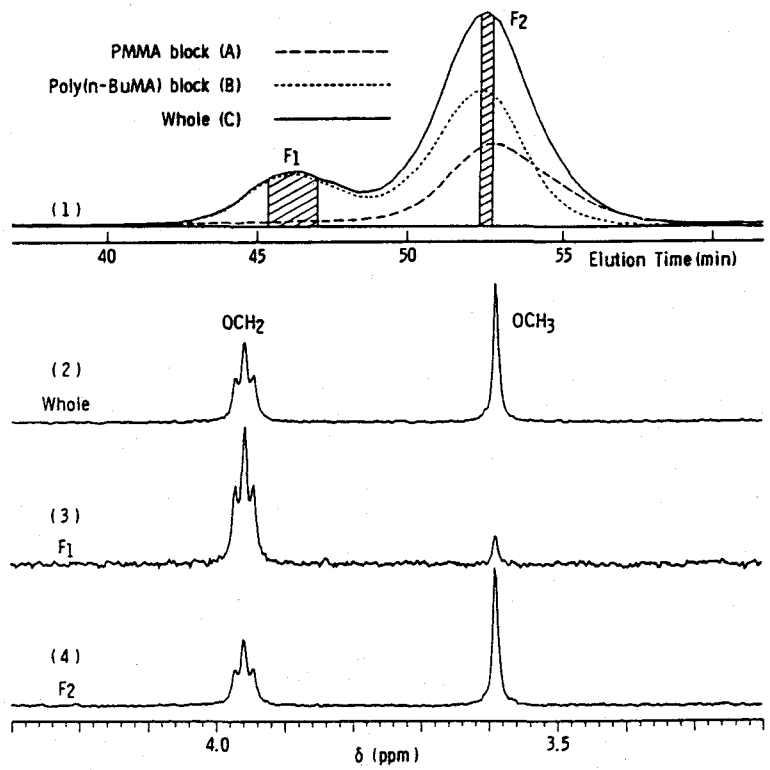

Figure 15. On-line GPC/NMR analysis of PMMA-*block*-poly(*n*-BuMA) prepared with *t*-C_4H_9MgBr in toluene at -60°C.

RI detection. Figure 15 also illustrates the ^1H NMR spectra (OCH_3 and OCH_2 region) obtained by summation of all the data blocks covering the whole elution peak (Figure 15-2) and by summation of the data blocks included in the parts of F_1 (Figure 15-3) and F_2 (Figure 15-4), both indicated in Figure 15-1. The total mole ratio of MMA and *n*-BuMA determined from Figure 15-2 was again 34.5 : 65.5. The results depicted in Figure 15 clearly show that the high molecular weight fraction is rich in *n*-BuMA units, while the low molecular weight fraction is rich in MMA units.

The GPC/NMR data of the PMMA-*block*-poly(*n*-BuMA) was divided into seven regions as indicated in Figure 16. The *Mn* for each region was calculated from the calibration curve made by using standard polystyrenes, and the chemical composition of each region was determined from the ^1H NMR spectrum for the region. Degrees of polymerization (*DP*'s) of the PMMA and poly(*n*-BuMA) blocks could be calculated from the *Mn*'s and the chemical compositions for the individual regions. Figure 16 shows the plots of the logarithmic *DP* of the PMMA and poly(*n*-BuMA) blocks for each region against the molecular weight of the copolymer. The average *DP* of PMMA blocks was about 30, which corresponds to the $[MMA]_0/[t\text{-}C_4H_9MgBr]_0$ ratio in the polymerization. From the weight fraction and *Mn* of each region, the *Mw/Mn* of the PMMA-*block*-poly(*n*-BuMA) against molecular weight of the block copolymer was roughly estimated to be 1.07. The value is close to that for the PMMA homopolymerized with $t\text{-}C_4H_9MgBr$ in toluene at -60°C. The *DP* of the PMMA block slightly increases with an increase in the molecular weight of the block copolymer. The result may suggest that the living PMMA anions with higher *DP* have higher reactivity than those with lower *DP* in the polymerization of *n*-BuMA. It is also noticeable that the chromatogram showed no detectable peak due to the PMMA homopolymer with *DP* of 30. On the other hand, *log(DP)* of poly(*n*-BuMA) block increased linearly with an increase in the Mn of the copolymer. These results show that the polymer is truly a block copolymer formed from the living PMMA anion. The bimodal MWD of the block copolymer indicates that at least two types of active species with different activity should be generated in the polymerization of

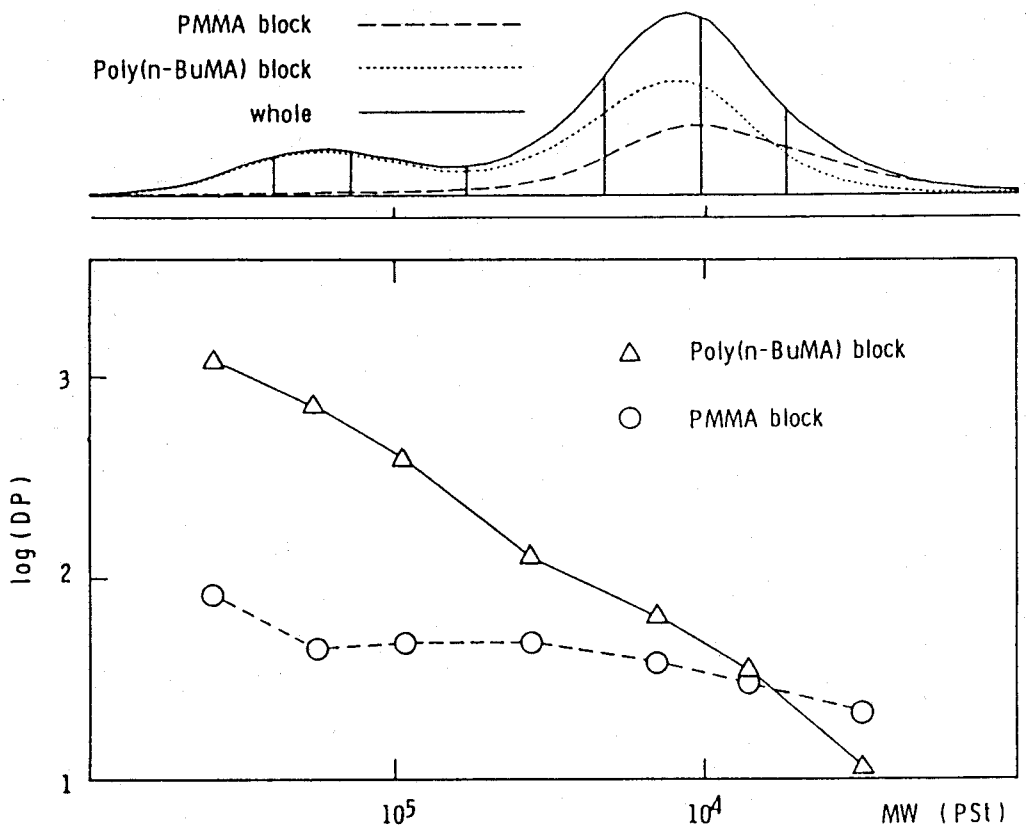

Figure 16. Plots of DP's of PMMA and poly(*n*-BuMA) blocks in the PMMA-*block*-poly(*n*-BuMA) against molecular weight of the block copolymer.

Table 3. The Number of Polymer Molecules in the High and Low Molecular Weight Fractions of Poly(MMA)-*block*-poly(*n*-BuMA)

Fraction	*Mn*	$\frac{Mw}{Mn}$	Number of polymer molecules (mmol)
High MW part	87800	1.19	0.028
Low MW part	9140	1.32	1.35

n-BuMA with the living PMMA anion, although the initiation reaction occurred quantitatively. *Mn*, *Mw/Mn* and the number of polymer molecule for the high and low molecular weight peaks in the bimodal GPC curve were estimated separately and listed in Table 3. The number of polymer molecules of the high molecular weight fraction was one-fiftieth as much as that of the low molecular weight fraction, although the *DP* of the former fraction was 10 times as large as that of the latter fraction. This means that about 2 % of the living PMMA anions form the propagating species for the high molecular weight fraction, whose activity was about 500 times as high as that for the low molecular weight fraction.

Polymerization of MMA with *t*-C_4H_9MgBr in toluene at low temperature gave highly isotactic PMMA with a narrow MWD, while polymerization of *n*-BuMA gave highly isotactic poly(*n*-BuMA) but with a multimodal MWD. Figure 17 shows the results obtained by GPC/NMR experiment on the random copolymer of MMA and *n*-BuMA (MMA/*n*-BuMA = 66.3/33.7) prepared with *t*-C_4H_9MgBr in toluene at -78°C. The chromatogram (Figure 17-1F) clearly shows multimodal MWD. The chromatograms D and E, based on MMA and *n*-BuMA units, respectively, indicate that the chemical composition is almost independent of its molecular weight. Figures 17-2 and 17-3 are the ^1H NMR spectra of fractions F_3 and F_4 indicated in the chromatogram, respectively. It is evident from the spectra that both the fractions are highly isotactic. These results suggest that multiple active species with different reactivities exist in the copolymerization system, but their monomer selectivities and stereoregularities are almost the same.

The present studies clearly show that the on-line GPC/NMR allows us to investigate the molecular weight dependence of the chemical composition of copolymer, in a short time (< 60 min), with a small amount of sample (< 1mg) without calibration, and to extract a wide variety of information from the data of a single experiment. The results obtained by this method will serve to investigate copolymerization mechanism. It is easy to imagine that the application of the GPC/NMR method is not restricted to the analysis of the chemical composition of binary copolymer but can be extended to the analysis of terpolymer or the higher order of multicomponent copolymers.

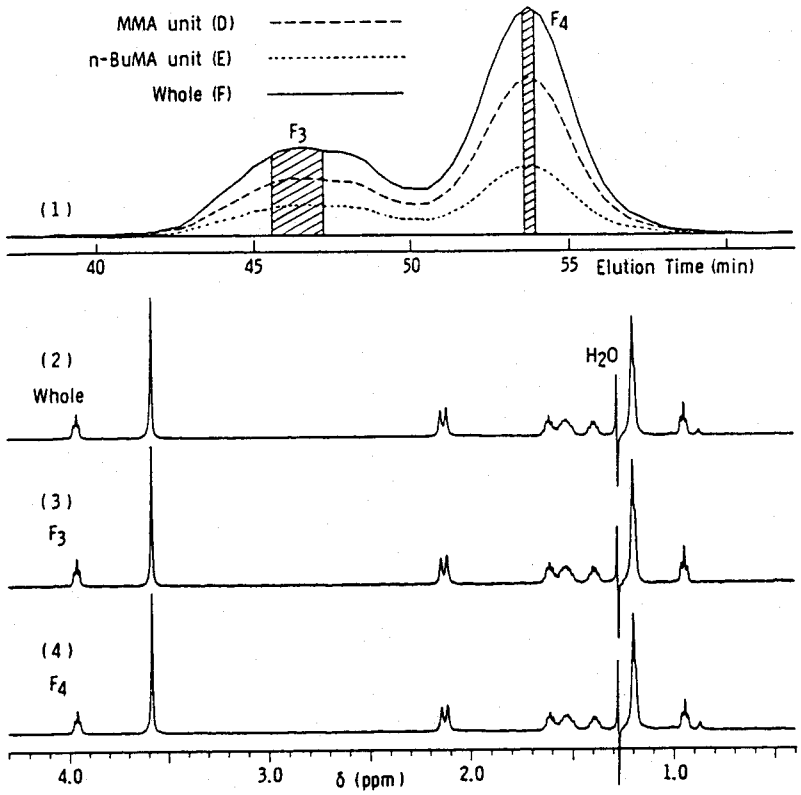

Figure 17. On-line GPC/NMR analysis of poly(MMA-*ran*-*n*-BuMA) prepared with *t*-C_4H_9MgBr in toluene at -78°C.

4.6 On-line GPC/NMR Analysis of the Mixture of Chloral Oligomers[6]

The on-line GPC/NMR method will also provide structural data of the homologous components in the oligomers such as chloral oligomers if a GPC column with small porosity is employed.

The stereochemistry of chloral oligomers has been investigated extensively[25-29], and it was shown that oligomers could be isolated when the polymerization of chloral was carried out near and slightly below the ceiling temperature of polymerization and was acetate end-capped.

$$t\text{-}C_4H_9OLi + n\ CCl_3CHO \xrightarrow[-\ CH_3CO_2Li]{(CH_3CO)_2O} t\text{-}C_4H_9O\text{-}\left(\text{-}\underset{\displaystyle CCl_3}{\underset{|}{CH}}\text{-}O\text{-}\right)_n\text{-}COCH_3$$

Gas chromatographic studies on a mixture of the chloral oligomers[26] revealed that the dimer (n = 2) exists in the *meso (m)* and *racemo (r)* diastereomers and that the trimer and tetramer fractions (n = 3 and 4) each tends to exhibit one main peak, accompanied by some small satellite peaks. NMR and X-ray crystallographic analyses[28,29] showed that the major isomer of dimer and the highly predominant isomers of trimer and tetramer were the *m*-, *mm*- and *mmm*-diastereomers, respectively. It is the objective of this work to analyze the oligomer components of the higher degree of polymerization ($3 \leq n \leq 7$) by the on-line GPC/NMR method.

The mixture of chloral oligomers was prepared by t-C_4H_9OLi initiation and acetate end-capping as reported previously (8,9). The residue of vacuum distillation (bp > 125°C, 1.0 mmHg) obtained from the mixture was subjected to the on-line GPC/NMR analysis.

Chloroform containing 10 % of chloroform-*d* and 0.5 % of ethanol was used as an eluent and the flow rate was 1.5 ml/min. The 10 % of chloroform-*d* was enough for internal lock of the magnetic field. The amount of the sample loaded was 10 mg. Ninety degree pulse (5.8 μs) and the repetition time of 6.0 s were employed for acquisition of ^1H NMR data. A total of 128 spectra, each consisted of 16K data points covering 4500 Hz, were collected during the elution time from 40.0 to 65.6 min and

stored as 2 coadded scans (time resolution of 12 s). Main band of the strong signal due to the eluent ($CHCl_3$) was suppressed by gated homonuclear irradiation as shown in Figure 18. A line-broadening factor of 0.27 Hz was applied.

Figure 19 shows the on-line GPC/NMR data of the mixture of chloral oligomers (5.45 - 6.35 ppm). Singlet signals due to acetal protons appear in the figure. ^1H NMR spectra of the oligomer components from heptamer to trimer were recorded successively during the elution time from 46.0 to 52.2 min.

Six spectra recorded in the elution time from 46.0 to 47.2 min (data #30 - #35) were accumulated to yield a spectrum of the chloral heptamer in much improved S/N (Figure 20a). Seven peaks observed at 5.713, 5.797, 5.969, 6.217, 6.231, 6.241 and 6.816 ppm are attributable to the seven acetal protons in the heptamer. Similarly, ^1H NMR spectra of the pure components from hexamer to trimer were obtained separately from the single GPC/NMR measurement (Figures 20b-20e); the spectra consist of 6, 5, 4 and 3 singlets, respectively. We have already confirmed by X-ray analysis that the spectra shown in Figures 20d and 20e are due to the *mmm*-tetramer and the *mm*-trimer, respectively[27]. Thus Figures 20a-20e indicate that the chloral oligomer consists exclusively of purely isotactic oligomers, although several unassigned peaks of weak intensity are found in the spectrum of trimer fraction (Figure 20e). The chain-growth reaction of the propagating species having *racemo*-sequence should be hindered by steric reasons over the trimer level.

Figure 21 shows the GPC traces recorded by RI-detection (Figure 21a) and by ^1H NMR-detection (Figure 21b). The difference between the time scales in Figures 21a and 21b resulted from the difference in the void volume of the connecting path. The ^1H NMR-detected elution curves were obtained by monitoring peak height of the acetal proton signals resonating at 6.231 ppm (heptamer), 5.677 ppm (hexamer), 5.837 ppm (pentamer), 5.705 ppm (tetramer) and 5.923 ppm (trimer). It is noteworthy that the ^1H NMR-detected GPC curves reflect accurately the molar concentrations of the oligomer components. The number average molecular weight *Mn* and the *Mw/Mn* values for the mixture of chloral oligom-

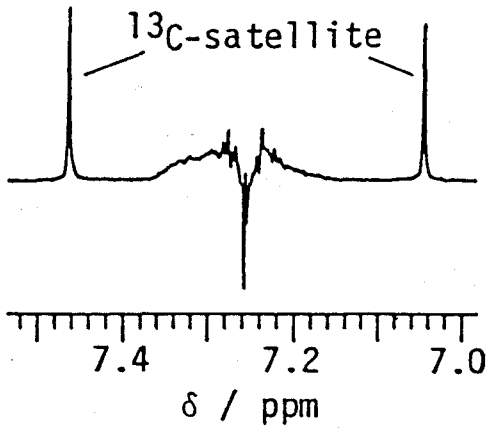

Figure 18. The suppressed signal due to the eluent ($CHCl_3$). This is a higher frequency part of the spectrum shown in Figure 19.

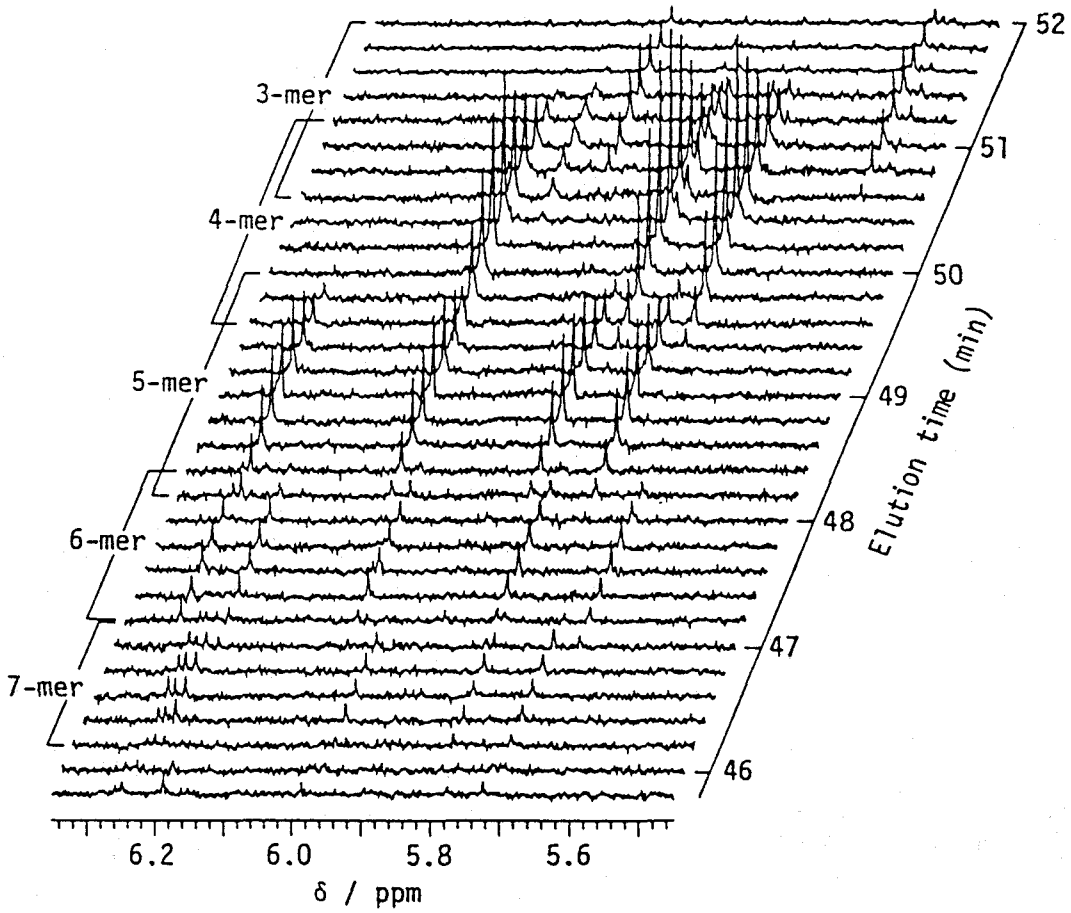

Figure 19. The on-line GPC/NMR data of the mixture of chloral oligomers.

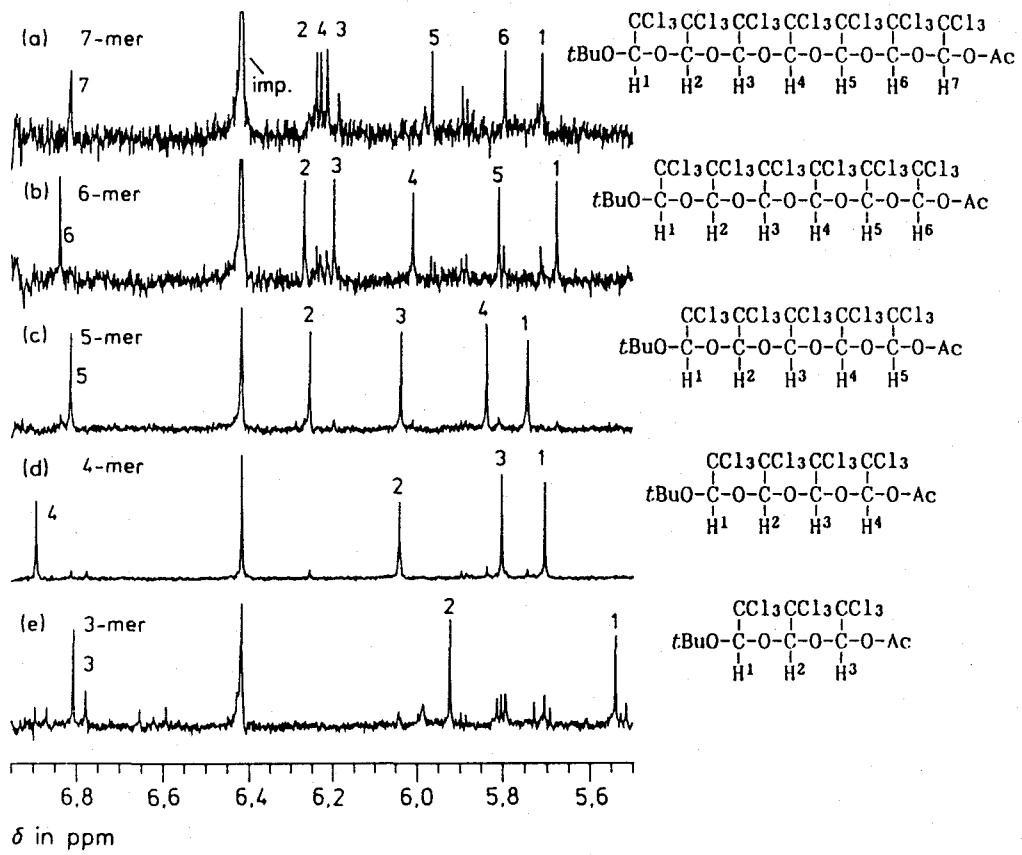

Figure 20. ^{1}H NMR spectra of the chloral oligomers (acetal proton region) derived from the on-line GPC/NMR data; (a): heptamer, elution time 46,0–47,2 min; (b): hexamer, 47,2–48,2 min; (c): pentamer, 48,2–49,4 min; (d): tetramer, 49,8–50,8 min; (e): trimer, 51,4–52,2 min. The signal at 6,43 ppm is due to an impurity in the eluent

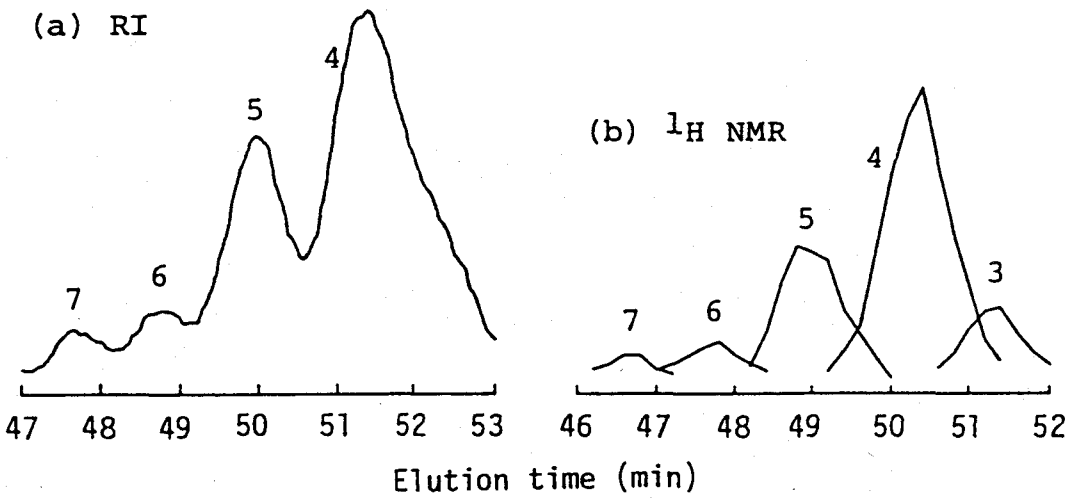

Figure 21. The RI-detected (a) and ^{1}H NMR-detected (b) GPC curves of the mixture of chloral oligomers.

ers were evaluated as 737 and 1.03 respectively, on the basis of the ^1H NMR-detected GPC curves.

The present results demonstrate the applicability of the on-line GPC/NMR method to the structural analysis of the oligomeric products.

4.7 Experimental Part

MMA and *n*-BuMA were purified by fractional distillation, dried over calcium dihydride, and then distilled under high vacuum just before use.

t-C_4H_9MgBr was prepared from *t*-C_4H_9Br and magnesium in dry diethyl ether ($[Mg^{2+}]/[t\text{-}C_4H_9] = 1.28$).

Toluene, purified in a usual manner and stored over sodium metal, was mixed with a small amount of *n*-C_4H_9Li and then vacuum-distilled.

The block copolymerization was carried out under dry nitrogen in a separable flask equipped with a mechanical stirrer. The polymerization of the first monomer, MMA, was initiated by adding the *t*-C_4H_9MgBr solution to the monomer solution in toluene at -60°C. After 4.5 h, toluene and then the second monomer, *n*-BuMA, were slowly added to the reaction mixture with stirring. The random copolymerization was carried out in a glass ampoule under dry nitrogen. The reaction was initiated by adding the *t*-C_4H_9MgBr solution to a 2:1 mixture of MMA and *n*-BuMA in toluene at -78°C. Both copolymerizations were terminated by adding a small amount of methanol to the reaction mixture. The solvent and unreacted monomers were removed from the reaction mixture by vacuum distillation. The residues were dissolved in benzene, and the insoluble materials were removed by centrifugation, and the copolymers were recovered from the benzene solutions by freeze drying.

References

1. J. C. Moore, *J. Polym. Sci., Part A*, **2**, 835 (1964).
2. K. Hatada, K. Ute, Y. Okamoto, M. Imanari, N. Fujii, *Polym. Bull.*, **20**, 317 (1988).
3. K. Hatada, K. Ute, M. Kashiyama, M. Imanari, *Polym. J.*, **22**, 218 (1990).
4. K. Hatada, K. Ute, T. Kitayama, T. Nishimura, M. Kashiyama, N. Fujimoto, *Polym. Bull.*, **22**, 549 (1990).
5. K. Hatada, K. Ute, T. Kitayama, M. Yamamoto, T. Nishimura, M. Kashiyama, *Polym. Bull.*, **21**, 489 (1989).
6. K. Ute, M. Kashiyama, K. Oka, K. Hatada, O. Vogl, *Makromol. Chem., Rapid Commun.*, **11**, 31 (1990).
7. E. Bayer, K. Albert, M. Nieder, E. Grom, T. Keller, *Adv. Chromatogr.*, **14**, 525 (1979).
8. H. C. Dorn, *Anal. Chem.*, **56**, 747A (1984).
9. D. A. Laude Jr., C. L. Wilkins, *Trends Anal. Chem.*, **5**, 230 (1986).
10. J. F. Haw, T. E. Glass, H. C. Dorn, *Anal. Chem.*, **53**, 2327 (1981).
11. K. Albert, E. Bayer, *Trends Alal. Chem.*, **7**, 288 (1988).
12. Z. Grubisic, P. Rempp, H. Benoit, *J. Polym. Sci.*, **B5**, 753 (1967).
13. W. Kaye, and A. J. Havlik, *Appl. Optics*, **12**, 541 (1973).
14. H. A. Andreetta, I. H. Sorokin, R. V. Figini, *Makromol. Chem., Rapid Commun.*, **6**, 419 (1985).
15. T. Q. Nguyen, H. H. Kausch, *J. Chromatogr.*, **449**, 63 (1988).
16. K. Hatada, K. Ute, K. Tanaka, T. Kitayama, Y. Okamoto, *Polym. J.*, **17**, 977 (1985); *ibid*, **18**, 1037 (1986).
17. K. Ute, T. Kitayama, K. Hatada, *Polym. J.*, **18**, 249 (1986).
18. H. Inagaki, T. Miyamoto, F. Kamiyama, *J. Polym. Sci., Part B* **7**, 329 (1969).
19. T. Miyamoto, S. Tomoshige, H. Inagaki, *Polym. J.*, **6**, 564 (1974).
20. D. M. Wiles, S. Bywater, *Trans. Farad Soc.*, **61**, 150 (1965).
21. T. Kitayama, T. Shinozaki, E. Masuda, M. Yamamoto, K. Hatada, *Polym. Bull.*, **20**, 505 (1988).
22. T. Kitayama, T. Shinozaki, T. Sakamoto, M. Yamamoto, K. Hatada, *Makromol. Chem., Suppl.*, **15**, 167 (1989).
23. S. Mori, *Adv. Chromat.*, **22**, 187 (1984).
24. T. Kitayama, K. Ute, M. Yamamoto, N. Fujimoto, K. Hatada, *Polym. J.*, **22**, 386 (1990).
25. O. Vogl, *The Chemist*, **62**, 16 (1985).
26. J. Zhang, G. D. Jaycox, O. Vogl, *Polymer*, **29**, 707 (1988).
27. K. Hatada, K. Ute, T. Nakano, F. Vass, O. Vogl, *Makromol. Chem.*, **190**, 2217 (1989).
28. O. Vogl, K. Ute, T. Nishimura, F. Xi, F. Vass, K. Hatada, *Macromolecules*, **22**, 4658 (1989).
29. K. Ute, T. Nishimura, K. Hatada, F. Xi, F. Vass, O. Vogl, *Makromol. Chem.*, **191** (1990).

PUBLICATION LIST

Chapter 1

1.1 NMR Assignment of the Terminal Methine Protons in Poly(methyl methacrylate) and Location of the Butyl Isopropenyl Ketone Unit in the Polymer Molecule Produced by Butyllithium and Butylmagnesium Chloride
Tatsuki Kitayama, Koichi Ute, Koichi Hatada, *Polym. J.*, **16**, 925 - 928 (1984).

1.2 Studies on the Polymerization of Methyl Methacrylate with Butylmagnesium Chloride by the Aid of Totally Deuterated Monomer
Koichi Ute, Tatsuki Kitayama, Koichi Hatada, *Polym. J.*, **18**, 249 - 261 (1986).

1.3 Studies on the Anionic Polymerization of Methyl Methacrylate with Butyllithium and Butylmagnesium Chloride Using Deuterated Monomer and Initiator
Koichi Ute, Tastuki Kitayama, Koichi Hatada, *Polym. J.*, to be submitted.

1.4 The NMR Chemical Shifts between the Nonequivalent Methylene Protons of Polymers and Oligomers of Methyl Methacrylate: The Revised *meso/racemo* Assignments for the ω-End Dyad Sequences
Koichi Hatada, Koichi Ute, Tatsuki Kitayama, Katsuji Tanaka, Mamoru Imanari, Naoyuki Fujii, *Polym. J.*, 21, 447 - 449 (1989).

1.5 Mechanism of Polymerization of MMA by Grignard Reagents and Preparation of Highly Isotactic PMMA with Narrow Molecular Weight Distribution
Koichi Hatada, Koichi Ute, Katsuji Tanaka, Tatsuki Kitayama, Yoshio Okamoto, *"Recent Advances in Anionic Polymerization"*, T. E. Hogen-Esch and J. Smid, Eds., Elsevier Science Publishing, 1987, p. 195-204.

Chapter 2

2.1 Preparation of Highly Isotactic Poly(methyl methacrylate) of Low Polydispersity
Koichi Hatada, Koichi Ute, Katsuji Tanaka, Tatsuki Kitayama, Yoshio Okamoto, *Polym. J.*, **17**, 977 - 980 (1985).

2.2 Living and Highly Isotactic Polymerization of Methyl Methacrylate by *t*-C_4H_9MgBr in Toluene
Koichi Hatada, Koichi Ute, Katsuji Tanaka, Yoshio Okamoto, Tatsuki Kitayama, *Polym. J.*, **18**, 1037 - 1047 (1986).

2.3 Two-Dimensional NMR Spectra of Isotactic Poly(methyl methacrylate) Prepared with *t*-C_4H_9MgBr and Detailed Examination of Tacticity
Koichi Hatada, Koichi Ute, Katsuji Tanaka, Mamoru Imanari, Naoyuki Fujii, *Polym. J.*, **19**, 425 - 436 (1987).

2.4 Preparation of Highly Isotactic and Syndiotactic Poly-(methyl methacrylate) Macromonomers Having the Same Chemical Structure and Their Polymerization
Koichi Hatada, Tatsuki Kitayama, Koichi Ute, Eiji Masuda, Tetsunori Shinozaki, Masanori Yamamoto, *Polym. Bull.*, **21**, 165 - 172 (1989).

2.5 Highly Isotactic and Living Polymerization of Ethyl Methacrylate with *t*-C_4H_9MgBr in Toluene and the Preparation of Block and Random Copolymers with High Stereoregularity
Tatsuki Kitayama, Koichi Ute, Masanori Yamamoto, Nobutaka Fujimoto, Koichi Hatada, *Polym. J.*, **22**, 386 - 396 (1990).

2.6 Synthesis of Stereoregular Polymers and Copolymers of Methacrylate by Living Polymerization and their Characterization by NMR Spectroscopy,
Tatsuki Kitayama, Koichi Ute, Koichi Hatada, *British Polym. J.*, **23**, 5 - 17 (1990).

Chapter 3

3.1 Stereochemistry of the Oligomerization of Methyl Methacrylate by *t*-C_4H_9MgBr in Toluene at -78°C
Koichi Hatada, Koichi Ute, Katsuji Tanaka, Tatsuki Kitayama, *Polym. J.*, **19**, 1325 - 1328 (1987).

3.2 Stereoregular Oligomers of Methyl Methacrylate: X-ray Crystal Structure Analysis and ^1H NMR Spectrum of the Trimer
Koichi Ute, Tohru Nishimura, Yoshiki Matsuura, Koichi Hatada, *Polym. J.*, **21**, 231 - 240 (1989).

3.3 Crystal Structure of Methyl Methacrylate Dimer. Revised *meso/racemo* Assignment for the Dimer
Tamaki Nakano, Koichi Ute, Yoshio Okamoto, Yoshiki Matsuura, Koichi Hatada, *Polym. J.*, **21**, 935 - 939 (1989).

3.4 Stereoregular Oligomers of Methyl Methacrylate III. ^{1}H and ^{13}C NMR Spectra of the Pure-Isotactic and Pure-Syndiotactic Oligomers from Dimers to Octamers
Koichi Ute, Tohru Nishimura, Koichi Hatada, *Polym. J.*, **21**, 1027 - 1041 (1989).

3.5 Stereoregular Oligomers of Methyl Methacrylate 4. Supercritical Fluid Chromatography of the Isotactic and Syndiotactic Oligomers of MMA
Koichi Hatada, Koichi Ute, Tohru Nishimura, Masaharu Kashiyama, Toshinori Saito, Makoto Takeuchi, *Polym. Bull.*, **23**, 157 - 162 (1990).

Chapter 4

4.1 On-line GPC/NMR Experiments Using the Isotactic Poly(methyl methacrylate) with Well-Defined Chemical Structure
Koichi Hatada, Koichi Ute, Yoshio Okamoto, Mamoru Imanari, Naoyuki Fujii, *Polym. Bull.*, **20**, 317 - 321 (1988).

4.2 On-line GPC/NMR Analyses of Block and Random Copolymers of Methyl and Butyl Methacrylates Prepared with *t*-C_4H_9MgBr
Koichi Hatada, Koichi Ute, Tatsuki Kitayama, Masanori Yamamoto, Tohru Nishimura, Masaharu Kashiyama, *Polym. Bull.*, **21**, 489 - 495 (1989).

4.3 On-line GPC/NMR Analysis of the Mixture of Chloral Oligomers
Koichi Ute, Masaharu Kashiyama, Ken-ichi Oka, Koichi Hatada *Makromol. Chem., Rapid Commun.*, **11**, 31 - 35 (1990).

4.4 Direct Determination of Molecular Weight and Its Distribution by the Absolute Calibration Method Using the On-line GPC/NMR
Koichi Hatada, Koichi Ute, Masaharu Kashiyama, Mamoru Imanari, *Polym. J.*, **22**, 218 - 222 (1990).

4.5 Studies on the Molecular Weight Dependence of Tacticity of Anionically Prepared PMMAs by On-line GPC/NMR
Koichi Hatada, Koichi Ute, Tatsuki Kitayama, Tohru Nishimura, Masaharu Kashiyama, Nobutaka Fujimoto, *Polym. Bull.*, **22**, 549 - 554 (1990).

Other Papers

Polymerization of Methacrylates

5.1 An Extraordinary Effect of Ether on the Polymerization of Methacrylates with Grignard Reagent in Toluene
Koichi Hatada, Koichi Ute, Tatsuki Kitayama, Mikiharu Kamachi, *Polym. J.*, **15**, 771 - 773 (1983).

5.2 Syntheses of Syndiotactic Poly(methyl methacrylate)s with Grignard Reagents (RMgBr)
Zun-Kui Cao, Koichi Ute, Tatsuki Kitayama, Yoshio Okamoto, Koichi Hatada, *Kobunshi Ronbunshu*, **43**, 435 - 441 (1986).

5.3 Studies of *p*- and *m*-Vinylbenzylmagnesium Chlorides as Initiators and monomers —— Preparations of Macromers and Poly(Grignard reagent)s
Koichi Hatada, Hideo Nakanishi, Koichi Ute, Tatsuki Kitayama, *Polym. J.*, **18**, 581 - 591 (1986).

5.4 Preparation of PMMA Macromers by *o*-Vinylbenzylmagnesium Chloride and Their Polymerization
Koichi Hatada, Tetsunori Shinozaki, Koichi Ute, Tatsuki Kitayama, *Polym. Bull.*, **19**, 231 - 237 (1988).

Structural Determination

5.5 Determination of Tacticity of Polymethacrylamide by ^{13}C NMR Spectroscopy
Koichi Hatada, Tatsuki Kitayama, Koichi Ute, *Polym. Bull.*, **9**, 241 - 244 (1983).

5.6 *E,Z* Assignments of Isophorone Diisocyanate (IPDI) and Their Implications on the Relative Reactivity of the Isocyanate Group
Koichi Hatada, Koichi Ute, S. Peter Pappas, *J. Polym. Sci., Part C: Polym. Lett.*, **25**, 477 - 480 (1987).

5.7 Unambiguous ^{13}C NMR Assignments for Isocyanate Carbons of Isophorone Diisocyanate and Reactivity of Isocyanate Groups in *Z*- and *E*-Stereoisomers
Koichi Hatada, Koichi Ute, Ken-ichi Oka, S. Peter Pappas, *J. Polym. Sci., Part A: Polym. Chem.*, **28**, 3019 - 3027 (1990).

5.8 Determination of Molecular Weight of Poly(methyl methacrylate) by Deuterium NMR and Its Reliability
Koichi Hatada, Koichi Ute, Masaharu Kashiyama, *Polym. J.*, **22**, 853 - 857 (1990).

5.9 Structure and Biosynthesis Mechanism of Rubber from "Fungi"
Yasuyuki Tanaka, Makio Mori, Koichi Ute, Koichi Hatada
Rubber Chem. Technol., **63**, 1 - 7 (1990).

Chloral Oligomers

5.10 Haloaldehyde Polymers, 34 ^{1}H and ^{13}C NMR Spectra of Chloral Oligomers Prepared by Lithium *tert*-butoxide Initiation and the Assignment of the *meso/racemo* Addition Products of the Dimers
Koichi Hatada, Koichi Ute, Tamaki Nakano, Frantisek Vass, Otto Vogl, *Makromol. Chem.*, **190**, 2217 - 2228 (1989).

5.11 Haloaldehyde Polymers XXXV. ^{1}H, ^{19}F and ^{13}C NMR Spectra and Stereochemistry of Bornyl Esters of Fluorochlorobromoacetic Acid
Koichi Hatada, Koichi Ute, Tamaki Nakano, Yoshio Okamoto, Thomas R. Doyle, Otto Vogl, *Polym. J.*, **21**, 171 - 177 (1989).

5.12 Direct Formation of the Helical Polymer Conformation in Stereospecific Polymer Synthesis. X-ray Crystallographic Determination of Linear Chloral Oligomers
Otto Vogl, Fu Xi, Frantisek Vass, Koichi Ute, Tohru Nishimura, Koichi Hatada, *Macromolecules*, **22**, 4658 - 4660 (1989).

5.13 Haloaldehyde Polymers, 40 Stereostructure of Chloral Oligomers Prepared with Lithium *tert*-butoxide: Helical Conformation of the Linear Isotactic Oligomers in Crystal and in Solution
Koichi Ute, Tohru Nishimura, Koichi Hatada, Fu Xi, Frantisek Vass, Otto Vogl, *Makromol. Chem.*, **191**, 557 - 569 (1990).

5.14 Haloaldehyde Polymers, 43 Structure of 2-Bornyloxy-Terminated Chloral Oligomers
Koichi Ute, Ken-ichi Oka, Masaharu Kashiyama, Koichi Hatada, Fu Xi, Otto Vogl, *Makromol. Chem.*, in press

Reviews

5.15 Stereoregular Polymerization of α-Substituted Acrylates
Koichi Hatada, Tatsuki Kitayama, Koichi Ute, *Prog. Polym. Sci.*, 13, 189 - 276 (1988).

5.16 「ＰＭＭＡマクロマーについての２、３の話題」
右手浩一・畑田耕一、高分子加工、36, 366 - 372 (1987).

5.17 「オンラインＧＰＣ／ＮＭＲによるポリマーの構造解析」
畑田耕一・右手浩一、高分子、38, 1029 (1989).

5.18 「高分子溶液の高分解能ＮＭＲ」
右手浩一、高分子、40 (1), 印刷中 (1991).